

UNIVERSITY OF BIRMINGHAM

**An Investigation on the Effect of
Solution Concentration, Applied Voltage and Collection
Distance on Electrospun Fibres of PVA Solutions**

by

Tasawar Iqbal

A thesis submitted to the College of Engineering and Physical Sciences for the degree of

MRes in Biomaterials

Supervisor: Dr. A. Stamboulis

Department of Metallurgy and Materials, University of Birmingham, UK

August 2010

UNIVERSITY OF
BIRMINGHAM

University of Birmingham Research Archive

e-theses repository

This unpublished thesis/dissertation is copyright of the author and/or third parties. The intellectual property rights of the author or third parties in respect of this work are as defined by The Copyright Designs and Patents Act 1988 or as modified by any successor legislation.

Any use made of information contained in this thesis/dissertation must be in accordance with that legislation and must be properly acknowledged. Further distribution or reproduction in any format is prohibited without the permission of the copyright holder.

ABSTRACT

This study investigates the effect of parameters including increasing concentrations, applied voltage and collection distance using poly (vinyl alcohol) (PVA) solutions on the fibre diameter and morphology of electrospun nanofibres. PVA solutions of 4%, 6% and 8% of mass percentage were used. The diameter and morphology of nanofibres formed were analysed under the Environmental Scanning Environmental Microscope (ESEM). The deposition rate and area were also analysed.

At lower concentrations of PVA 4% and PVA 6% beaded fibres were formed. The average fibre diameter with PVA 4% ranged from 43-92nm, PVA 6% ranged from 72-128nm and with PVA 8% ranging from 144-215nm.

Increasing the applied voltage produced thinner fibres with PVA 4%. With PVA 6%, at a shorter distance increasing the applied voltage increased the average fibre diameter from 18-20kV and at a longer distance decreased it. With PVA 8% increasing the applied voltage at a shorter distance decreased the average fibre diameter and at a longer distance slightly increased it.

With increasing collection distance the average fibre diameter increased with PVA 4% using 8kV and 20kV. With PVA 6% at 18kV it increased with increasing collection distance, at 20kV decreases and at 12kV decreases from 7cm to 10cm. With PVA 8% the average fibre diameter increases with increasing collection distance.

Results concluded that concentration had a significant effect on the fibre diameter and morphology. Altering the voltage and collection distance altered fibre diameter.

DEDICATION

Bismillah-Arrahmaan-Niraheem.

In the name of Allah, the Beneficent, the Merciful.

Thank you Allah, for everything you have given me. May Allah send peace and blessings upon our beloved Prophet Muhammad (sallallahu alaihi wasalam)

I would like to dedicate this thesis to my Mother, Shamim Akhtar. Love you Mum.

ACKNOWLEDGMENTS

I would to thank my supervisor Dr. Artemis Stamboulis for giving me the opportunity to work in my area of interest, nanoscience. I would also thank Theresa Morris and Paul Stanley for the help they gave in training me on the ESEM. Finally, I am grateful to have completed my MRes at the University of Birmingham.

I would like to give a special thanks to my Mother. Also, a special thanks to my brother Dr. Mushaud Iqbal for all the time and support he gave, and finally, a very special thanks to my niece Imaan Iqbal.

CONTENTS

1. INTRODUCTION	page 19
2. LITERATURE REVIEW	page 20
2.1. Electrospinning Process	page 20
2.2. Process Parameters	page 22
2.3. Effect of Solution Concentration	page 23
2.4. Effect of Applied Voltage	page 28
2.5. Effect of Collection Distance	page 34
2.6. Applications of Electrospun Fibres in Tissue Engineering	page 37
2.7. Poly (vinyl alcohol)	page 39
3. METHODS AND MATERIALS	page 40
3.1. Preparation of PVA Solutions	page 40
3.2. Electrospinning Preparation	page 40
3.3. Electrospinning Parameters	page 43
3.4. Materials and Characterisation	page 43
4. RESULTS	page 45
<u>4.1. Solution Concentration</u>	page 45
4.1.1. Effect of Increasing Concentration on Fibre Diameter and Morphology	page 45
4.1.2. Effect of Increasing Concentration on Fibre Diameter Distribution	page 51
4.1.3. Effect of Increasing Concentration on Deposition Rate	page 59
<u>4.2. Applied Voltage</u>	page 62
4.2.1. Effect of Increasing Voltage on Fibre Diameter and Morphology	page 62
4.2.2. Effect of Increasing Voltage on Fibre Diameter Distribution	page 73

4.2.3. Effect of Increasing Voltage on Deposition Rate	page 85
<u>4.3. Collection Distance</u>	page 88
4.3.1. Effect of Increasing Collection Distance on Fibre Diameter and Morphology	page 88
4.3.2. Effect of Increasing Concentration on Fibre Diameter Distribution	page 100
4.3.4. Effect of Increasing Concentration on Deposition Rate	page 113
<u>4.4. Beaded Fibre Morphology</u>	page 115
4.4.1. Effect of Increasing Voltage on Bead Morphology	page 117
4.4.2. Effect of Increasing Collection Distance on Bead Morphology	page 121
<u>4.3. Observations of the Electrospinning Process: Jet Formation and Deposition</u>	page 124
4.4. Droplet Formation and Ejection onto the Collector	page 139
5. DISCUSSION	page 142
5.5. Effect of Concentration	page 142
5.5. Effect of Applied Voltage	page 148
5.6. Effect of Collection Distance	page 153
5.7. Electrospinning Process: Jet Formation and Deposition	page 159
6. CONCLUSION	page 160
7. FUTURE WORK	page 166
8. APPENDICES	page 168
9. REFERENCES	page 187

LIST OF FIGURES

Figure 1. A typical electrospinning setup.

Figure 2. The effect of increasing concentration on bead morphology.

Figure 3. Relationship between solution concentration and surface tension.

Figure 4. The above image is of the electric field generated during electrospinning.

Figure 5. Change in morphology of the beads on the fibres with increasing collection distance.

Figure 6. Electrospinning setup for ES1a.

Figure 7. Electrospinning Apparatus encased in periplex glass box. (Appendix IX)

Figure 8. SEM images at different concentrations, a) PVA 4%, b) PVA 6% and c) PVA 8%

Figure 9. Overall Average, Maximum and Minimum Fibre Diameter at 10cm Collection Distance and 12kV with Increasing Concentration

Figure 10. SEM images at different concentrations, a) PVA 4%, b) PVA 6% and c) PVA 8%

Figure 11. Overall Average, Maximum and Minimum Fibre Diameter at 10cm Collection Distance and 20kV with Increasing Concentration

Figure 12. SEM images at different concentrations, a) PVA 4%, b) PVA 6% and c) PVA 8%.

Figure 13. Overall Average, Maximum and Minimum Fibre Diameter at 15cm Collection Distance and 12kV with Increasing Concentration.

Figure 14. SEM images at different concentrations, a) PVA 4%, b) PVA 6% and c) PVA 8%.

Figure 15. Overall Average, Maximum and Minimum Fibre Diameter at 15cm Collection Distance and 20kV with Increasing Concentration.

Figure 16. Total Percentage of Fibre Diameter Distribution of PVA 4% Solution at 10cm Collection Distance and 12kV.

Figure 17. Overall Percentage of Fibre Diameter Distribution of PVA 6% Solution at 10cm Collection Distance and 12kV.

Figure 18. Percentage of Fibre Diameter Distribution of PVA 8% Solution at 10cm Collection Distance and 12kV

Figure 19. Total Percentage of Fibre Diameter Distribution of PVA 4% Solution at 10cm Collection Distance and 20kV

Figure 20. Total Percentage of Fibre Diameter Distribution of PVA 6% Solution at 10cm Collection Distance and 20kV

Figure 21. Total Percentage of Fibre Diameter Distribution of PVA 8% Solution at 10cm Collection Distance and 20kV

Figure 22. Total Percentage of Fibre Diameter Distribution of PVA 4% Solution at 15cm Collection Distance and 12kV

Figure 23. Total Percentage of Fibre Diameter Distribution of PVA 6% Solution at 15cm Collection Distance and 12kV

Figure 24. Percentage of Fibre Diameter Distribution of PVA 8% Solution at 15cm Collection Distance and 12kV

Figure 25. Total Percentage of Fibre Diameter Distribution of PVA 4% Solution at 15cm Collection Distance and 20kV.

Figure 26. Total Percentage of Fibre Diameter Distribution of PVA 6% Solution at 15cm Collection Distance and 20kV.

Figure 27. Total Percentage of Fibre Diameter Distribution of PVA 8% Solution at 15cm Collection Distance and 20kV.

Figure 28. Deposition Rate of PVA 4%, 6% and 8% Solutions Electrospun at 10cm Collection Distance and 12kV.

Figure 29. Deposition Rate of PVA 4%, 6% and 8% Solutions Electrospun at 10cm Collection Distance and 20kV.

Figure 30. Deposition Rate of PVA 4%, 6% and 8% Solutions Electrospun at 15cm Collection Distance and 12kV.

Figure 31. Deposition Rate of PVA 4%, 6% and 8% Solutions Electrospun at 15cm Collection Distance and 20kV

Figure 32. SEM images of electrospun PVA 4% at 7cm collection distance with application of increasing voltage, a) 8kV, b) 12kV and c) 20kV

Figure 33. Overall Average, Maximum and Minimum Fibre Diameter of Electrospun PVA 4% Solution at 7cm Collection Distance with Increasing Voltage

Figure 34. SEM images of electrospun PVA 4% % at 10cm collection distance with application of increasing voltage, a) 8kV, b) 12kV and c) 20kV

Figure 35. Overall Average, Maximum and Minimum Fibre Diameter of Electrospun PVA 4% Solution at 10cm Collection Distance with Increasing Voltage

Figure 36. SEM images of electrospun PVA 4% at 15cm collection distance with application of increasing voltage, a) 8kV, b) 12kV and c) 20kV

Figure 37. Overall Average, Maximum and Minimum Fibre Diameter of Electrospun PVA 4% Solution at 15cm Collection Distance with Increasing Voltage

Figure 38. SEM images of electrospun PVA 6% at 10cm collection distance with application of increasing voltage, a) 12kV, b) 18kV and c) 20kV

Figure 39. Overall Average, Minimum and Maximum Diameter of Electrospun Fibres of PVA 6% Solution at 10cm Collection Distance with Increasing Voltage

Figure 40. SEM images of electrospun PVA 6% at 15cm collection distance with application of increasing voltage, a) 12kV, b) 18kV and c) 20kV

Figure 41. Overall Average, Minimum and Maximum Diameter of Electrospun Fibres of PVA 6% Solution at 15cm Collection Distance with Increasing Voltage

Figure 42. SEM images of electrospun PVA 8% at 10cm collection distance with application of increasing voltage, a) 12kV and b) 20kV

Figure 43. Overall Average, Minimum and Maximum Fibre Diameter of Electrospun PVA 8% Solution at 10cm Collection Distance with Increasing Voltage

Figure 44. SEM images of electrospun PVA 8%% at 15cm collection distance with application of increasing voltage, a) 12kV and b) 20kV

Figure 45. Overall Average, Minimum and Maximum Fibre Diameter of Electrospun PVA 8% Solution at 15cm Collection Distance with Increasing Voltage

Figure 46. Total Percentage of Fibre Diameter Distribution of PVA 4% Solution at 7cm Collection Distance and 8kV

Figure 47. Total Percentage of Fibre Diameter Distribution of PVA 4% Solution at 7cm Collection Distance and 12kV

Figure 48. Total Percentage of Fibre Diameter Distribution of PVA 4% Solution at 10cm Collection Distance and 8kV

Figure 49. Total Percentage of Fibre Diameter Distribution of PVA 4% Solution at 10cm Collection Distance and 12kV

Figure 50. Total Percentage of Fibre Diameter Distribution of PVA 4% Solution at 10cm Collection Distance and 20kV

Figure 51. Total Percentage of Fibre Diameter Distribution of PVA 4% Solution at 15cm Collection Distance and 8kV

Figure 52. Total Percentage of Fibre Diameter Distribution of PVA 4% Solution at 15cm Collection Distance and 12kV

Figure 53. Total Percentage of Fibre Diameter Distribution of PVA 4% Solution at 15cm Collection Distance and 20kV

Figure 54. Overall Percentage of Fibre Diameter Distribution of PVA 6% Solution at 10cm Collection Distance and 12kV

Figure 55. Total Percentage of Fibre Diameter Distribution of PVA 6% Solution at 10cm Collection Distance and 18kV

Figure 56. Total Percentage of Fibre Diameter Distribution of PVA 6% Solution at 10cm Collection Distance and 20kV

Figure 57. Total Percentage of Fibre Diameter Distribution of PVA 6% Solution at 15cm Collection Distance and 12kV

Figure 58. Total Percentage of Fibre Diameter Distribution of PVA 6% Solution at 15cm Collection Distance and 18kV

Figure 59. Total Percentage of Fibre Diameter Distribution of PVA 6% Solution at 15cm Collection Distance and 20kV

Figure 60. Percentage of Fibre Diameter Distribution of PVA 8% Solution at 10cm Collection Distance and 12kV

Figure 61. Total Percentage of Fibre Diameter Distribution of PVA 8% Solution at 10cm Collection Distance and 20kV

Figure 62. Percentage of Fibre Diameter Distribution of PVA 8% Solution at 15cm Collection Distance and 12kV

Figure 63. Total Percentage of Fibre Diameter Distribution of PVA 8% Solution at 15cm Collection Distance and 20kV

Figure 64. Deposition Rate of 4wt% PVA Solution Electrospun Fibres Collected on an Area of 2cm² Al Foil Collector

Figure 65. Deposition Rate of 6wt% PVA Solution Electrospun Fibres Collected on an Area of 2cm² Al Foil Collector

Figure 66. Deposition Rate of 8wt% PVA Solution Electrospun Fibres Collected on an Area of 2cm² Al Foil Collector

Figure 67. SEM images of electrospun PVA 4% using 8kV with increasing collection distance, a) 7cm, b) 10cm and c) 15cm

Figure 68. Overall Average, Maximum and Minimum Fibre Diameter of Electrospun PVA 4% Solution at 8kV with Increasing Collection Distance

Figure 69. SEM images of electrospun PVA 4% using 12kV with increasing collection distance, a) 7cm, b) 10cm and c) 15cm

Figure 70. Overall Average, Maximum and Minimum Fibre Diameter of Electrospun PVA 4% Solution at 12kV with Increasing Collection Distance

Figure 71. SEM images of electrospun PVA 4% using 20kV with increasing collection distance, a) 7cm, b) 10cm and c) 15cm

Figure 72. Overall Average, Maximum and Minimum Fibre Diameter of Electrospun PVA 4% Solution at 20kV with Increasing Collection Distance

Figure 73. SEM images of electrospun PVA 6% using 12kV with increasing collection distance, a) 7cm, b) 10cm and c) 15cm

Figure 74. Overall Average, Minimum and Maximum Fibre Diameter of Electrospun Fibres of PVA 6% Solution at 12kV with Increasing Collection Distance

Figure 75. SEM images of electrospun PVA 6% using 18kV with increasing collection distance, a) 10cm and b) 15cm

Figure 76. Overall Average, Minimum and Maximum Fibre Diameter of Electrospun Fibres of PVA 6% Solution at 18kV with Increasing Collection Distance

Figure 77. SEM images of electrospun PVA 6% using 20kV with increasing collection distance, a) 10cm and b) 15cm

Figure 78. Overall Average, Minimum and Maximum Fibre Diameter of Electrospun Fibres of PVA 6% Solution at 20kV with Increasing Collection Distance

Figure 79. SEM images of electrospun PVA 8% using 12kV with increasing collection distance, a) 10cm and b) 15cm

Figure 80. Overall Average, Minimum, Maximum Fibre Diameter of Electrospun PVA 8% Solution at 12kV with Increasing Collection Distance

Figure 81. SEM images of electrospun PVA 8% using 20kV with increasing collection distance, a) 10cm and b) 15cm

Figure 82. Overall Average, Minimum and Maximum Fibre Diameter of Electrospun PVA 8% Solution at 20kV with Increasing Collection Distance

Figure 83. Total Percentage of Fibre Diameter Distribution of PVA 4% Solution at 7cm Collection Distance and 8kV

Figure 84. Total Percentage of Fibre Diameter Distribution of PVA 4% Solution at 10cm Collection Distance and 8kV

Figure 85. Total Percentage of Fibre Diameter Distribution of PVA 4% Solution at 15cm Collection Distance and 8kV

Figure 86. Total Percentage of Fibre Diameter Distribution of PVA 4% Solution at 7cm Collection Distance and 12kV

Figure 87. Total Percentage of Fibre Diameter Distribution of PVA 4% Solution at 10cm Collection Distance and 12kV

Figure 88. Total Percentage of Fibre Diameter Distribution of PVA 4% Solution at 15cm Collection Distance and 12kV

Figure 89. Total Percentage of Fibre Diameter Distribution of PVA 4% Solution at 10cm Collection Distance and 20kV

Figure 90. Total Percentage of Fibre Diameter Distribution of PVA 4% Solution at 15cm Collection Distance and 20kV

Figure 91. Total Percentage of Fibre Diameter Distribution of PVA 6% Solution at 7cm Collection Distance and 12kV

Figure 92. Overall Percentage of Fibre Diameter Distribution of PVA 6% Solution at 10cm Collection Distance and 12kV

Figure 93. Total Percentage of Fibre Diameter Distribution of PVA 6% Solution at 15cm Collection Distance and 12kV

Figure 94. Total Percentage of Fibre Diameter Distribution of PVA 6% Solution at 10cm Collection Distance and 18kV

Figure 95. Total Percentage of Fibre Diameter Distribution of PVA 6% Solution at 15cm Collection Distance and 18kV

Figure 96. Total Percentage of Fibre Diameter Distribution of PVA 6% Solution at 10cm Collection Distance and 20kV

Figure 97. Total Percentage of Fibre Diameter Distribution of PVA 6% Solution at 15cm Collection Distance and 20kV

Figure 99. Percentage of Fibre Diameter Distribution of PVA 8% Solution at 10cm Collection Distance and 12kV

Figure 100. Percentage of Fibre Diameter Distribution of PVA 8% Solution at 15cm Collection Distance and 12kV

Figure 101. Total Percentage of Fibre Diameter Distribution of PVA 8% Solution at 10cm Collection Distance and 20kV

Figure 102. Total Percentage of Fibre Diameter Distribution of PVA 8% Solution at 15cm Collection Distance and 20kV

Figure 103. Deposition Rate of 4wt% PVA Solution Electrospun Fibres Collected on an Area of 2cm² Al Foil Collector

Figure 104. Deposition Rate of 6wt% PVA Solution Electrospun Fibres Collected on an Area of 2cm² Al Foil Collector

Figure 105. Deposition Rate of 8wt% PVA Solution Electrospun Fibres Collected on an Area of 2cm² Al Foil Collector

Figure 106. Elongated Bead

Figure 107. Bead

Figure 108. Bead/Spindle

Figure 109. Spindle-like

Figure 110. Average Bead Width and Length on Electrospun Fibres of PVA 4% Solution at 7cm Collection Distance and Increasing Voltage

Figure 111. Average Bead Width and Length on Electrospun Fibres of PVA 4% Solution at 10cm Collection Distance and Increasing Voltage

Figure 112. Average Bead Width and Length on Electrospun Fibres of PVA 4% Solution at 15cm Collection Distance and Increasing Voltage

Figure 113. Average Bead Width and Length on Electrospun Fibres of PVA 6% Solution at 10cm Collection Distance and Increasing Voltage

Figure 114. Average Bead Width and Length on Electrospun Fibres of PVA 6% Solution at 15cm Collection Distance and Increasing Voltage

Figure 115. Average Bead Width and Length on Electrospun Fibres of PVA 4% Solution at 8kV and Increasing Collection Distance

Figure 116. Average Bead Width and Length on Electrospun Fibres of PVA 4% Solution at 12kV and Increasing Collection Distance

Figure 117. Average Bead Width and Length on Electrospun Fibres of PVA 4% Solution at 20kV and Increasing Collection Distance

Figure 118. Average Bead Width and Length on Electrospun Fibres of PVA 6% Solution at 12kV and Increasing Collection Distance

Figure 119. Average Bead Width and Length on Electrospun Fibres of PVA 6% Solution at 18kV and Increasing Collection Distance

Figure 120. Average Bead Width and Length on Electrospun Fibres of PVA 6% Solution at 20kV and Increasing Collection Distance

Figure 121. Initiation of mesh formation as jet continues to deposit fibres.

Figure 122. Mesh becomes larger with subsequent deposition of fibres.

Figure 123. The structure of the mesh at the end of the experiment after without voltage application.

Figure 124a. SEM image of the tip of the mesh.

b. x2000 magnification

Figure 125a. SEM image of upper middle region of the mesh.

b.x10 000 magnification

Figure 126a. SEM image of the lower middle region of the mesh.

b. x2000 magnification

c. x10 000 magnification

Figure 127a. SEM image of the base of the mesh.

b. x2000 magnification

c. x10000 magnification

Figure 128. a) Single jet and b) Dual jets

Figure 129a. Electrospinning jet.

b. Electrospinning jet stops.

c. Drop grows larger at the tip protrudes towards the collector.

d. Drop is ejected and electrospinning jet forms immediately and continues the process.

Figure 130. The average fibre diameter with the Berry number for PVA at M_w of A: 9500g/mol, B: 18,000g/mol, C: 40,500g/mol, D: 67,000g/mol, E: 93,500g/mol & F: 155,000g/mol. The $[\eta]C$ critical values for the transition from extremely dilute to dilute to highly entangled polymer chain regimes are shown.

Appendix VIII

Figure 131. Image above shows the collector and region of collection. The image on the left gives an example of the circular deposition which comprises of an oval shaped collection with no visible region of the collector surface within the deposition. The image on the right is an example of a ringed collection which consists of the circular deposition of PVA with a region in the centre of the visible collector surface.

Figure 132. The image above shows the collection of light and dense collection, spraying during electrospinning, ejection of drops on the collector and regions of the solution collection due to insufficient drying the jet before reaching the collector.

LIST OF TABLES

Appendix VIII

- Table 1. PVA 4%, 12kV, 15cm, H=25cm
- Table 2. PVA 4%, 12kV, 10cm, H=25cm
- Table 3. PVA 4%, 20kV, 10cm, H=25cm
- Table 4. PVA 4%, 20kV, 15cm, H=24-25cm
- Table 5. PVA 4%, 8kV, 10cm, H=24-25cm
- Table 6. PVA 4%, 12kV, 7cm, H=25cm
- Table 7. PVA 4%, 8kV, 15cm, H=24.5-25cm
- Table 8. PVA 4%, 8kV, 7cm, H=25cm
- Table 9. PVA 6%, 12kV, 10cm, H=25-25.5cm
- Table 10. PVA 6%, 20kV, 15cm, H=25cm
- Table 11. PVA 6%, 20kV, 10cm, H=24-24.5cm
- Table 12. PVA 6%, 18kV, 10cm, H=25cm
- Table 13. PVA 6%, 12kV, 7cm, H=24.5-25cm
- Table 14. PVA 6%, 18kV, 15cm, H=25cm
- Table 15. PVA 6%, 12kV, 15cm, H=25.5-25cm
- Table 16. PVA 8%, 12kV, 10cm, H=25-26cm
- Table 17. PVA 8%, 20kV, 10cm, H=25-26cm
- Table 18. PVA 8%, 12kV, 15cm, H=25-26cm

1. INTRODUCTION

The electrospinning or electrostatic spinning technique has become increasingly popular in recent years as method of producing polymeric nanofibres for a variety of applications¹. The electrospinning technique possesses many benefits as the fibres produced can offer unique properties. Manipulation of structures on a nanoscale level can control the chemical, physical, electrical, optical and magnetic properties. Nanotechnology and nanomaterials have a range of potential use pharmaceutical and biomedical applications^{2,3,4}. For example, drug delivery by transporting therapeutic drugs in nanospheres and biocompatible implantable devices and structures⁴.

A variety of techniques are used to produce polymeric nanofibres such drawing, template synthesis, temperature induced phase separation, molecular self assembly and electrospinning. However, these techniques possess disadvantages limiting their use which include discontinuous fabrication process, non scalable production, polymer-specific processes and lack of control over diameter and orientation of fibres produced².

Electrospinning is an emerging technique which allows the fabrication of polymeric nanofibres using polymer solutions and polymer melts with more control over the processing parameters to enable manipulation of the fibres produced. Fibres ranging from approximately 3nm to 10 μ m can be fabricated using the same experimental setup whilst varying the parameters².

This study aims to investigate the effect electrospinning parameters which include of concentrations, applied voltage and collection distance using poly (vinyl alcohol) (PVA) solutions on the fibre diameter and morphology of electrospun nanofibres.

2. LITERATURE REVIEW

2.1. Electrospinning Process

The electrospinning process involves applying a known voltage to a capillary containing polymer solution (or polymer melt) and using the electrical field applied to draw the viscous liquid from the tip of the capillary to a target where the fibres are collected. The solvent evaporates from the liquid jet as it travels from the tip to form fibres which deposit on the collector. The fibres formed vary in diameter depending on the processing parameters⁵.

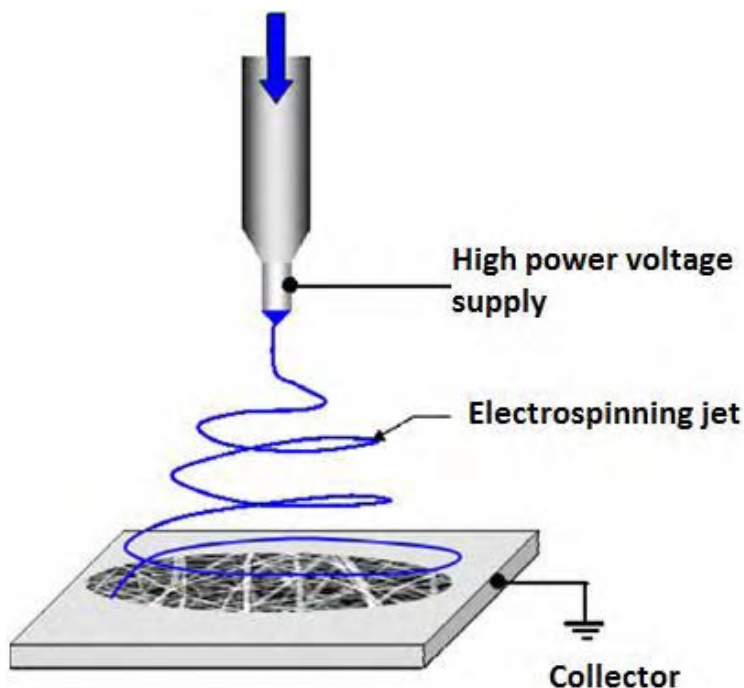


Figure 1. A typical electrospinning setup⁶.

The base region is where the solution is held within the capillary with a drop maintained on its tip under the action of the surface tension. An electrical potential or voltage is applied to

the solution. The intensity of the electric field induces electrostatic charges within the solution changing the shape of the drop. The electric forces concentrate on the most protruding region of the drop, inducing mutual charge repulsion on its surface. The drop protrudes more and as the charge is the greatest on the protruding region the surface is pulled put into a conical shape, altering the drop morphology from a spherical droplet shape into a protruding drop, known as a Taylor cone. The formation of the Taylor cone will be discussed in more detail later. The electric charges continue to increase in the protruding part of the Taylor cone decreasing its radius. The continuing increase in charge repulsion exceeds the surface tension of the solution and a jet is ejected from the Taylor cone and initiates electrospinning^{7,8}.

An equilibrium of electric forces, flow rate, viscoelastic properties and surface tension of the solution maintain the shape and size of the Taylor cone at the tip during electrospinning⁹ allowing the continuous electrospinning of the polymer jet⁷.

The jet region comprises of acceleration and elongation of the jet by electrical forces. The stretching of the jet decreases its diameter and increases its length at constant rate as it travels towards the collector, during which the jet undergoes bending and whipping instabilities¹⁰. The jet accelerates towards the metal screen collector and the solvent evaporates as it is stretched continuously¹⁰ leaving the polymer behind in the form of fibres on the collector⁷.

When the electrical potential exceeds the cohesive forces within the solution it undergoes splitting and splaying. Splaying occurs during the stretching and evaporation of the jet¹¹.

As the jet thins during elongation, the charge expands the jet in the radial direction from the forces acting on the polymer mass from the surrounding electric field. The jet resists the radial expansion by electric forces by the viscoelastic elongational flow of the jet. As the jet becomes thinner the electric forces become greater and strong enough to overcome the jet cohesive forces causing the jet to splay. The radial forces on the axis of the jet become large enough to overcome the cohesive forces and a single jet may split into many charged jets carrying approximately the same charge and of similar diameters accelerating towards the collector in the direction of the electric field⁷.

The collection region is where the jet trajectory ends and the charge carried on the jet is grounded by the collection of polymer fibres on collector^{7,12}. Fibres which arrive at the collector carry a certain amount of charge which can be dissipated by using a conducting collector, such as metal collector⁷. Any remaining solvent evaporates and deposited fibres solidify¹³.

2.2. Process Parameters

The parameters that manipulate the type and diameter size of the fibres produced include the system parameters or solution properties, process parameters and ambient conditions^{4,14}.

The system parameters comprise of the concentration, molecular weight, viscosity, conductivity and surface tension¹². Process parameters control the external variables of the equipment applied to the solution which include electric potential or voltage, flow rate, distance between the capillary tip and target. Ambient parameters include humidity

surrounding the electrospinning solution, along with air velocity and room temperature, which are also considered^{1,4}.

Many researchers have investigated the effect of process and system parameters on fibre morphology using various polymer solutions. This study focuses on the effect of the solution concentration, applied voltage, distance between needle tip and collector or collection distance on fibre formation.

2.3. Effect of Solution Concentration

Factors which influence the ability of a polymer solution to produce fibres, the 'spinnability', are essentially the solution concentration and polymer molecular weight. The degree of polymer chain entanglements within the solution is governed by these properties⁸. This study focuses on the effect of the solution concentration, at a constant molecular weight, on the morphology of the fibres.

The factors which govern the morphological transition of bead-only structures to smooth fibres are two critical concentrations; C_i and C_f . Only beads are produced below C_i due to insufficient entanglement of the polymer chains. Fibres begin to appear above C_i . Between C_i and C_f , a combination of fibres and bead of various sizes and morphologies are observed^{15,16,17}.

Below C_i electrospinning occurs with the production of beads or droplets^{8,16}. The solution possesses a dilute regime as the chains are separated and interact mainly with the solvent molecules¹⁸. There are insufficient chain entanglements and no chain overlapping, which is

necessary for the viscoelastic alignment of chains in the charged solution jet to obtain uniform fibres. High concentration of solvent molecules in the solution causes the molecules to congregate to form spherical shapes which appear as beads. The effect of the surface tension of solvent molecules reduces the surface area per unit mass of fluid as solvent molecules contract inwards from the perimeter of the droplet surface forming spherical or bead shaped structures¹⁹.

As the concentration increases above C_i the solution possesses a semi-dilute regime. The chains overlap and entangle with relatively reduced mobility in comparison to the dilute regime¹⁸. Between C_i and C_f chain entanglements are sufficient for fibre forming. With increasing concentration the jet break up is inhibited and production of droplets is minimised. Beads may form on the jet as it travels towards the collector, forming a mixture of beads and fibres¹⁹. Higher amount of solvent molecules cause surface tension to dominate leading to bead formation along the jet and the resultant fibre. At C_f the increased concentration increases chain entanglements. The interactions increase between solvent and polymer molecules as the solution become more viscous. The solvent molecules distribute over the entangled polymer chains under the influence of the charge when the jet is stretched. Increased chain entanglements add an increased resistance to stretching under the electrostatic forces. Therefore, beads are less likely to form as the solvent molecules do not assemble together. Fibres of increased diameters are formed compared to those fibres produced with beaded morphologies^{8,19}.

Above C_f only smooth fibres are electrospun^{15,16,17}. In the highly concentrated solution the mobility of the chains is limited by high level of chain entanglement making the solution

extremely viscous¹⁸. The electrospinning of high viscosity solution is difficult and little fibre forming can be observed. Highly viscous or concentrated solutions prohibit the continuous flow of the solution to the capillary and a constant flow rate is difficult to maintain^{8,20}. Dietzel *et al* (2002) found that spinning poly (ethylene oxide) (PEO) solutions with concentration of 15wt% or above could not develop a sustainable jet. Instead, a thick protrusion of the drop on the tip extends towards the collector in the presence of the electric field and oscillates under its influence until it eventually departs from the tip on to the collector²¹.

In order for the electrospinning process to initiate, the charge applied must be sufficient enough to overcome the surface tension of the solution for the jet to emerge from the droplet on the tip of the capillary¹⁹.

2.3.1. **Morphology**

The morphology of subsequent fibres formed with increasing concentrations changes from beads with no fibres, to beads with developing fibres, then to beaded fibres with varying bead morphologies, then fibres with no beads and globular fibres or macro-beads⁸. Megelski *et al* (2002) found the frequency of beads reduced, and the fibre diameter and bead size increased with increasing concentration. Morphology of the beads also changes from spherical beads to spindle-like features as concentration increases due to the effect of the surface tension decreasing with increasing polymer concentration^{22,23}.

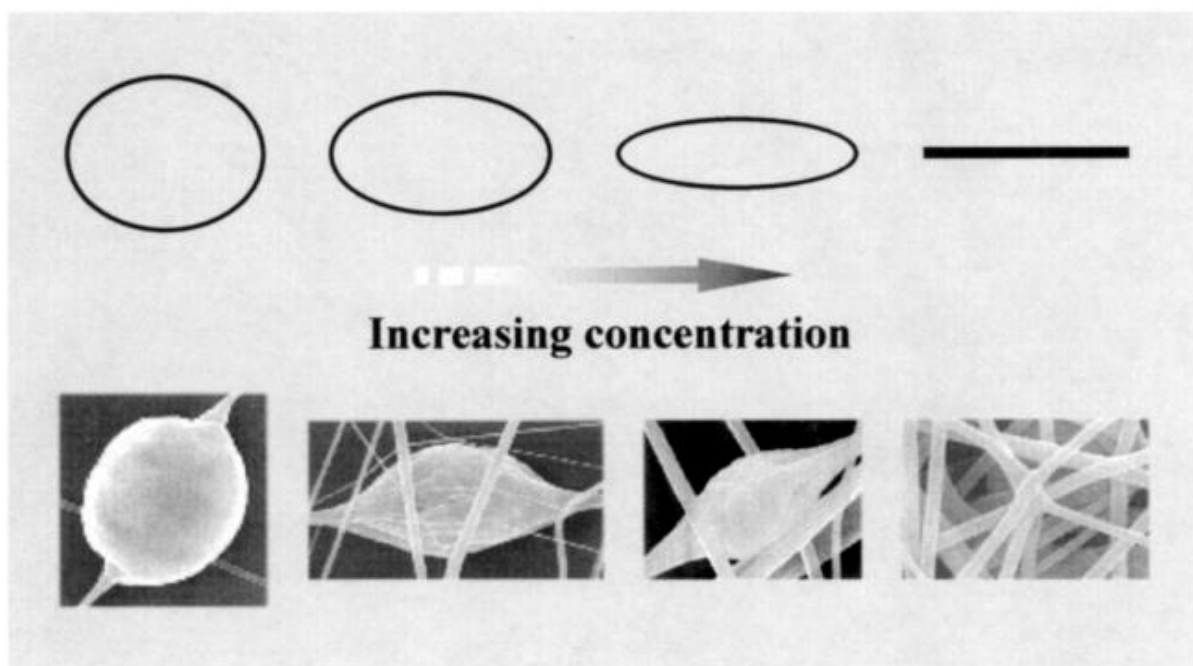


Figure 2. The effect of increasing concentration on bead morphology²⁰.

Formation of beads on fibres is mainly caused by surface tension of the solvent within the solution. Lower surface tension causes a greater number of bead formation which is observed in fibres electrospun from low concentration solutions. The surface tension becomes larger with increasing concentrations which cause fewer beads to form²⁴.

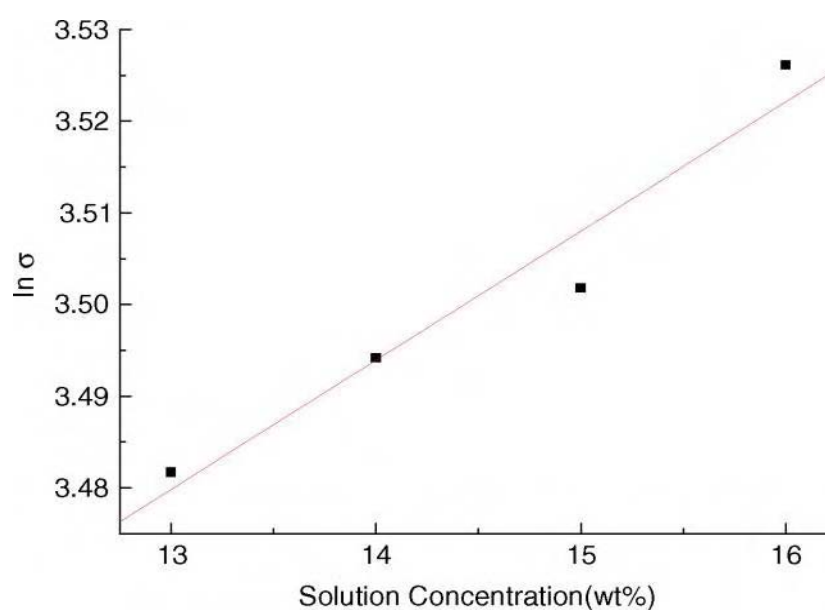


Figure 3. Relationship between solution concentration and surface tension²⁴.

Demir *et al* (2002) found the fibre morphologies changes with concentration. High concentrations polyurethaneurea solutions produced fibres of curly, wavy and straight structures, whereas, with low viscosity thinner beaded fibres were formed¹⁰.

It is common to find beaded morphologies of electrospun fibres whilst electrospinning with low concentration or viscosity solutions. However, the presence of beads reduces the large surface area to volume ratio, which is crucial property of nanoscale fine fibres. Curled structures also have the same effect. Therefore, beaded and curled fibres are undesirable and are considered as defects or 'by-products' on the structure. It is important to allocate parameters which reduce defects during formation on fibres^{10,17}.

2.3.2. **Fibre Diameter**

The solution and charge interaction on the jet determines the fibre diameter distribution of resulting electrospun fibres¹⁹. Demir *et al* (2002) found the fibre diameter increased with increasing concentration. However, fibre distribution was not uniform for high concentration solutions¹⁰.

At a certain viscosity a secondary jet may erupt from the main jet or Taylor cone during the electrospinning, which is able to yield fibres of a narrower diameter¹⁹. Therefore, differential fibre distribution may result producing fibre of varying fibre diameters. Demir *et al* (2002) found that with low viscosity solution of 3.8 wt% multiple jets were ejected from the drop on the capillary tip in the presence of high electrical fields. More viscous solutions can reduce the eruption of secondary jets forming fibres of larger diameters. At 12.8 wt% only one jet emerged from the drop on the tip¹⁰.

A smaller deposition area is observed of electrospun fibres by increasing the concentration. The onset of the jet instability occurs at a further distance from the capillary tip. The viscoelastic force is sufficient enough to withstand the electrical bending instability to allow the jet to leave the needle tip and travel for a longer distance in a straight path before bending instability initiates¹⁵. The projection of the jet in this manner reduces the jet path and the resultant bending instability of the jet deposits over a smaller region. The fibres collected from these regions have large diameters as they have undergone less stretching from the reduced jet path¹⁹.

Dietzel *et al* (2001) found at low PEO concentrations the fibre diameter distribution varied. The research found undulating variations in the fibre diameter along a single fibre of low concentration solutions. At higher concentrations the fibre diameter was relatively larger and more uniform²¹. Zhong *et al* (2002) found with PDLA solutions the average bead diameter and the distance between the beads increased with concentration²³.

Gomes *et al* (2007) show higher concentration solutions produce larger average fibre diameter, in comparison to lower concentration solutions which produced smaller average fibre diameter, when the same voltage is applied. Therefore, the fibre diameter increases with solution concentration⁵.

2.4. Applied Voltage

In the presence of no external electrical field an ionic polymer solution has equal number of positive and negative ions present within each volume unit. Applying the voltage causes the ions to accumulate under attractive and repulsive forces. The ions are attracted by and

migrate towards their oppositely charged electrodes, hence, positive ions move to the negative electrode and negative to the positive electrode¹⁹. The difference between the positive and negative ions in specific region is called the charge. The charge establishes an electrical field which extends over large distances⁹.

The electric field begins from the capillary tip, which is the point electrode, where the solution drop is suspended, and follows to the oppositely charged electrode, the collector. The electrospinning solution follows the vector path of the electric field. The fibres deposit on the centre and surrounding regions of the collector²⁵.

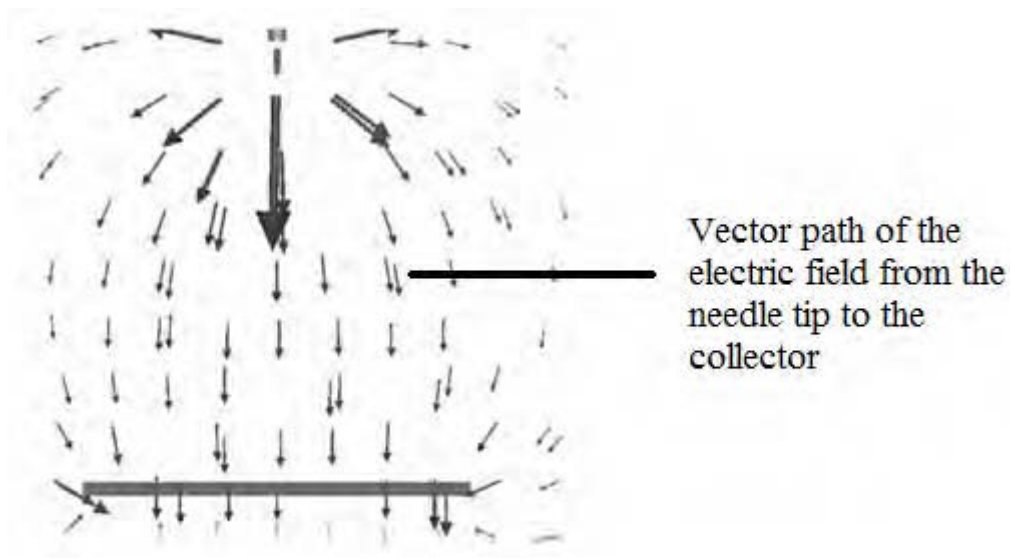


Figure 4. The above image is of the electric field generated during electrospinning²⁵.

Applying an increasing voltage, to the solution drop on the tip of the capillary induces charge on the solution surface and ions migrate on the surface of the drop, distorting its shape into a Taylor cone. When the voltage applied is high enough to overcome the surface tension of the solution, a stable solution jet is ejected from the surface of the drop to

transport the excess ions, which migrate to the surface, towards the collector. Increasing the voltage increases the charge on the drop and jet^{9,21}.

In the presence of the applied voltage and the resulting external electrical field, several forces act on the jet during its flight towards the target. Forces acting on the jet include the electrostatic force, the viscoelastic force, the columbic force and the surface tension. The columbic repulsive forces repel charged carriers within regions of the viscoelastic jet which cause further elongation during the flight. The electrostatic forces transport the charges from the capillary tip as the jet stretches towards the collector. The viscoelastic forces and surface tension resist stretching of the charged jet. The actions of surface tension, Columbic and viscoelastic forces have a significant effect on the morphology of the fibres produced²⁶. The applied voltage induces and maintains charges within the solution and the action of repulsive forces between the ions deforms the viscoelastic solution to maintain the continuity of the Taylor cone and jet²⁷. The charged jet travels towards the collector in the electrical field in order to complete the circuit¹².

The surface tension determines the initiating voltage for electrospinning⁶. A highly viscous or high concentration solution requires a high application of voltage to overcome its surface tension to initiate electrospinning^{11,28,29}. The solution drop at the needle tip is distorted to form the Taylor cone from which a jet is ejected to initiate electrospinning on the application of a negative or positive voltage greater than 5kV⁶. Doshi *et al* (1995) investigated the voltage values needed in order to initiate the jet from the Taylor cone. Jet initiation for PEO solutions of various concentrations were above 8kV. The voltage values

for the onset of the jet increased with increasing concentration. However, above and below critical concentrations a jet is not attainable due to solution properties¹¹.

As the applied voltage is increased the electric field strength increases. The amount of repulsive charge increases and jet acceleration increases towards the collector. Increased acceleration draws more solution from the needle tip, leaving the Taylor cone less stable¹⁴. The unstable oscillating Taylor cone causes beaded fibres to form. Further increasing the voltage increases the jet velocity, causing the solution to be drawn out quicker than the rate at which the needle obtains the solution from its source. Consequently, the Taylor cone recedes into the tip continuing electrospinning directly from inside the capillary tip^{19,23}. The acceleration of the jet causes it to stretch which thins the diameter²⁸. The increased draw stress on the solution from the needle tip, due to increased voltage application can also lead to deposition of more fibres on the collector²⁹.

In order to yield fibres of a reduced diameter a higher voltage is applied to the solution. This leads to increased stretching of the jet from the effect of higher electrostatic forces induced by the charges and higher repulsive forces within segments of the jet^{30,31}. Voltage affects the feedrate, jet acceleration, jet and fibre morphology, fibre diameter size and the electric field strength³².

2.4.1. Morphology

Application of increasing voltage was found to change the morphology from smooth to highly beaded fibres. Instability of the jet arises from applying the high voltage which causes the Taylor cone to recede into the needle from the tip and electrospinning continues from

within the needle, which may cause bead formation^{19,28}. Dietzel *et al* (2001) found smooth fibres to form at low voltage application and highly beaded fibres at a higher voltage. Increasing the voltage decreases the solution volume of the Taylor cone until the jet recedes into the needle tip. The jet continues from the edge of the tip indicating it continues from solution in contact on the inside wall of the needle. Beaded fibres begin to form and bead density increases²¹. Beads change from spindle-like to spherical like morphology²³.

Gomes *et al* (2007) found with low concentration of polyacrylonitrile (PAN) solutions the bead density, average fibre diameter and the frequency of fibres deposited increased with increasing voltage. Beaded fibres possessed numerous beads with short and thin fibres⁵. Demir *et al* (2002) found that lowering the electric field strength decreased bead density¹⁰.

Doshi *et al* (1995) found that by small increases in voltage changed the deposition of fibres from a random orientation to straight alignments. Majority of the fibres formed were of a circular cross section with electrospun coils, loops and beads¹¹. Megelski *et al* (2002) found the fibres formed were twisted with ribbon-shaped morphologies²².

Samatham and Kim (2006) investigated the effect of the electric current on the diameter and morphologies of electrospun PAN solution fibres. Four different jet regimes were obtained from varying the electric current which consisted of a fluctuating jet, a stable jet, a stable jet with intermittent collection of polymer drops and multiple jets. The fluctuating jet was obtained with application of a high electric field. At a lower electric field the stable jet is formed yielding smooth fibres. The droplets also formed with the stable jet. The drop grew large on the tip and fell on the collector. The beads formed on the fibres were

spherical due to the presence of lower electric forces. Multiple jets formed directly from the drop on tip. The higher voltage application increases the electric field strength which induces more charges in the solution allowing more jets to emerge. Beaded fibres were obtained with elongated beads stretched by the electrostatic forces³³.

2.4.2. Fibre Diameter

During the flight of the solution jet, it undergoes bending instability and deforms plastically, under the influence of the electric field by the repulsive forces. The viscoelastic jet reduces the instability by stretching. The jet elongates as it spirals and loops and thins the jet diameter³⁴. The instability allows the jet to elongate greatly within the space of a small distance³⁵. Megelski *et al* (2002) and Sukigara *et al* (2004) found the fibre size to decrease with increasing voltage, whilst all other variables remained constant^{22,36}.

Demir *et al* (2002) found the jet diameter increases with increasing voltage. Multiple jets emerged in the presence of high electric fields with low viscosity solutions. The jets rotated in a clockwise direction from the tip to collector as fibres deposited. The flowing charges on the surface of the fibres collected causing the fibres to repel each other and disperse over a larger area¹⁰. Multiple electrospinning jets resulted in larger collection regions on the collector^{10,21}.

Applying an even higher voltage can form fibres with larger diameters as beads on fibres merge together^{19,37}. Alternatively, the increased removal of solution mass from the capillary can form larger fibres³⁰. Increased solution removal also results in a higher deposition rate³⁸.

Baumgarten's (1971) work on electrostatic spinning of acrylic fibres found the diameter did not decrease monotonically with increasing electric field strength, but rather a minimum diameter size was reached after increasing the electric field. However, with further increase of the electric field the fibre diameter increased rather than further decreasing³⁹. It has been suggested that a high voltage application may have a significant effect on fibre diameter by producing either large or small diameter fibres³².

2.5. Effect of Collection Distance

The distance between the needle tip and collector is the collection distance. The collection distance has influence on the jet flight time and the electric field strength on the resultant fibres²⁸.

Shortening the collection distance decreases the jets flight time and solvent evaporation time. The field strength increases due to the shorter distance which has the same effect on electrospinning if the voltage were increased^{19,21,23}.

The electric field strength is increased with reduced collection distance, which causes instability of the Taylor cone and jet initiation. Kong *et al* (2007) found that increasing the collection distance led to a greater amount of jet ejection and solution removal, causing the Taylor cone to retract into the tip and continuing the jet ejection from the edge of the capillary tip. The jet ejected to produce two separate electrospun fibre webs. Increasing the collection distance resulted in reduced electric field strength which stabilised the Taylor cone producing a single jet²⁵.

2.5.1. Morphology

Buchko *et al* (1991) found that reduced collection distance reduced the flight time of the jet which is needed for solvent evaporation. As a result the fibres collected were flat instead of cylindrical and the spherical bead structures instead were flat and coin-shaped²⁹. Fibres collected on the target contained excessive amounts of solvent causing fibres to merge together when they come into contact. The resulting interconnected fibre mesh or web is formed from bonding of these fused fibres²⁹.

Several studies have found that fibres also have the tendency to form beads at shorter collection distances. Dietzel *et al* (2002) and Megelski *et al* (2002) found that decreasing the collection distance induced the formation of beaded fibres^{21,22}. Demir *et al* (2002) and Patra *et al* (2009) found increasing the collection distance decreased the bead density^{10,31}. Equally, Lee *et al* (2003) found the bead diameters increased with increasing collection distance²⁰. Increased collection distance weakens the electrical field at a constant voltage reducing the drawing stress and jet acceleration, therefore, increasing the bead diameters²⁰.

The high field strength as a result of a shorter distance can be the cause of bead formation and enhance bead density on fibres^{19,21,23,28}. However, bead density reduces with increasing collection distance and the bead morphology changes from spherical to spindle-like³². Bead formation can be decreased if the given distance provides optimal field strength to allow sufficient elongation of the jet^{19,26}.

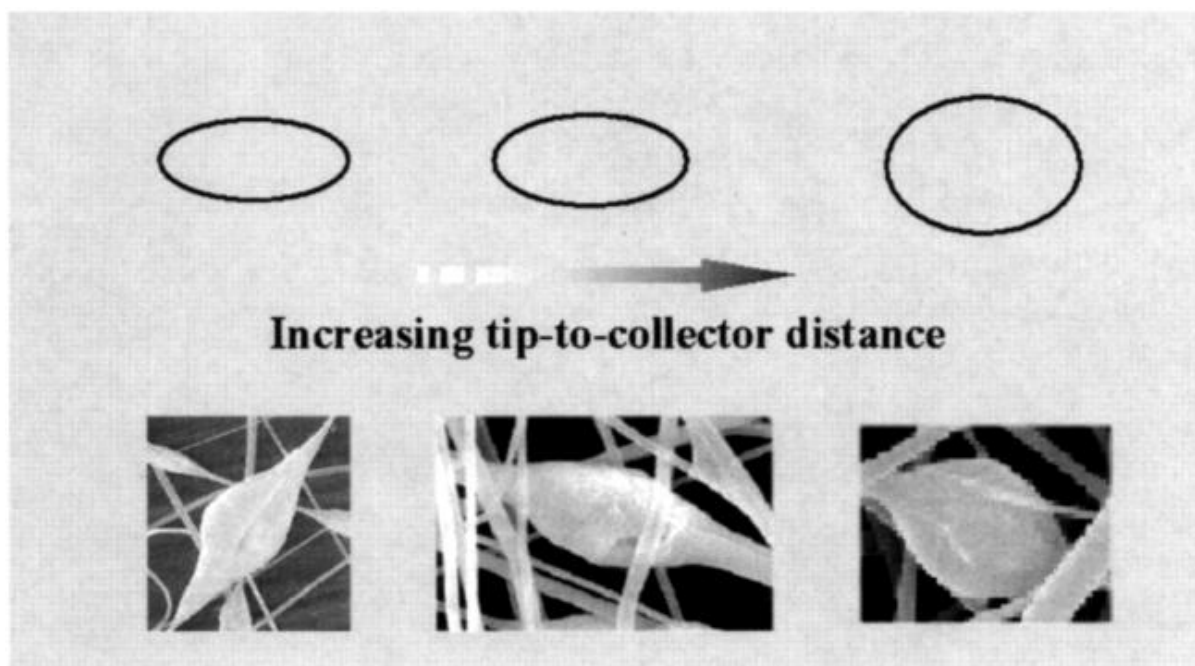


Figure 5. Change in morphology of the beads on the fibres with increasing collection distance²⁰.

2.5.2. Fibre Diameter

The fibre diameter may decrease with increasing collection distance as more time is given for solvent evaporation which further thins and splits the jet producing finer fibres^{7,40}. Li *et al* (2006) found that increasing the collection distance from 10cm to 15cm significantly reduces the fibre diameter⁴¹. Yördem *et al* (2008) and Ayutsede *et al* (2005) found increasing the distance resulted with fibres of lower average diameter^{42,43}. Homayoni *et al* (2009) found that longer collection distances also improved quality of the fibres²⁸.

Conversely, studies have shown that increasing the collection distance can lead to increased fibre diameter. Lee *et al* (2004) suggest the electric field strength is weaker due to the longer distance and affects the jet by reducing its stretching resulting in fibres with larger diameters¹³. However, Zhao *et al* (2004) found too large distances resulted in no fibres

reaching the collector⁴⁴. On the other hand, Yuan *et al* (2004) found that decreasing the collection distance increased the average fibre diameter due to insufficient time for solvent evaporation⁴⁰.

Depending on the distance there is a certain optimal value for the electrostatic field at which fine fibres can be produced. Below the value, the diameter of fibre increases as weaker electric field causes the jet stretching to decrease¹⁹.

Studies show that decreasing the collection distance has similar effect to that of increasing the voltage^{28,39,45}. Reducing the collection distance, increases electric field strength increasing jet acceleration and elongation, yielding finer fibres. The fibres may be wet on reaching the collector due to insufficient solvent evaporation and fibres collected may not be uniform. Increasing the collection distance, weakens the electric field strength, which can also yield non-uniform fibres. The increased distance yields drier fibres which may also be due to the ambient humidity factor as well as increased flight time for solvent evaporation³².

2.6. Application of Electrospun Fibres in Tissue Engineering

The application of nanotechnology in biomedical applications establishes the field of nanomedicine. Nanomedicine aims to produce biomimetic structures, with simple fabrication methods, to be utilised for tissue engineering⁴⁶.

Tissue engineering is utilised for the repair, replacement or restoration of diseased or damaged tissue caused by congenital defects or injury with the use of manufactured

biocompatible scaffolds combined with human cell systems or cell responsive biomolecules³. The scaffold material must be biocompatible to induce the desired cell response in the body which is determined by the architecture and surface topography of the engineered scaffolds, and its physical and chemical properties⁴⁷. The material should be manipulated to achieve the desired structure for a specific tissue replacement³.

The process of electrospinning allows manipulation of parameters to attain optimal conditions and achieve the desired scaffold architecture according to specific tissue structures⁴⁸. For example, aligned fibrous structures are used to control cell orientation³. Randomly orientated fibres produce internally porous structures needed for cell habitation and migration⁴⁷.

Polymers are the best-suited scaffold material for a three-dimensional template. They possess the capability to promote cell adhesion and maintain function of differentiated cells without hindrance to proliferation which are essential properties of scaffold material⁴⁹. Nanostructures produced have the high surface area to volume ratio and are highly porous providing adequate properties to allow cells to maintain function and viability³.

Polymers chosen for tissue scaffolding include natural and synthetic, as well as hybrid materials⁵⁰. Hybrid materials are a blend of different materials which achieve desired mechanical and structural properties, such as, improved electrospinnability, mechanical stability, increased porosity, reduced mass and more chemical reactivity may be obtained on nanoscale^{3,46,48}. Synthetic biopolymers include poly (lactic acid) (PLA), polycaprolactone (PCL) and poly (glycolide) which have been extensively investigated as tissue scaffolding⁵¹.

This study investigates electrospinning using poly (vinyl alcohol) (PVA). It is a water-soluble, biocompatible and biodegradable polymer. It is non-toxic because degrades into water and carbon dioxide^{52,53, 54}. It is also relatively better at fibre forming than other polymers^{52,55}.

2.7. **Poly (vinyl alcohol)**

The rheological properties of PVA solutions can vary with molecular weight, polymer concentration, ambient temperatures and DH⁵⁵. The viscosity of the PVA solutions is primarily dependent on the molecular weight and concentration, with an increase in viscosity observed with increase in polymer concentration.

3. METHODS AND MATERIALS

3.1. Preparation of PVA Solutions

Polyvinyl alcohol (degree of hydrolysis $\geq 98\%$) with a molecular weight of 72,000 Da was obtained from the company Merck, Germany, and was used as received. All PVA solutions were made using distilled water as the solvent. The distilled water was heated to 90°C before adding the measured mass of PVA powder. The mixture was stirred in a closed container moderately for 2 hours and left to cool to room temperature before use for electrospinning. The solutions prepared consisted of wet weight percentage (wt%) concentrations of 4wt%, 6wt% and 8wt% PVA.

3.2. Electrospinning Preparation

The electrospinning apparatus, ES1a, was made by and purchased from the company Electrospinz Limited, New Zealand. The machine components consist of the electrospinning platform and control box, which is the power supply for electrospinning, connected to the platform and the electrical socket. The electrospinning platform consisted of the glass header or solution tank, connected to a silicon rubber hose (30cm length), which connected to the constant head system. The needle (Axygen Scientific, yellow T-200-Y pipette tips, 200 microlitres in volume) was made of high density polypropylene with the internal diameter of 0.61mm and external diameter of 0.84mm measured in micrometers. The needle was fixed on to the head system and aiming linearly towards the collector or target plane (300x350x10mm polyethylene). A shield casing was made from periplex glass that contained the electrospinning platform to prevent fibres escaping into the surroundings and for protection from the fibres during electrospinning. A black card was placed on far side of the casing adjacent to the collector screen, as it was easier to observe the needle tip, Taylor

cone and its jet, and to detect fibres. A stable Taylor cone was maintained by adjusting the height of the solution tank, which controlled the flow rate of the solution to the needle tip. A 30cm metal ruler was aligned parallel to the rod on which the tank was fixated behind on the shield casing, to measure the height of the tank when adjustments were made to the flow rate. Height measurements started at 0cm from the base of the rod and increasing vertically. Measurements were taken using the top edge of the tank being level with the measurement on the ruler.

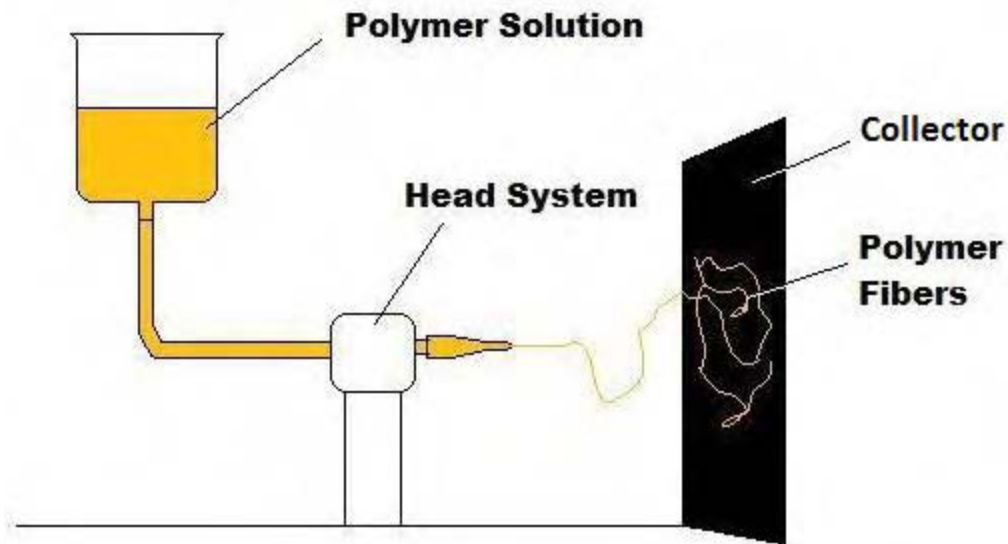


Figure 6. Electrospinning setup for ES1a.

Before the start of each experiment 4-5ml of the solution, that was to undergo electrospinning, was run through the head system, without the application of the voltage. This reduced solution friction allowing adequate flow of the solution through the electrospinning system and eliminate any air bubbles present within the solution in the head system, needle or at the needle tip. Solution running out from the needle was collected by a small container placed on the electrospinning platform beneath the needle

tip. Excess large drops hanging from the tip were carefully soaked up but residue solution was not wiped off the needle or its tip as this aided electrospinning. For each experiment 20ml of the solution was poured into the tank and covered with parafilm, which was loosened by stretching the film to prevent the effect of suction of solution back into the tank from the hose. Covering the solution tank also reduced the evaporation of the solvent which can change the viscosity of the solution. The tank height was adjusted to allow a small droplet of solution to protrude from the needle tip. Aluminium foil was the collector used to deposit fibres. A rectangle sheet covered the central region of the collector screen in line with the needle.

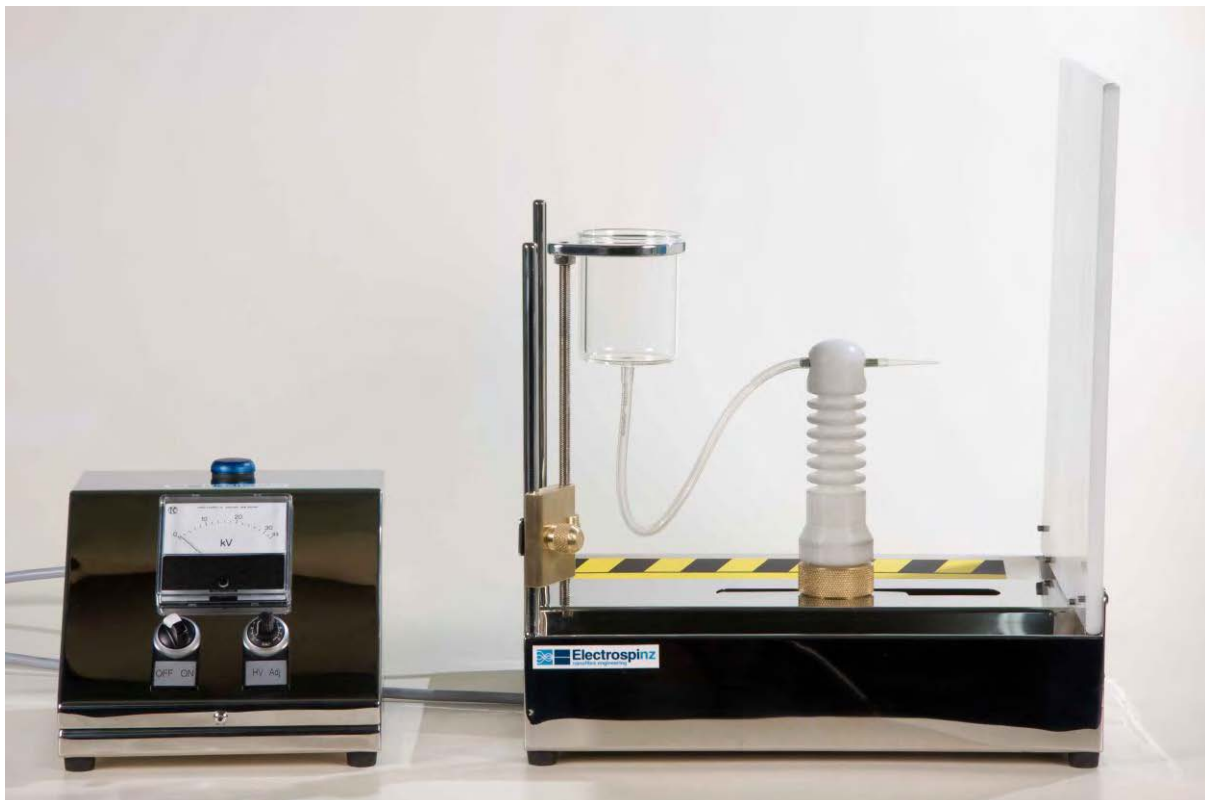


Figure 7. *Electrospinning Apparatus encased in periplex glass box. (Appendix IX)*

3.3. Electrospinning Parameters

The parameters manipulated consisted of the voltage and the collection distance (CD). The voltages applied were 12kV and 20kV, and the distance values were 10cm and 15cm for each concentration of PVA solution. Additional parameters investigated for 4% PVA solution were the collection distance of 7cm and voltage of 8kV. For 6% PVA, additional parameters included a collection distance of 7cm and 18kV voltage in combination with the standard parameters mentioned previously. Each experiment was conducted for 1 hour.

The height of the tank was adjusted accordingly to obtain an adequate flow rate which formed a Taylor cone ejecting a jet. Flow rate was manipulated to minimise the formation of droplets and spraying of the solution during electrospinning. The fibres were subsequently left to dry for 24 hours.

3.4. Measurement and Characterisation

The deposition rate was measured as the change in average mass of fibres deposited on the collector. The mass output of electrospinning for each solution at the given parameters was measured by weighing the mass of the Al foil before and after the electrospinning. For a more accurate measure 3 samples of 2cm² were cut carefully from the Al foil using a metal blade in a successive vertical order, in the central region of heavy deposition of fibres. The measures were taken for each experiment. The samples of the Al foil were weighed individually to give an average mass value of a single 2cm² sample. The samples were weighed using an analytical balance measuring to 0.00001g, giving the mass of electrospun material and the collector. The average mass of the collector was obtained and this value

was subtracted from the sample value to give mass of the electrospun output. The deposition rate and area were analysed^{56,57,58}.

The fibres obtained from the electrospinning process were analysed using the Philips Environmental Scanning Electron Microscope (ESEM) XL-30. The fibres analysed were collected from the region of the collector linear to the needle tip. The samples were platinum coated for 1minute and the nanofibres were observed under the microscope. The average fibre diameter, bead size including bead width perpendicular to the fibre axis, and bead length in line with the fibre axis were measured using Paintshop Pro V.9⁵⁹. A total of 4 experiments were carried out for each variable parameter. For each experiment, 73-90 fibre diameters were measured. For PVA 4% and PVA 6%, 1-7 beads were measured to obtain the average bead size. Fibre diameter distribution and fibre morphology were also analysed using Paintshop Pro V.9 from images obtained by the ESEM.

4. RESULTS

4.1. Solution Concentration

4.1.1. Effect of Increasing Concentration on Fibre Diameter and Morphology

Morphology of electrospun fibres of PVA 4%, 6% and 8% solutions were observed with ESEM images. The changes observed in fibre morphology with increasing solution concentration are shown below in Figure 8, 10, 12 and 14. Solutions of 4%, 6% and 8% concentrations were electrospun at given parameters and the resulting average, maximum and minimum fibre diameter obtained are displayed in the graphs below in Figures 9, 11, 13 and 15.

Effect of Increasing Concentration using Parameters of 10cm Collection Distance and 12kV on Fibre Diameter and Morphology

Figure 8 shows the morphology consisting of beaded fibres at PVA 4% with large spherical beads linked together by thin cylindrical fibres. With PVA 6% the bead sizes are considerably smaller with greater density of fibres intercepting the beads. Bead morphology varies between spherical and spindle-like. No beads are observed with PVA 8%, the fibres appear smooth but the morphology may vary between cylindrical and flat ribbon fibres. Figure 9 shows the average fibre diameter increases with increasing concentration of PVA solution.

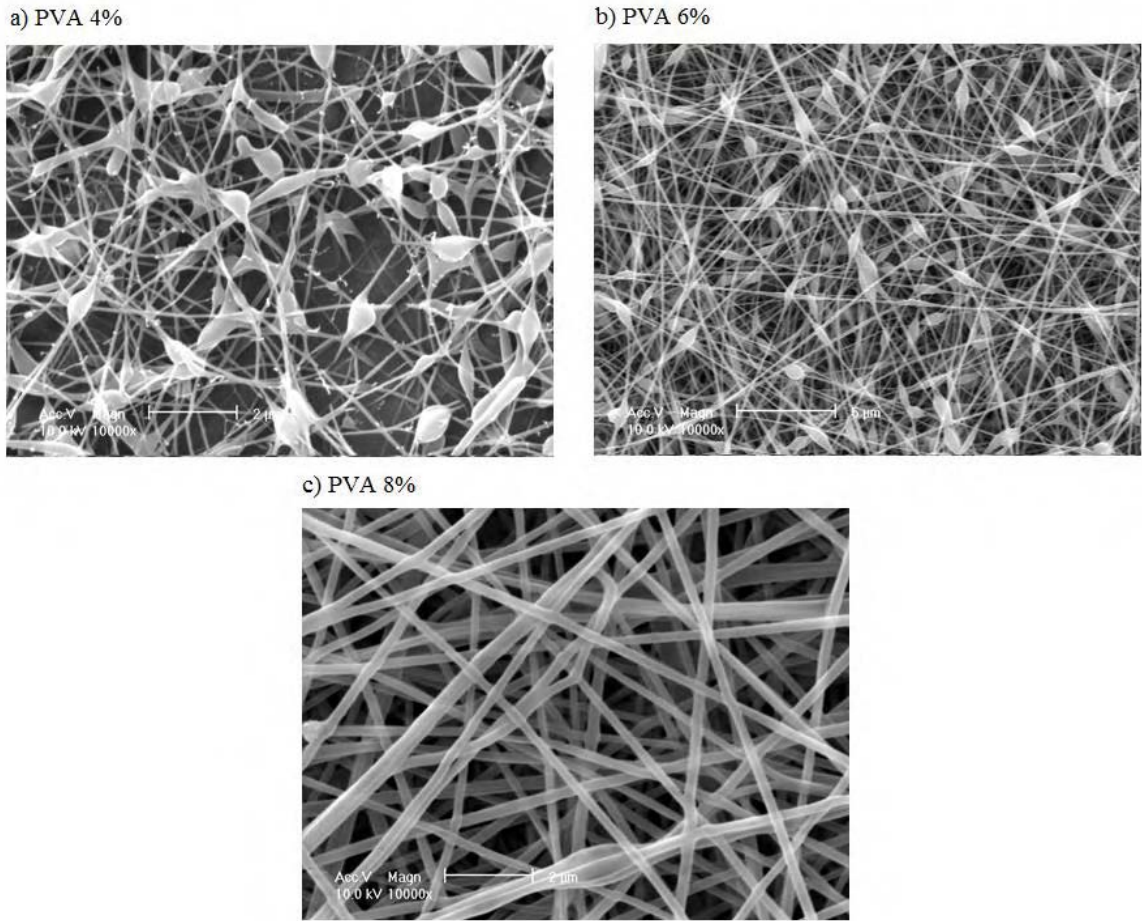


Figure 8. SEM images at different concentrations, a) PVA 4%, b) PVA 6% and c) PVA 8%

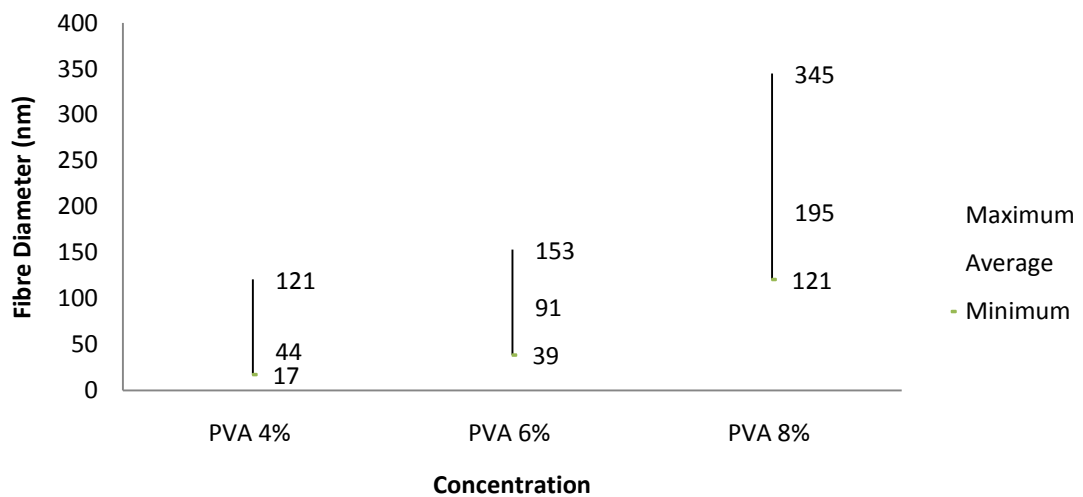
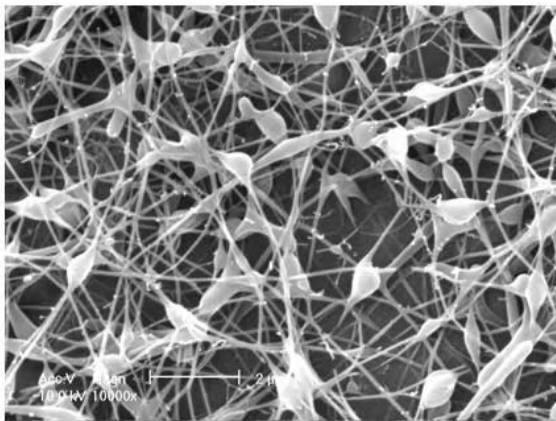


Figure 9. Overall Average, Maximum and Minimum Fibre Diameter at 10cm Collection Distance and 12kV with Increasing PVA Concentration

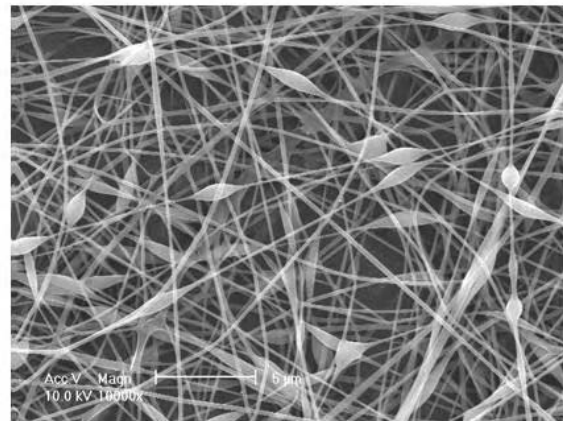
Effect of Increasing Concentration using Parameters of 10cm Collection Distance and 20kV on Fibre Diameter and Morphology

A much larger diameter range is observed with PVA 6% and PVA 8% compared to PVA 4%, as shown in Figure 10. Similar average fibre diameters are obtained at PVA 6% and PVA 8% ranging between 120-150nm. PVA 4% yielded the smallest diameter of 48nm (Figure 11). Beaded fibres formed with large spherical beads at PVA 4%. The beads reduce in size and density and attain spindle-shaped morphologies at PVA 6%. Conglutination occurs as fibres are collected with PVA 8%. Fibres merge together to form webs and small regions of solidified solution (Figure 10c). The results show the average fibre diameter increases with increasing concentration shown in Figure 11.

a) PVA 4%



b) PVA 6%



c) PVA 8%

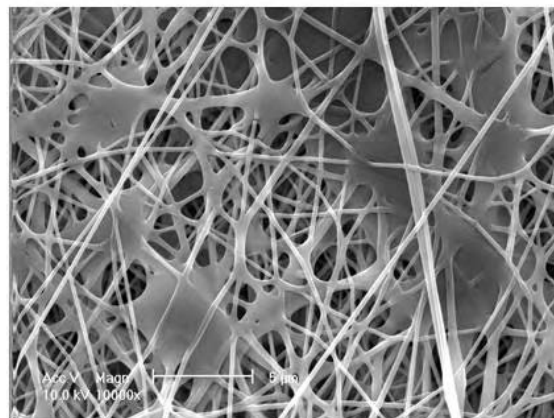


Figure 10. SEM images at different concentrations, a) PVA 4%, b) PVA 6% and c) PVA 8%

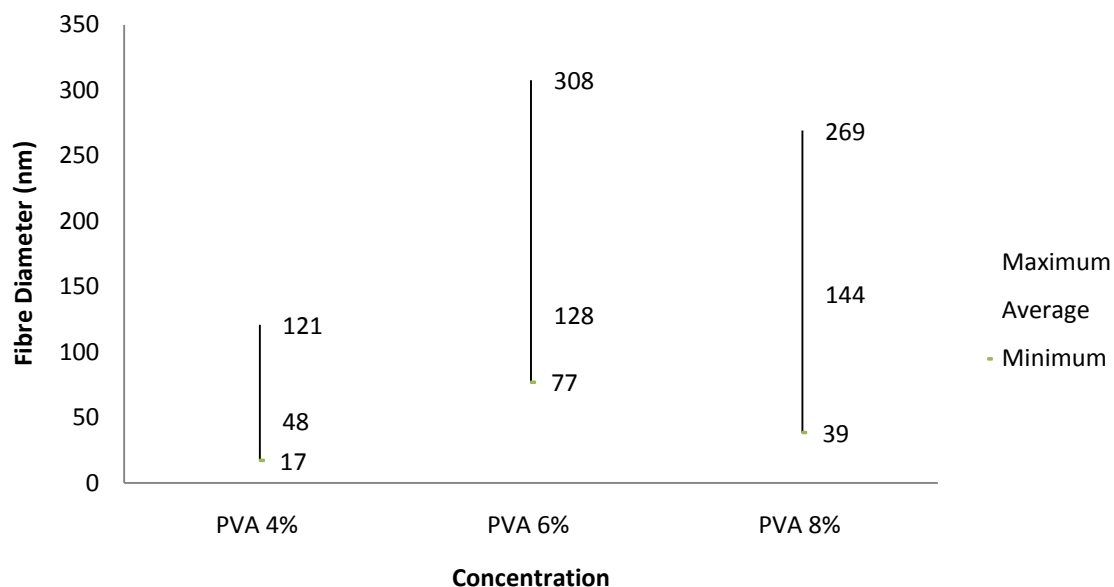


Figure 11. Overall Average, Maximum and Minimum Fibre Diameter at 10cm Collection Distance and 20kV with Increasing Concentration

Effect of Increasing Concentration using Parameters of 15cm Collection Distance and 12kV on Fibre Diameter and Morphology

Figure 12 shows fibres formed at PVA 4% possess a mixture of spindle shaped and elongated beads linked to fibres. With PVA 6% only a few beaded fibres are visible and PVA 8% formed only smooth fibres. Figure 13 shows the average fibre diameter increases with increasing concentration. PVA 4% and 6% possess average diameters below 80nm and PVA 8% in comparison possesses more than double the diameter size with 204nm.

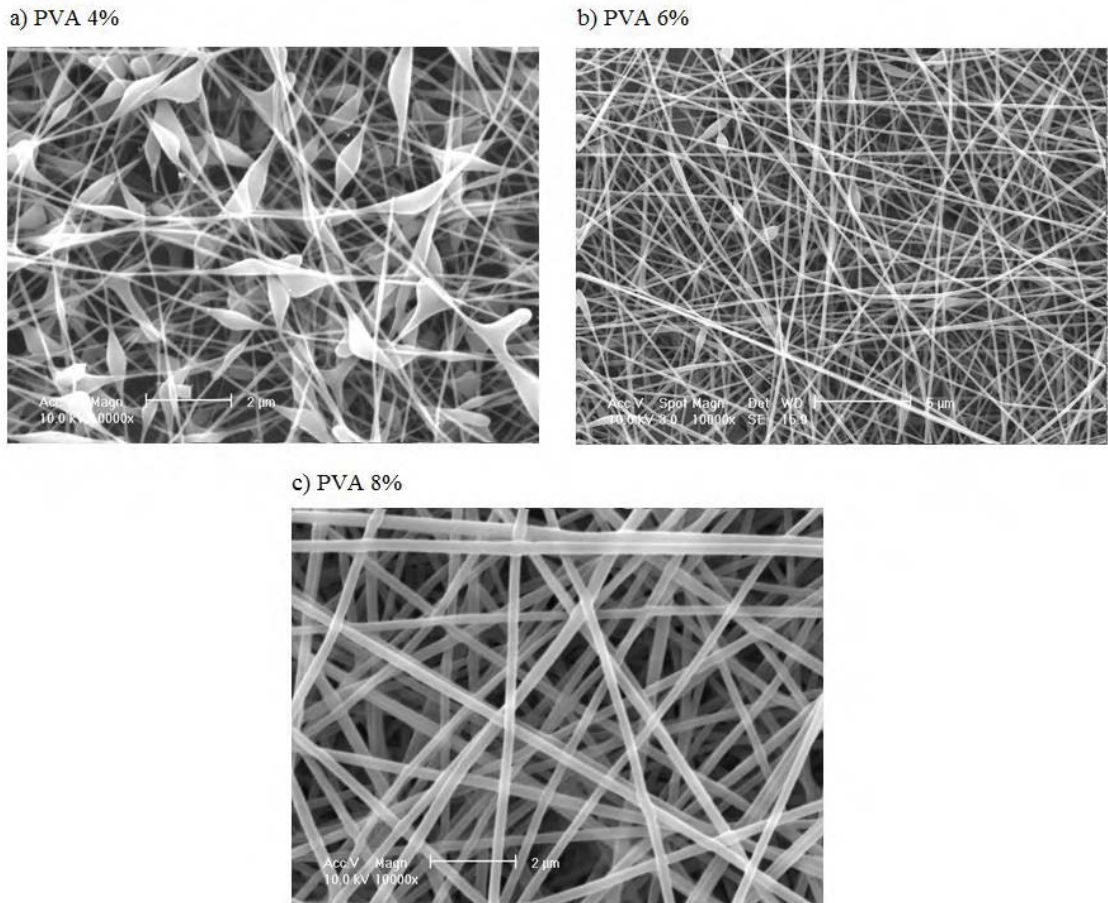


Figure 12. SEM images at different concentrations, a)PVA 4%, b) PVA 6% and c) PVA 8%.

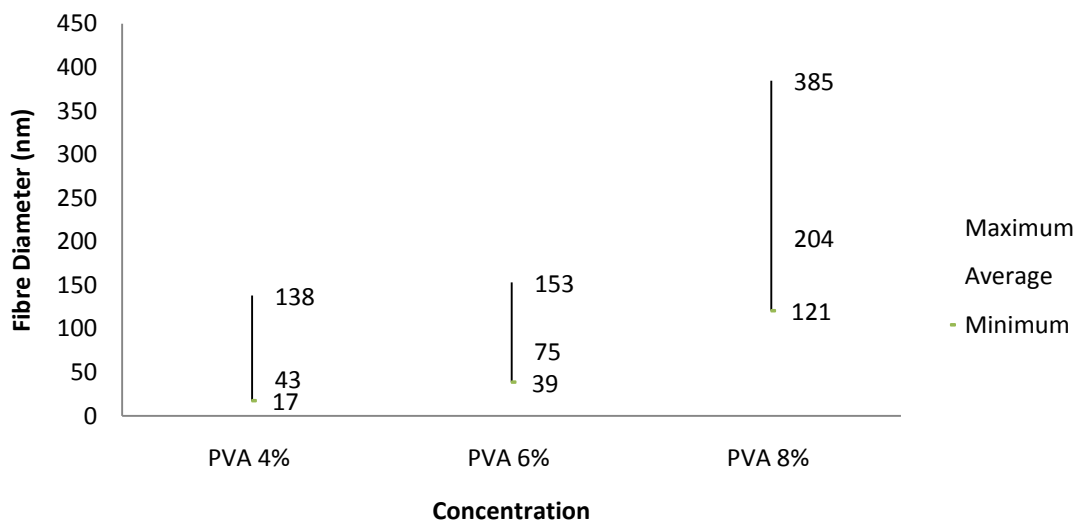
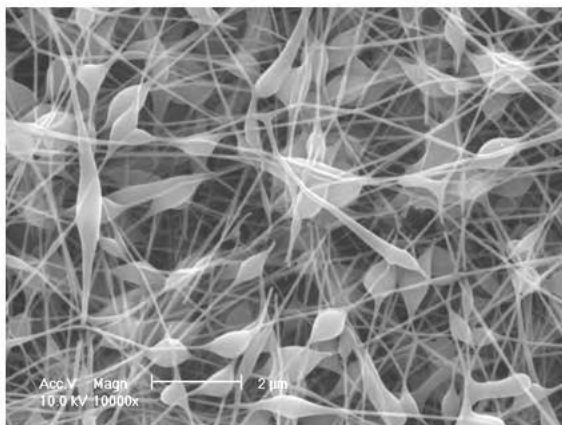


Figure 13. Overall Average, Maximum and Minimum Fibre Diameter at 15cm Collection Distance and 12kV with Increasing Concentration.

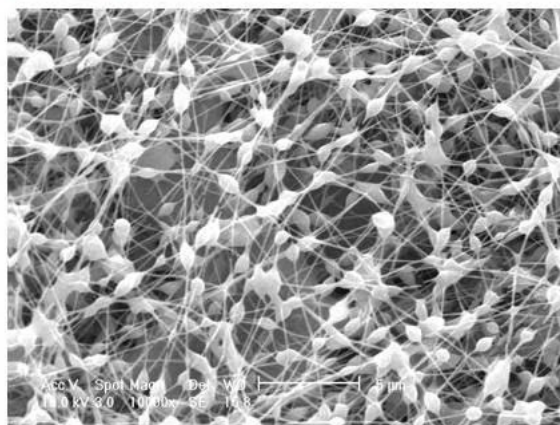
Effect of Increasing Concentration using Parameters of 15cm Collection Distance and 20kV
on Fibre Diameter and Morphology

Figure 14 shows a mixture of spindle shaped and elongated beads linked to thin fibres with PVA 4%. With PVA 6% a higher density of smaller sized beads were formed. PVA 8% only smooth fibres with some that merge together to form a single large fibre and flat ribbon fibres were observed. Figure 15 shows the average fibre diameter increases with concentration. The average diameters are below 80nm for PVA 4% and 6%. In comparison, PVA 8% produced fibres with diameters more than double the size of PVA 4% and PVA 6%.

a) PVA 4%



b) PVA 6%



c) PVA 8%

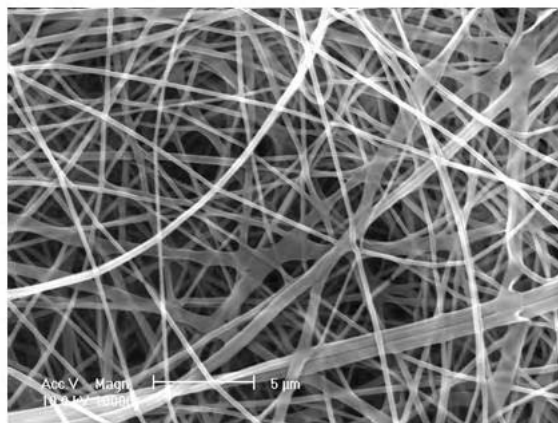


Figure 14. SEM images at different concentrations, a) PVA 4%, b) PVA 6% and c) PVA 8%.

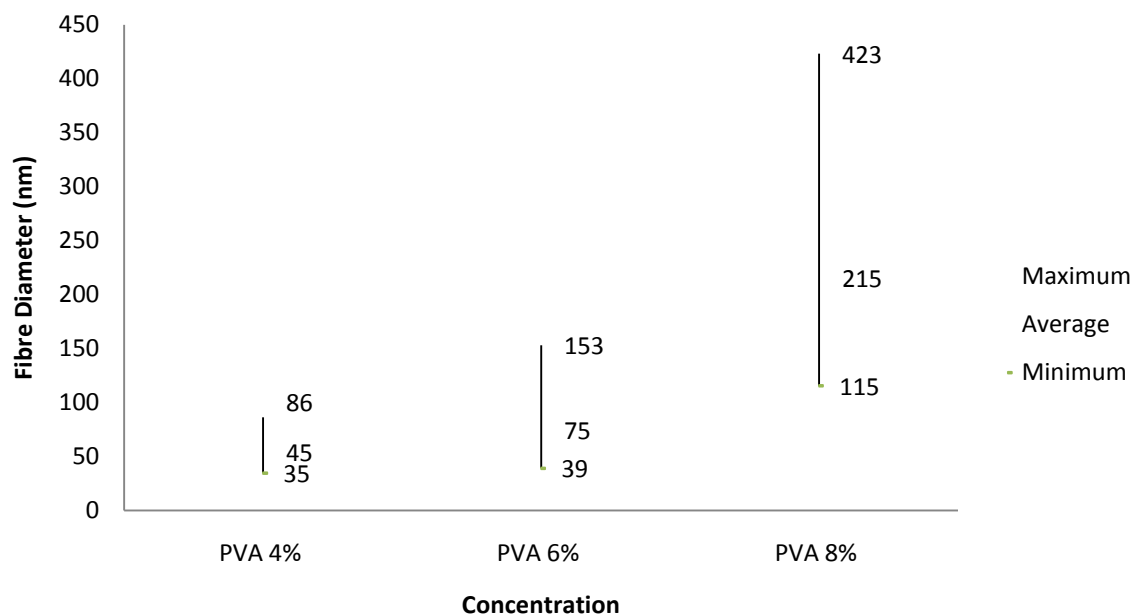


Figure 15. Overall Average, Maximum and Minimum Fibre Diameter at 15cm Collection Distance and 20kV with Increasing Concentration.

4.1.2. Effect of Increasing Concentration Fibre Diameter Distribution

Effect of Increasing Concentration at Parameters of 10cm Collection Distance and 12kV on Fibre Distribution

Figure 16 to 18 show the fibre diameter distribution for PVA 4%, 6% and 8% at the given parameters of 10cm collection distance and 12kV. Fibre diameter distribution increases with increasing concentration. Figure 16 shows the distribution of fibres at PVA 4% were relatively narrow with the fibre diameters below 130nm. The diameter of fibres ranged from 17–121nm. Figure 17 shows the fibre diameter distribution for PVA 6% which is slightly larger than PVA 4%. Fibres with distinct diameters were obtained. The diameter of fibres ranged from 39–192nm. Figure 18 shows the fibre diameter distribution of PVA 8% which had the largest diameter distribution. The diameter of fibres ranged from 121-345nm.

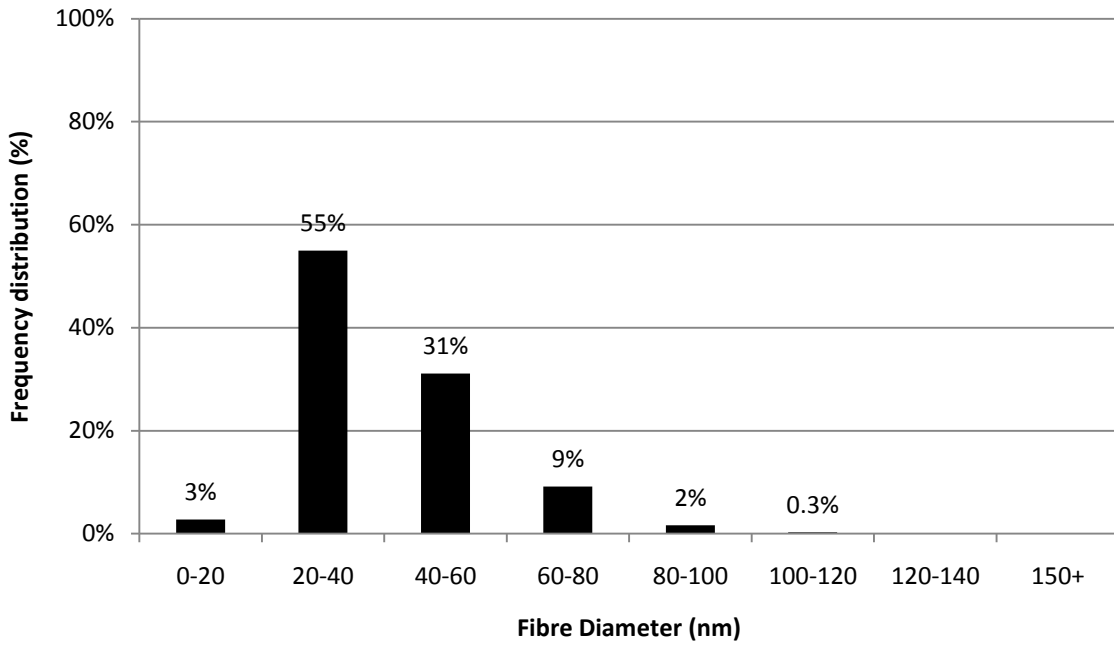


Figure 16. Total Percentage of Fibre Diameter Distribution of PVA 4% Solution at 10cm Collection Distance and 12kV.

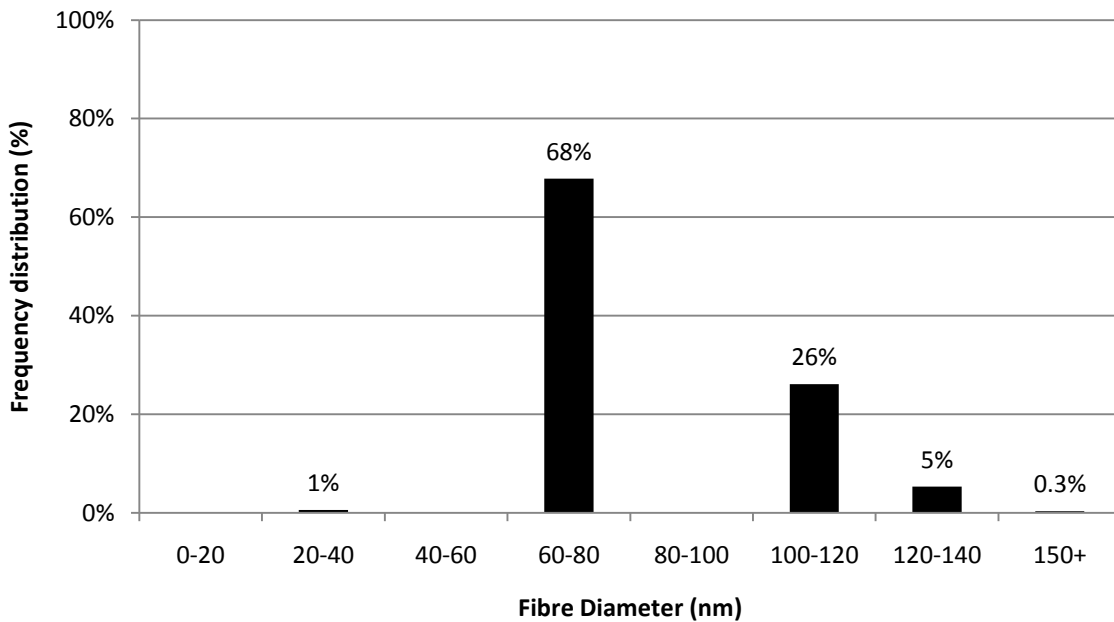


Figure 17. Overall Percentage of Fibre Diameter Distribution of PVA 6% Solution at 10cm Collection Distance and 12kV.

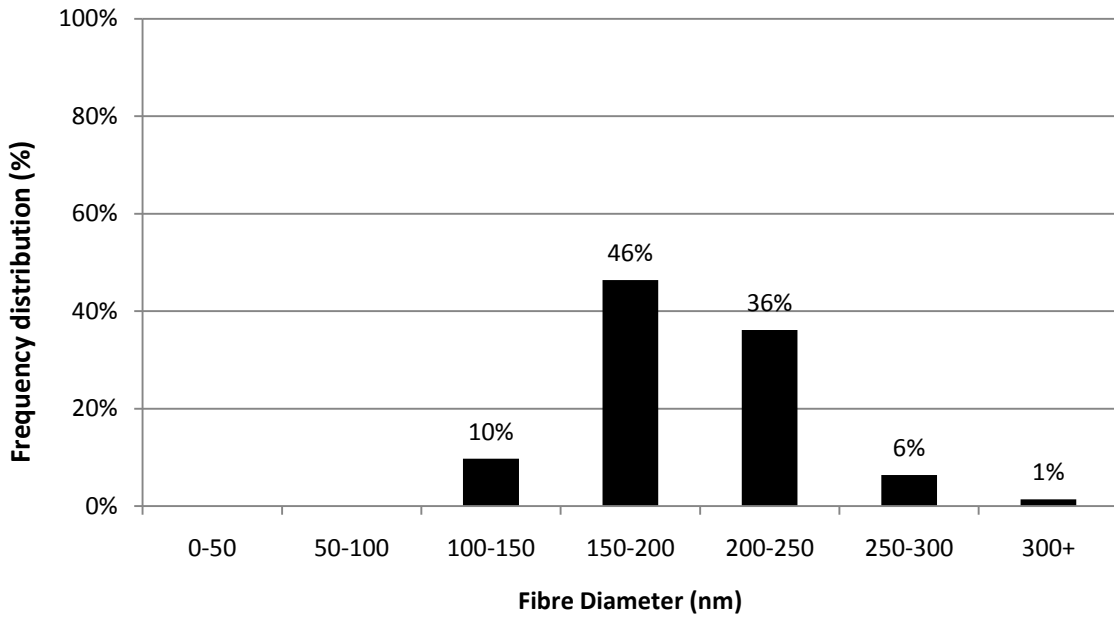


Figure 18. Percentage of Fibre Diameter Distribution of PVA 8% Solution at 10cm Collection Distance and 12kV

Effect of Increasing Concentration at Parameters of 10cm Collection Distance and 20kV on Fibre Distribution

Figures 19 to 21 show the fibre diameter distribution for PVA 4%, 6% and 8%. Increases in fibre diameter distribution were observed from PVA 4% to 6%, however, decreases were observed from PVA 6% to 8%. Figure 19 shows the diameter distribution for PVA 4% with diameters ranging from 17–121nm. Figure 20 shows the distribution for PVA 6% with diameters ranging from 39-308nm, which in comparison is much broader than PVA 4%. Figure 21 shows the distribution of fibre diameters for PVA 8% which consist of diameters ranging from 39-269nm.

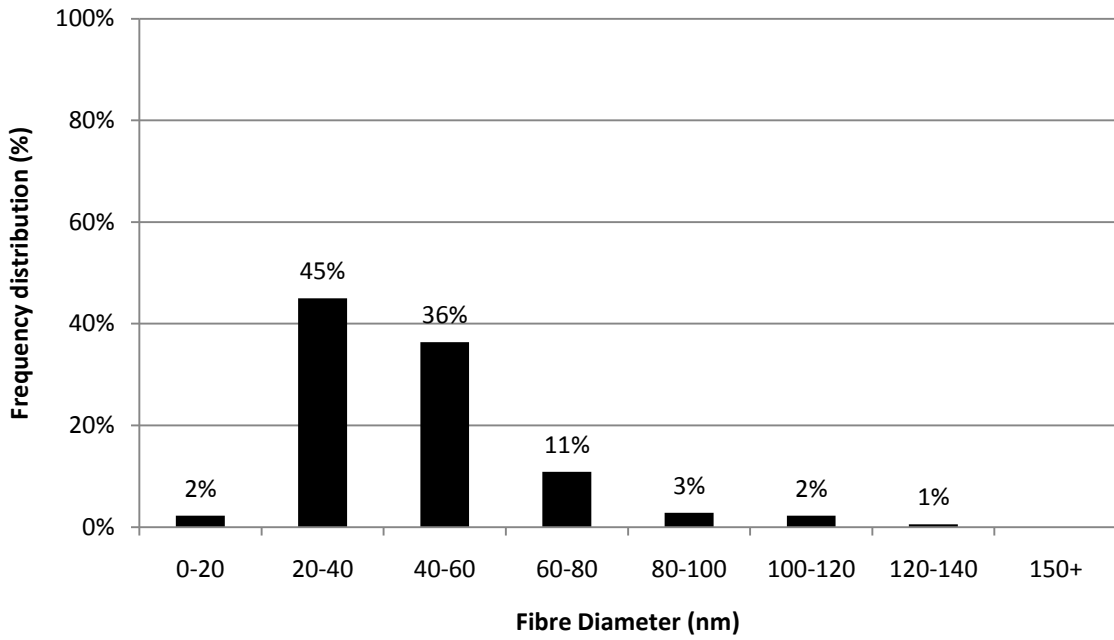


Figure 19. Total Percentage of Fibre Diameter Distribution of PVA 4% Solution at 10cm Collection Distance and 20kV

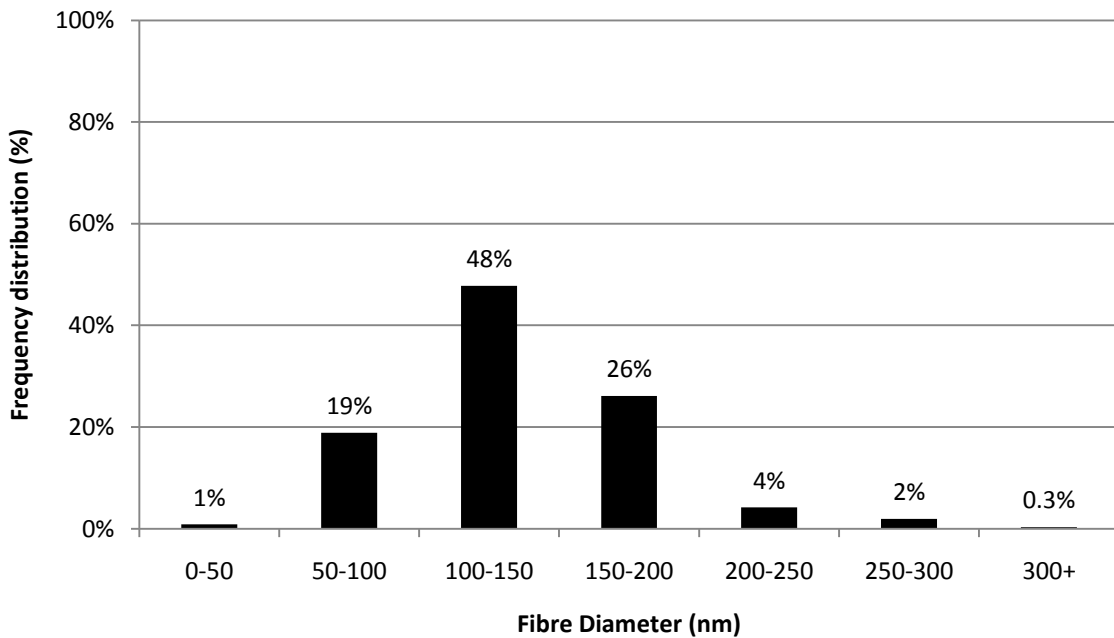


Figure 20. Total Percentage of Fibre Diameter Distribution of PVA 6% Solution at 10cm Collection Distance and 20kV

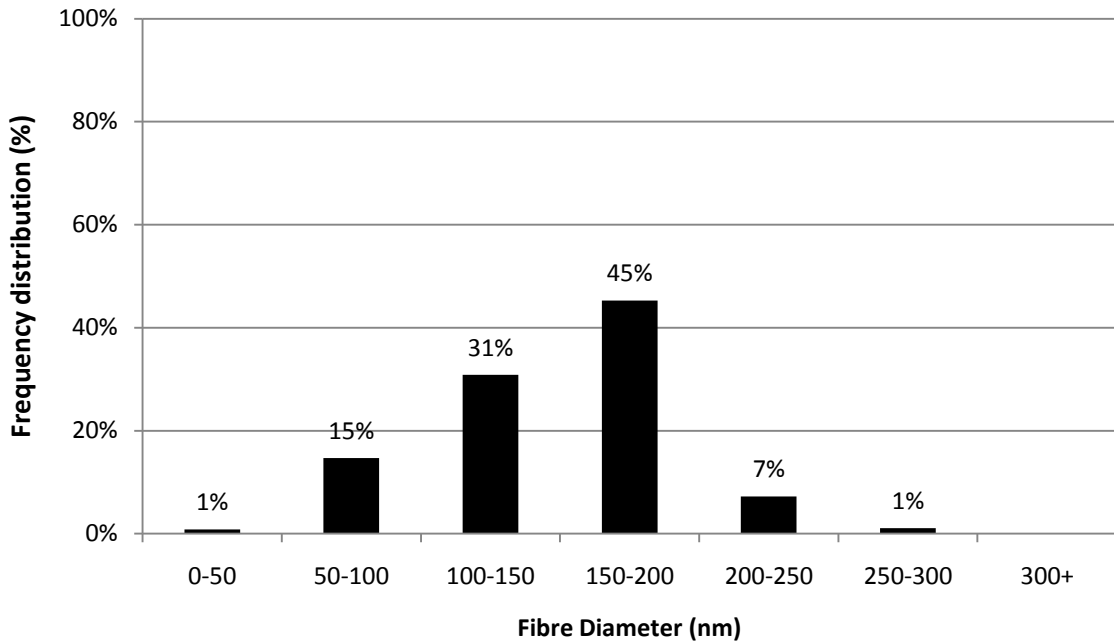


Figure 21. Total Percentage of Fibre Diameter Distribution of PVA 8% Solution at 10cm Collection Distance and 20kV

Effect of Increasing Concentration at Parameters of 15cm Collection Distance and 12kV on Fibre Distribution

Figures 22 to 24 show the fibre diameter distribution for PVA 4%, 6% and 8% which increases with increasing concentration at 15cm collection distance and 12kV. Figure 22 shows the fibre diameter distribution for PVA 4%, with diameters ranging from 17-138nm. Figure 23 shows fibre diameter distribution at PVA 6%, with diameters ranging from 39-231nm. Figure 24 shows the distribution at PVA 8% with diameters ranging from 121-385nm.

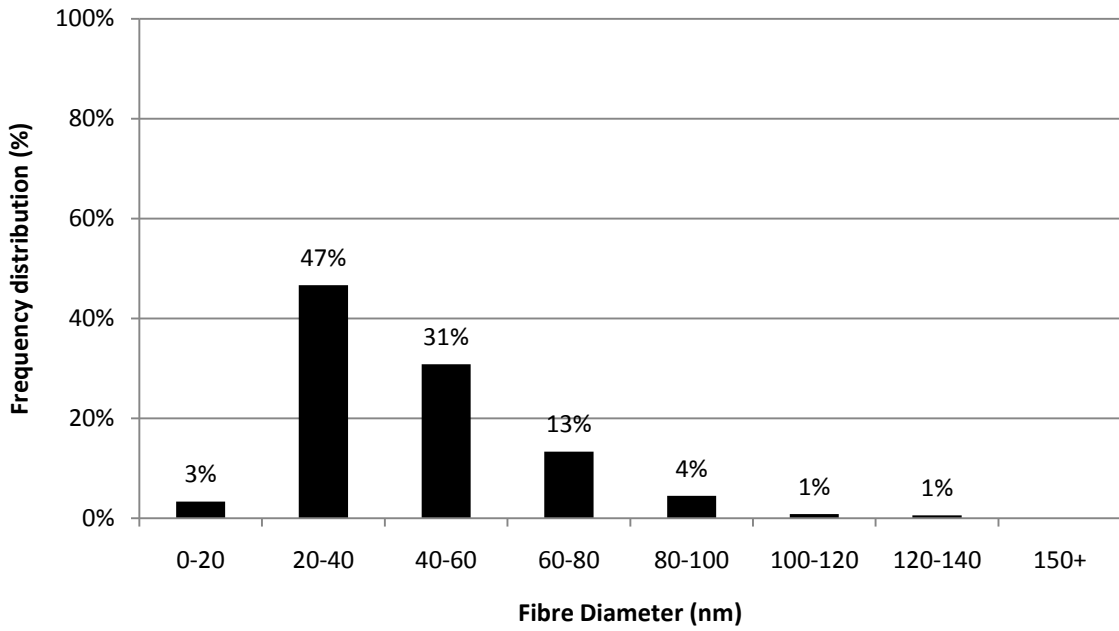


Figure 22. Total Percentage of Fibre Diameter Distribution of PVA 4% Solution at 15cm Collection Distance and 12kV

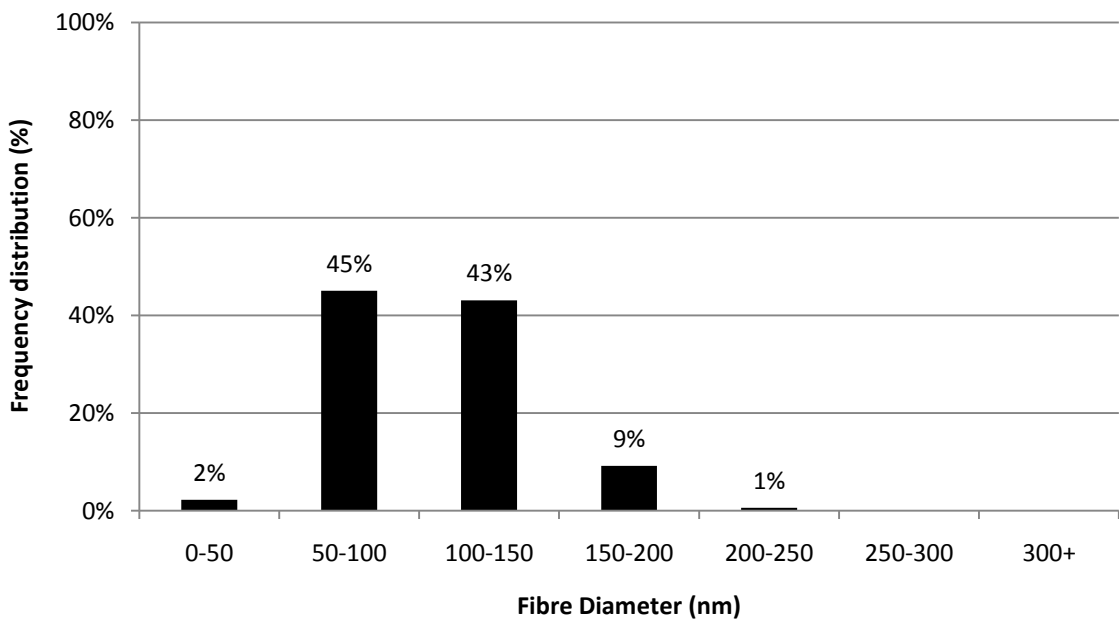


Figure 23. Total Percentage of Fibre Diameter Distribution of PVA 6% Solution at 15cm Collection Distance and 12kV

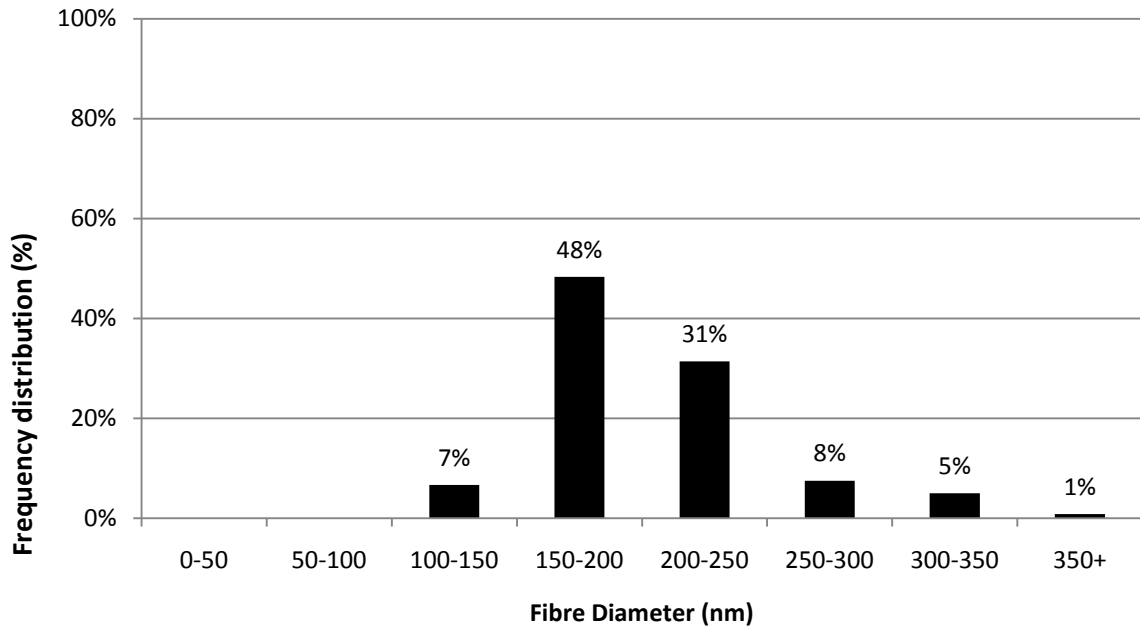


Figure 24. Percentage of Fibre Diameter Distribution of PVA 8% Solution at 15cm Collection Distance and 12kV

Effect of Increasing Concentration at Parameters of 15cm Collection Distance and 20kV on Fibre Distribution

Figures 25 to 27 show the fibre diameter distribution for PVA 4%, 6% and 8%, which increases with increasing concentration at 15cm collection distance and 20kV. Figure 25 shows the fibre diameter distribution at PVA 4% consisting of diameters ranging from 17-121nm. Figure 26 shows the distribution at PVA 6% which consists of diameters ranging from 39-153nm. Figure 27 shows the distribution at PVA 8% with diameters ranging from 115-423nm, which has the largest distribution.

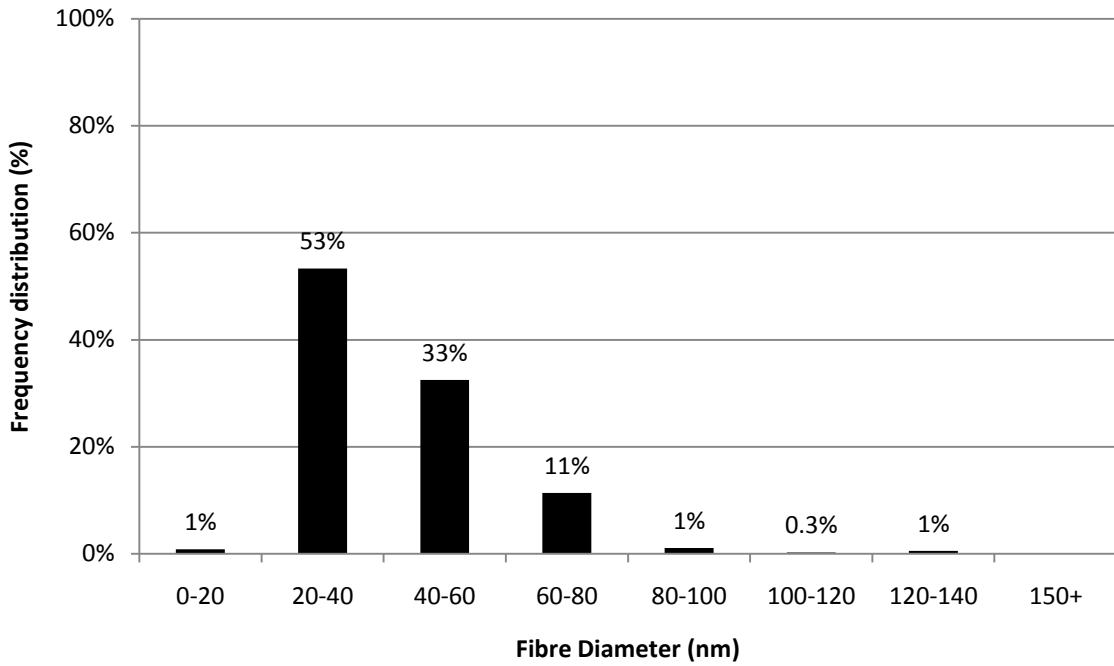


Figure 25. Total Percentage of Fibre Diameter Distribution of PVA 4% Solution at 15cm Collection Distance and 20kV.

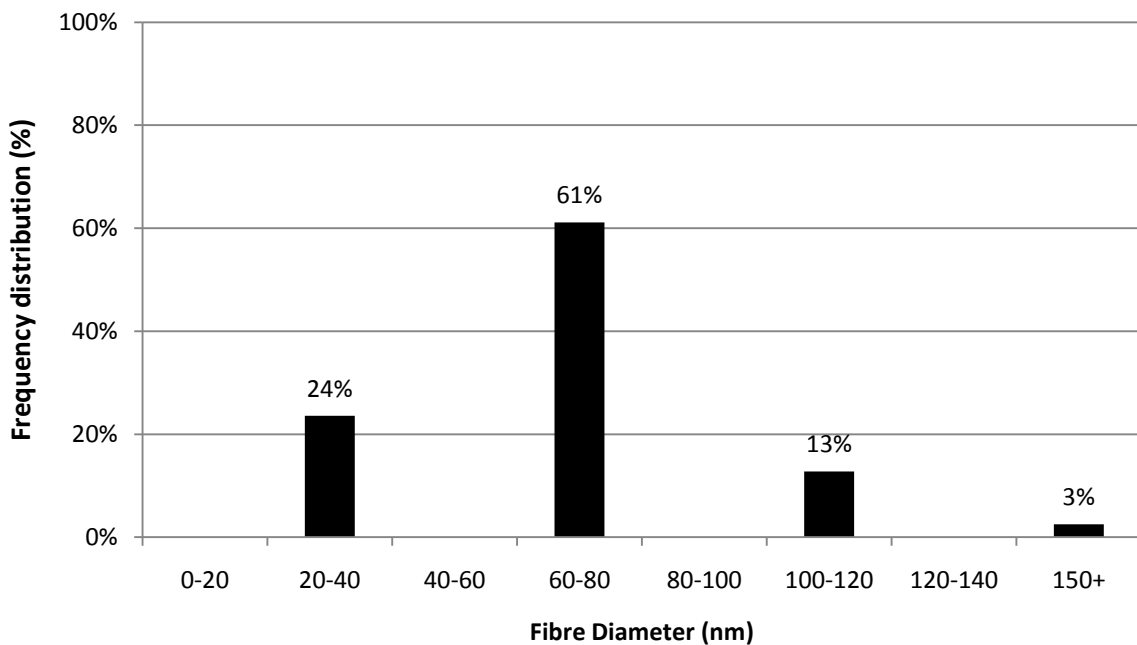


Figure 26. Total Percentage of Fibre Diameter Distribution of PVA 6% Solution at 15cm Collection Distance and 20kV.

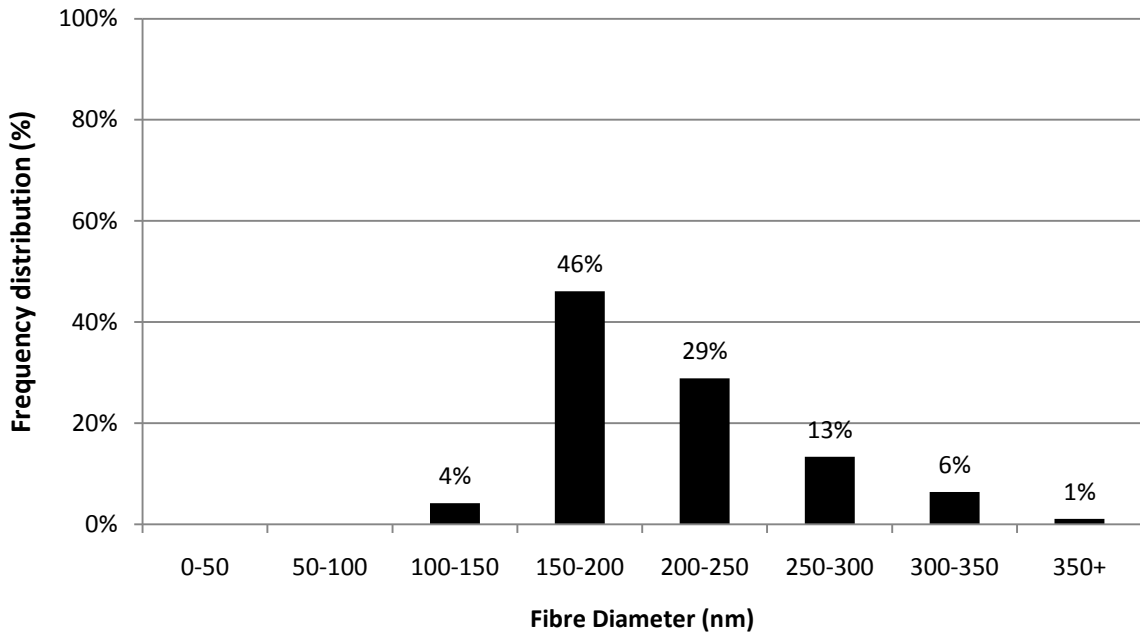


Figure 27. Total Percentage of Fibre Diameter Distribution of PVA 8% Solution at 15cm Collection Distance and 20kV.

4.1.3. Effect of Increasing Solution Concentration on Deposition Rate

Figures 28 to 31 show the effect of increasing solution concentration on deposition rate with varied parameters. Figure 28 shows at parameters of 12kV and 10cm collection distance, the deposition rate increases with increasing concentration. Figure 29 shows at 20kV and 10cm collection distance, the deposition rate varies with increasing solution concentration, as it decreases from PVA 4% to 6% and increases from PVA 6% to 8%. Figure 30 shows at 12kV and 15cm collection distance, the deposition rate varies slightly, with only a very small decrease from PVA 4% to 6% and slight increase from PVA 6% to 8%. Figure 31 shows at 15cm collection distance and 20kV, the deposition rate varies with concentration. A decrease from PVA 4% to 6% and increase from PVA 6% to 8% is observed.

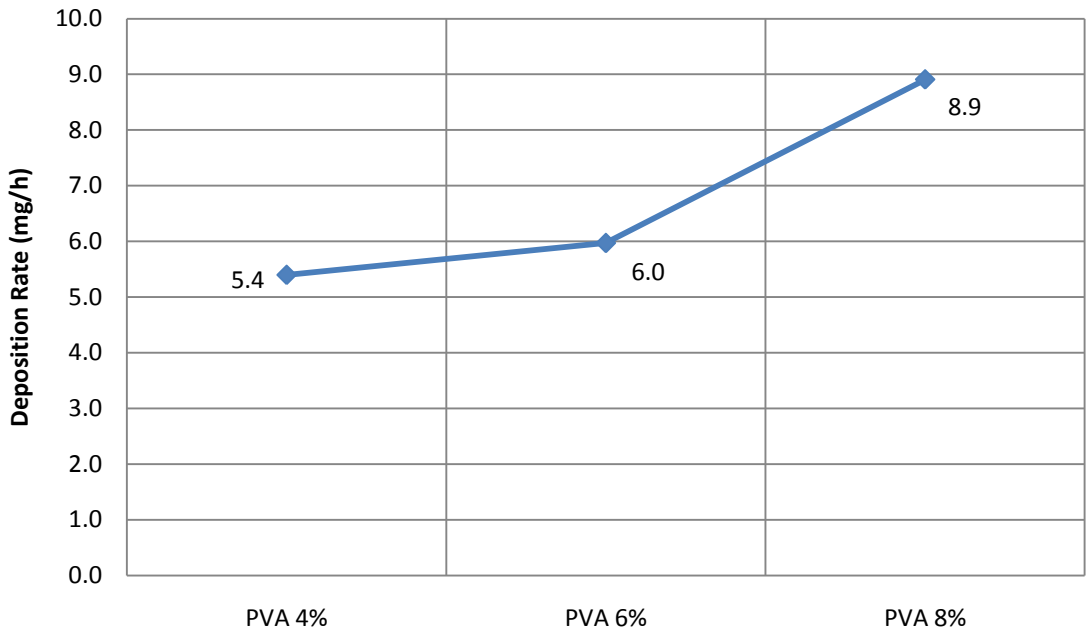


Figure 28. Deposition Rate of PVA 4%, 6% and 8% Solutions Electrospun at 10cm Collection Distance and 12kV.

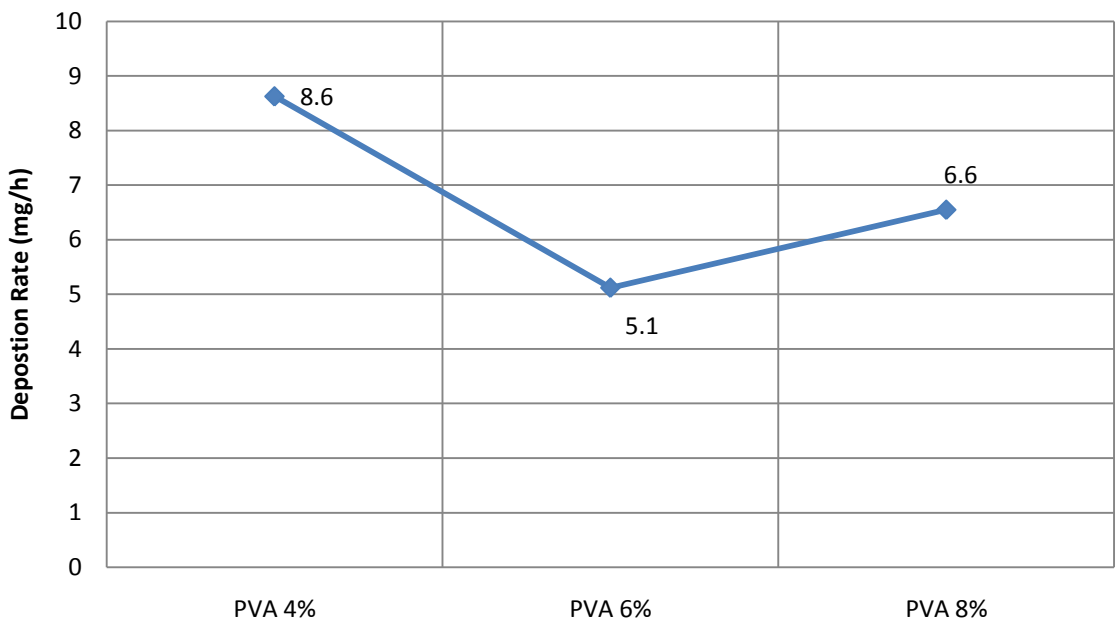


Figure 29. Deposition Rate of PVA 4%, 6% and 8% Solutions Electrospun at 10cm Collection Distance and 20kV.

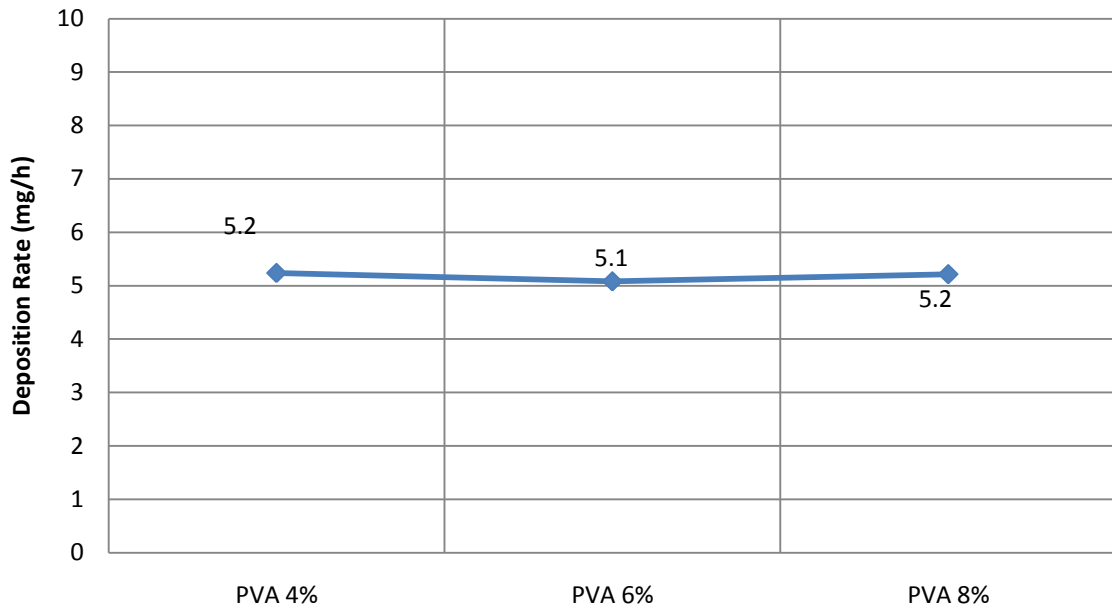


Figure 30. Deposition Rate of PVA 4%, 6% and 8% Solutions Electrospun at 15cm Collection Distance and 12kV.

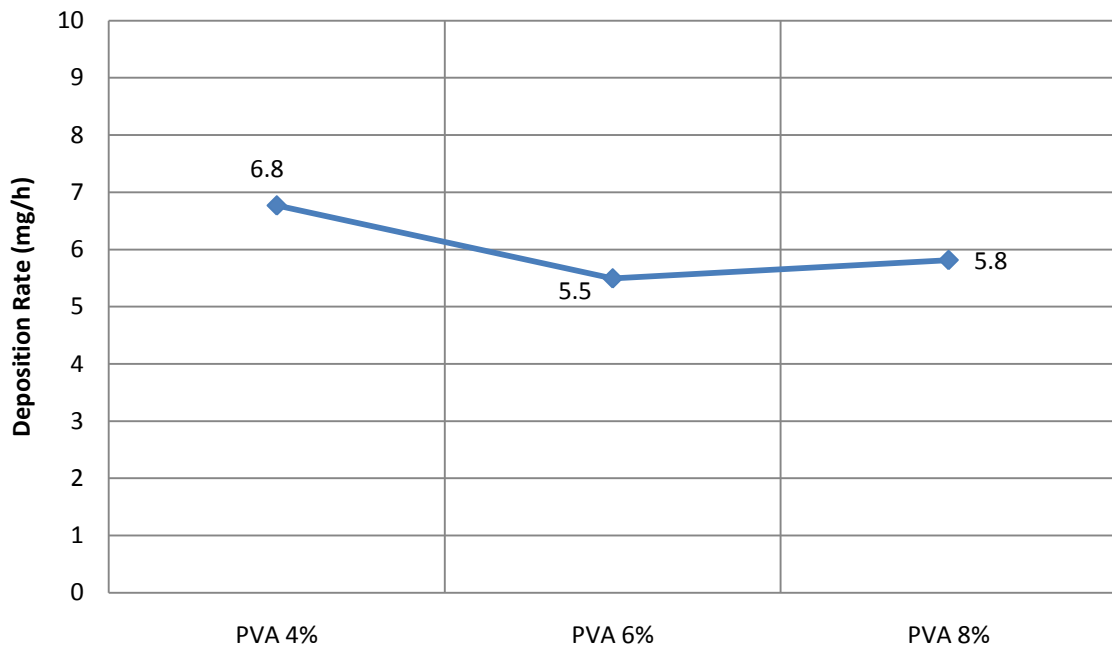


Figure 31. Deposition Rate of PVA 4%, 6% and 8% Solutions Electrospun at 15cm Collection Distance and 20kV

4.2. Applied Voltage

4.2.1. Effect of Increasing Voltage on Fibre Diameter and Morphology

Effect of Increasing Voltage on Fibre Diameter and Morphology using PVA 4%

Figures 32 to 37 show the effect of increasing voltage on the average, maximum and minimum diameter and morphology of the fibres at PVA 4% concentration using different collection distances. The collection distances of 7cm (Figure 32, and 33), 10cm (Figure 34 and 35) and 15cm (Figure 36 and 37) were used whilst applying voltages of 8kV, 12kV and 20kV at each collection distance.

Effect of Increasing Voltage on Fibre Diameter and Morphology at 7cm Collection Distance using PVA 4%

Figure 32 shows as the voltage increases the morphology does not change significantly. Combinations of large spherical and elongated beads were formed. Some regions showed webbing occurred as the beads merged with fibres distorting their morphologies. At 20kV no distinct fibres were formed, however, some signs of beaded fibre morphology were observed. Figure 33 shows the average fibre diameter decreased with increasing voltage from 8kV to 12kV at 7cm collection distance. At 20kV no fibres were formed, therefore, fibre diameter measurements could not be obtained.

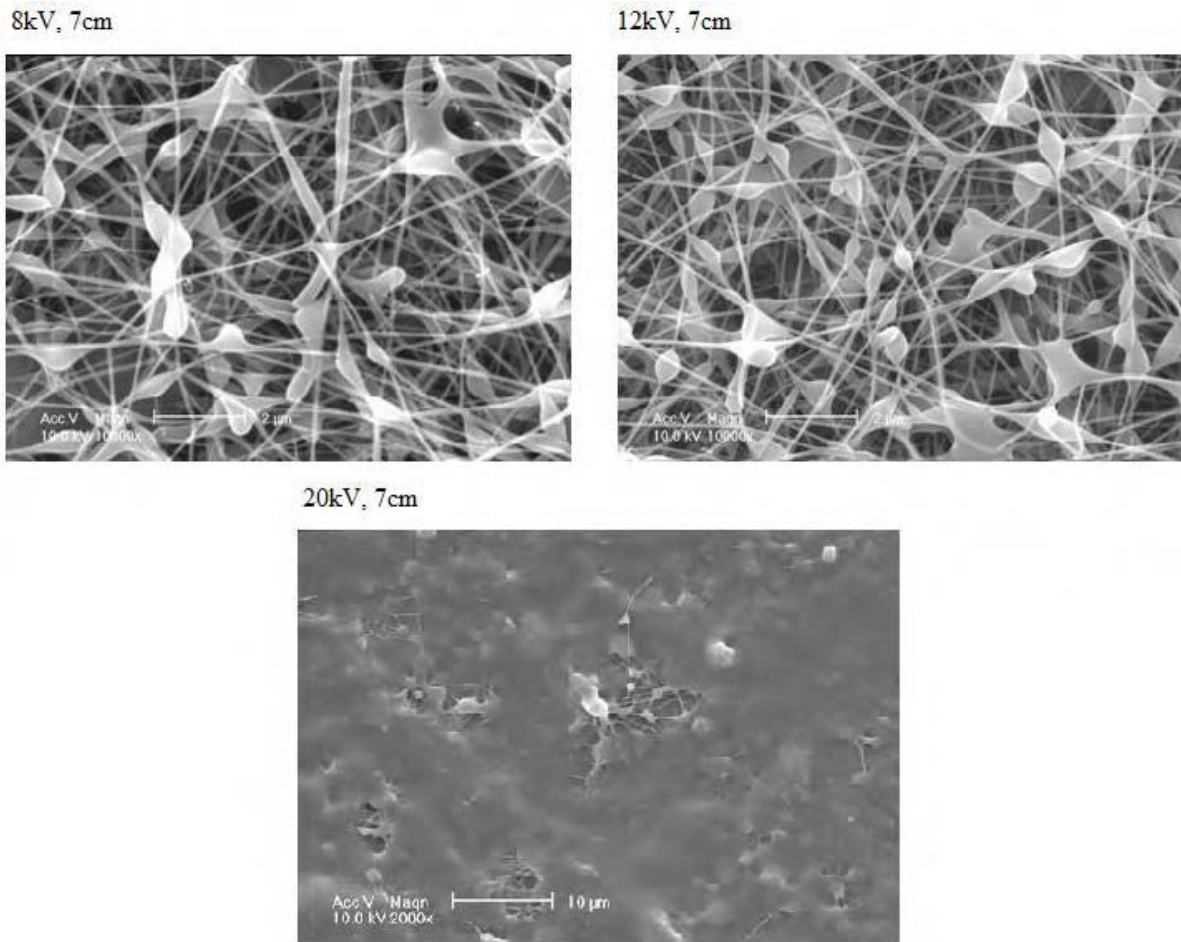


Figure 32. SEM images of electrospun PVA 4% at 7cm collection distance with application of increasing voltage, a) 8kV, b) 12kV and c) 20kV

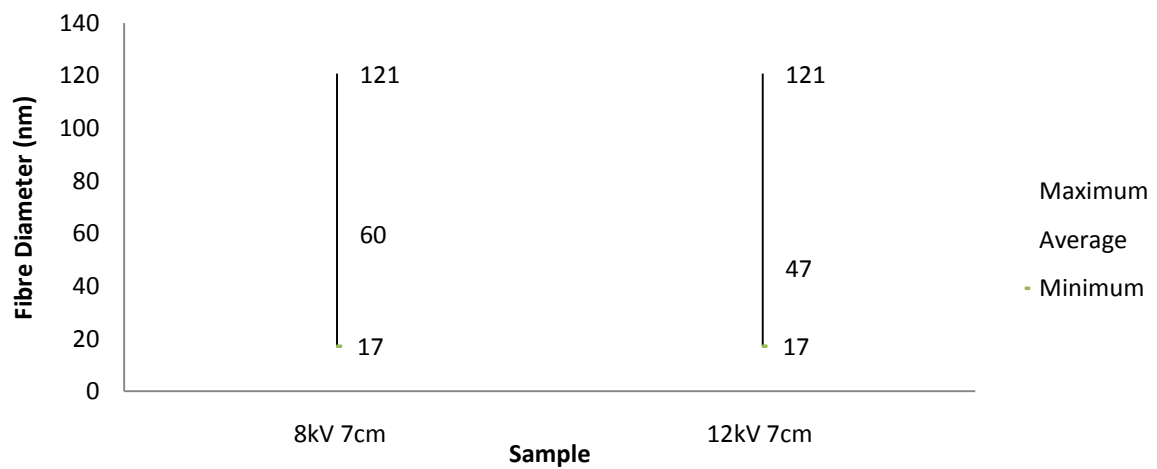


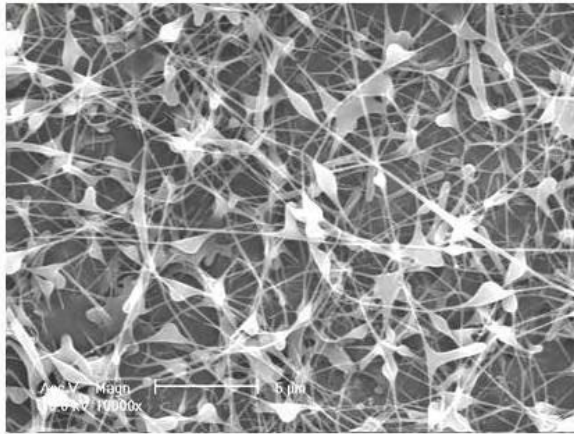
Figure 33. Overall Average, Maximum and Minimum Fibre Diameter of Electrospun PVA 4% Solution at 7cm Collection Distance with Increasing Voltage

Increasing Voltage on Fibre Diameter and Morphology at 10cm Collection Distance using

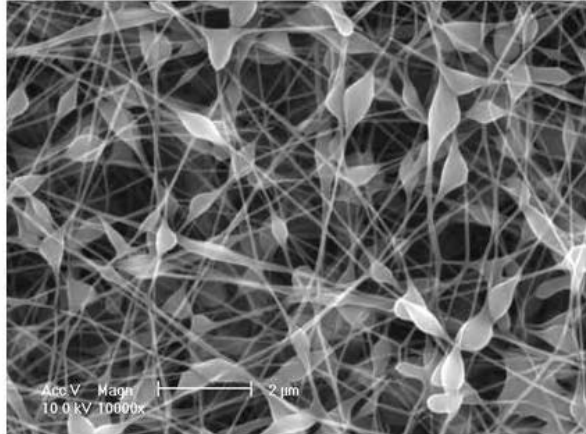
PVA 4%

Figure 34 shows at 10cm collection distance a mixture of spindle shaped and elongated beads on the fibres at 8kV and 12kV were formed. At 20kV the beads appear to merge with fibres and other beads to form fibre webs. Figure 35 shows from 8kV to 12kV the average fibre diameter decreased and at 20kV only a slight increase from 12kV.

a) 8kV, 10cm



b) 12kV, 10cm



c) 20kV, 10cm

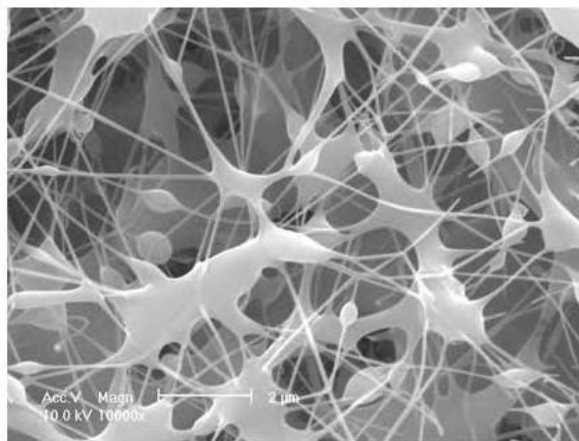


Figure 34. SEM images of electrospun PVA 4% % at 10cm collection distance with application of increasing voltage, a) 8kV, b) 12kV and c) 20kV

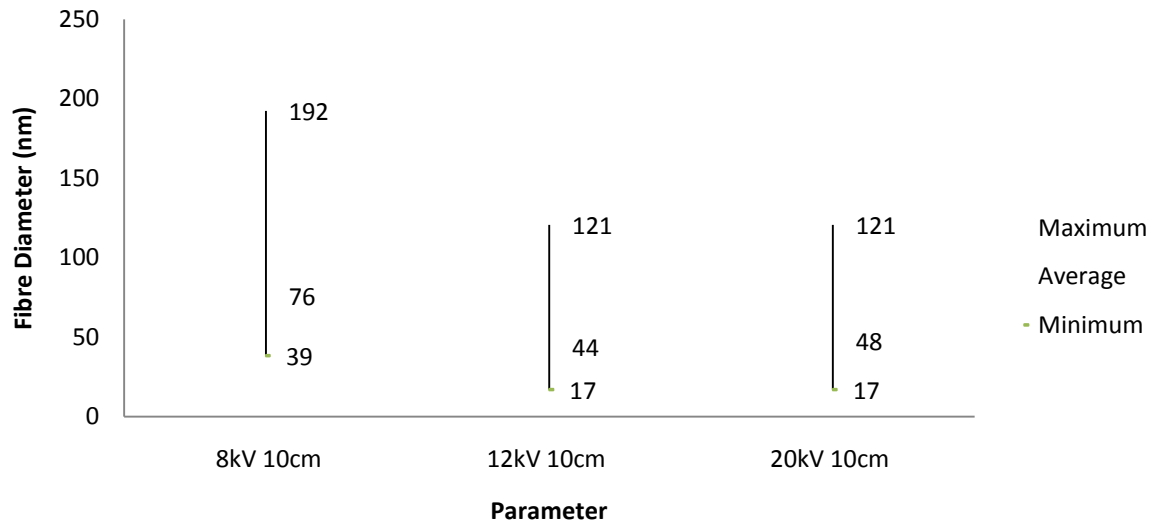


Figure 35. Overall Average, Maximum and Minimum Fibre Diameter of Electrospun PVA 4% Solution at 10cm Collection Distance with Increasing Voltage

Effect of Increasing Voltage on Fibre Diameter and Morphology at 15cm Collection Distance using PVA 4%

Figure 36 shows a mixture of spherical, spindle-bead and elongated beads on the fibres were formed. Some beads elongating greatly in the direction perpendicular from the fibre axis. The density of the beaded fibres increases with increasing voltage. Figure 37 shows from 8kV to 12kV the average fibre diameter decreased. At 20kV the fibre diameter decreases only slightly from 12kV.

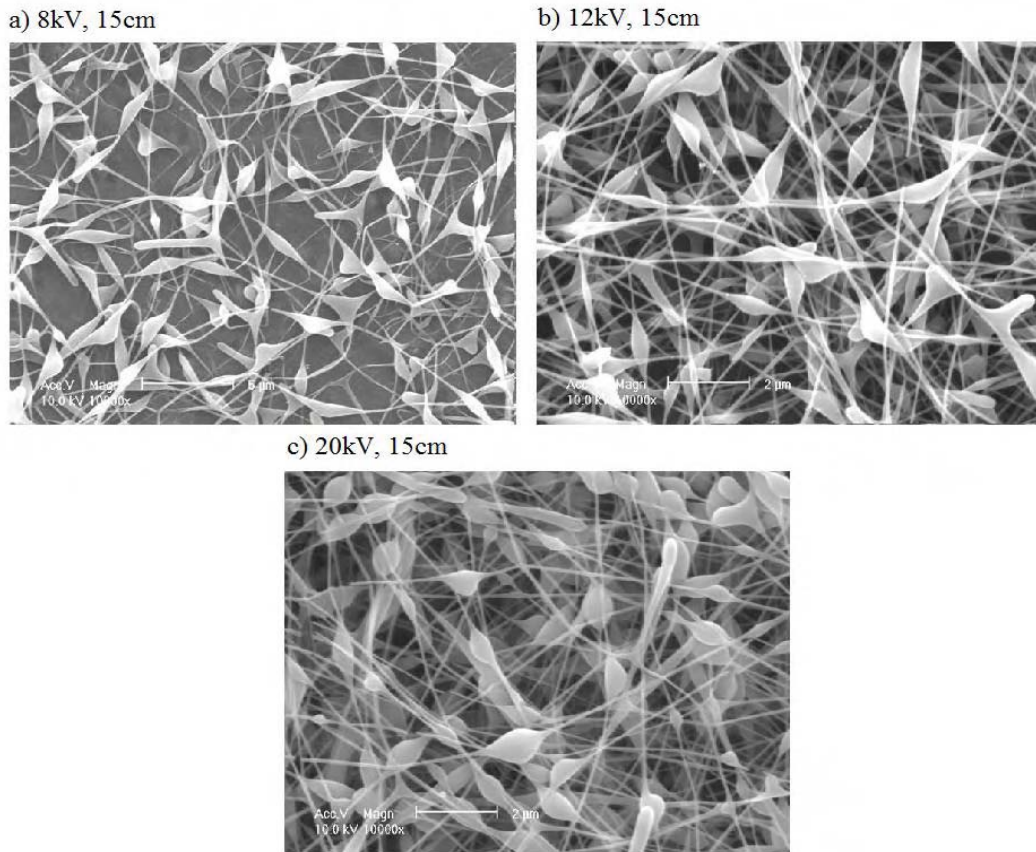


Figure 36. SEM images of electrospun PVA 4% at 15cm collection distance with application of increasing voltage, a) 8kV, b) 12kV and c) 20kV

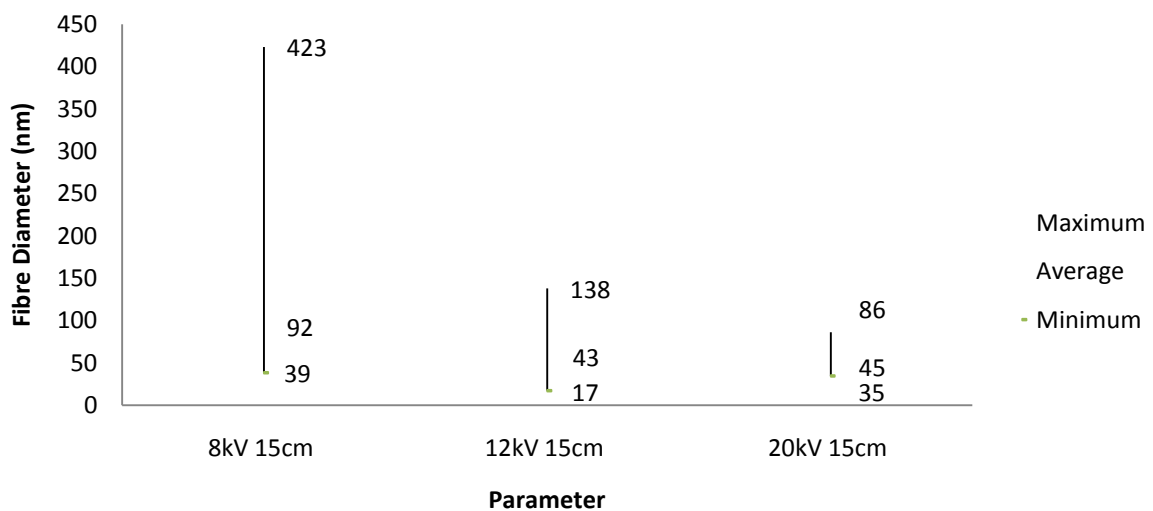


Figure 37. Overall Average, Maximum and Minimum Fibre Diameter of Electrospun PVA 4% Solution at 15cm Collection Distance with Increasing Voltage

Effect of Increasing Voltage on Fibre Diameter and Morphology using PVA 6%

Figures 38 to 41 show the effect of increasing voltage applied to 6% PVA solutions at different collection distances on the average, maximum and minimum diameter and morphology of the electrospun fibres. The collection distances of 10cm (Figure 38 and 39) and 15cm (Figure 40 and 41) were used whilst voltages of 12kV, 18kV and 20kV were applied to the solution.

Effect of Increasing Voltage on Fibre Diameter and Morphology at 10cm Collection

Distance using PVA 6%

Figure 38 shows the fibre morphology consists of large spherical beads on the fibres at 18kV and spindle-like beads on the fibres at 12kV and 20kV. Applying 18kV to the solution formed regions of fibre webs, as the beads and fibres merged together. The fibres intercepted through the surface of the large beads and with other fibres. The higher density of beaded fibres is observed at 12kV, with small spherical to spindle-like beads. At 20kV the beads are slightly larger with spindle-like morphology. Figure 39 shows the average fibre diameter decreased slightly with increasing voltage from 12kV to 18kV. The average diameter further increased at 20kV from 18kV.

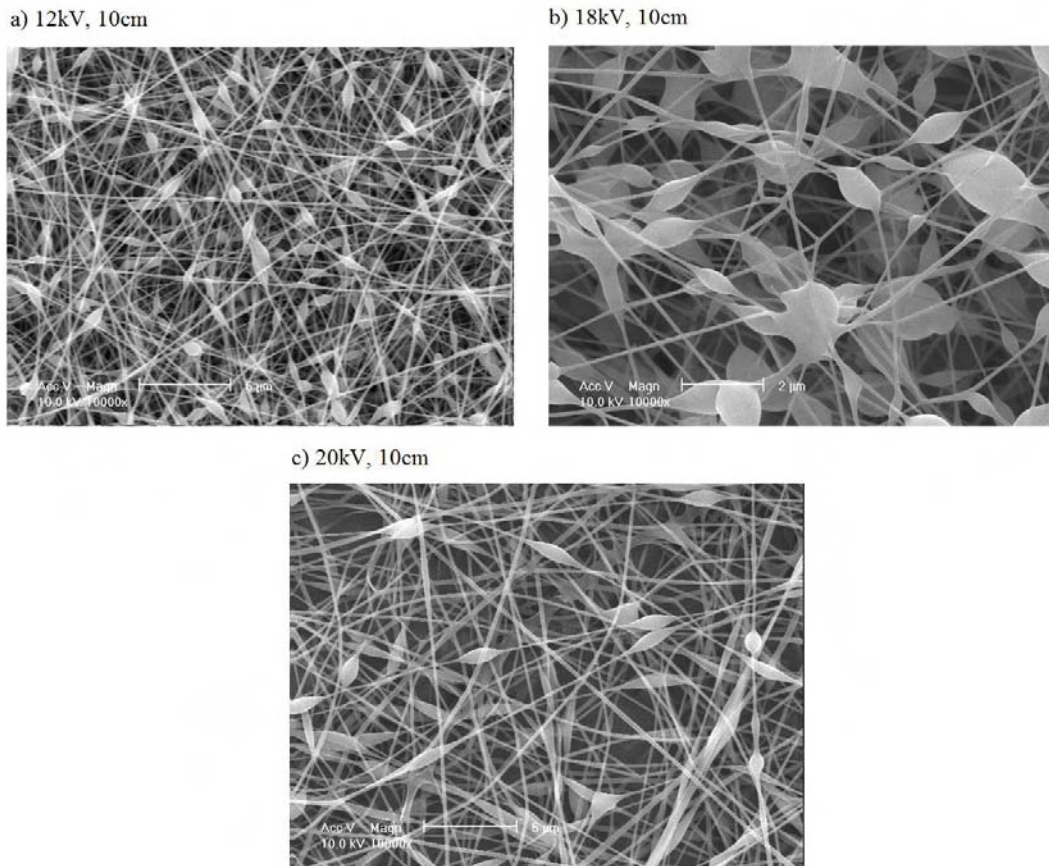


Figure 38. SEM images of electrospun PVA 6% at 10cm collection distance with application of increasing voltage, a) 12kV, b) 18kV and c) 20kV

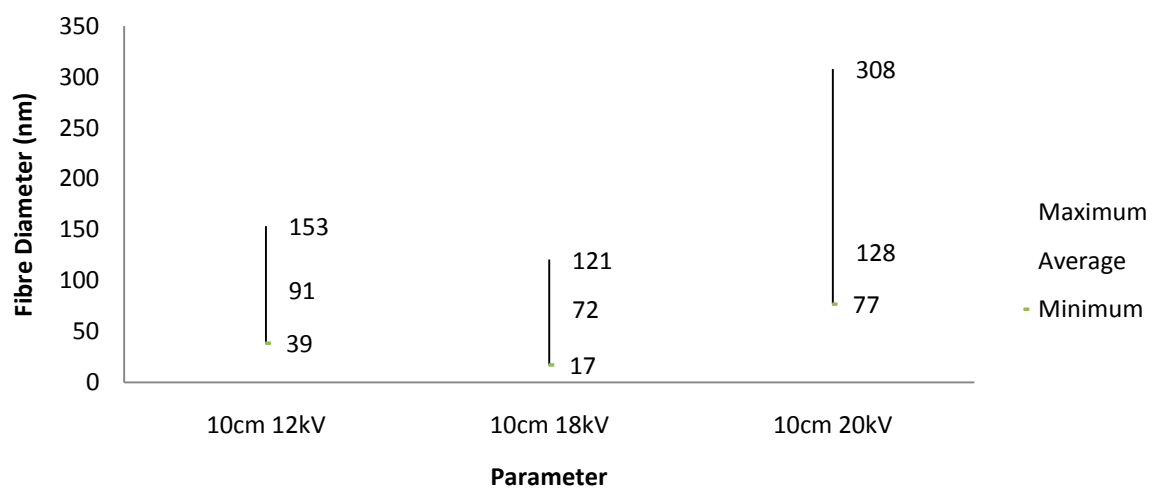


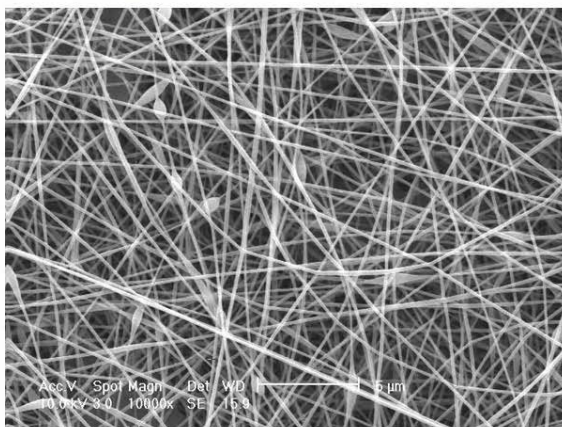
Figure 39. Overall Average, Minimum and Maximum Diameter of Electrospun Fibres of PVA 6% Solution at 10cm Collection Distance with Increasing Voltage

Increasing Voltage on Fibre Diameter and Morphology at 15cm Collection Distance using

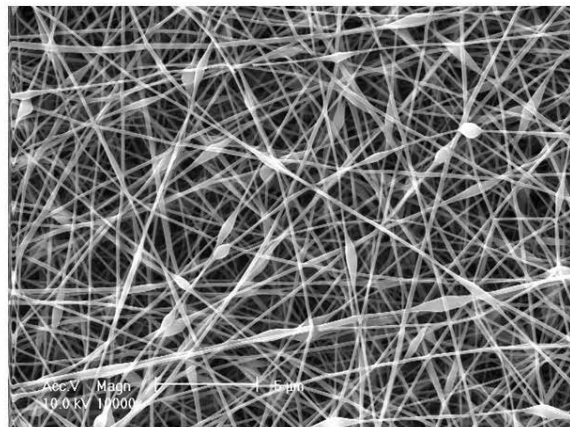
PVA 6%

Figure 40 shows distinct changes in morphology with increasing voltage. Only a few beaded fibres are observed at 12kV. The density increases slightly at 18kV with spherical and spindle-shaped beads. At 20kV the bead density increased drastically with larger, more spherical shaped beads on the fibres. Figure 41 shows the average fibre diameter increased slightly by increasing the voltage from 12kV to 18kV. The average diameter decreases with further increase to 20kV.

a) 12kV, 15cm



b) 18kV, 15cm



c) 20kV, 15cm

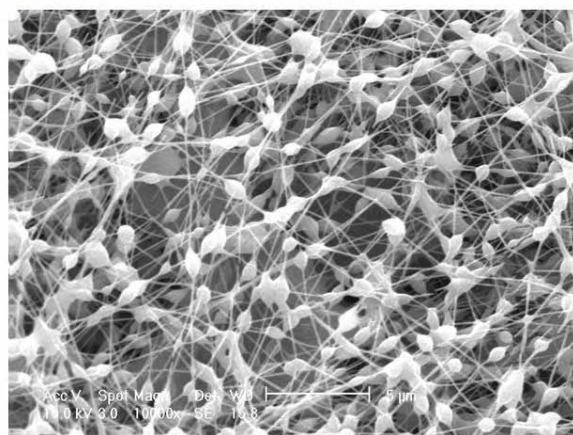


Figure 40. SEM images of electrospun PVA 6% at 15cm collection distance with application of increasing voltage, a) 12kV, b) 18kV and c) 20kV

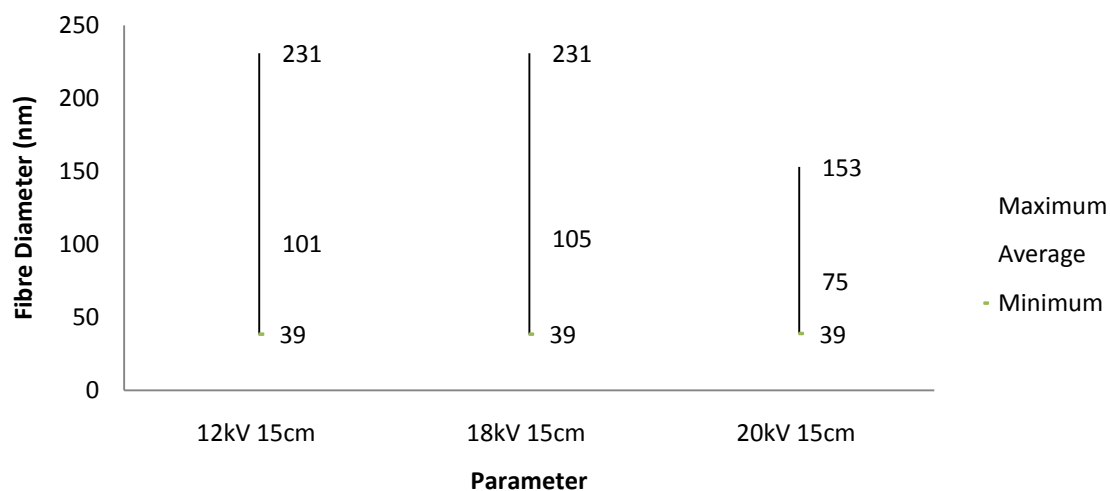


Figure 41. Overall Average, Minimum and Maximum Diameter of Electrospun Fibres of PVA 6% Solution at 15cm Collection Distance with Increasing Voltage

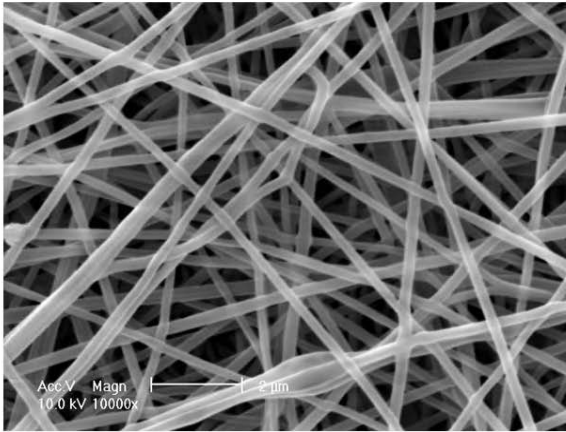
Effect of Increasing Voltage on Fibre Diameter and Morphology using PVA 8%

Figures 42 to 45 show the effect of increasing voltage on the average, maximum and minimum diameter, and morphology of the resultant electrospun fibres at PVA 8% using different collection distances. The collection distances of 10cm (Figure 42 and 43) and 15cm (Figure 44 and 45) were used whilst voltages of 12kV and 20kV were applied to the solution.

Effect of Increasing Voltage on Fibre Diameter and Morphology at 10cm Collection Distance using PVA 8%

Figure 42 shows beadless fibres were formed with increasing voltage at PVA 8%. At 12kV, these fibres possessed smooth and cylindrical morphologies. Some of the fibres merged together to form a single large fibre. Overlapping fibres adhered to fibres beneath altering the shape of the fibre at the region of contact. At 20kV undulating fibres and fibre webs were formed. These fibres also consisted of cylindrical and flat ribbon fibres. Figure 43 shows the average fibre diameter decreased with increasing voltage.

a) 12kV, 10cm



b) 20kV, 10cm

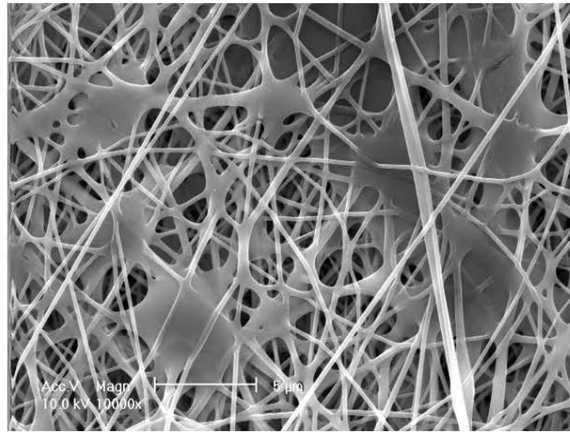


Figure 42. SEM images of electrospun PVA 8% at 10cm collection distance with application of increasing voltage, a) 12kV and b) 20kV

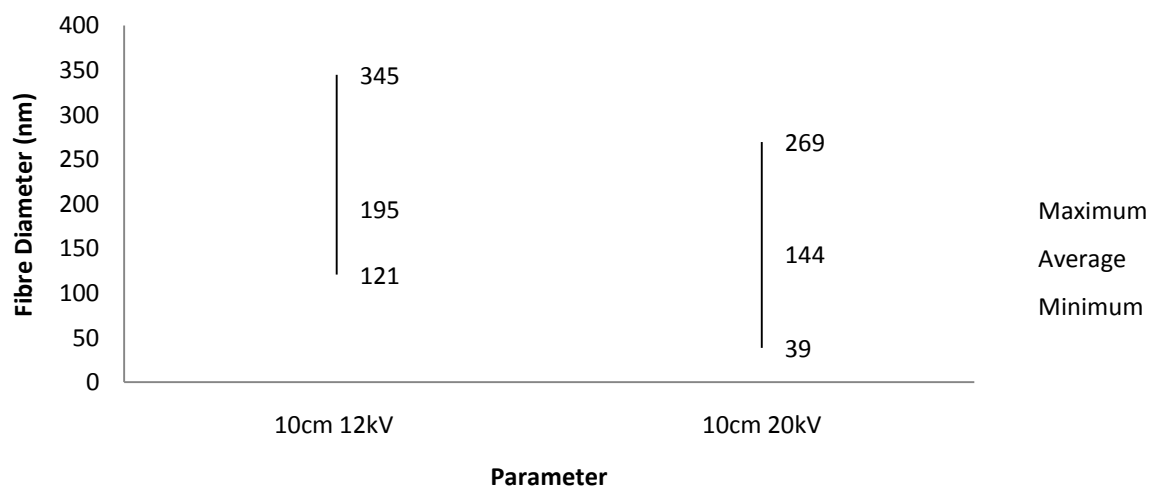


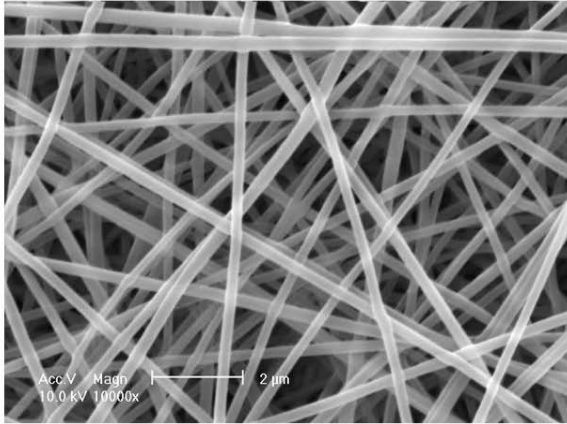
Figure 43. Overall Average, Minimum and Maximum Fibre Diameter of Electrospun PVA 8% Solution at 10cm Collection Distance with Increasing Voltage

Increasing Voltage on Fibre Diameter and Morphology at 15cm Collection Distance using PVA 8%

Figure 44 shows smooth and beadless fibres were produced with increasing voltage. At 12kV the fibre morphology was cylindrical and uniform. At 20kV a mixture of cylindrical

and flat ribbon fibres were produced of undulating diameters. Figure 45 shows the average fibre diameter increased slightly with increasing.

a) 12kV, 15cm



b) 20kV, 15cm

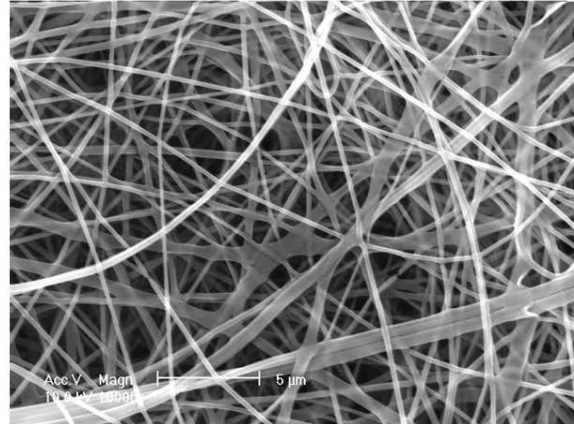


Figure 44. SEM images of electrospun PVA 8%% at 15cm collection distance with application of increasing voltage, a) 12kV and b) 20kV

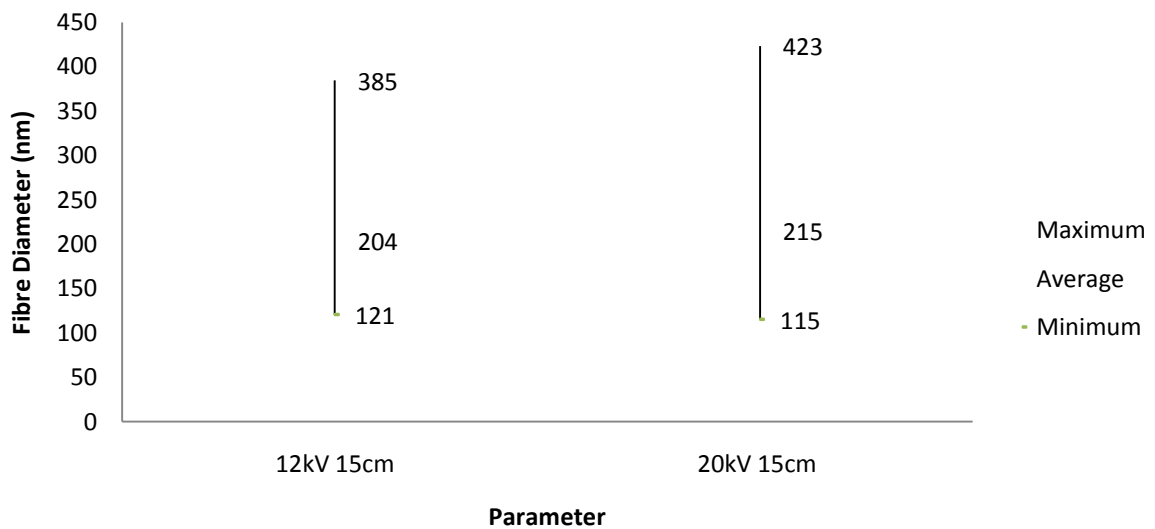


Figure 45. Overall Average, Minimum and Maximum Fibre Diameter of Electrospun PVA 8% Solution at 15cm Collection Distance with Increasing Voltage

4.2.2. Effect of Increasing Voltage on Fibre Diameter Distribution

Effect of Voltage of Increasing Voltage on Fibre Diameter Distribution using PVA 4%

Figures 46 to 53 show the effect of increasing voltage on the fibre diameter distribution at the collection distances of 7cm, 10cm and 15cm for PVA 4%.

Effect of Increasing Applied Voltage on the Fibre Diameter Distribution at 7cm Collection

Distance with 8kV and 12kV using PVA 4%

Figures 46 and 47 shows at 7cm collection distance the fibre diameter distribution decreases with increasing voltage. Figure 46 shows the fibre diameter distribution at 8kV with diameters ranging from 17-241nm. Figure 47 shows the distribution of fibres obtained at 12kV with diameters ranging from 17-121nm.

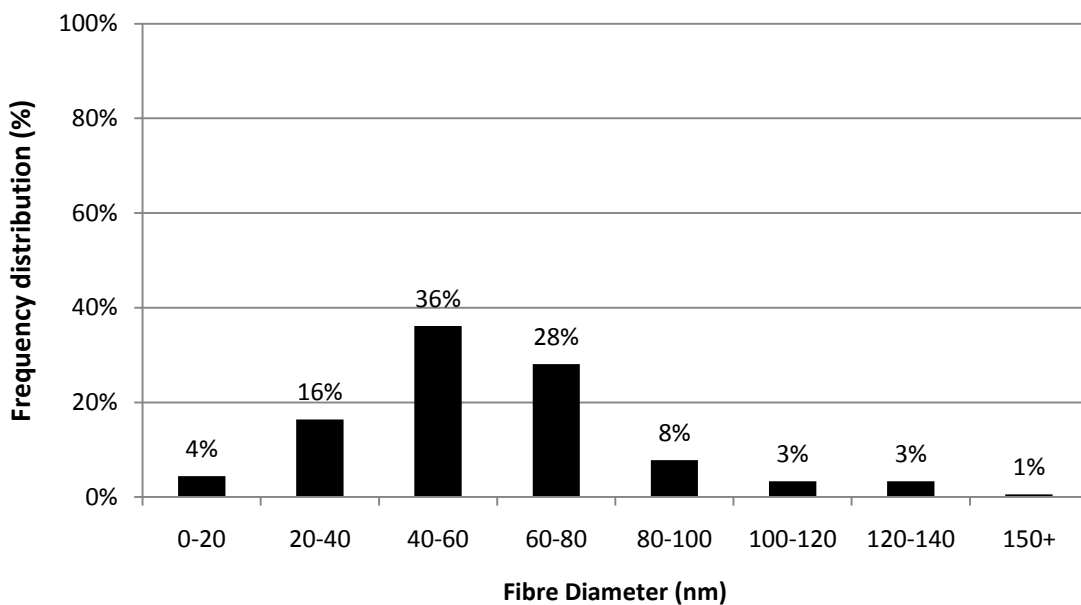


Figure 46. Total Percentage of Fibre Diameter Distribution of PVA 4% Solution at 7cm Collection Distance and 8kV

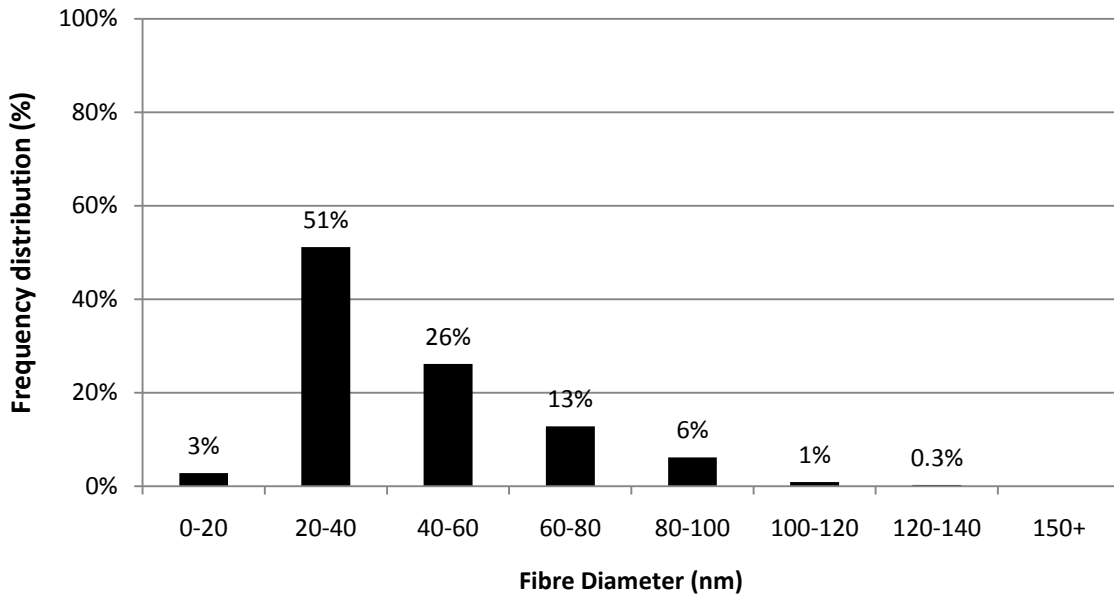


Figure 47. Total Percentage of Fibre Diameter Distribution of PVA 4% Solution at 7cm Collection Distance and 12kV

Effect of Increasing Applied Voltage on the Fibre Diameter Distribution at 10cm Collection Distance with 8kV, 12kV and 20kV using PVA 4%

At 10cm collection distance, Figures 48 and 49 show the fibre diameter distribution decreases from 8kV to 12kV and Figure 49 to 50 shows no alteration from 12kV to 20kV. Figure 48 shows the diameter distribution of fibres formed at 8kV, where fibres of distinct sizes are formed, with diameters ranging from 39-192nm. Figure 49 shows the diameter distribution of fibres formed at 12kV, which comprises of fibres with diameters ranging from 17-121nm. Figure 49 shows the diameter distribution of fibres formed at 20kV with diameters ranging from 17-121nm.

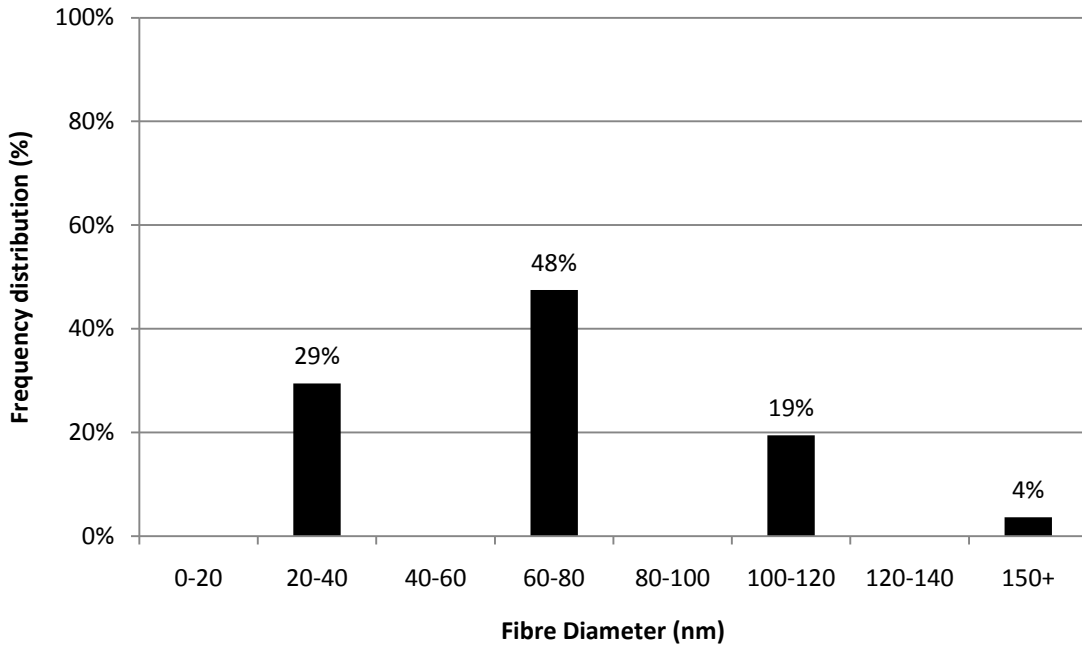


Figure 48. Total Percentage of Fibre Diameter Distribution of PVA 4% Solution at 10cm Collection Distance and 8kV

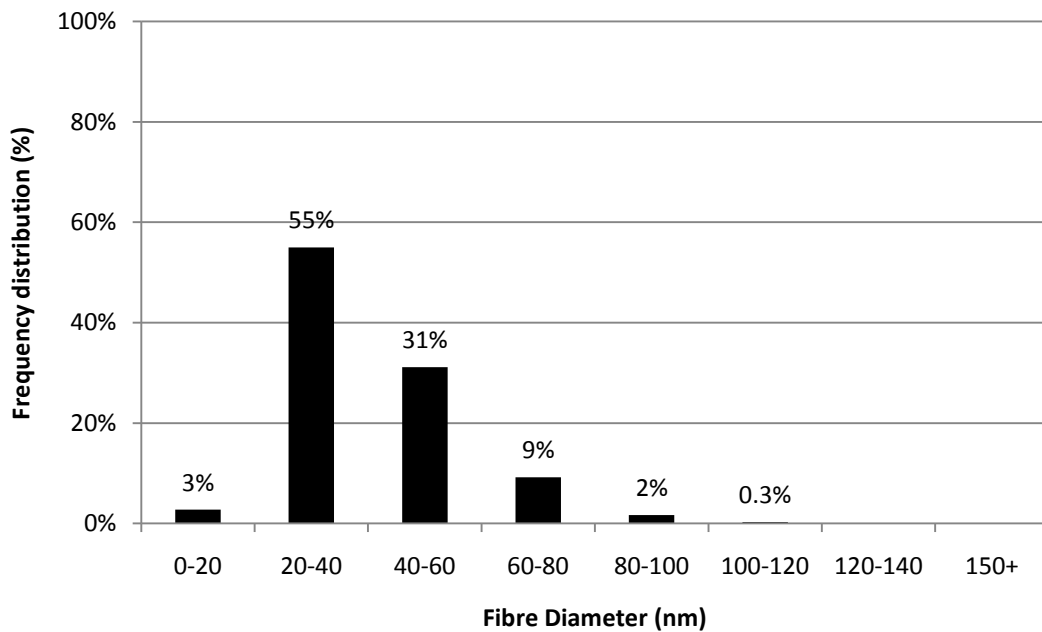


Figure 49. Total Percentage of Fibre Diameter Distribution of PVA 4% Solution at 10cm Collection Distance and 12kV

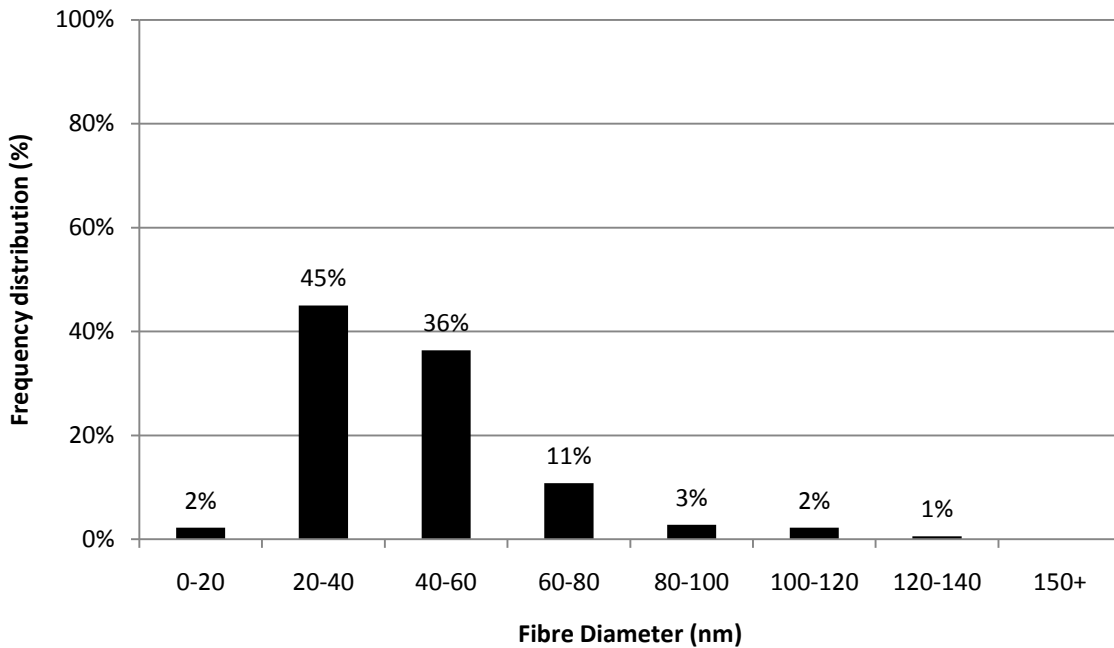


Figure 50. Total Percentage of Fibre Diameter Distribution of PVA 4% Solution at 10cm Collection Distance and 20kV

Effect of Increasing Applied Voltage on the Fibre Diameter Distribution at 15cm Collection

Distance with 8kV, 12kV and 20kV using PVA 4%

Figures 51 to 53 show the average fibre diameter distribution decreases with increasing voltage at 15cm collection distance. Figure 51 shows the fibre diameter distribution at 8kV with diameters ranging from 39-423nm. Figure 52 shows the diameter distribution obtained at 12kV with diameters ranging from 17-138nm. Figure 53 shows the distribution at 20kV with diameters ranging from 17-121nm.

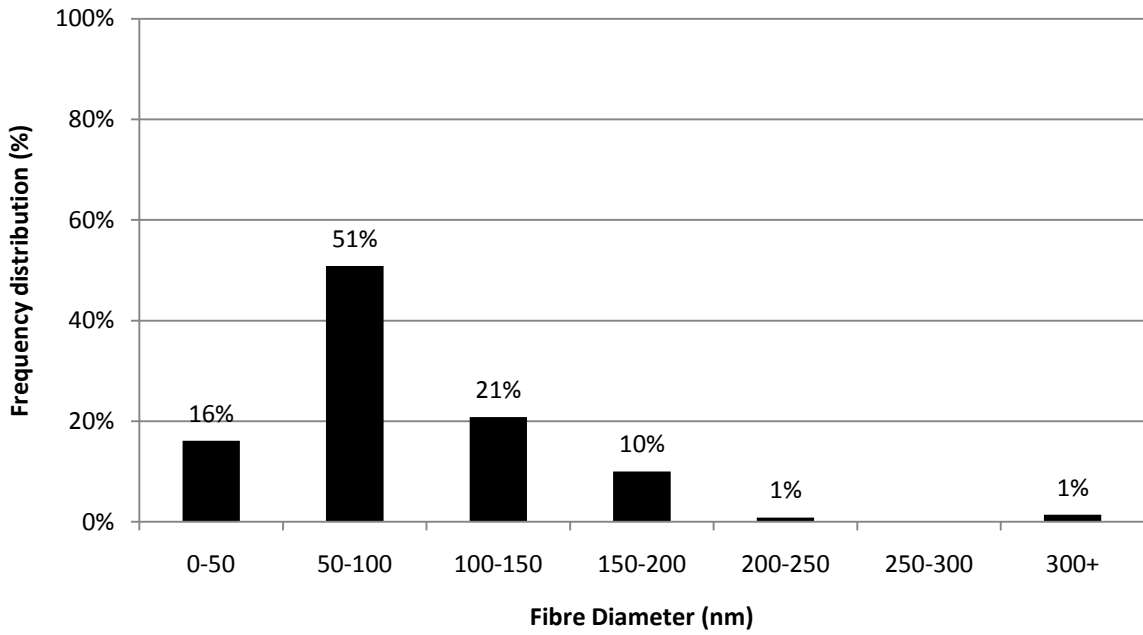


Figure 51. Total Percentage of Fibre Diameter Distribution of PVA 4% Solution at 15cm Collection Distance and 8kV

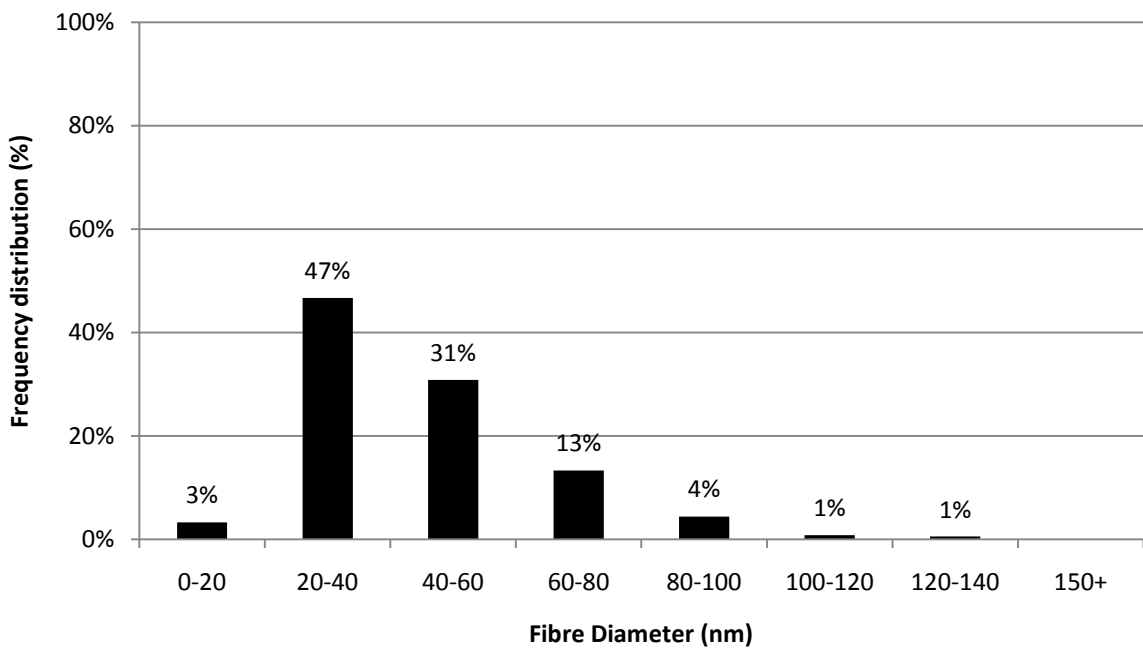


Figure 52. Total Percentage of Fibre Diameter Distribution of PVA 4% Solution at 15cm Collection Distance and 12kV

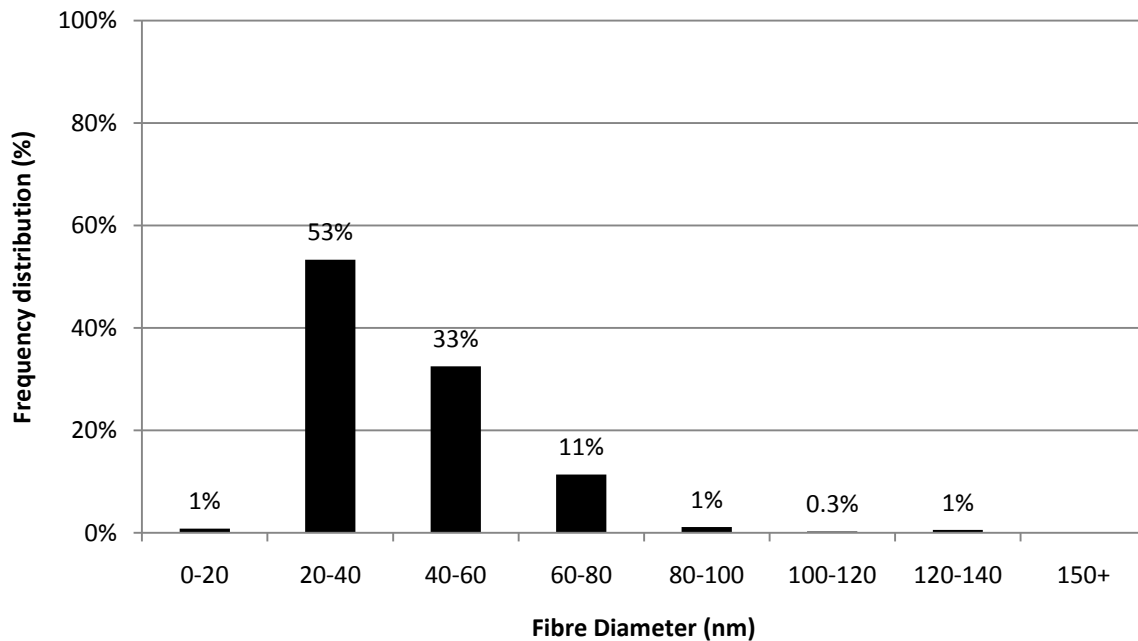


Figure 53. Total Percentage of Fibre Diameter Distribution of PVA 4% Solution at 15cm Collection Distance and 20kV

Effect of Voltage of Increasing Voltage on Fibre Diameter Distribution using PVA 6%

Figures 54 and 59 show the effect of increasing voltage on the fibre diameter distribution, using PVA 6% at the collection distances of 10cm and 15cm.

Effect of Increasing Applied Voltage on the Fibre Diameter Distribution at 10cm Collection Distance with 12kV, 18kV and 20kV using PVA 6%

Figure 55 and 56 shows the fibre diameter distribution decreases from 12kV to 18kV and Figure 54 and 55 shows it increases from 18kV to 20kV at 10cm collection distance. Figure 54 shows the distribution at 12kV with diameters ranging from 39-192nm. Figure 55 show the distribution at 18kV with diameters ranging from 17-138nm. Figure 56 shows the distribution at 20kV with diameters ranging from 39-308nm.

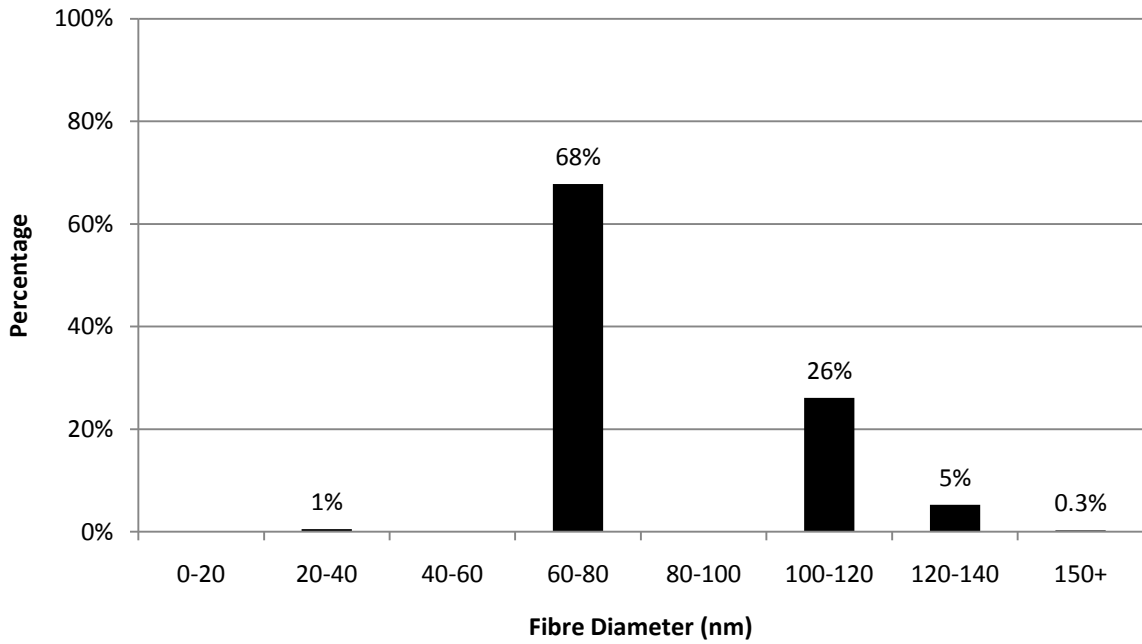


Figure 54. Overall Percentage of Fibre Diameter Distribution of PVA 6% Solution at 10cm Collection Distance and 12kV

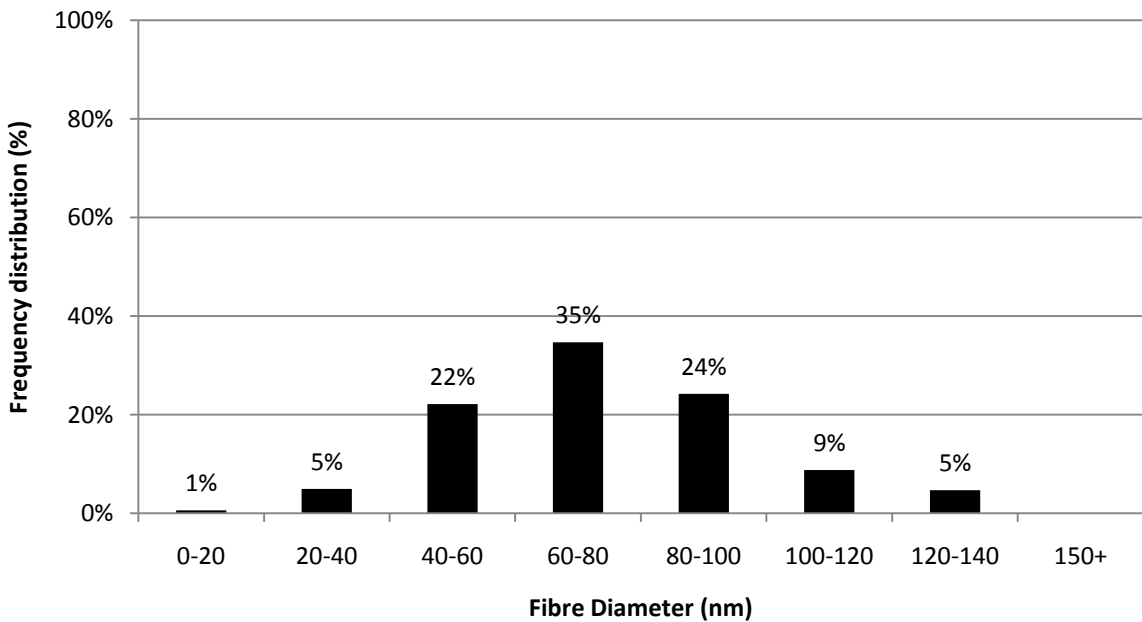


Figure 55. Total Percentage of Fibre Diameter Distribution of PVA 6% Solution at 10cm Collection Distance and 18kV

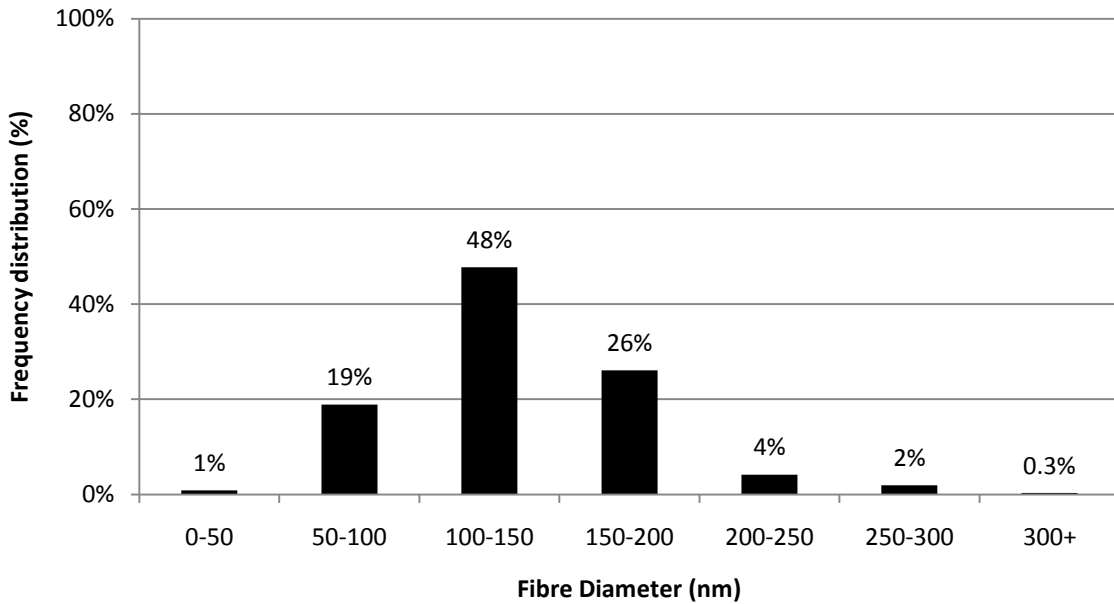


Figure 56. Total Percentage of Fibre Diameter Distribution of PVA 6% Solution at 10cm Collection Distance and 20kV

Effect of Increasing Applied Voltage on the Fibre Diameter Distribution at 15cm Collection Distance with 12kV, 18kV and 20kV using PVA 6%

Figure 57 to 59 shows the fibre diameter distribution decreases with increasing voltage at 15cm collection distance. Figure 57 shows the distribution at 12kV with diameters ranging from 39-231nm. Figure 58 shows the distribution at 18kV with diameters ranging from 39-231nm. Figure 59 shows the distribution at 20kV with diameters ranging from 39-153nm.

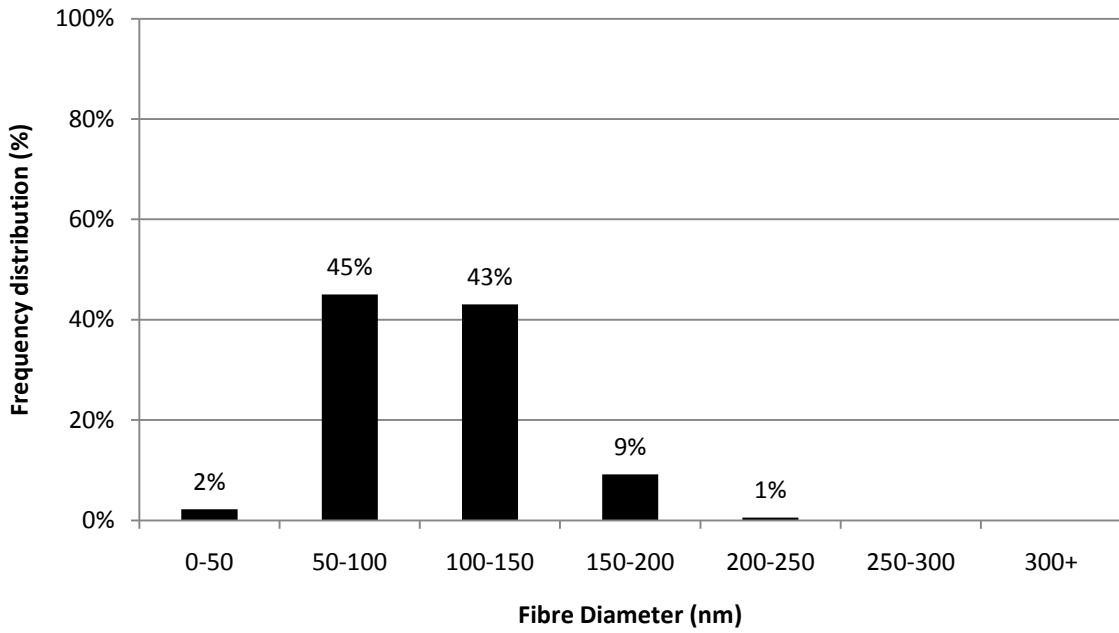


Figure 57. Total Percentage of Fibre Diameter Distribution of PVA 6% Solution at 15cm Collection Distance and 12kV

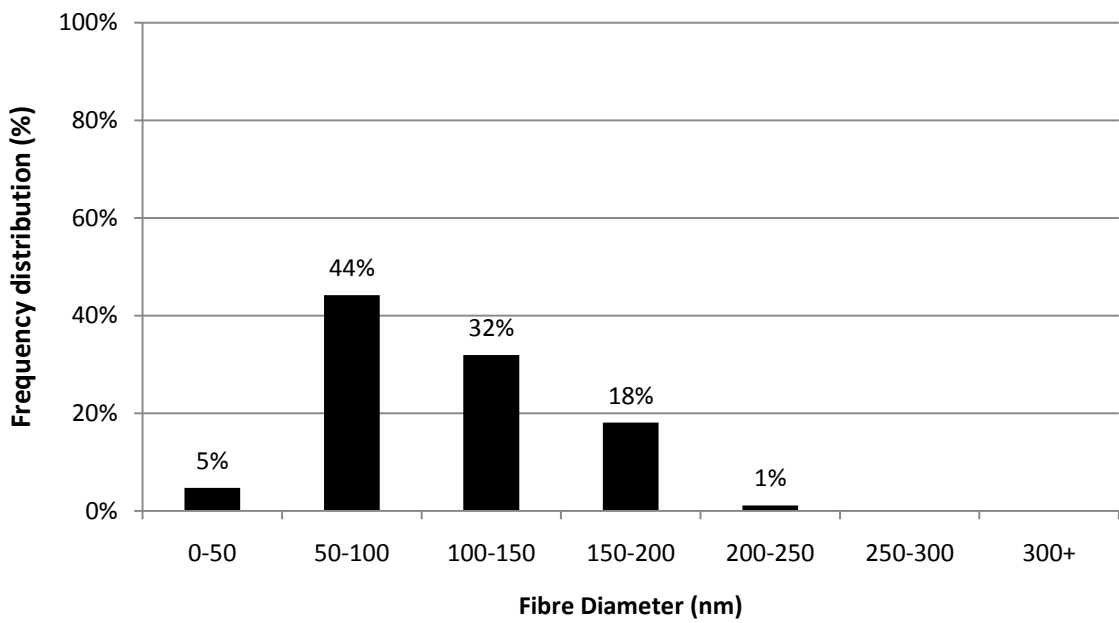


Figure 58. Total Percentage of Fibre Diameter Distribution of PVA 6% Solution at 15cm Collection Distance and 18kV

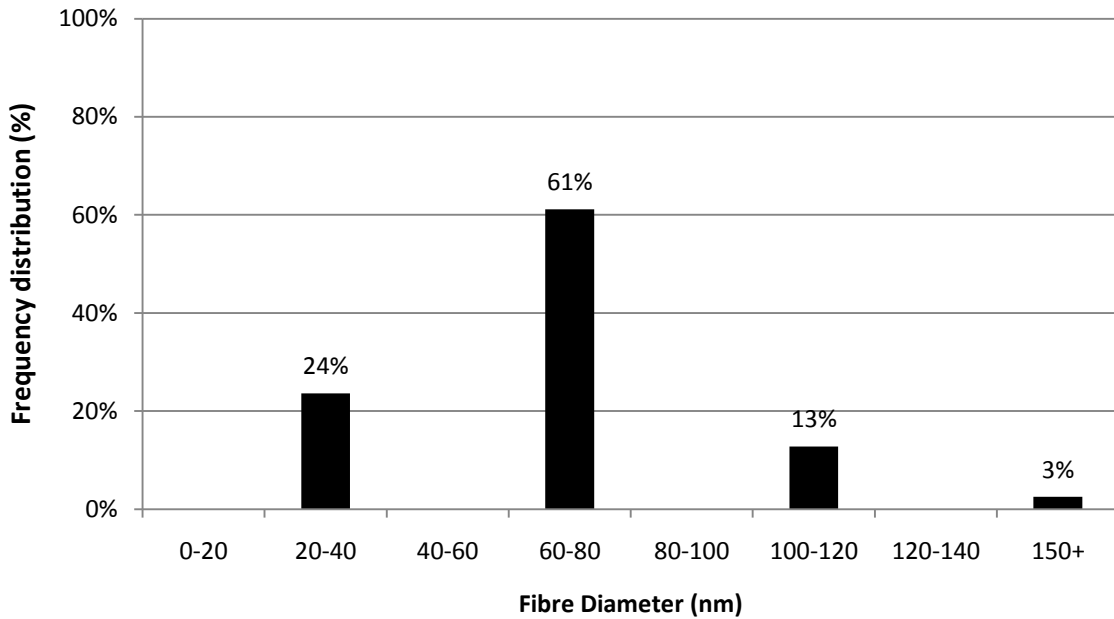


Figure 59. Total Percentage of Fibre Diameter Distribution of PVA 6% Solution at 15cm Collection Distance and 20kV

Effect of Voltage of Increasing Voltage on Fibre Diameter Distribution using PVA 8%

Figures 60 to 63 show the effect of increasing applied voltage using PVA 8% on the fibre diameter distribution at the collection distances of 10cm and 15cm.

Effect of Increasing Applied Voltage on the Fibre Diameter Distribution at 10cm Collection Distance at 12kV and 20kV using PVA 8%

Figure 60 and 61 show the fibre diameter distribution increases with increasing voltage at 10cm collection distance. Figure 60 shows the distribution at 12kV with diameters ranging from 121-345nm. Figure 61 shows the distribution at 20kV with diameters ranging from 39-269nm.

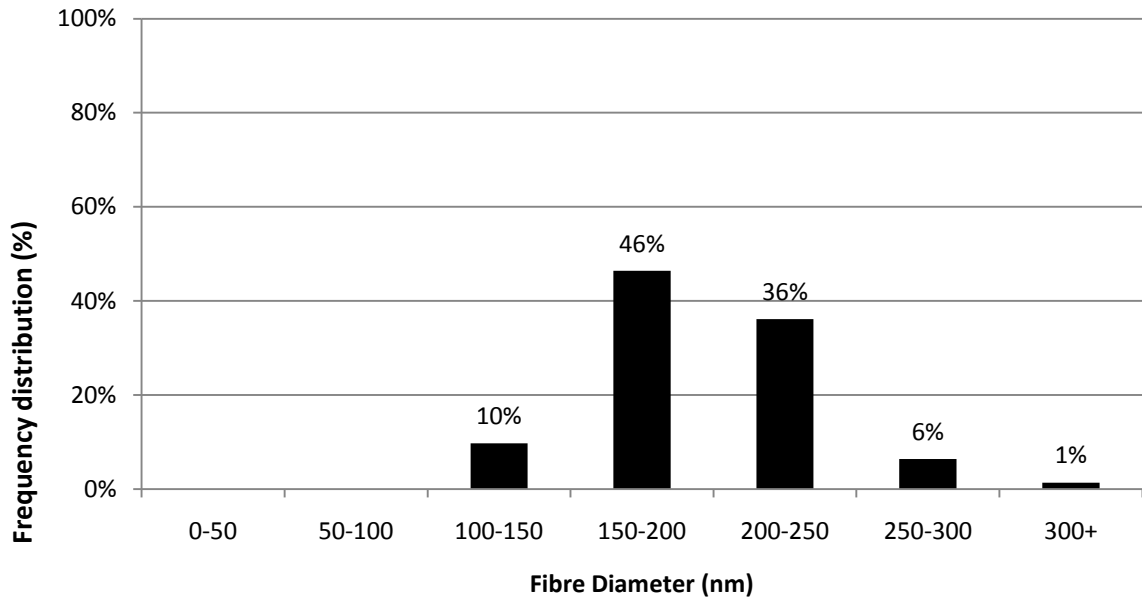


Figure 60. Percentage of Fibre Diameter Distribution of PVA 8% Solution at 10cm Collection Distance and 12kV

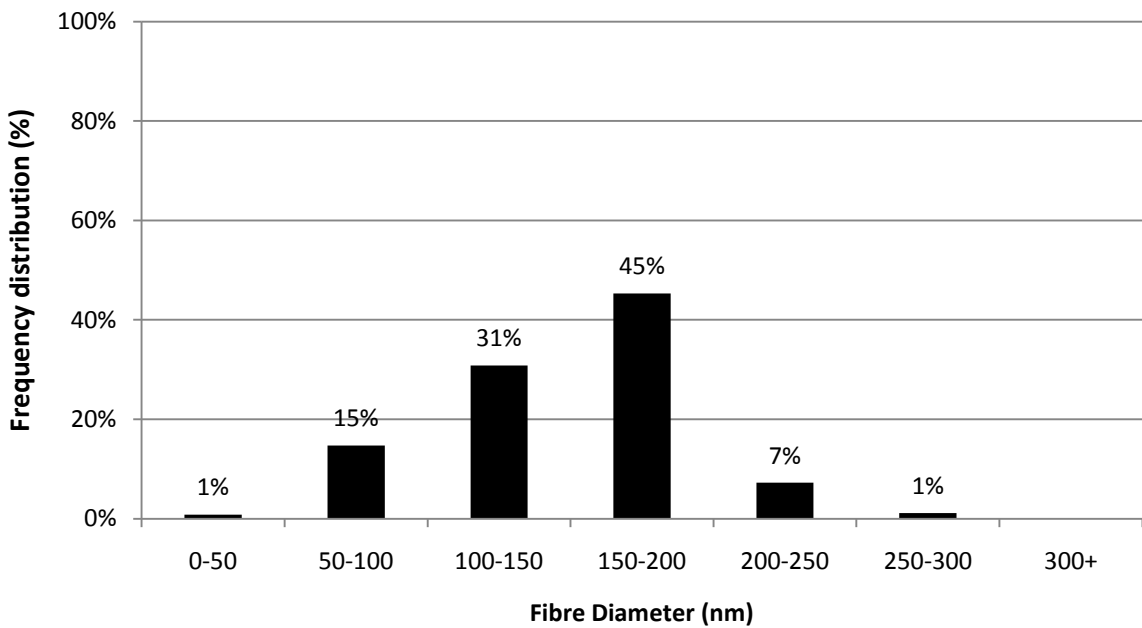


Figure 61. Total Percentage of Fibre Diameter Distribution of PVA 8% Solution at 10cm Collection Distance and 20kV

Effect of Increasing Applied Voltage on the Fibre Diameter Distribution at 15cm Collection

Distance at 12kV and 20kV using PVA 8%

Figure 62 and 63 shows the fibre diameter distribution increases with increasing voltage at 15cm collection distance. Figure 62 shows the fibre diameter distribution at 12kV consisting of diameters ranging from 121-385nm. Figure 63 shows the distribution at 20kV consisting of diameters ranging from 115-423nm.

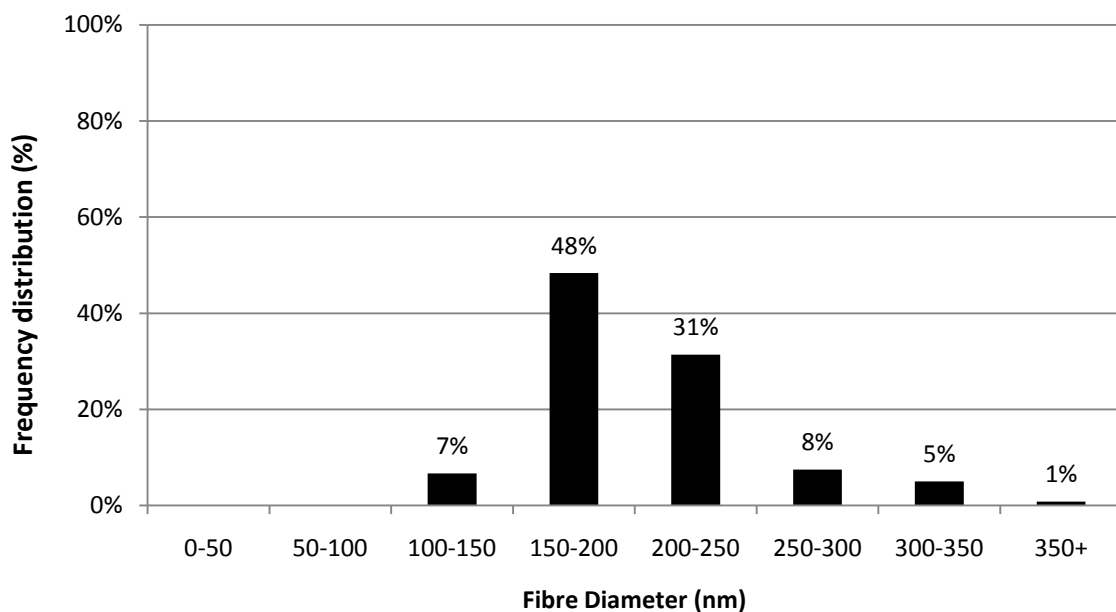


Figure 62. Percentage of Fibre Diameter Distribution of PVA 8% Solution at 15cm Collection Distance and 12kV

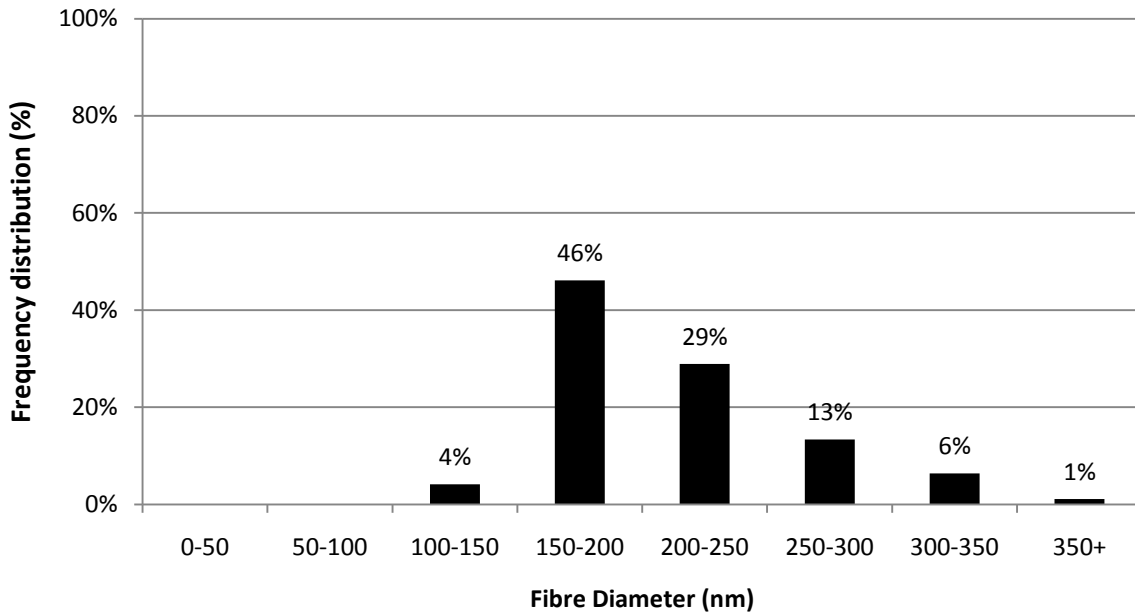


Figure 63. Total Percentage of Fibre Diameter Distribution of PVA 8% Solution at 15cm Collection Distance and 20kV

4.2.3. Effect of Increasing Voltage on Deposition Rate

Figure 64 shows the effect of increasing applied voltage on deposition rate using PVA 4%, at voltages of 8kV, 12kV and 20kV with collection distances of 7cm, 10cm and 15cm. The results showed the deposition rate increased with increasing voltage. Figure 65 shows the deposition rate using PVA 6% with increasing voltages of 12kV, 18kV and 20kV at collection distances of 10cm and 15cm. At 10cm and 15cm collection distances the deposition rate varied with voltage. The rate increased from 12kV to 18kV, then decreased from 18kV to 20kV. Figure 66 shows the deposition rate at PVA 8% with increasing voltage using 12kV and 20kV, at collection distances of 10cm and 15cm. At 10cm collection distance the deposition rate decreased and at 15cm the rate increased with increasing voltage.

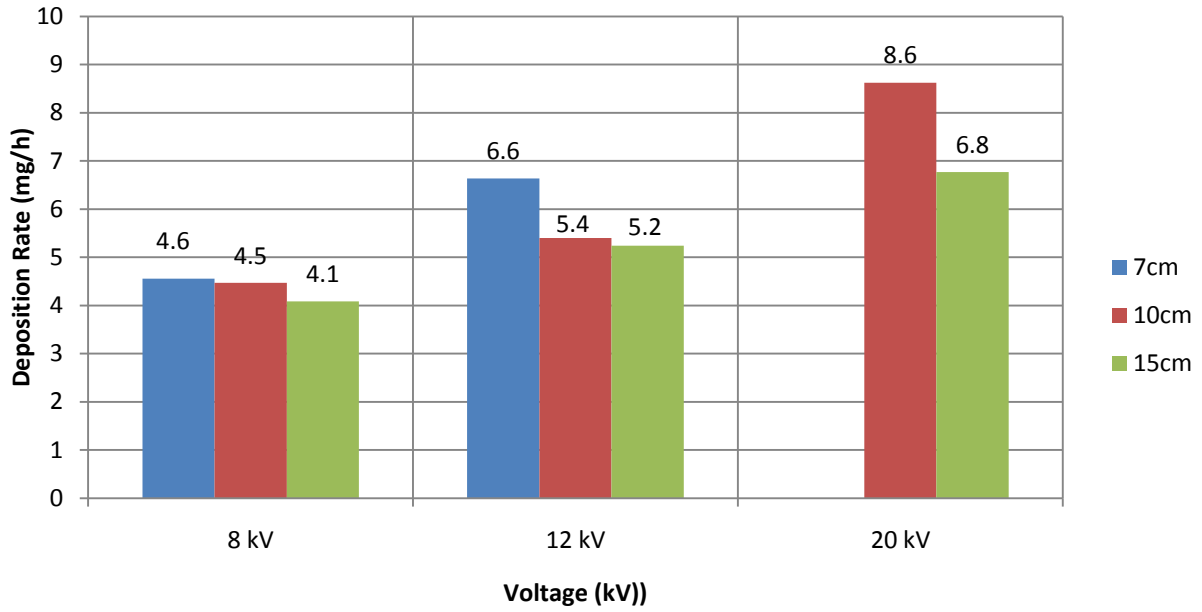


Figure 64. Deposition Rate of 4wt% PVA Solution Electrospun Fibres Collected on an Area of 2cm² Al Foil Collector

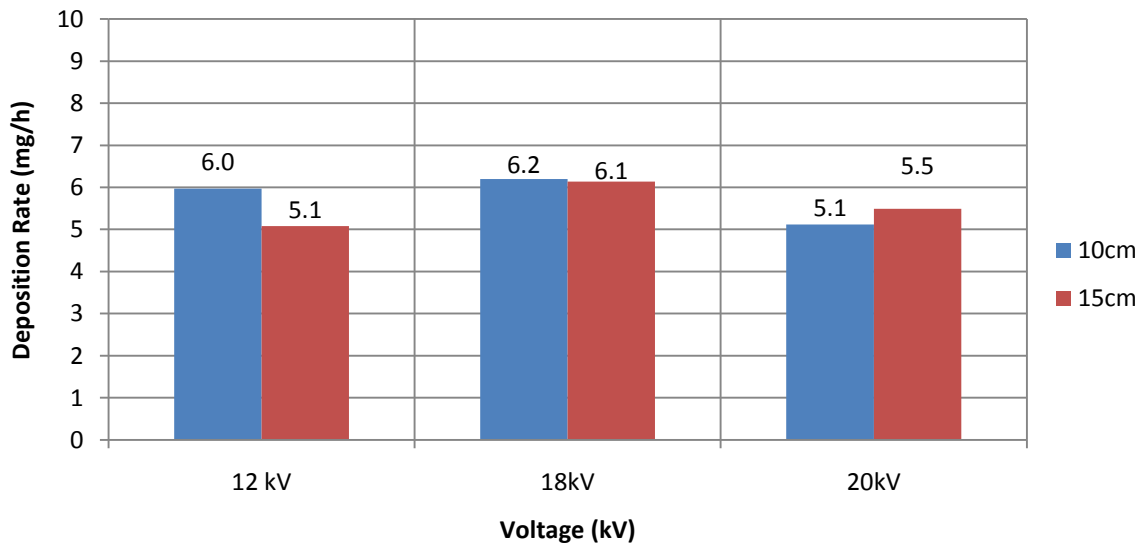


Figure 65. Deposition Rate of 6wt% PVA Solution Electrospun Fibres Collected on an Area of 2cm² Al Foil Collector

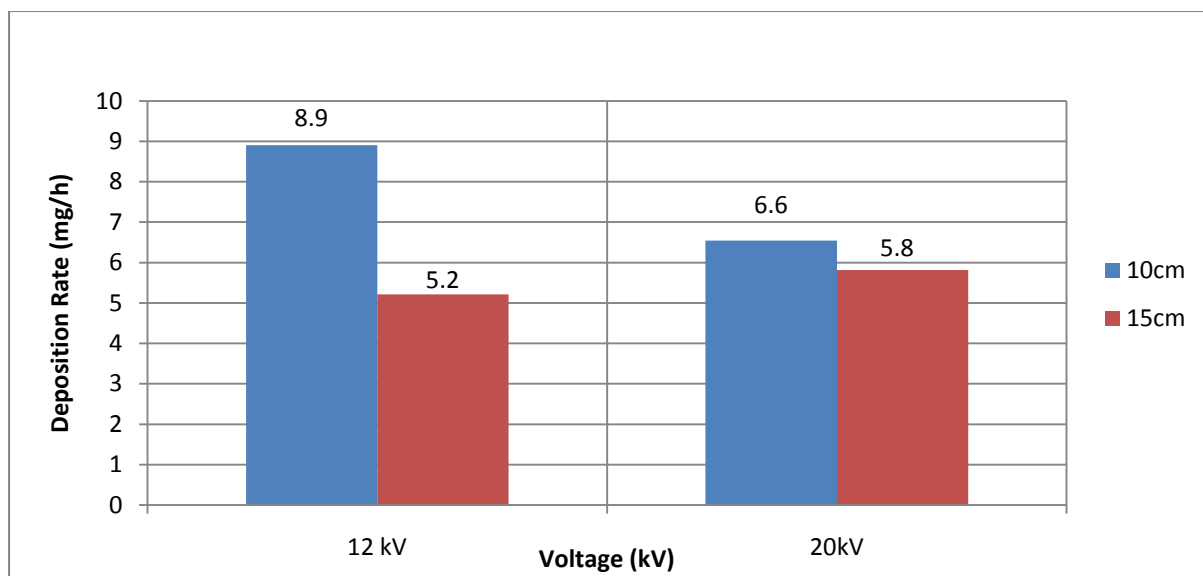


Figure 66. Deposition Rate of 8wt% PVA Solution Electrospun Fibres Collected on an Area of 2cm^2 Al Foil Collector

4.3. Collection Distance

4.3.1. Effect of Increasing Collection Distance on Fibre Diameter and Morphology

Effect of Increasing Collection Distance on Fibre Diameter and Morphology using PVA 4%

Figures 67 to 72 show the effect of increasing the collection distance on the average, maximum and minimum diameter and morphology of the fibres using PVA 4%. Collection distances of 7cm, 10cm and 15cm were used at voltages of 8kV, 12kV and 20kV.

Effect of Increasing Collection Distance on Fibre Diameter and Morphology at 8kV using PVA 4%

Figure 67 shows only beaded fibres were formed, consisting of a combination of spherical, spindle-like and elongated beads with increasing collection distance. The density of beaded fibres decreased with increasing collection distance. Fibre webbing also occurred at 7cm, which decreased with increasing collection distance. Figure 68 shows the average fibre diameter increased with increasing collection distance.

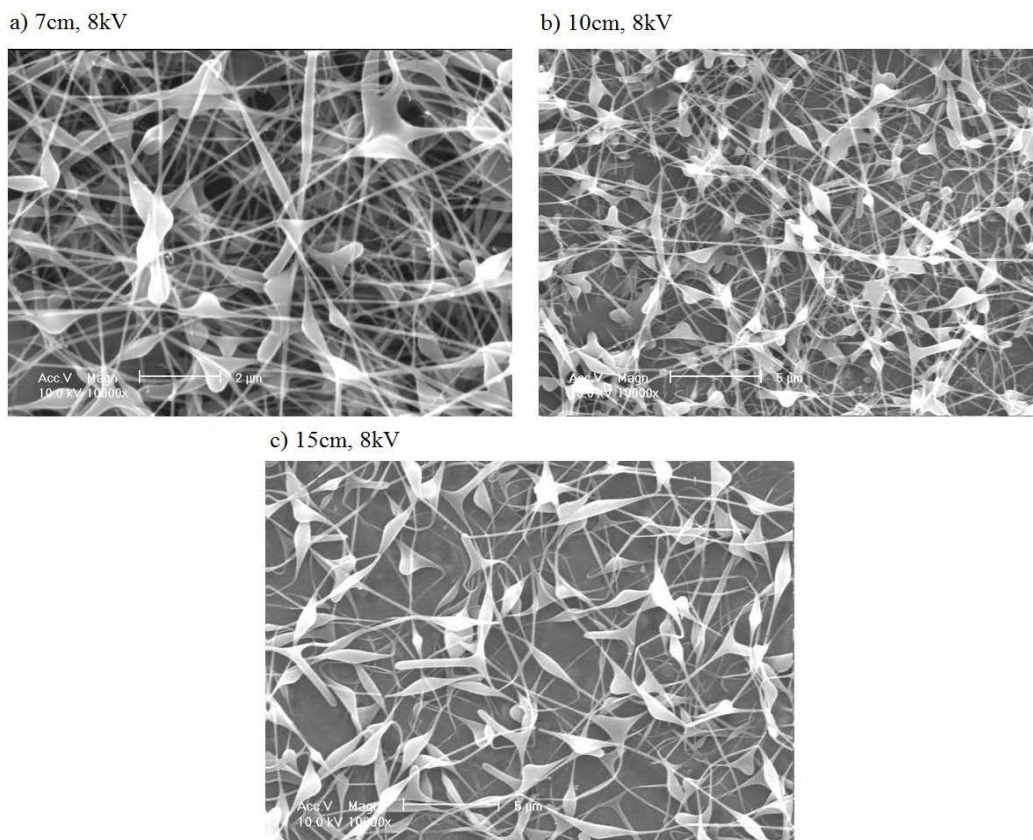


Figure 67. SEM images of electrospun PVA 4% using 8kV with increasing collection distance, a) 7cm, b) 10cm and c) 15cm

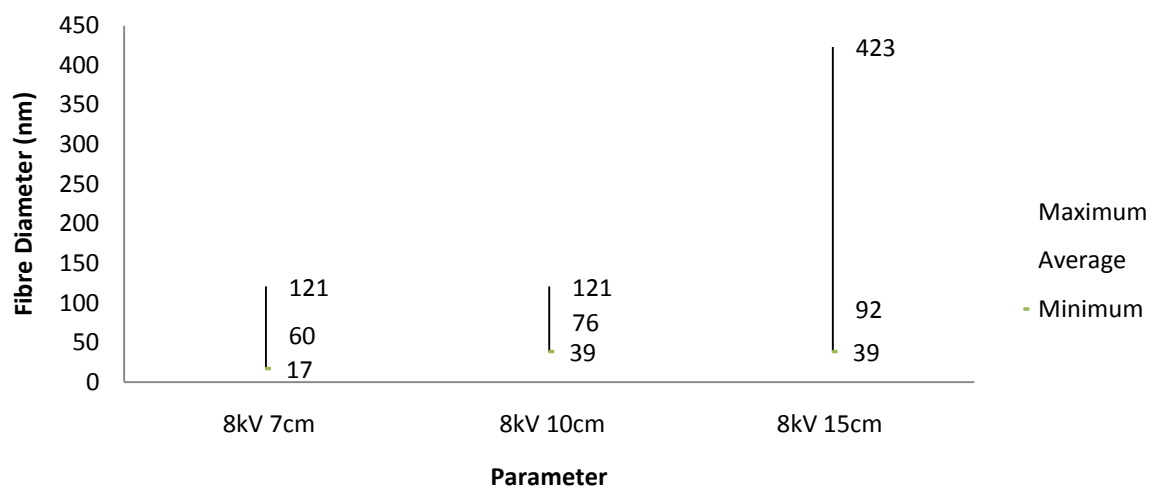


Figure 68. Overall Average, Maximum and Minimum Fibre Diameter of Electrospun PVA 4% Solution at 8kV with Increasing Collection Distance

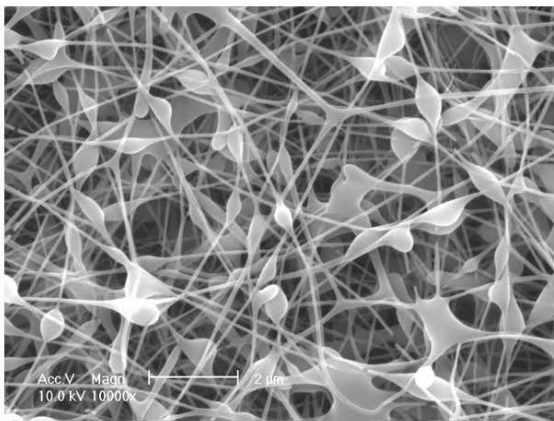
Effect of Increasing Collection Distance on Fibre Diameter and Morphology at 12kV using

PVA 4%

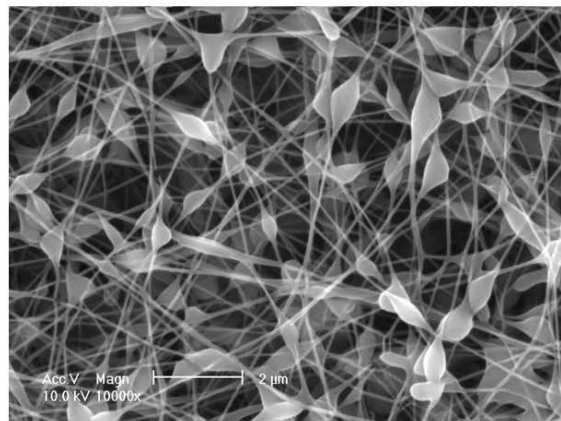
Figure 69 shows high densities of beads on fibres were formed at each collection distance.

Bead morphology consisted of spherical, spindle-like and elongated beads. Figure 70 shows the average fibre diameter decreased slightly as the collection distance increased.

a) 7cm, 12kV



b) 10cm, 12kV



c) 15cm, 12kV

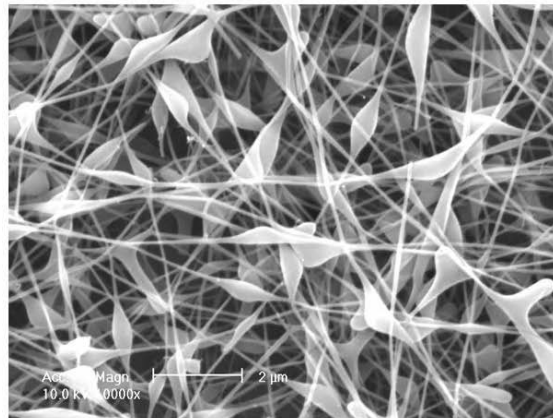


Figure 69. SEM images of electrospun PVA 4% using 12kV with increasing collection distance,

a) 7cm, b) 10cm and c) 15cm

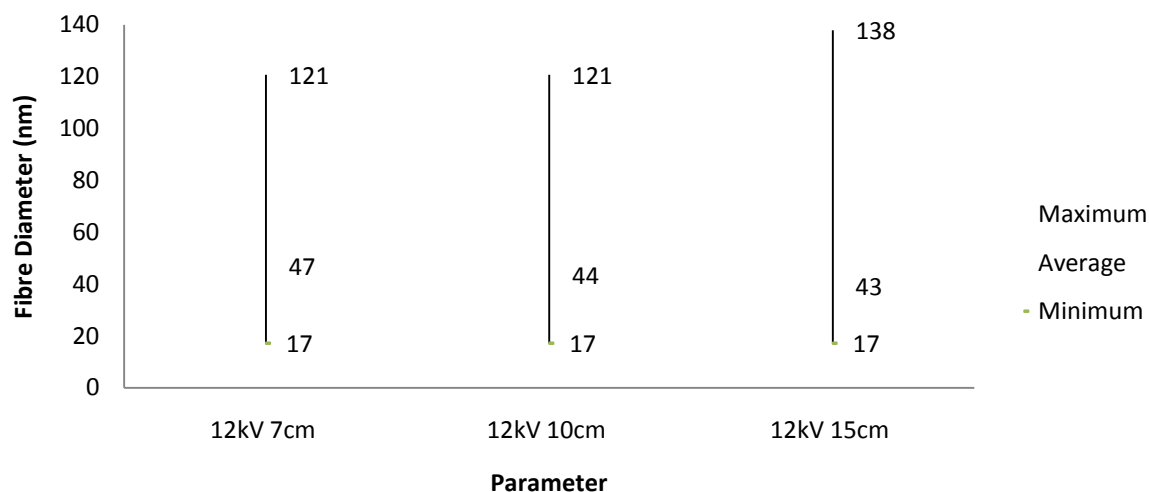
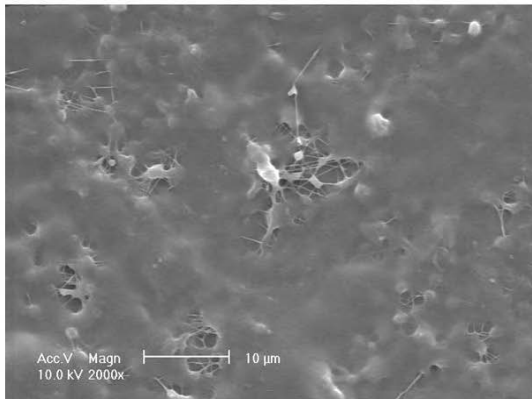


Figure 70. Overall Average, Maximum and Minimum Fibre Diameter of Electrospun PVA 4% Solution at 12kV with Increasing Collection Distance

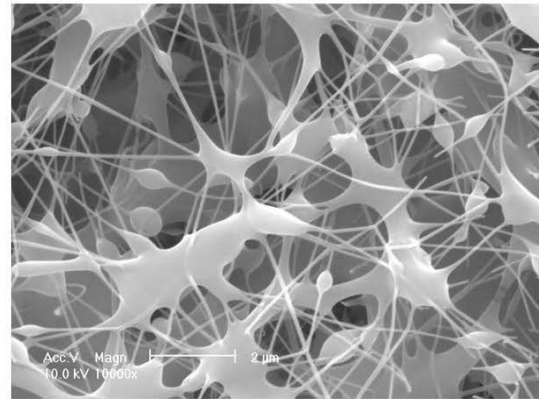
Effect of Increasing Collection Distance on Fibre Diameter and Morphology at 20kV using PVA 4%

Figure 71 shows no individual fibres were deposited at 7cm collection distance. At 10cm collection distance, the morphology consists of spherical shaped beads and fibre webs formed by merged beads and fibres. At 15cm collection distance, the beads on the fibres consisted of spherical, spindle- like and elongated beads and no fibre webs were observed. Figure 72 shows the average fibre diameter increased slightly with increasing collection distance.

a) 7cm, 20kV



b) 10cm, 20kV



c) 15cm, 20kV

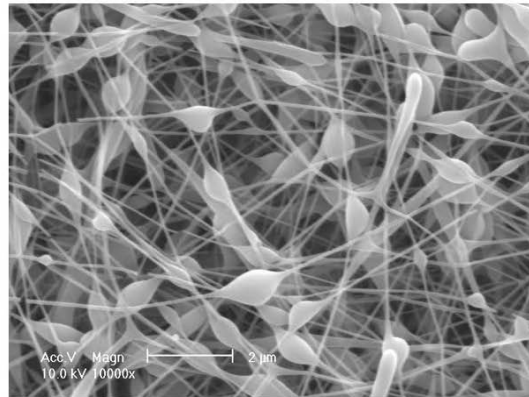


Figure 71. SEM images of electrospun PVA 4% using 20kV with increasing collection distance, a) 7cm, b) 10cm and c) 15cm

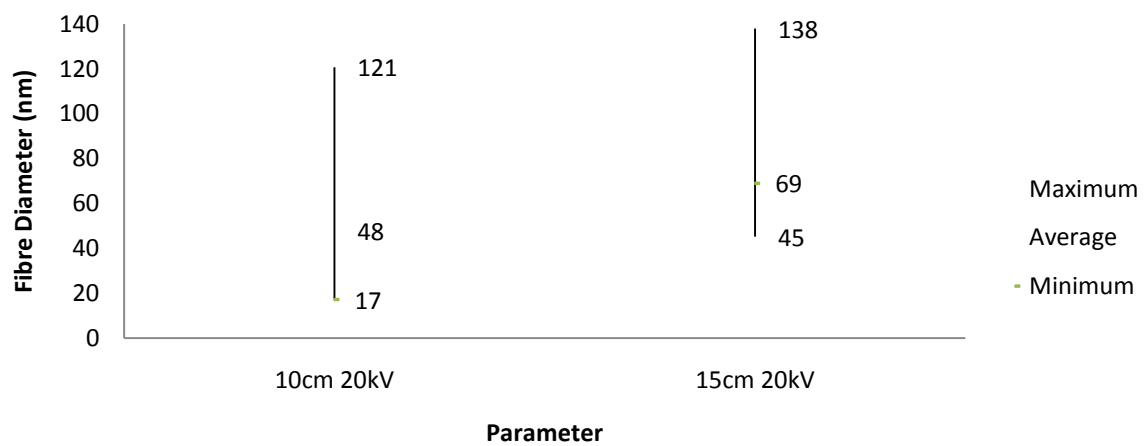


Figure 72. Overall Average, Maximum and Minimum Fibre Diameter of Electrospun PVA 4% Solution at 20kV with Increasing Collection Distance

Effect of Increasing Collection Distance on Fibre Diameter and Morphology using PVA 6%

Figures 73 to 78 show the effect of increasing the collection distance for PVA 6% on the average, maximum and minimum diameter and morphology of the fibres. The applied voltages of 12kV, 18kV and 20kV were used with increasing collection distances of 7cm (only at 12kV), 10cm and 15cm.

Effect of Increasing Collection Distance on Fibre Diameter and Morphology at 12kV using PVA 6%

Figure 73 shows a mixture of spherical and spindle-like beads on cylindrical fibres were formed with increasing collection distance. At 7cm collection distance the beads merged with neighbouring fibres or beads to form fibre webs. Fibre webs are not formed at 10cm and 15cm collection. The density of beaded fibres increased from 7cm to 10cm and reduced from 10cm to 15cm collection distance. At 15cm collection distance, majority of the fibres were beadless and uniform. Figure 74 shows the average fibre diameter decreases from 7cm to 10cm, increased slightly from 10cm to 15cm collection distance.

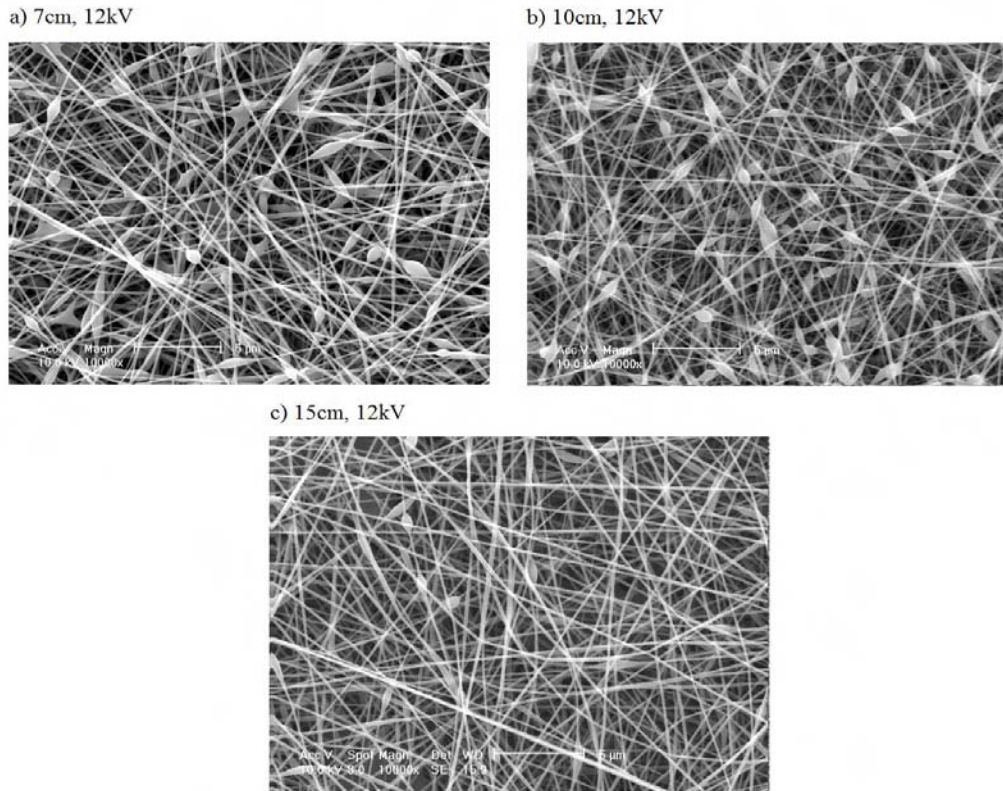


Figure 73. SEM images of electrospun PVA 6% using 12kV with increasing collection distance, a) 7cm, b) 10cm and c) 15cm

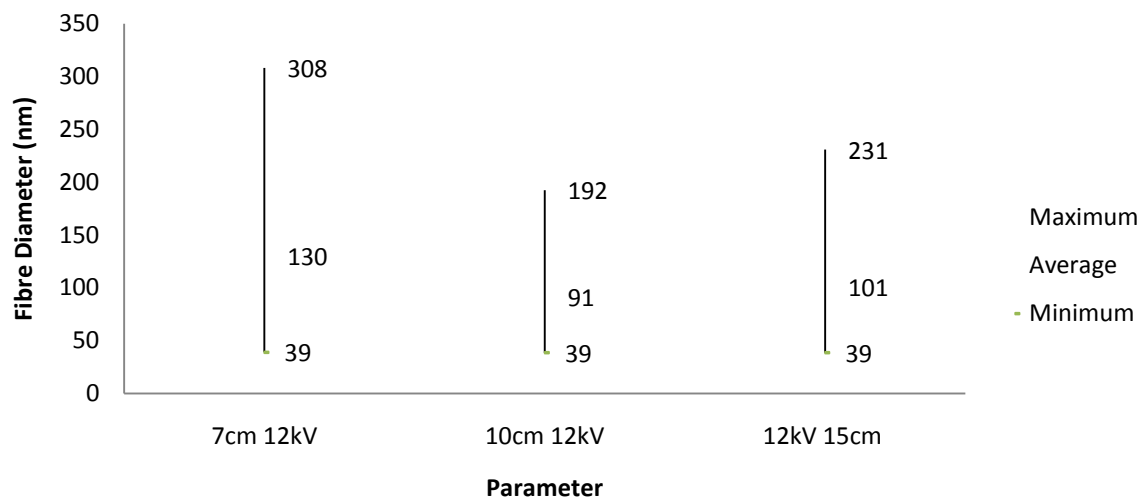


Figure 74. Overall Average, Minimum and Maximum Fibre Diameter of Electrospun Fibres of PVA 6% Solution at 12kV with Increasing Collection Distance

Effect of Increasing Collection Distance on Fibre Diameter and Morphology at 18kV using

PVA 6%

Figure 75 shows a distinct variation in the morphology observed with increasing collection distance. Large spherical and globular beads formed on fibres at 10cm collection distance and small, spindle-like beads formed on fibres at 15cm collection distance. The number and size of beads decreased with increasing collection distance. Figure 76 shows the average fibre diameter increased with increasing collection distance.

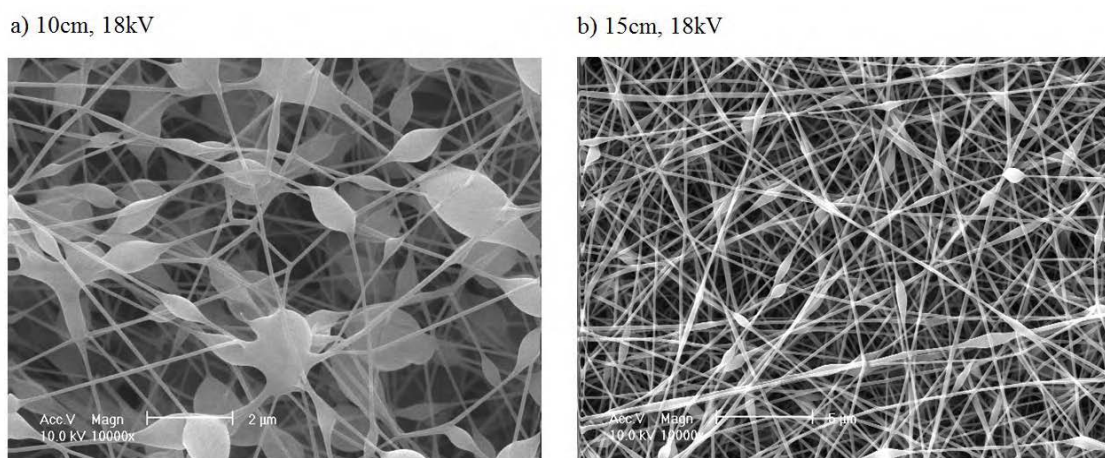


Figure 75. SEM images of electrospun PVA 6% using 18kV with increasing collection distance,

a) 10cm and b) 15cm

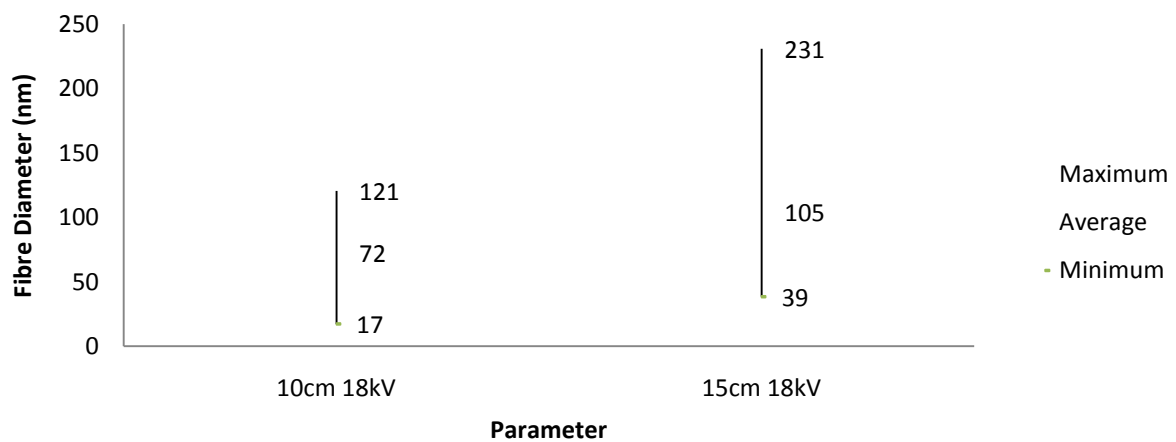


Figure 76. Overall Average, Minimum and Maximum Fibre Diameter of Electrospun Fibres of PVA 6% Solution at 18kV with Increasing Collection Distance

Effect of Increasing Collection Distance on Fibre Diameter and Morphology at 20kV using

PVA 6%

Figure 77 shows the number of beads increased with increasing collection distance. The bead morphology changed with increasing collection distance. Stretched, spindle-like beads formed on cylindrical fibres at 10cm collection distance. Smaller, spherical beads formed on fibres at 15cm collection distance. Figure 78 shows the average fibre diameter decreased with increasing collection distance.

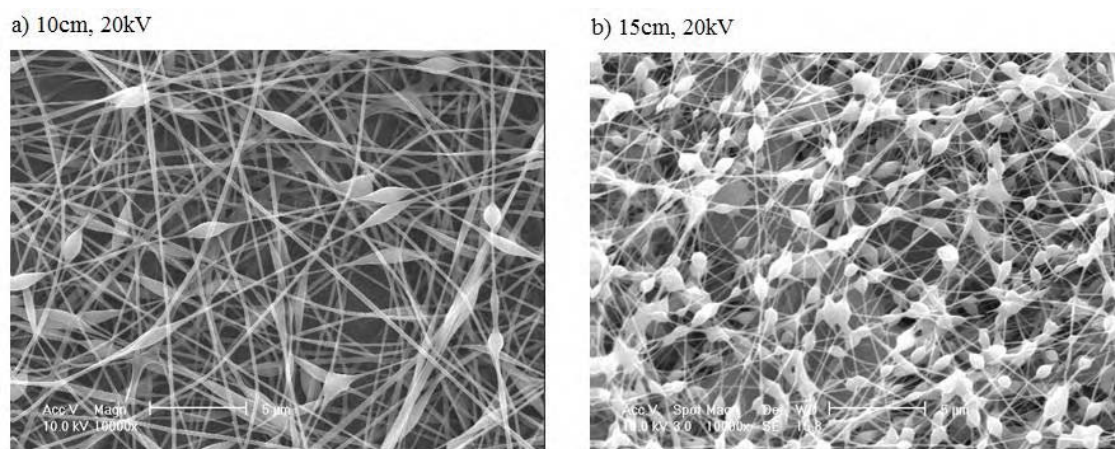


Figure 77. SEM images of electrospun PVA 6% using 20kV with increasing collection distance,

a) 10cm and b) 15cm

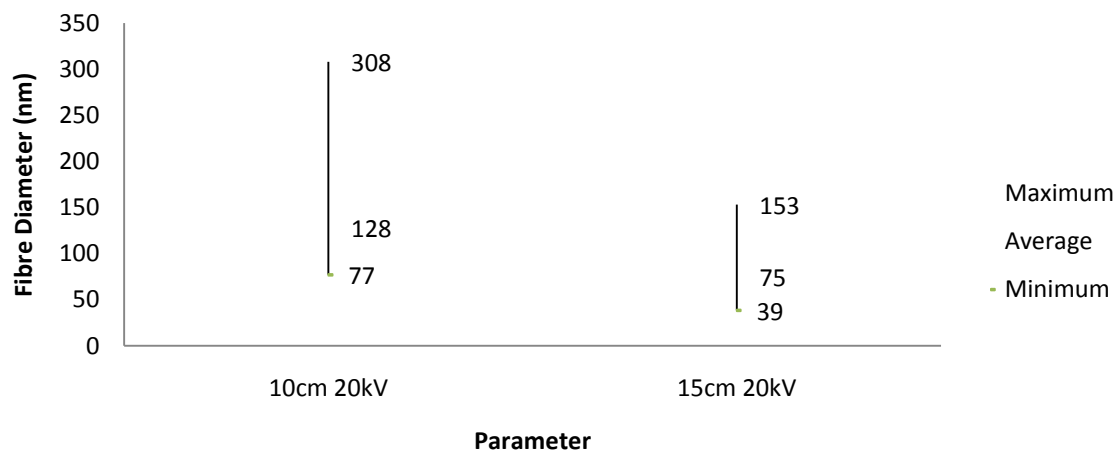


Figure 78. Overall Average, Minimum and Maximum Fibre Diameter of Electrospun Fibres of PVA 6% Solution at 20kV with Increasing Collection Distance

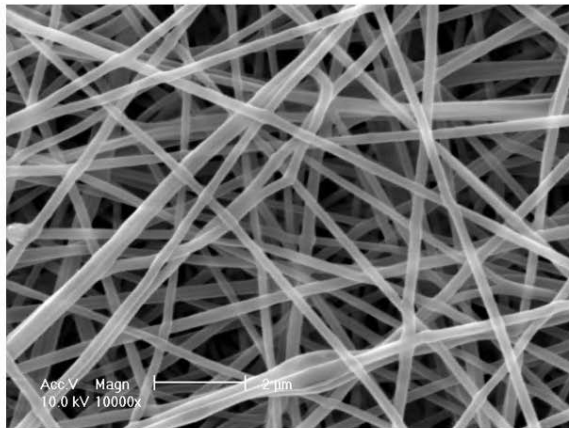
Effect of Increasing Collection Distance on Fibre Diameter and Morphology using PVA 8%

Figures 79 to 82 show the effect of increasing the collection distance using PVA 8% on the average, maximum and minimum diameter and morphology of the fibres formed. The applied voltages of 12kV and 20kV were used with increasing collection distances from 10cm and 15cm.

Effect of Increasing Collection Distance on Fibre Diameter and Morphology at 12kV using PVA 8%

Figure 79 shows smooth, beadless cylindrical fibres formed with increasing collection distance. At 10cm collection distance regions were formed where fibres overlapped and adhered to fibres beneath. Figure 80 shows the average fibre diameter increased slightly with increasing collection distance.

a) 10cm, 12kV



b) 15cm, 12kV

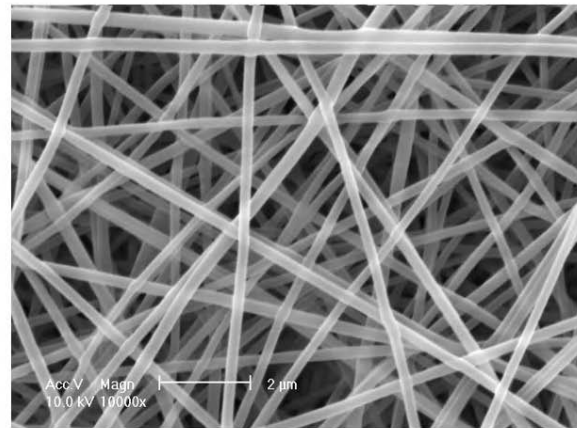


Figure 79. SEM images of electrospun PVA 8% using 12kV with increasing collection distance, a) 10cm and b) 15cm

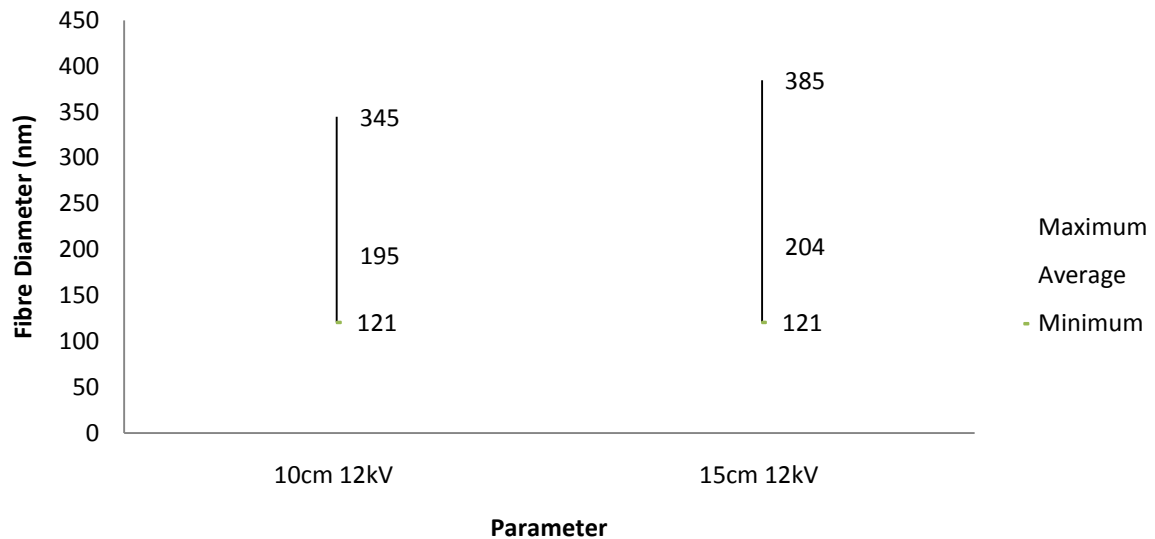
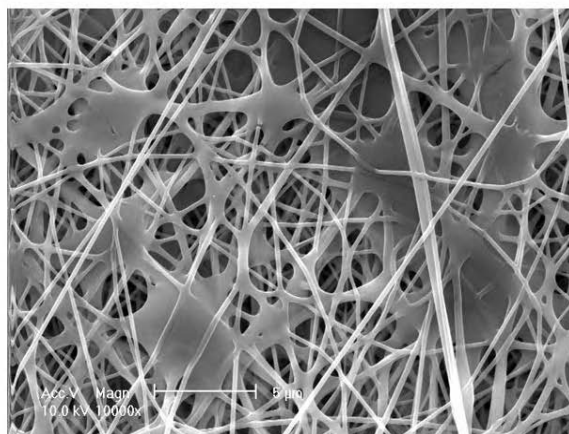


Figure 80. Overall Average, Minimum, Maximum Fibre Diameter of Electrospun PVA 8% Solution at 12kV with Increasing Collection Distance

Effect of Increasing Collection Distance on Fibre Diameter and Morphology at 20kV using PVA 8%

Figure 81 shows that beadless fibres with undulating fibre diameters were formed. At 10cm collection distance, fibre webbing occurred which diminished as the collection distance increased. Some features of flat ribbon fibres emerged at a reduced distance but which became more evident as distance increased. At 15cm collection distance, a mixture of flat ribbon and cylindrical fibres deposit on the collector. Fibres merged together to form a single large fibre at both collection distances. Figure 82 shows the average fibre diameter increased slightly with increasing collection distance.

a) 10cm, 20kV



b) 15cm, 20kV

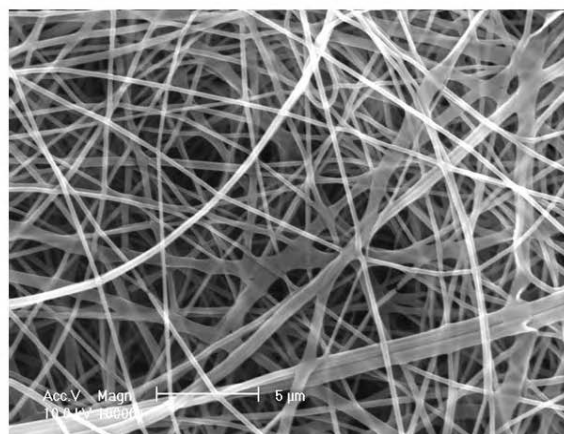


Figure 81. SEM images of electrospun PVA 8% using 20kV with increasing collection distance, a) 10cm and b) 15cm

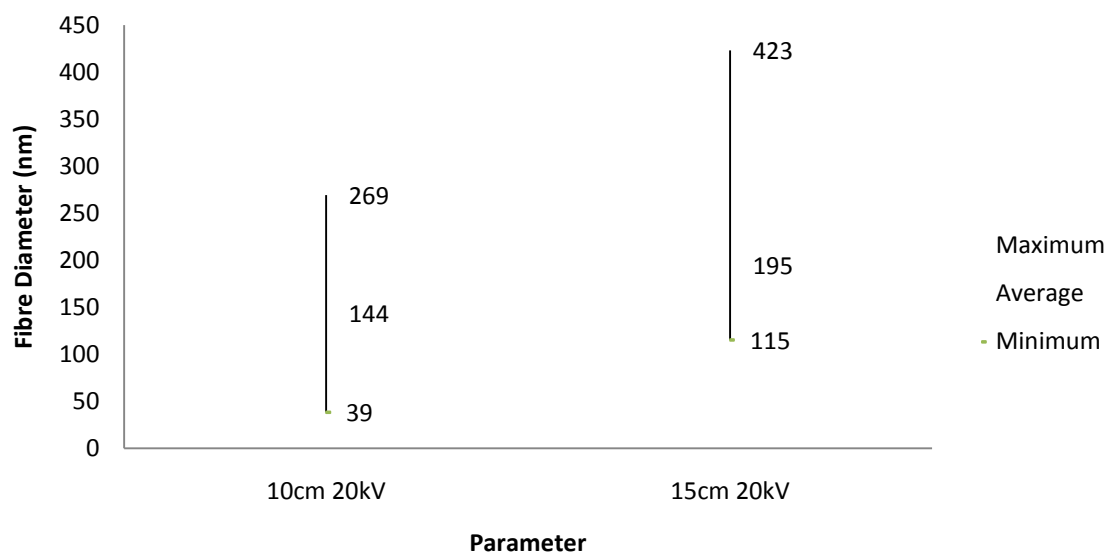


Figure 82. Overall Average, Minimum and Maximum Fibre Diameter of Electrospun PVA 8% Solution at 20kV with Increasing Collection Distance

4.3.2. Effect of Increasing Collection Distance on Fibre Diameter Distribution

Effect of Increasing Collection Distance on Fibre Diameter Distribution using PVA 4%

Figures 83 to 90 show the effect of increasing collection distance on the fibre diameter distribution using PVA 4%. Increasing collection distances of 7cm, 10cm and 15cm at the voltages of 8kV, 12kV and 20kV were used.

Effect of Increasing Collection Distance on the Fibre Diameter Distribution at 8kV using PVA 4%

Figure 83 to 85 shows from 7cm to 10cm collection distance the fibre diameter distribution decreased and from 10cm to 15cm collection distance increased at 8kV. Figure 83 shows the fibre diameter distribution at 7cm collection distance with diameters ranging from 17-241nm. Figure 84 shows the distribution of fibres obtained at 10cm with diameters ranging from 39-192nm. Figure 85 shows the distribution at 15cm with diameters ranging from 39-423nm.

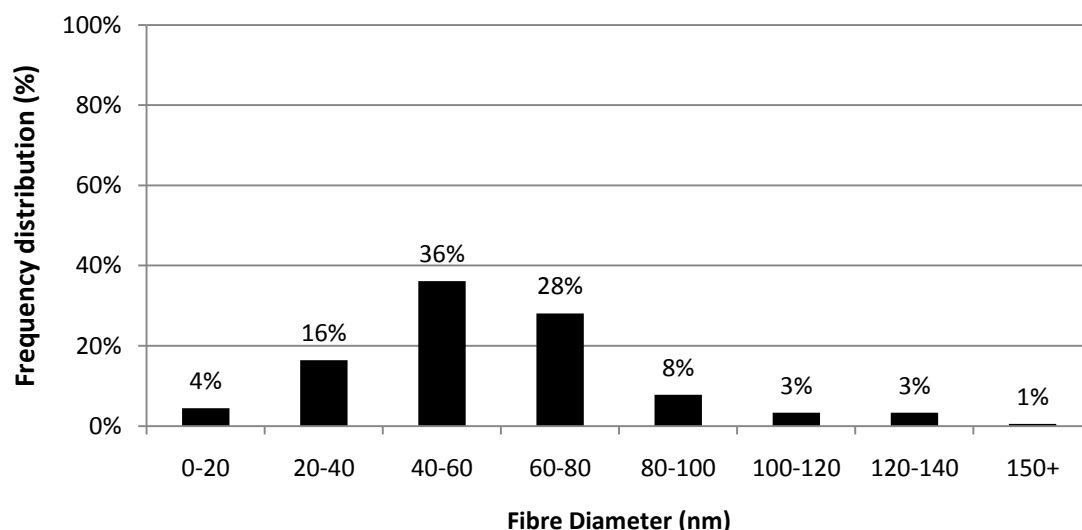


Figure 83. Total Percentage of Fibre Diameter Distribution of PVA 4% Solution at 7cm Collection Distance and 8kV

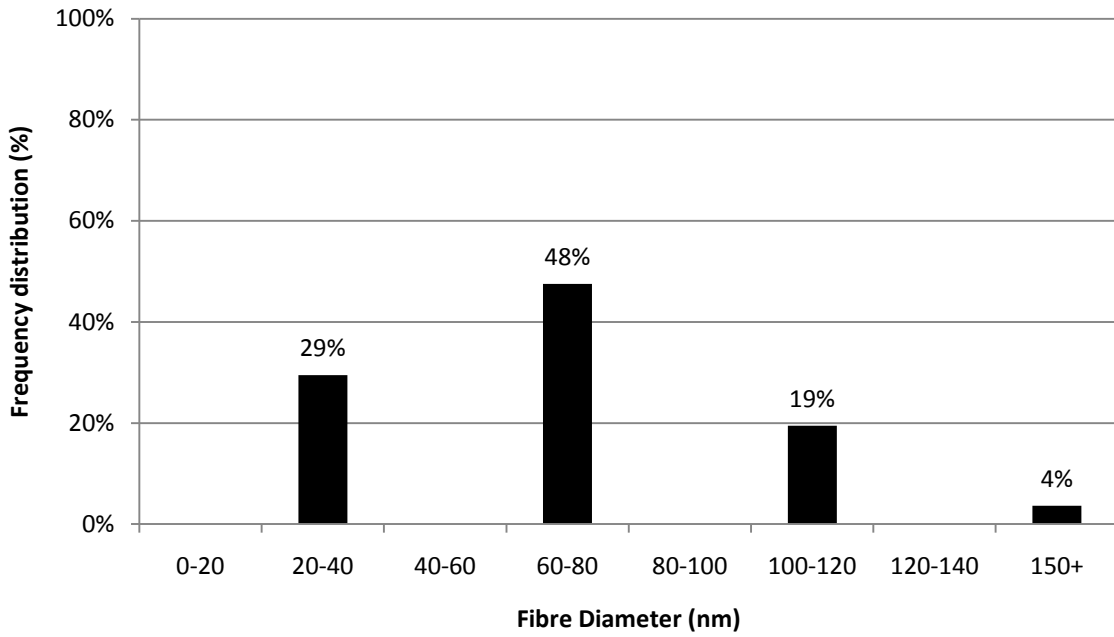


Figure 84. Total Percentage of Fibre Diameter Distribution of PVA 4% Solution at 10cm Collection Distance and 8kV

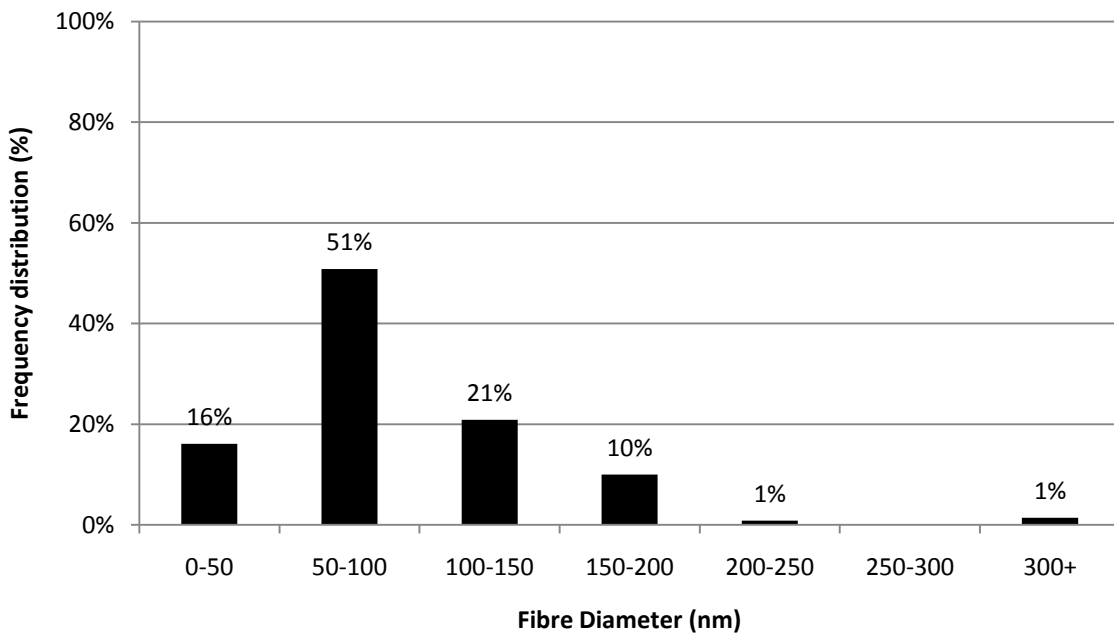


Figure 85. Total Percentage of Fibre Diameter Distribution of PVA 4% Solution at 15cm Collection Distance and 8kV

Effect of Increasing Collection Distance on the Fibre Diameter Distribution at 12kV using

PVA 4%

Figure 86 to 88 shows from 7cm to 10cm the fibre diameter distribution does not alter and from 10cm to 15cm collection distance increased at 12kV. Figure 86 shows the fibre diameter distribution at 7cm collection distance with diameters ranging from 17-121nm. Figure 87 shows the distribution of fibres obtained at 10cm collection distance with diameters ranging from 17-121nm. Figure 88 shows the distribution at 15cm collection distance with diameter ranging from 17-138nm.

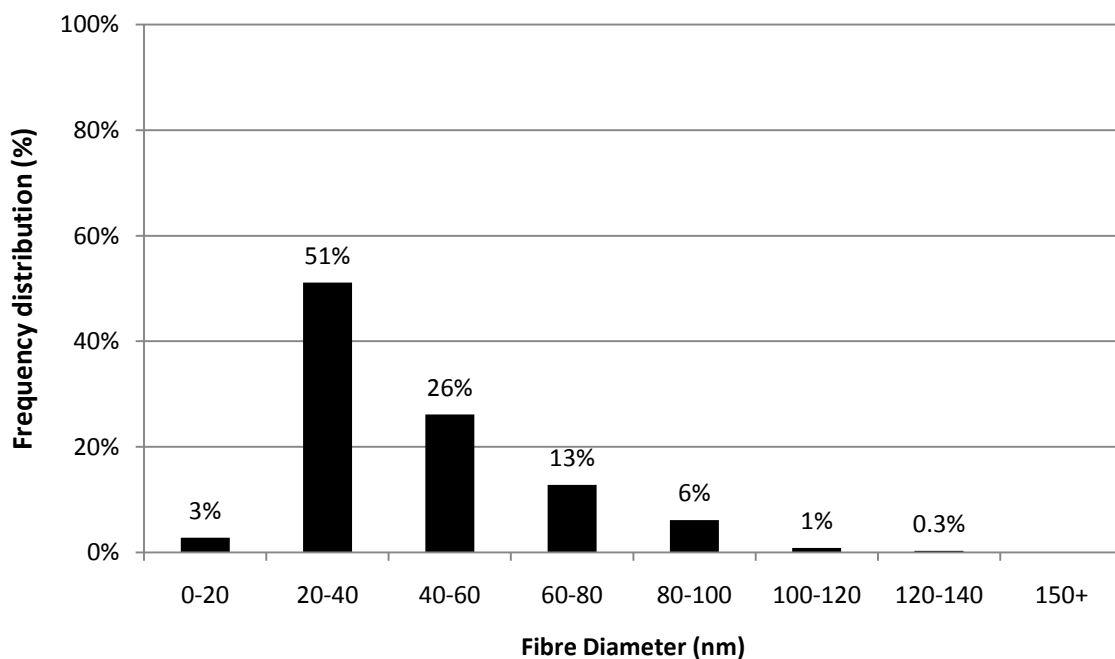


Figure 86. Total Percentage of Fibre Diameter Distribution of PVA 4% Solution at 7cm Collection Distance and 12kV

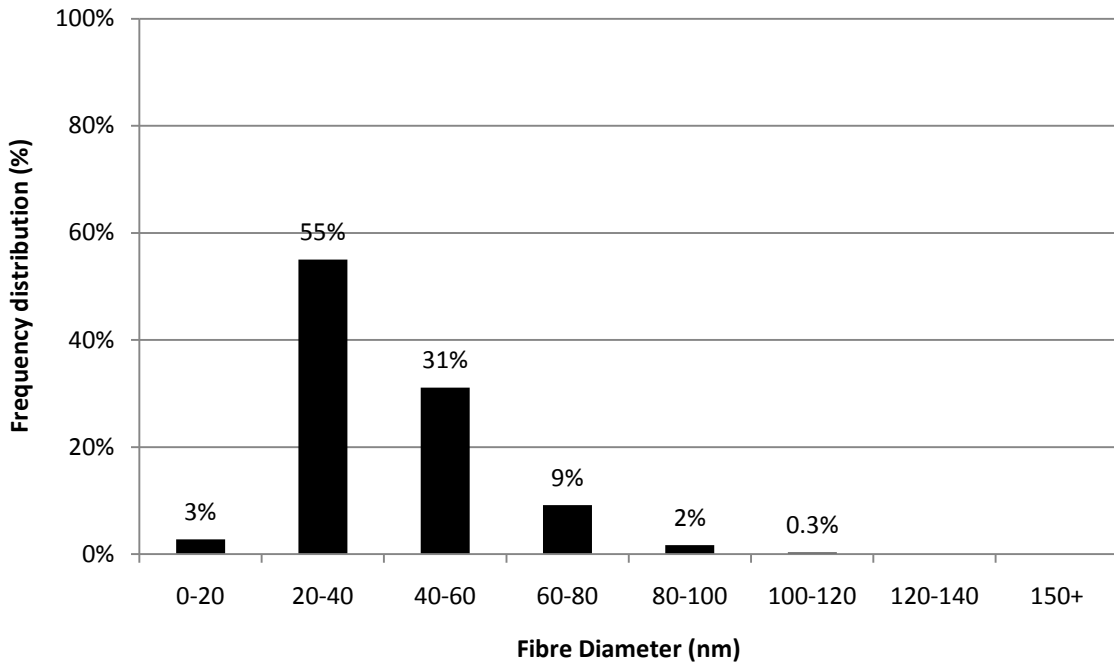


Figure 87. Total Percentage of Fibre Diameter Distribution of PVA 4% Solution at 10cm Collection Distance and 12kV

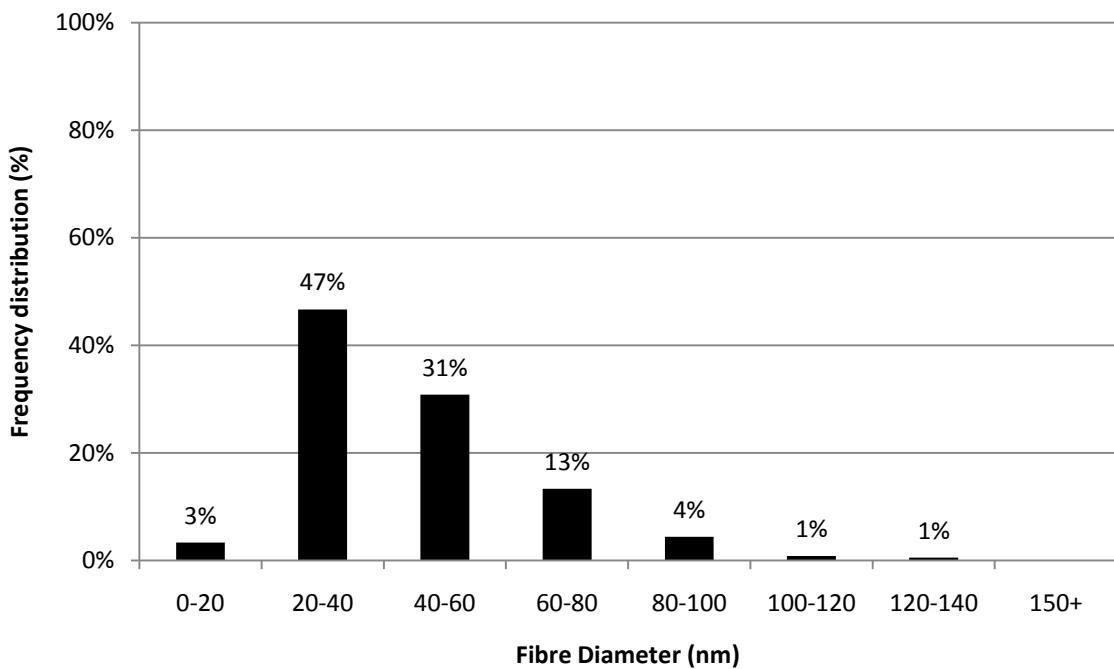


Figure 88. Total Percentage of Fibre Diameter Distribution of PVA 4% Solution at 15cm Collection Distance and 12kV

Effect of Increasing Collection Distance on the Fibre Diameter Distribution at 20kV using

PVA 4%

Figure 89 to 90 shows the fibre diameter distribution does not alter with increasing collection distance at 20kV. Figure 89 shows the fibre diameter distribution at 10cm collection distance with diameters ranging from 17-121nm. Figure 90 shows the distribution at 15cm with diameters ranging from 17-121nm.

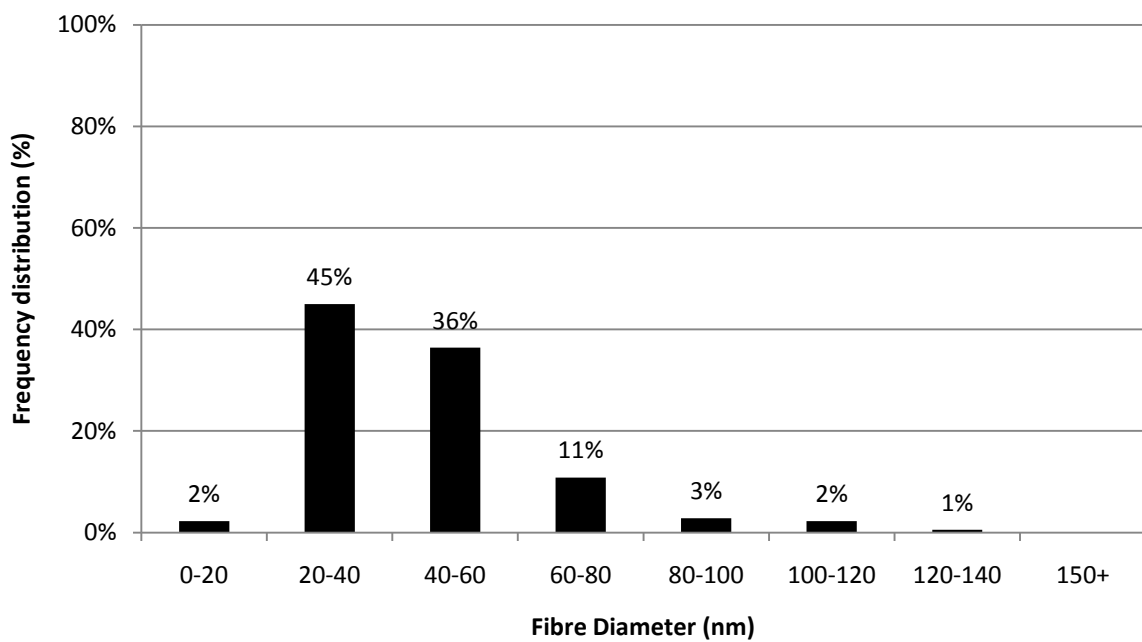


Figure 89. Total Percentage of Fibre Diameter Distribution of PVA 4% Solution at 10cm Collection Distance and 20kV

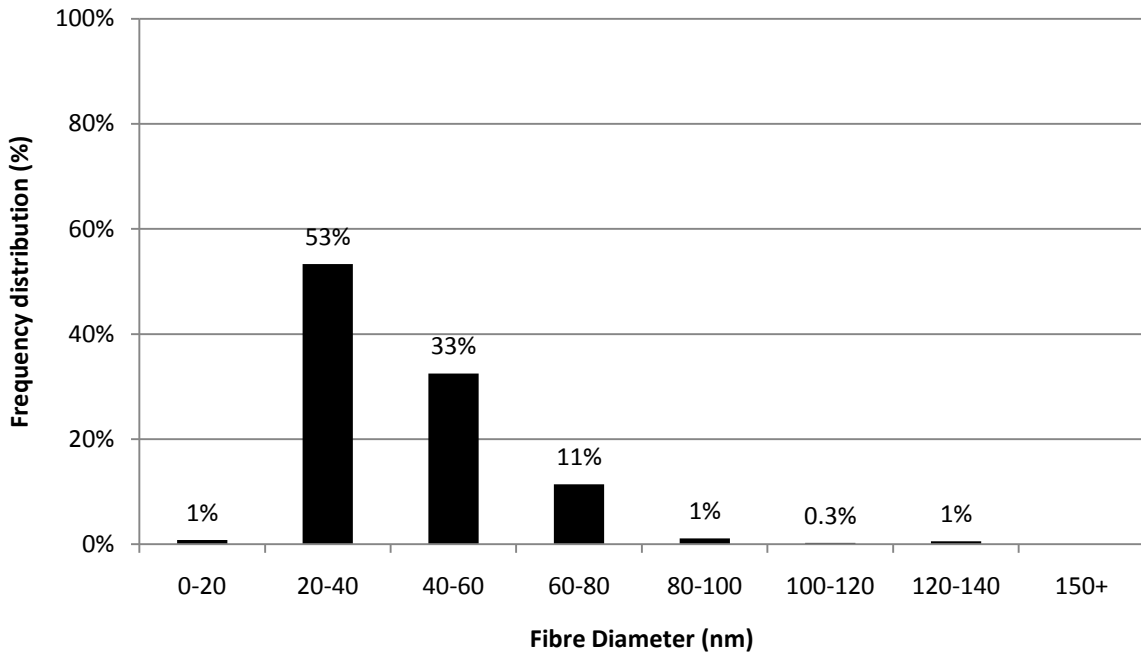


Figure 90. Total Percentage of Fibre Diameter Distribution of PVA 4% Solution at 15cm Collection Distance and 20kV

Effect of Increasing Collection Distance on Fibre Diameter Distribution using PVA 6%

Figures 83 to 90 show the effect of increasing collection distance using PVA 6% on the fibre diameter distribution at voltages of 8kV, 12kV and 20kV.

Effect of Increasing Collection Distance on the Fibre Diameter Distribution at 12kV using PVA 6%

Figure 91 to 93 shows from 7cm to 10cm collection distance the fibre diameter distribution decreased and from 10cm to 15cm collection distance the distribution increased. Figure 91 shows the fibre diameter distribution at 7cm collection distance with diameters ranging from 39-308nm. Figure 92 shows the distribution of fibres obtained at 10cm with diameters

ranging from 39-192nm. Figure 93 shows the distribution at 15cm collection distance with diameter ranging from 39-231nm.

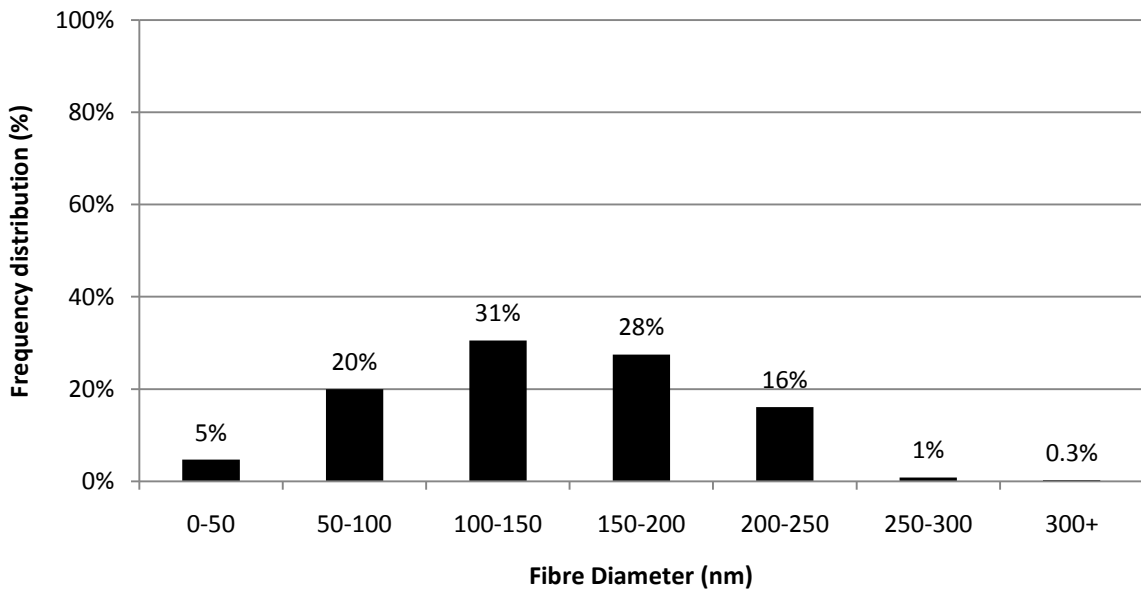


Figure 91. Total Percentage of Fibre Diameter Distribution of PVA 6% Solution at 7cm Collection Distance and 12kV

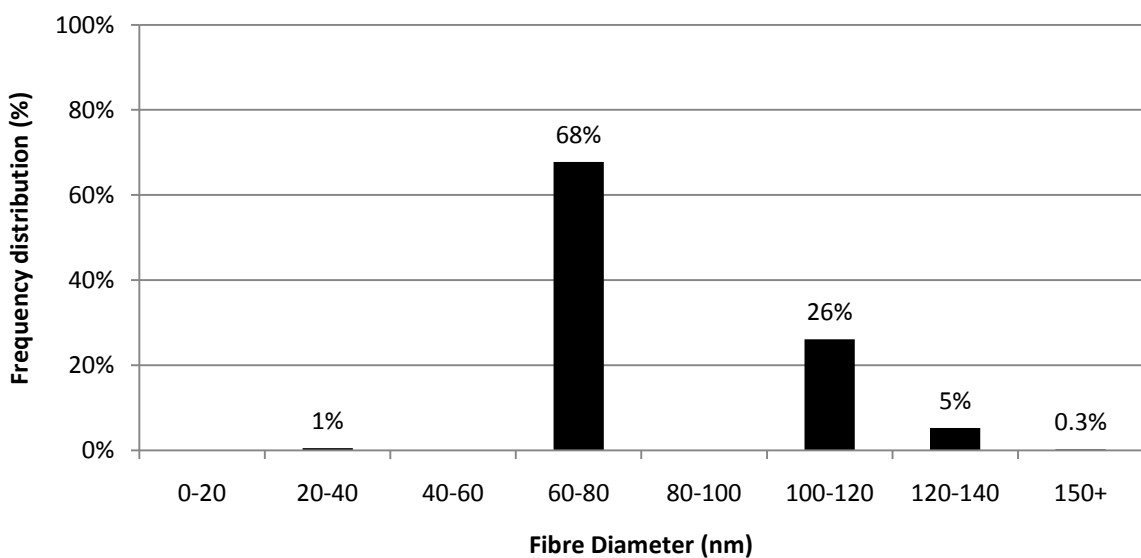


Figure 92. Overall Percentage of Fibre Diameter Distribution of PVA 6% Solution at 10cm Collection Distance and 12kV

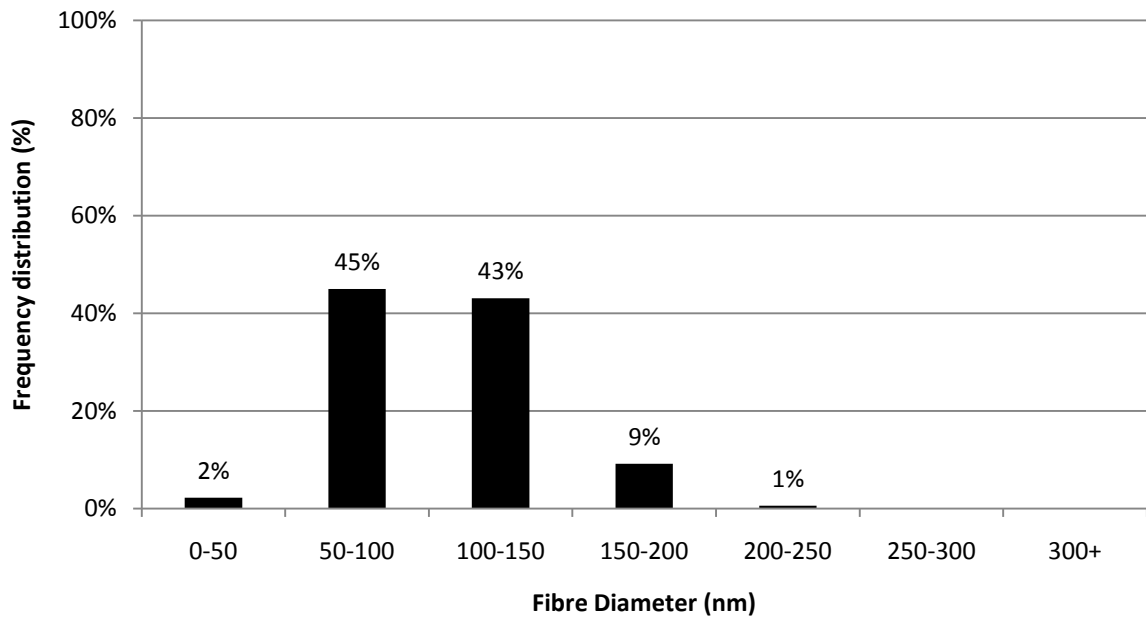


Figure 93. Total Percentage of Fibre Diameter Distribution of PVA 6% Solution at 15cm Collection Distance and 12kV

Effect of Increasing Collection Distance on the Fibre Diameter Distribution at 18kV using PVA 6%

Figure 94 and 95 show the fibre diameter distribution increased with increasing collection distance at 18kV. Figure 94 shows the fibre diameter distribution at 10cm collection distance with diameters ranging from 17-138nm. Figure 95 shows the distribution at 15cm collection distance with diameters ranging from 39-231nm.

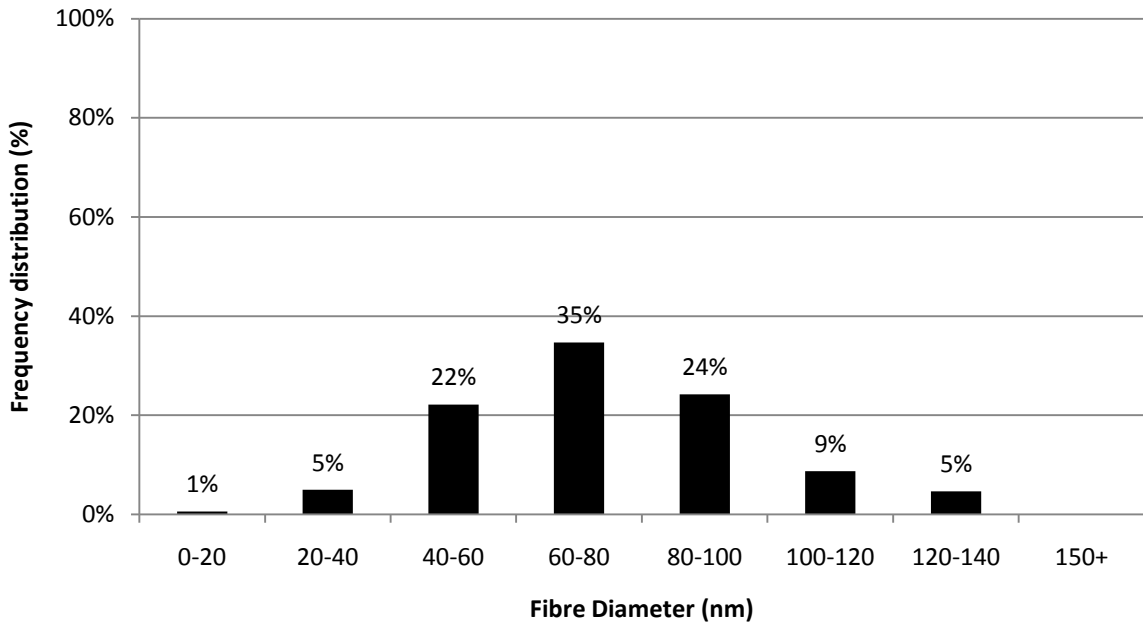


Figure 94. Total Percentage of Fibre Diameter Distribution of PVA 6% Solution at 10cm Collection Distance and 18kV

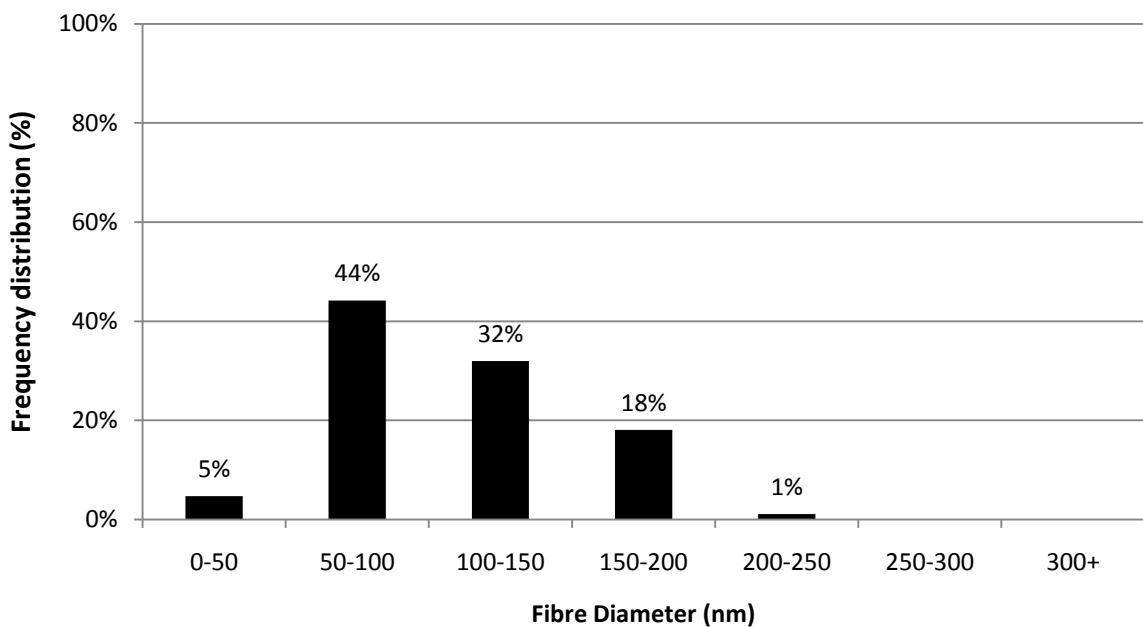


Figure 95. Total Percentage of Fibre Diameter Distribution of PVA 6% Solution at 15cm Collection Distance and 18kV

Effect of Increasing Collection Distance on the Fibre Diameter Distribution at 20kV using

PVA 6%

Figures 96 and 97 show the fibre diameter distribution decreased with increasing collection distance at 20kV. Figure 96 shows the fibre diameter distribution at 10cm collection distance with diameters ranging from 39-308nm. Figure 97 shows the distribution at 15cm collection distance with diameters ranging from 39-153nm.

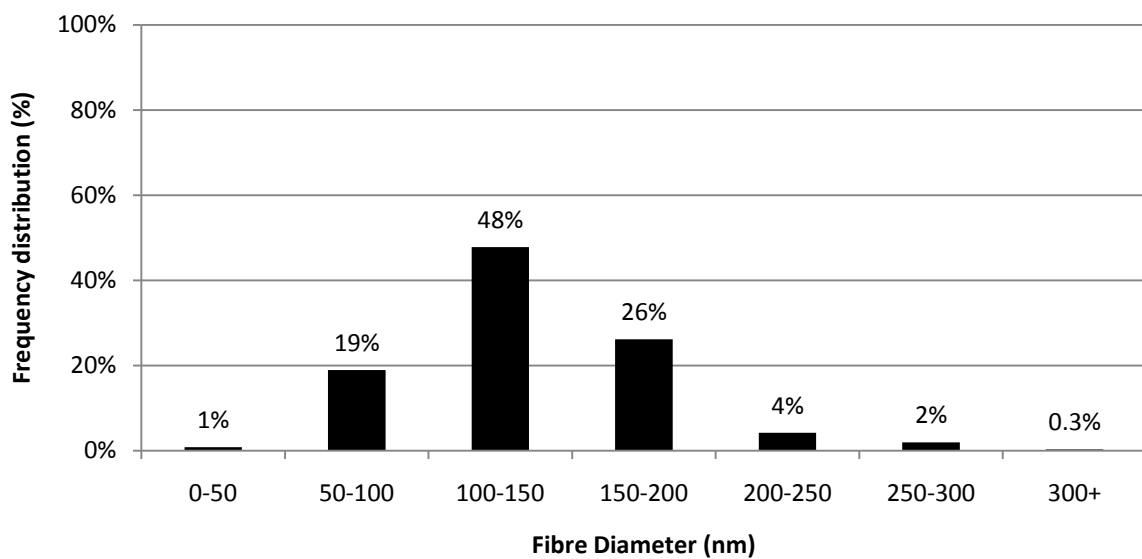


Figure 96. Total Percentage of Fibre Diameter Distribution of PVA 6% Solution at 10cm Collection Distance and 20kV

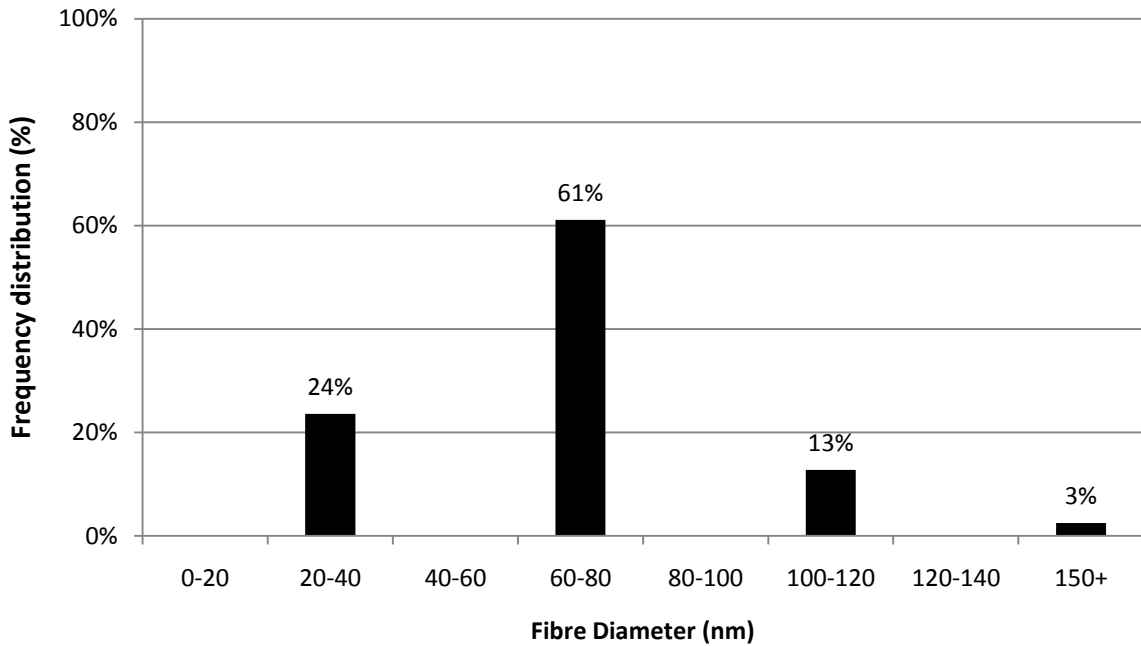


Figure 97. Total Percentage of Fibre Diameter Distribution of PVA 6% Solution at 15cm Collection Distance and 20kV

Effect of Increasing Collection Distance on Fibre Diameter Distribution using PVA 8%

Figures 99 to 102 show the effect of increasing collection distance using PVA 8% on the fibre diameter distribution at voltages of 12kV and 20kV.

Effect of Increasing Collection Distance on the Fibre Diameter Distribution at 12kV using PVA 8%

Figures 99 and 100 show the fibre diameter distribution increased with increasing collection distance at 12kV. Figure 99 shows the fibre diameter distribution at 10cm collection distance with diameters ranging from 121-345nm. Figure 100 shows the distribution of fibres obtained at 15cm collection distance with diameters ranging from 121-385nm.

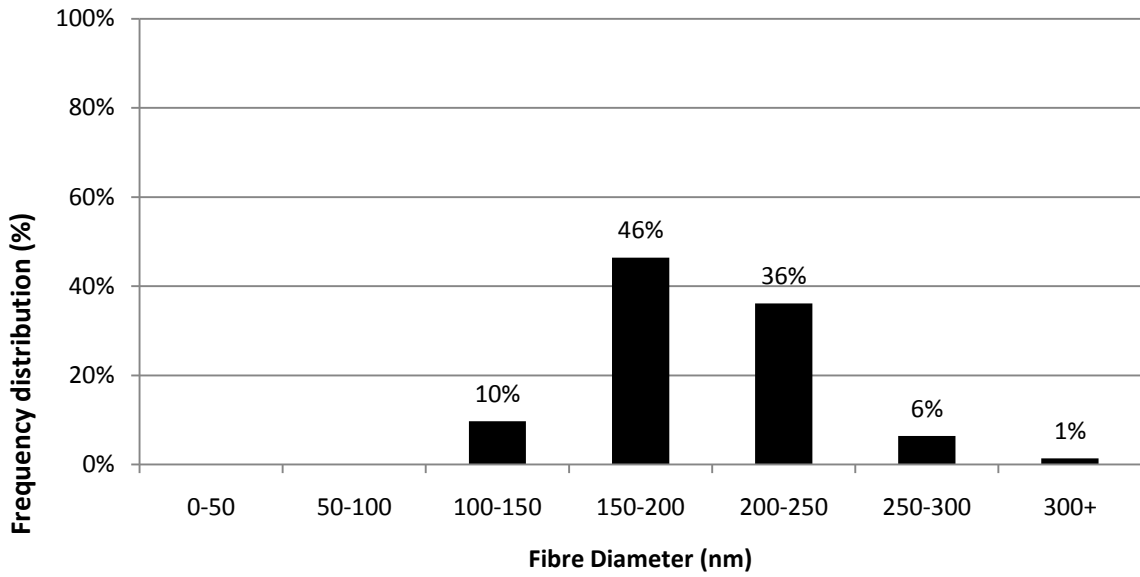


Figure 99. Percentage of Fibre Diameter Distribution of PVA 8% Solution at 10cm Collection Distance and 12kV

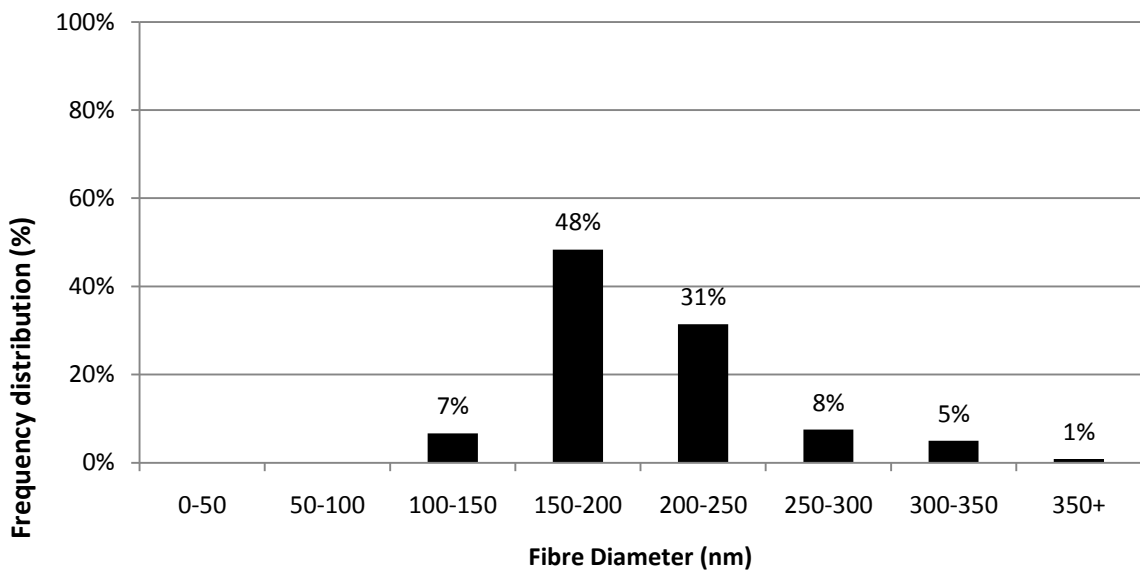


Figure 100. Percentage of Fibre Diameter Distribution of PVA 8% Solution at 15cm Collection Distance and 12kV

Effect of Increasing Collection Distance on the Fibre Diameter Distribution at 20kV using

PVA 8%

Figures 101 and 102 show the fibre diameter distribution increased with increasing collection distance at 20kV. Figure 101 shows the fibre diameter distribution at 10cm collection distance with diameters ranging from 39-269nm. Figure 102 shows the distribution of fibres obtained at 15cm collection distance with diameters ranging from 115-423nm.

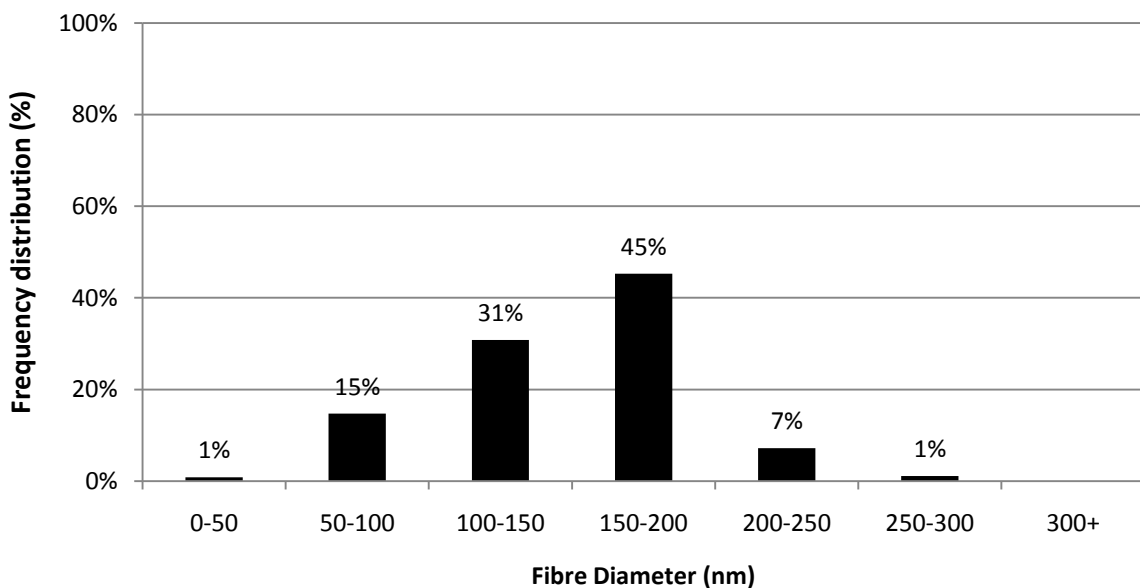


Figure 101. Total Percentage of Fibre Diameter Distribution of PVA 8% Solution at 10cm Collection Distance and 20kV

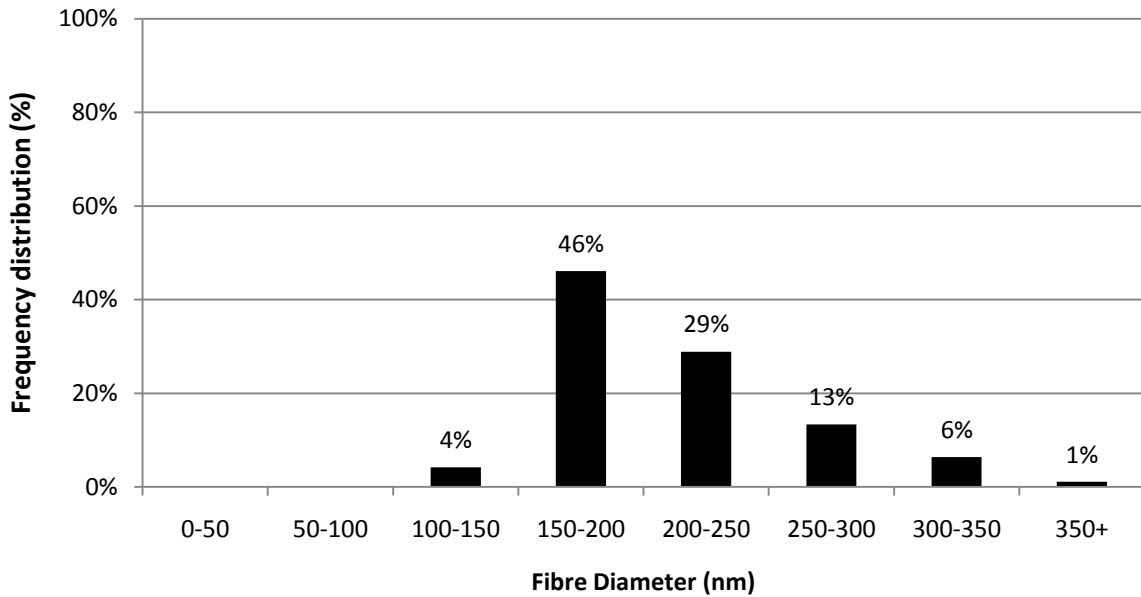


Figure 102. Total Percentage of Fibre Diameter Distribution of PVA 8% Solution at 15cm Collection Distance and 20kV

4.3.3. Effect of Increasing Collection Distance on Deposition Rate

Figure 103 shows using PVA 4%, at 8kV with increasing collection distance, an increase in deposition rate was observed from 7cm to 10cm collection distance and a decrease was observed from 10cm to 15cm collection distance. At 12kV, the deposition rate decreased with increasing collection distance, however, only a slight decrease was observed from 10cm to 15cm collection distance. At 20kV, the deposition rate decreased with increasing collection distance. Figure 104 shows at 12kV using PVA 6%, the deposition rate decreased with increasing collection distance. At 18kV the deposition rate decreased slightly with increasing collection distance. At 20kV the deposition rate increased with increasing collection distance. Figure 105 shows at 12kV using PVA 8% and at 20kV the deposition rate decreased with increasing collection distance.

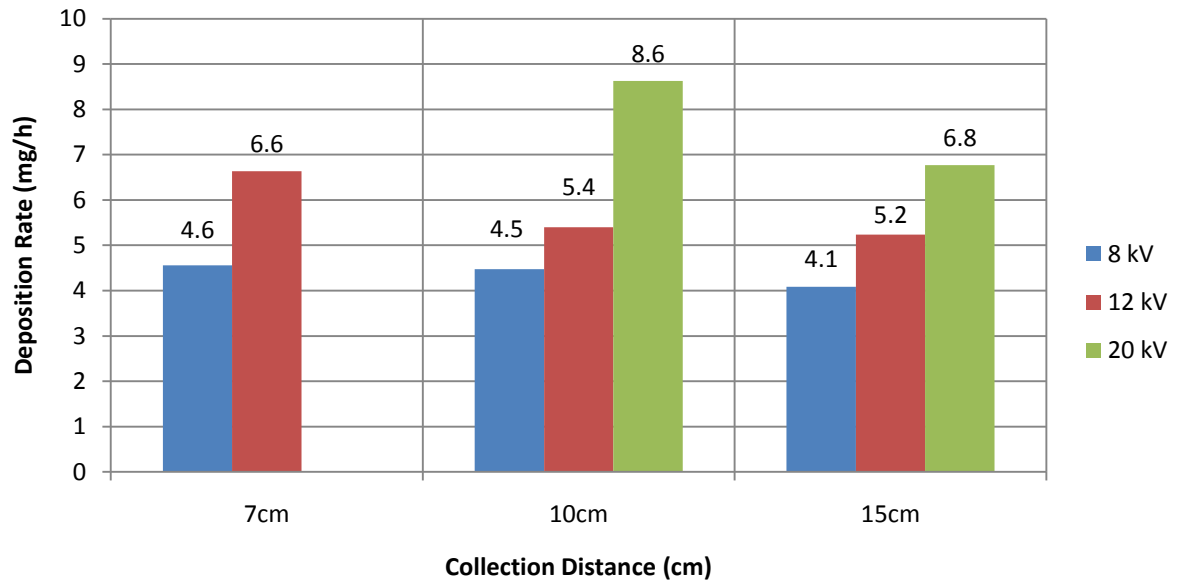


Figure 103. Deposition Rate of 4wt% PVA Solution Electrospun Fibres Collected on an Area of 2cm² Al Foil Collector

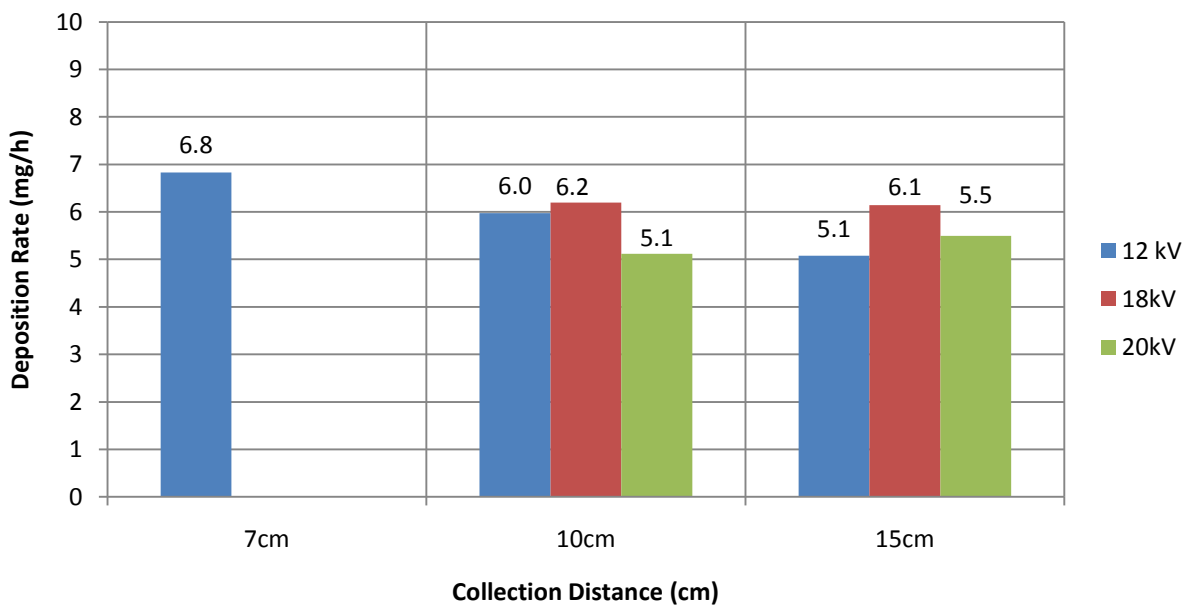


Figure 104. Deposition Rate of 6wt% PVA Solution Electrospun Fibres Collected on an Area of 2cm² Al Foil Collector

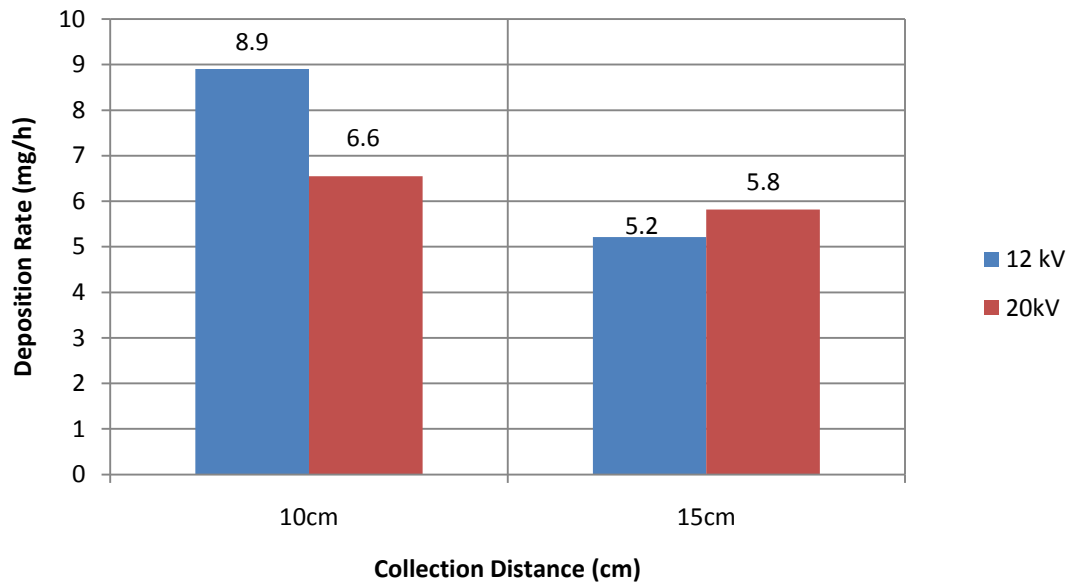


Figure 105. Deposition Rate of 8wt% PVA Solution Electrospun Fibres Collected on an Area of 2cm² Al Foil Collector

4.4. Beaded Fibre Morphology

Various bead morphologies were observed with fibres formed using PVA 4% and PVA 6%.

The observations are shown below.

The elongated bead width is greater than half the bead length, hence giving it an elongated shape.

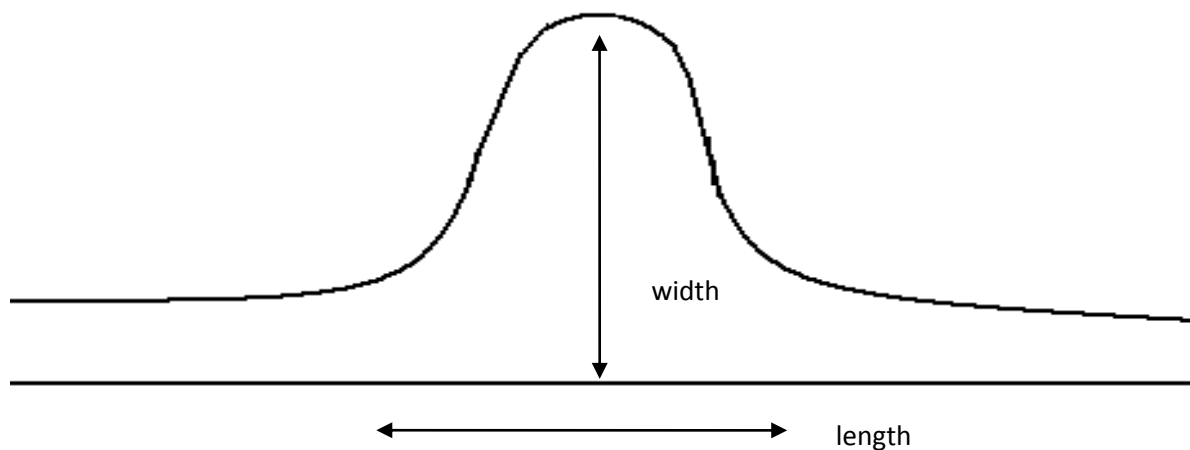


Figure 106. Elongated Bead

The spherical bead has a length equal to or up to double the width giving it a spherical shape.

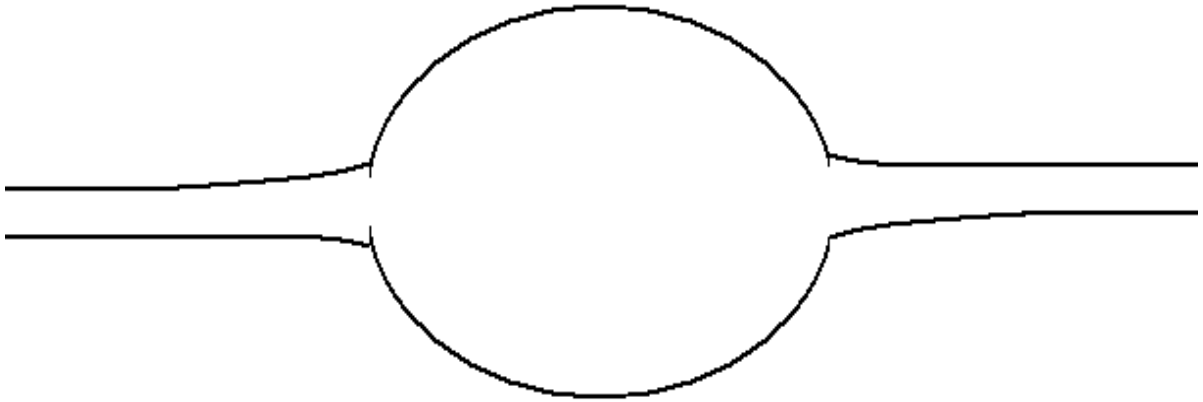


Figure 107. *Spherical Bead*

The spindle-bead has a length is double the width forming a shape that resembled a spindle. The bulge of the bead remained prominent. Sizes of these beads can be similar to that of 'spindle-like' morphology.

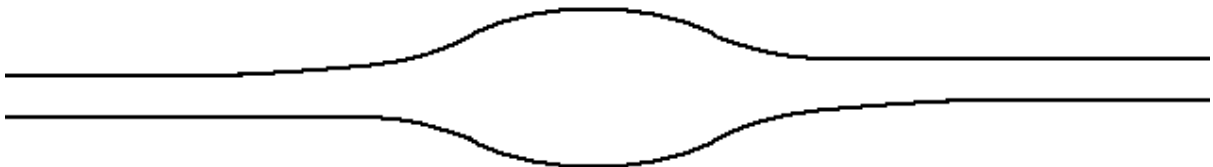


Figure 108. *Spindle-Bead*

The spindle-like bead length is double the width but the bulge was less prominent. The bulge stretches further to resemble a spindle, therefore, is characterised as a spindle-like bead.



Figure 109. *Spindle-like bead*

4.4.1. Effect of Increasing Voltage on Bead Size

Effect of Increasing Voltage on Bead Morphology using PVA 4%

Figures 110 to 112 show the effect of increasing voltage using PVA 4% on the average bead size, obtained at collection distances of 7cm, 10cm and 15cm with increasing voltages of 8kV, 12kV and 20kV. Figures 110 to 112 shows the bead size (length and width) decreased with increasing voltage with the exception of Figure 112 which shows the bead width increased from 12kV to 20kV at 15cm collection distance. At 8kV, a wider bead width produced elongated beads. Further voltage increase to 12kV reduced the bead width, whilst maintaining the ratio of the length, and produced spherical beads. At 20kV, a reduction in bead width produced spindle-bead and spindle-like morphologies. Figures 110 to 112 show at 8kV mainly elongated beads were formed, at 12kV a mixture of elongated beads, spherical beads, beads with spindle-bead and spindle-like morphologies were formed and at 20kV mainly spherical beads were formed.

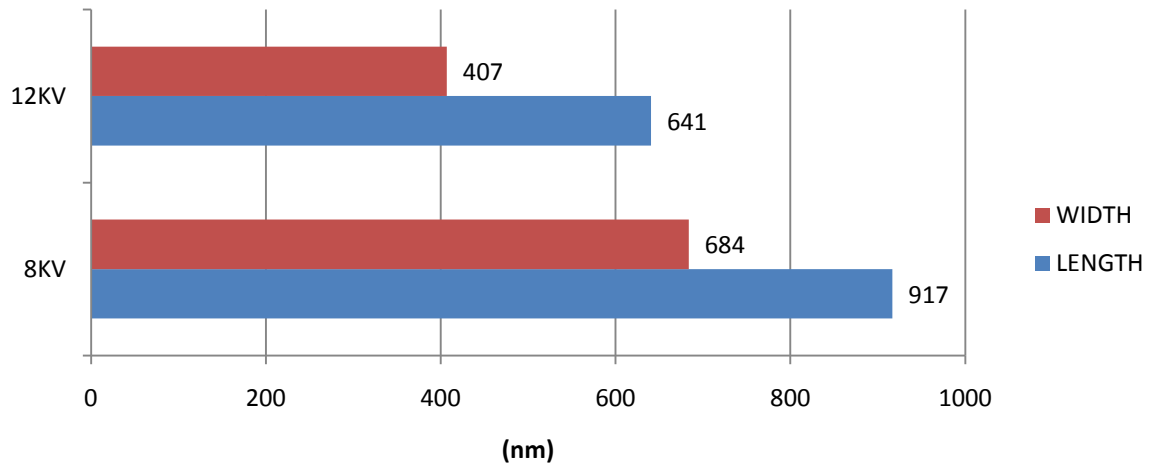


Figure 110. Average Bead Width and Length on Electrospun Fibres of PVA 4% Solution at 7cm Collection Distance and Increasing Voltage

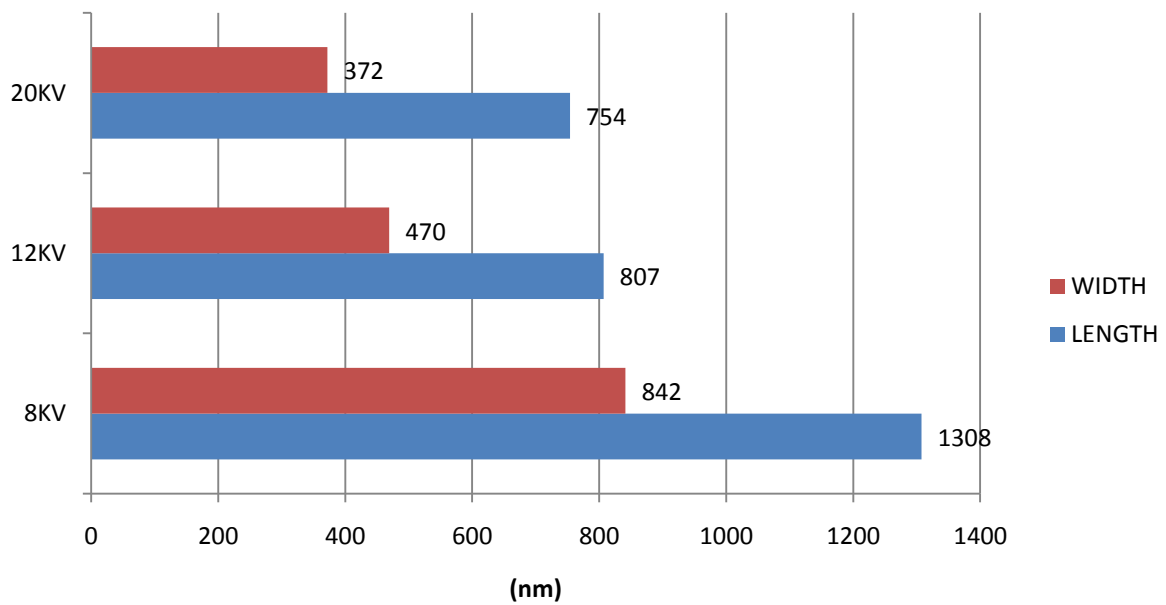


Figure 111. Average Bead Width and Length on Electrospun Fibres of PVA 4% Solution at 10cm Collection Distance and Increasing Voltage

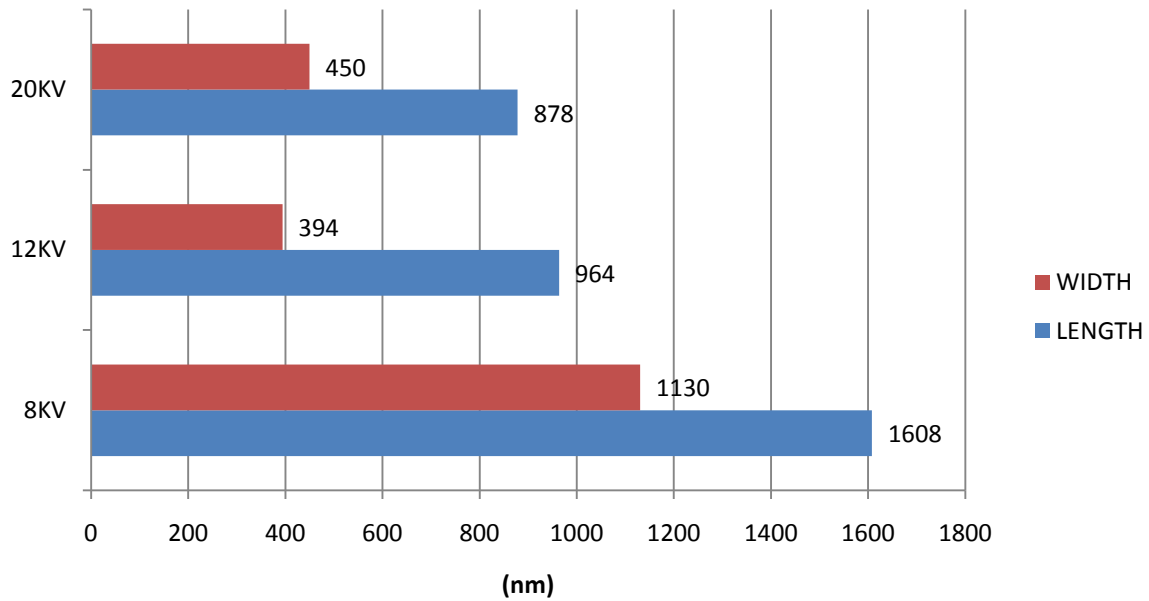


Figure 112. Average Bead Width and Length on Electrospun Fibres of PVA 4% Solution at 15cm Collection Distance and Increasing Voltage

Effect of Voltage on Bead Morphology using PVA 6%

Figure 113 and 114 shows the effect of increasing voltage using PVA 6% on the average bead width, perpendicular to the fibre axis, and the average bead length obtained whilst collection distances of 10cm and 15cm were maintained and increasing voltages of 12kV, 18kV and 20kV were applied. Figure 113 shows the bead size increased from 12kV to 18kV but decreased from 18kV to 20kV at 10cm collection distance. The morphology consisted of spindle-like beads on fibres at 12kV, beads with spindle-like and spindle-bead morphologies at 18kV and mainly spindle-like beads on fibres at 20kV. Figure 114 shows the bead size decreased slightly from 12kV to 18kV and 18kV to 20kV the bead length decreased with a slight increase in bead width at 15cm collection distance. However, the changes in bead width were small in comparison to the decrease in bead length with the increasing voltage.

Figure 114 the morphology changed from spindle-like at 12kV and 18kV to spherical bead at 20kV.

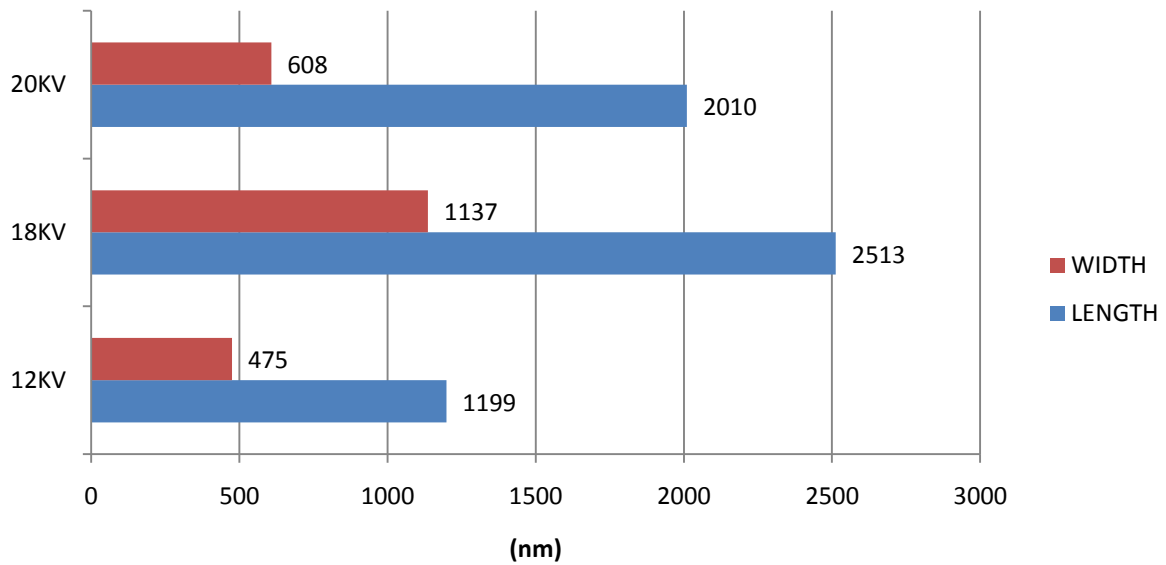


Figure 113. Average Bead Width and Length on Electrospun Fibres of PVA 6% Solution at 10cm Collection Distance and Increasing Voltage

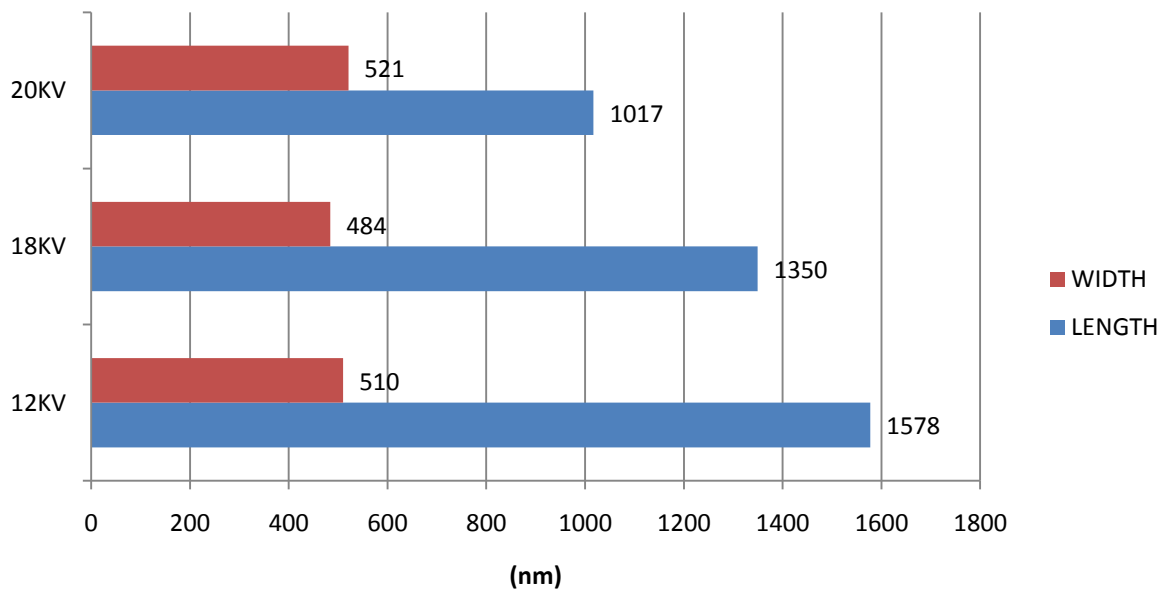


Figure 114. Average Bead Width and Length on Electrospun Fibres of PVA 6% Solution at 15cm Collection Distance and Increasing Voltage

4.4.2. Effect of Increasing Collection Distance on Bead Morphology

Effect of Collection Distance on Bead Morphology using PVA 4%

Figure 115 to 117 shows the effect of increasing collection distance using PVA 4% on the average bead length and width. Increasing collection distances of 7cm, 10cm and 15cm were used at voltages of 8kV, 12kV and 20kV. Figure 115 shows the bead size increased with increasing collection distance at 8kV. Figure 118 shows the bead size increased at 20kV. Figure 116 shows the bead size increased from 7cm to 10cm at 12kV. Figure 115 shows the elongated beads were formed at 8kV with increasing collection distance. Figure 116 shows at 12kV the morphology changed from elongated bead to spindle-like. Figure 117 shows at 20kV only spherical shaped beads were formed.

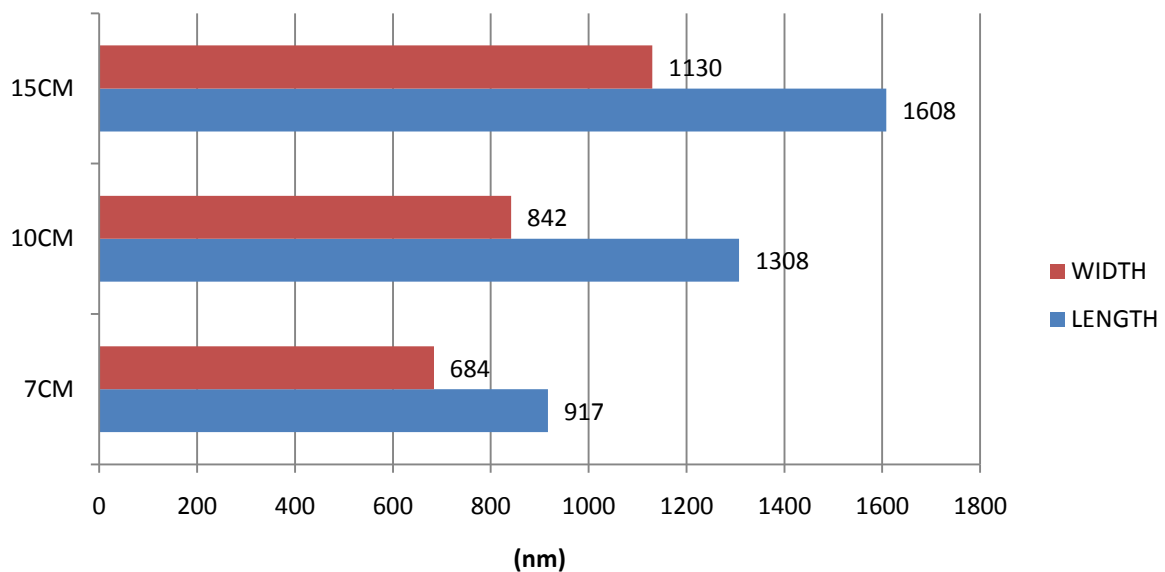


Figure 115. Average Bead Width and Length on Electrospun Fibres of PVA 4% Solution at 8kV and Increasing Collection Distance

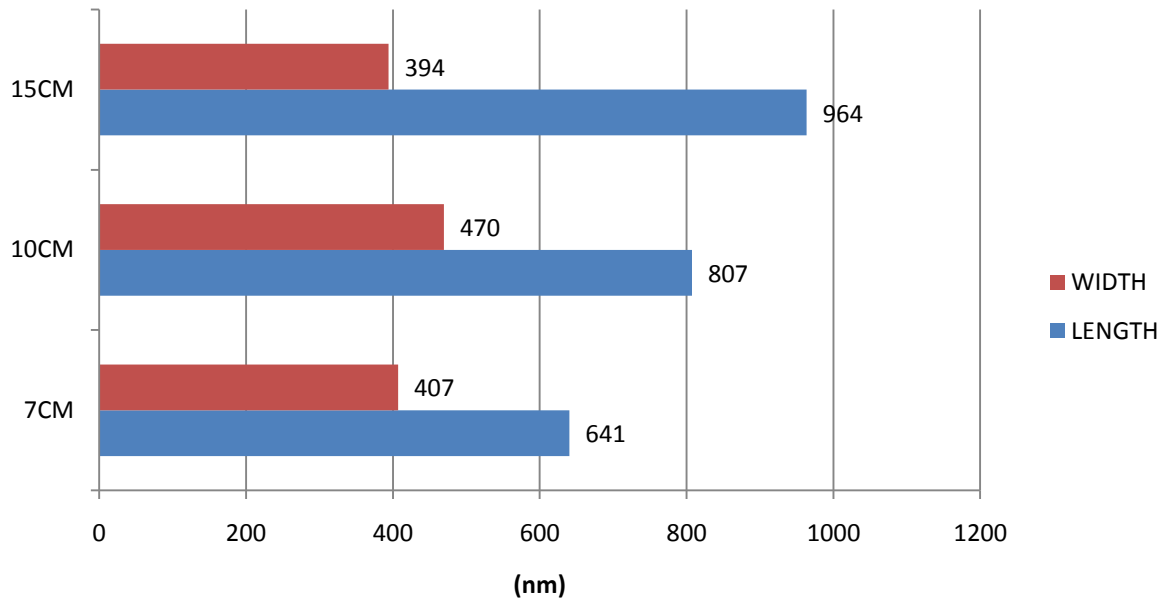


Figure 116. Average Bead Width and Length on Electrospun Fibres of PVA 4% Solution at 12kV and Increasing Collection Distance

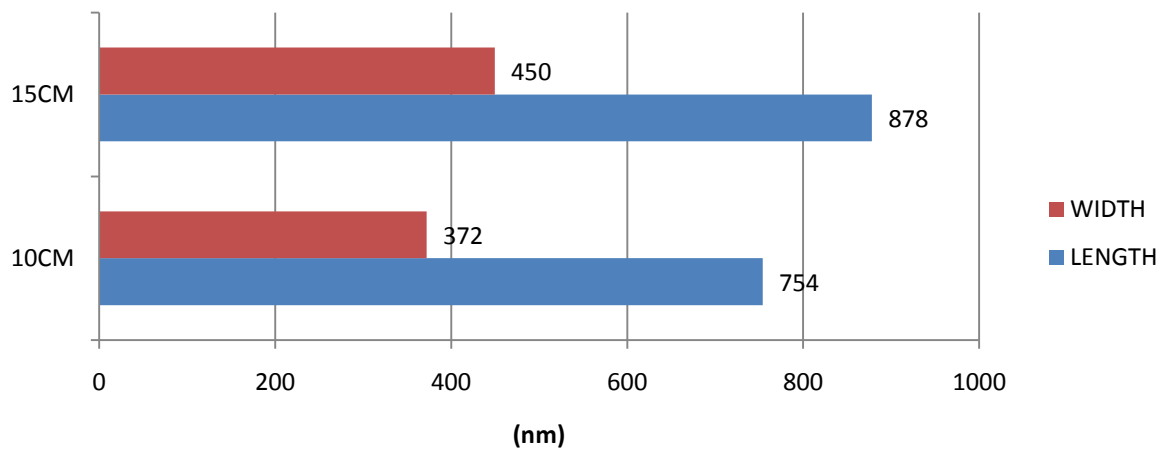


Figure 117. Average Bead Width and Length on Electrospun Fibres of PVA 4% Solution at 20kV and Increasing Collection Distance

Effect of Increasing Collection Distance on Bead Morphology using PVA 6%

Figure 118 to 120 shows the effect of increasing collection distance using PVA 6% on the average bead length and width at voltages of 12kV, 18kV and 20kV. Figure 119 and 120 show the bead size decreased with increasing collection distance at 18kV and 20kV. Figure 118 shows the length decreased from 7cm to 10cm collection distance and increased from 10cm to 15cm collection distance at 12kV. Figure 118 shows the bead width increased slightly with increasing collection distance. The morphologies varied between spindle-like and spherical bead. Figure 118 to 120 show as the collection distance increased, the beads maintain the spindle-like morphology at 12kV, the morphology changes from spherical bead shape to spindle-like at 18kV and from spindle-like to spherical bead shape at 20kV.

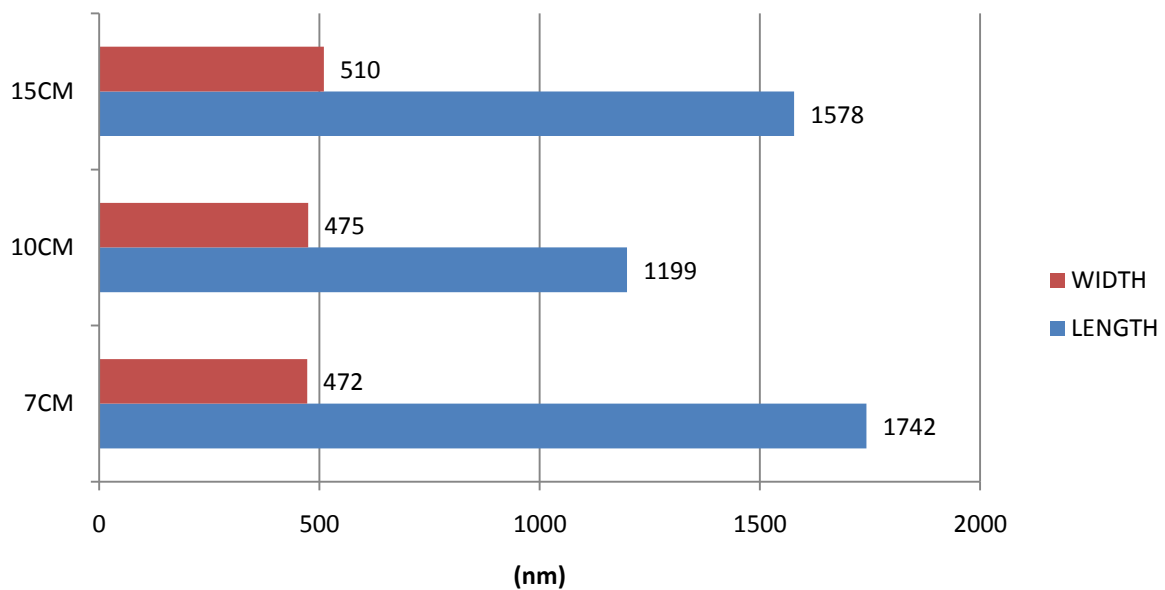


Figure 118. Average Bead Width and Length on Electrospun Fibres of PVA 6% Solution at 12kV and Increasing Collection Distance

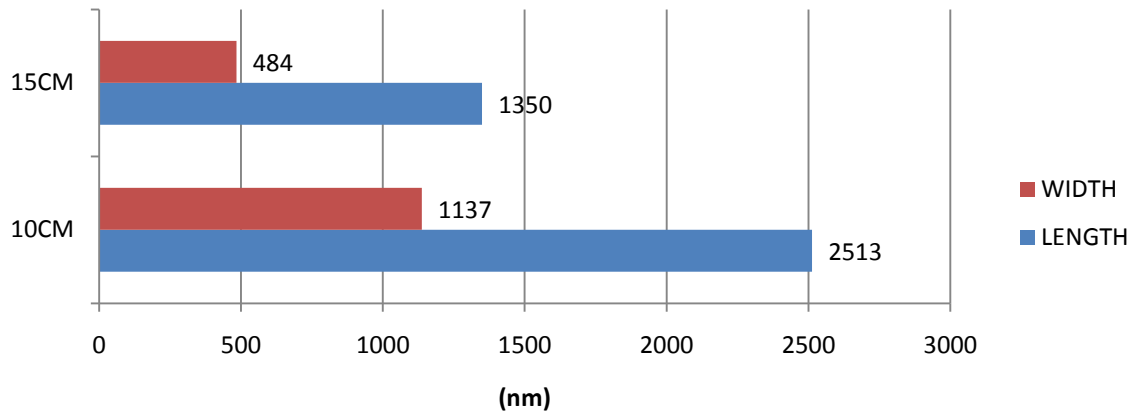


Figure 119. Average Bead Width and Length on Electrospun Fibres of PVA 6% Solution at 18kV and Increasing Collection Distance

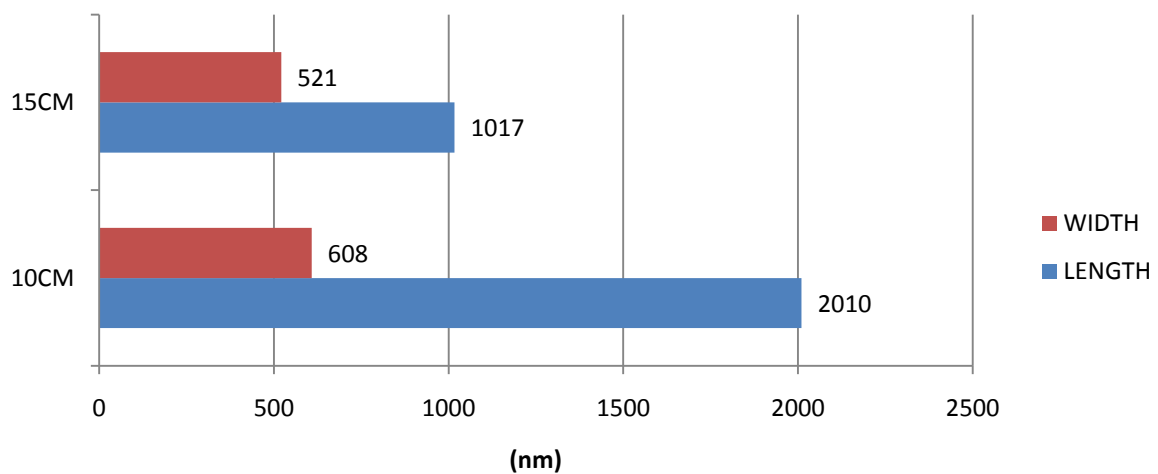


Figure 120. Average Bead Width and Length on Electrospun Fibres of PVA 6% Solution at 20kV and Increasing Collection Distance

4.5. Observations of the Electrospinning Process: Jet formation and Deposition

Observations were made during the electrospinning of the solutions at the different parameters which describe the electrospinnability of the solution, jet formation and its deposition on the collector.

4.5.1. PVA 4%

Observations at Parameters of 10cm collection distance and 12kV applied voltage using

PVA 4%

The electrospinning of PVA 4% solution consisted of fibre and droplet formation. On application of the voltage a few droplets, approximately 0.5mm in diameter, are released on to the collector. The electrospinning initiated with spraying of droplets on to the collector, followed by the formation of the Taylor cone ejecting the jet. The size the Taylor cone fluctuated whilst maintaining its shape and formed a polymer beat, as it continuously increased and shrunk in size at the needle tip. The polymer beat remained for majority of the experiment. The electrospinning jet did not split into mini-jets but remained as a single jet. A collection of drops and fibres were obtained on the target. A rough texture was visible of the fibre mat, which was due to the beads formed on the fibres collected.

Observations at Parameters of 10cm collection distance and 20kV applied voltage using

PVA 4%

Initially a single jet was ejected with a polymer beat. The jet alternated between forming fibres with and without a polymer beat. Few drops were also ejected in the duration of the fibre formation which deposited on the collector but for majority of the experiment the single jet was maintained.

Observations at Parameters of 15cm collection distance and 12kV applied voltage –using

PVA 4%

Electrospinning initiated with the formation of the Taylor cone emitting a single jet in the presence of a polymer beat. The electrospinning of the jet was constant and was not

disrupted by the formation of large droplets or spraying during the experiment. No drops were collected on the target.

Observations at Parameters of 15cm collection distance and 20kV applied voltage using

PVA 4%

Electrospinning initiated with the combination of spraying small droplets (1/2 mm in size) and ejection of large droplets on to the collector. The polymer beat was observed to be much faster in comparison with the lower voltage. The adjustment of the tank height from 25cm to 24cm reduced the ejection of large droplets but the spraying of smaller drops continued. Adjusting the height did not eliminate the polymer beat but enabled a single jet to be emitted from the needle tip. Some droplets that accumulated on the target were also contributed by residual solution present on the outer part of the needle surrounding the tip. The residual solution would gradually accumulate under the influence of the charge, edge towards the tip and merge with the Taylor cone. The addition of excess solution on the tip merged with and disrupted the Taylor cone shape forming a small drop which ejected on to the collector. However, residual solution surrounding the tip helped with electrospinning by preventing the solution at the tip from drying out and to overcome the surface tension to for jet initiation.

4.5.2. PVA 6%

Observations at Parameters of 10cm collection distance and 12kV applied voltage using

PVA 6%

The voltage is applied to the solution and initially electro spraying or ejection of small droplets on to the target, approximately 1mm in diameter was observed. The drops

reached the collector in solution state, accumulating on regions of fibre collection or linearly level with the needle forming a layer of solution on the collector. Jet initiation occurred once the drop was ejected from the tip. A Taylor cone formed instantly and spun fibres for a few seconds before it resumed back to ejecting a single drop, or occasionally several drops, and once again returning to spinning fibres. Once the height of the tank was adjusted fewer drops were released from the needle but this did not eliminate accumulation of solution on target. The solution layer continued to grow larger with continued electrospinning. Eventually the layer of solution becomes a large drop which travelled down the collector dissolving collected fibres in its path. No minijets were formed. It was difficult to achieve a tank height at which the droplet formation at the tip could be eliminated.

Observations at Parameters of 10cm collection distance and 20kV applied voltage using PVA 6%

Initially few small droplets of solution were ejected on to the collector. Once the spraying had ceased, after a few seconds the Taylor cone immersed with the jet. A distinct polymer beat was observed with the release of the jet at the Taylor cone region. The Taylor cone increased in size, whilst releasing the jet, protruded slightly out of the needle tip and was visible as a miniature drop, the size of a millimetre. The jet continued to release but had a narrower diameter. After reaching this size the drop instantaneously returned back into its original Taylor cone shape, with the diameter of the jet returning to its increased size and continuing the electrospinning of the solution. This process repeated throughout the experiment, with the polymer beats occurring once or twice per second. During the experiments the height of the tank was adjusted from 24.5cm to 24cm to reduce the

spraying of droplets and/or ejection of large droplets. As drops continued to release on to the collector, a layer of solution accumulated on the region in linearly to the needle tip. Subsequent depositing fibres started to form a mesh which extended from the layer of solution and protruding towards the needle. The mesh maintained its integrity throughout the experiment as successive fibres increased the size of the mesh. Fibres continued to deposit simultaneously on the collector and on the mesh. During the mesh forming process, the solution would cease to eject as droplets and only fibres were electrospun. A combination of fibres, droplets, ranging from sizes of a half to one millimetre, and a small mesh deposited in the centre of the collector. Images below show the mesh formation during electrospinning.

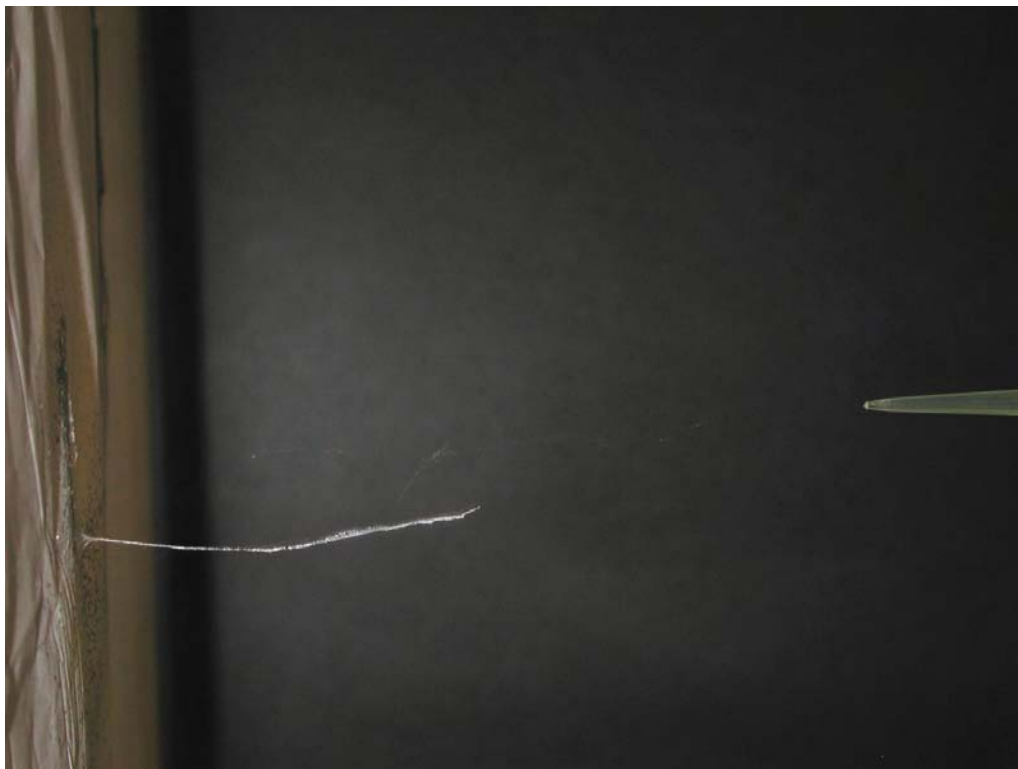


Figure 121. *Initiation of mesh formation as jet continues to deposit fibres.*



Figure 122. Mesh becomes larger with subsequent deposition of fibres.



Figure 123. *The structure of the mesh at the end of the experiment after without voltage application.*

Below the SEM images taken of the mesh show the surface structure formed at different regions of the mesh.

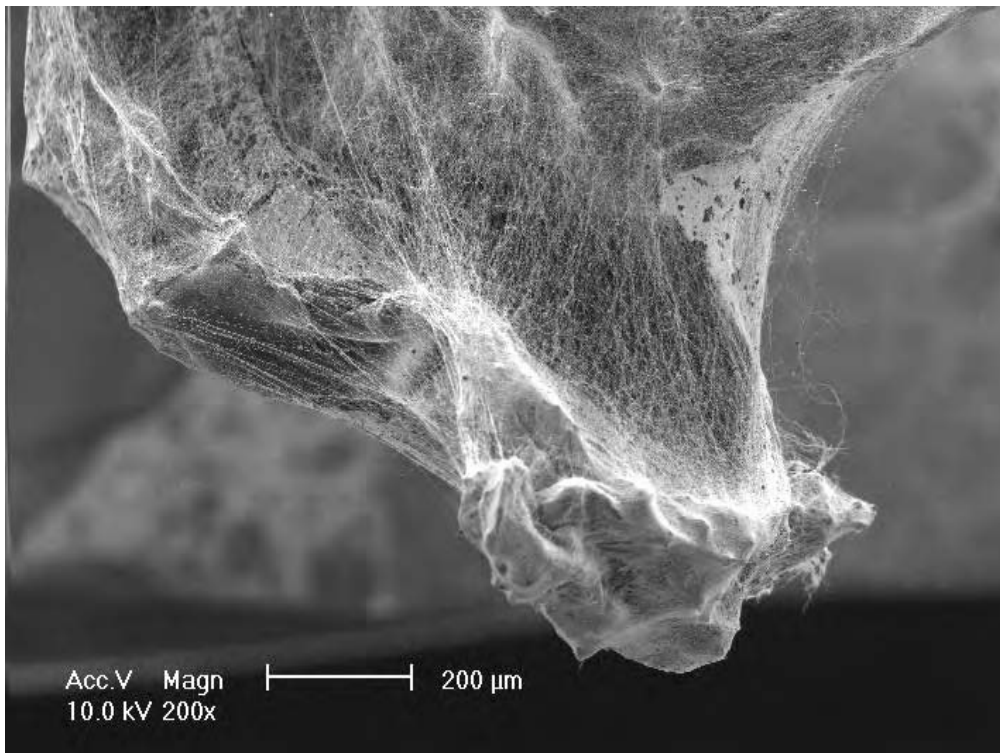
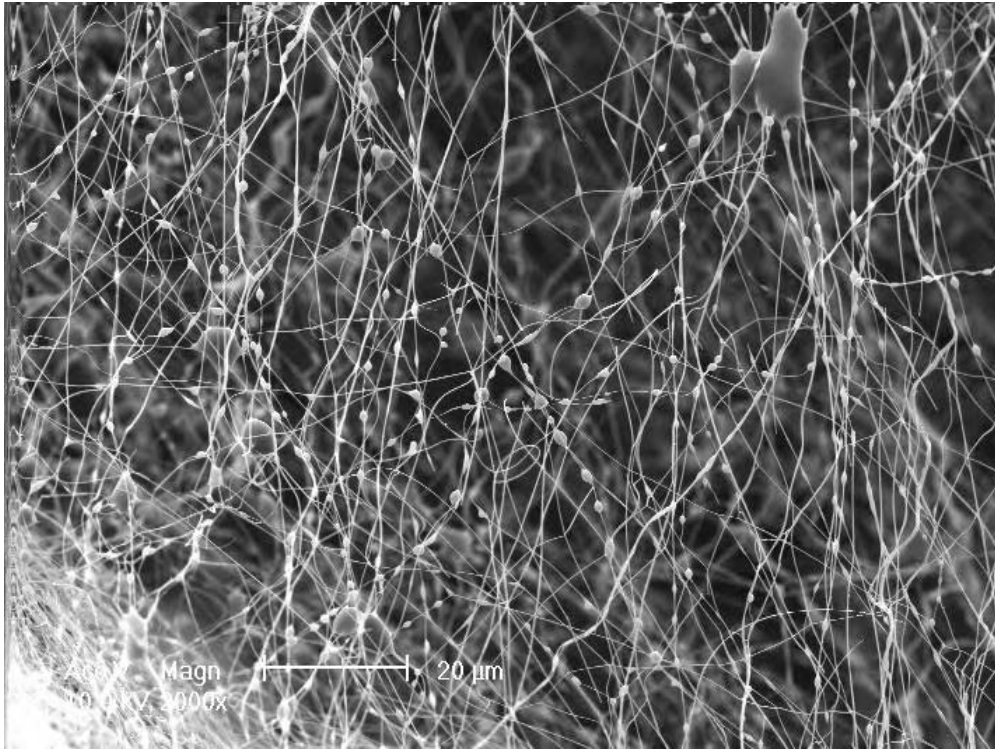


Figure 124a. *SEM image of the tip of the mesh.*



b. x2000 magnification

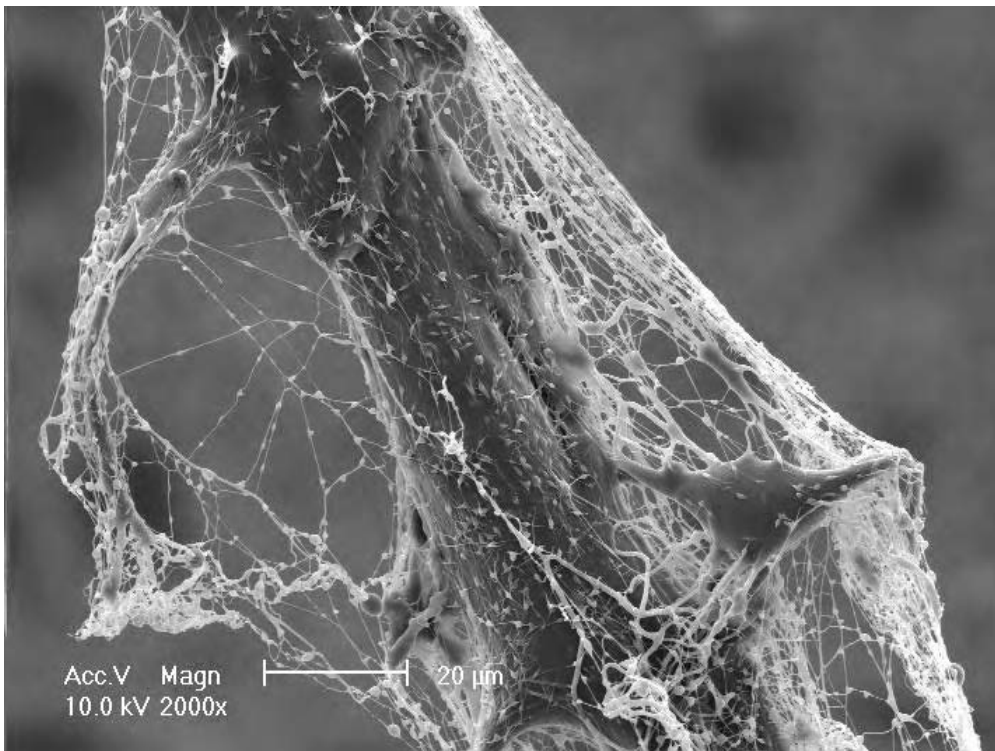
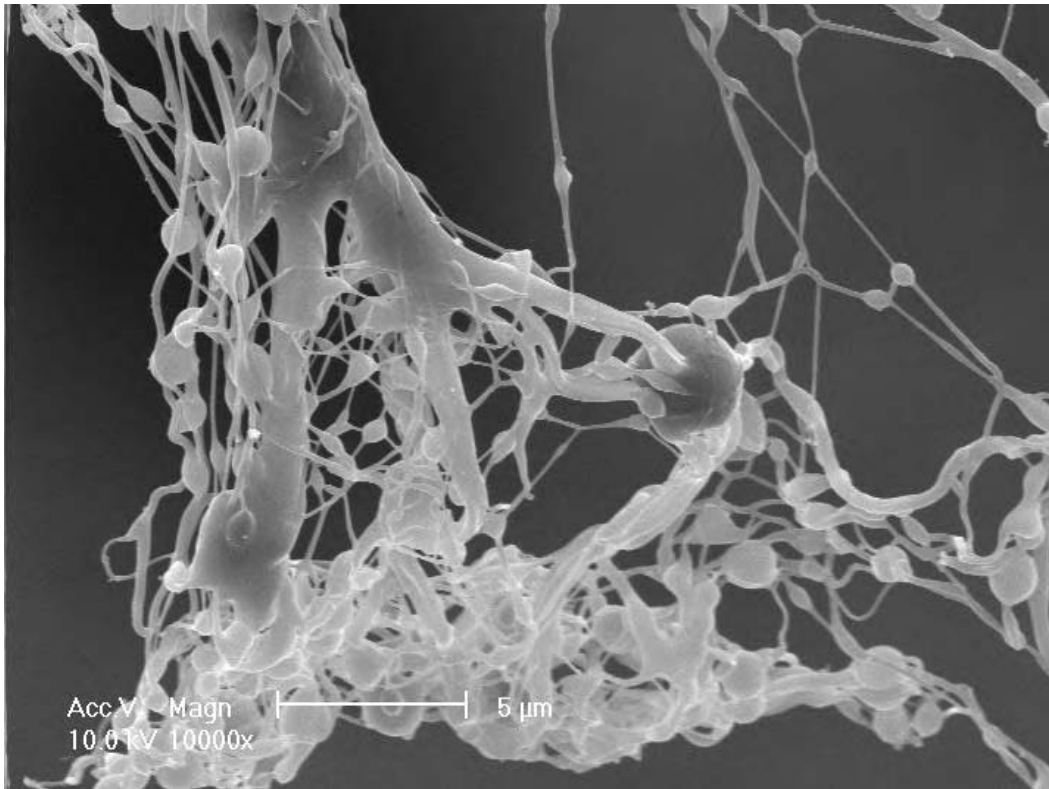


Figure 125a. SEM image of upper middle region of the mesh.



b. x10 000 magnification

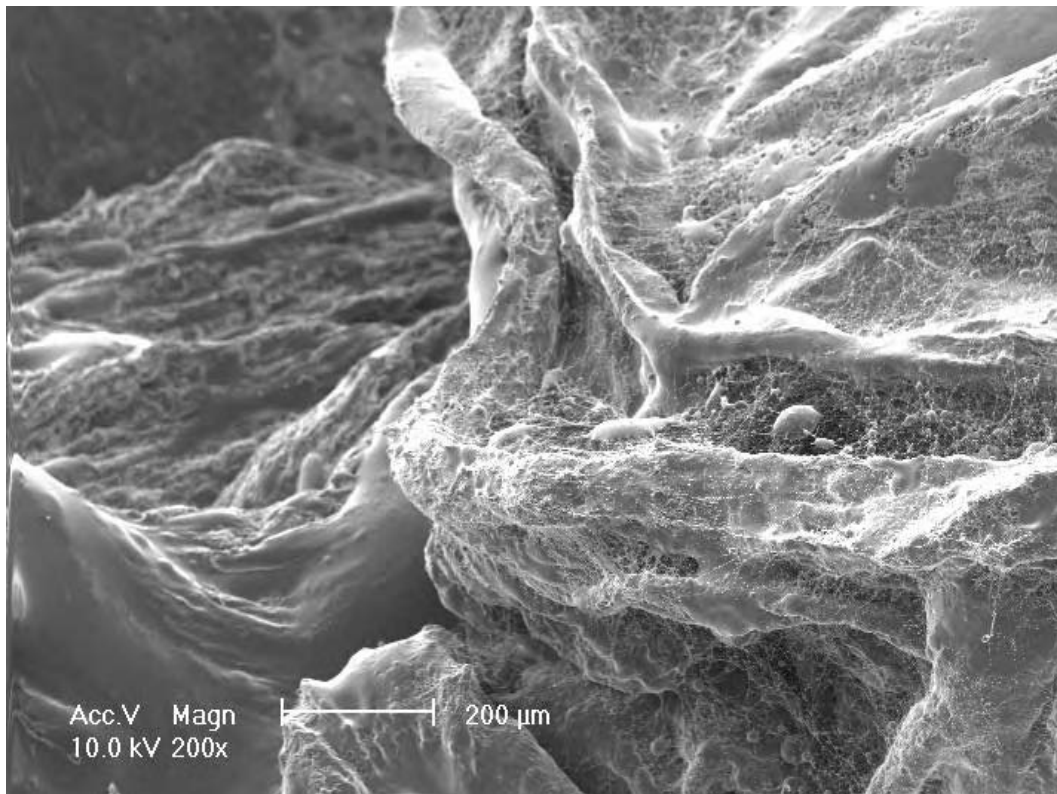
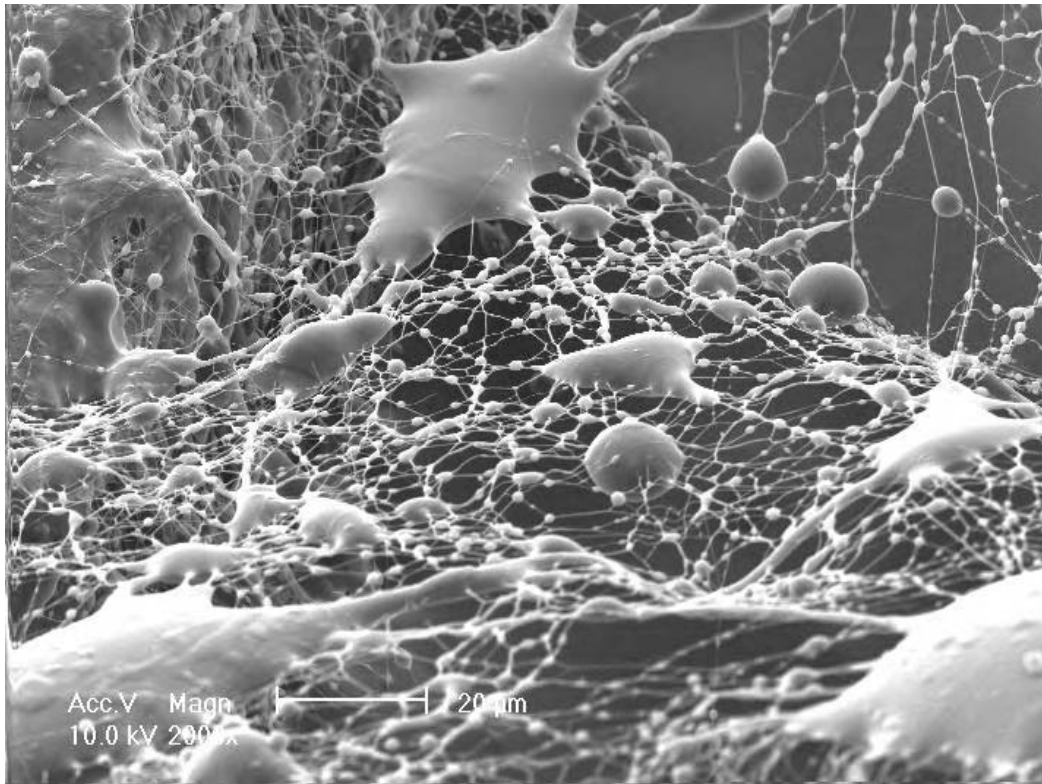
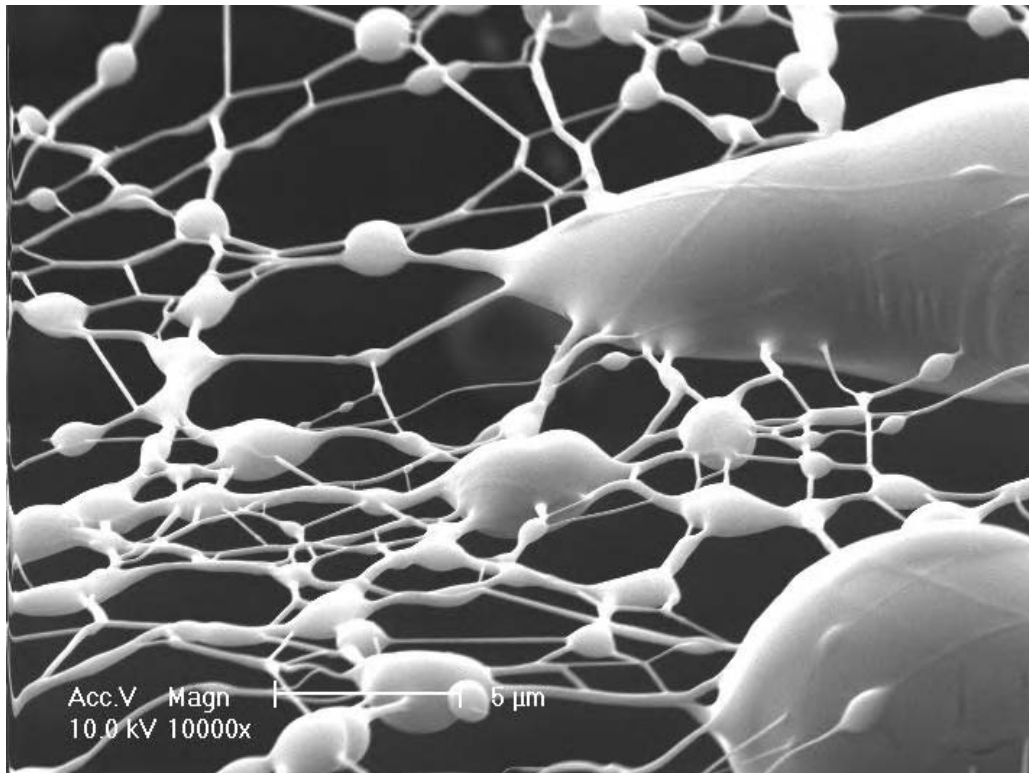


Figure 126a. SEM image of the lower middle region of the mesh.



b. x2000 magnification



c. x10 000 magnification

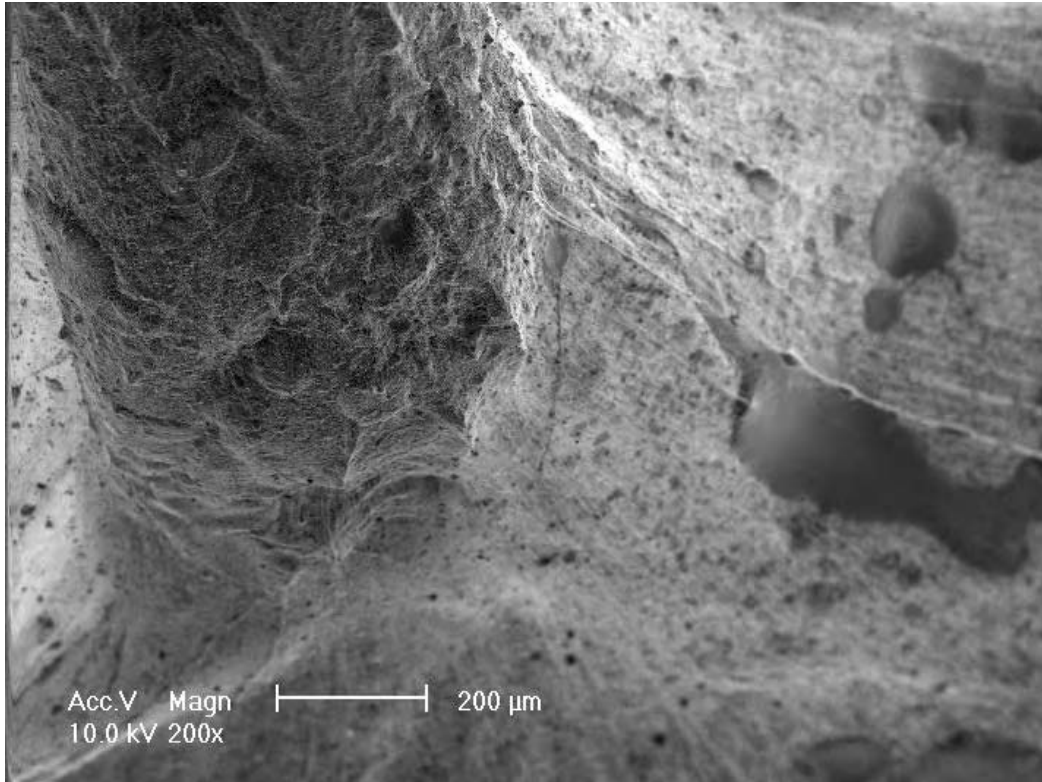
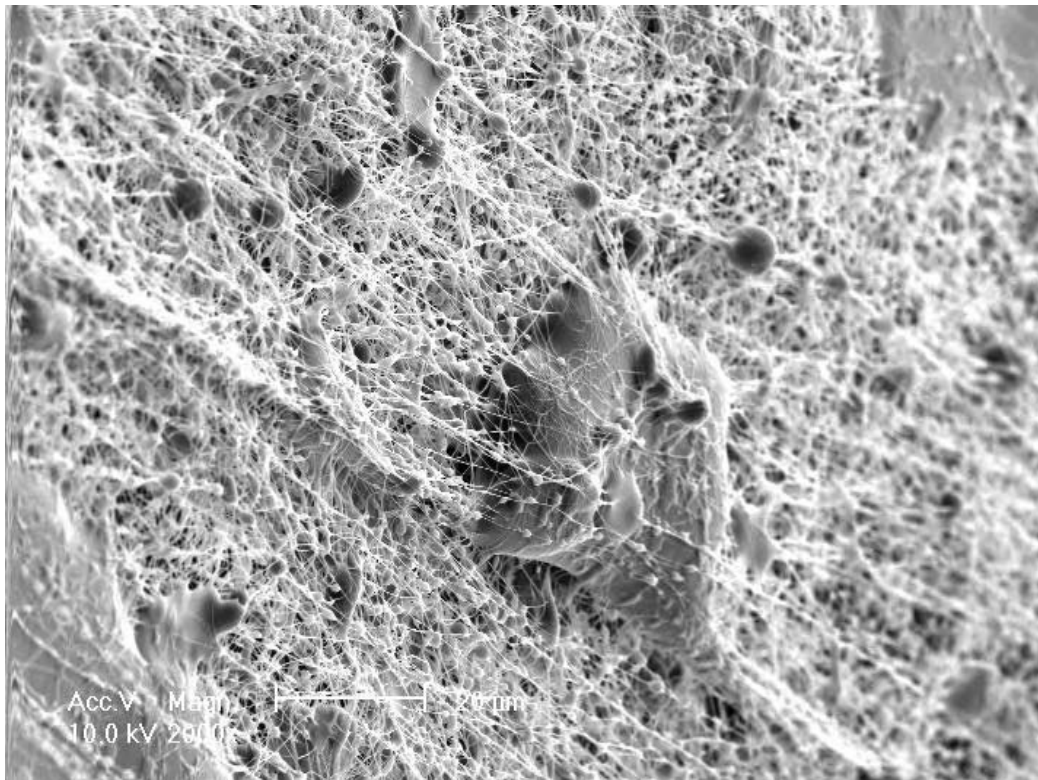
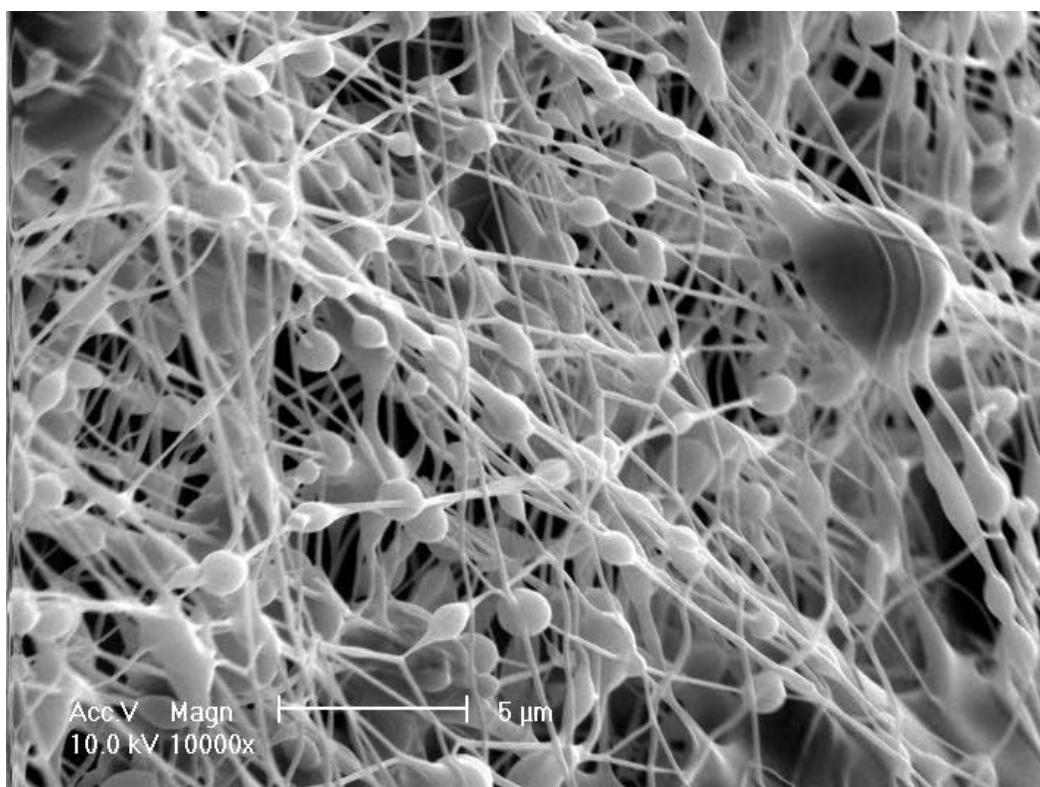


Figure 127a. SEM image of the base of the mesh.



b. x2000 magnification



c. x10000 magnification

Observations at Parameters of 15cm collection distance and 12kV applied voltage using

PVA 6%

Initially several small drops in the form of spraying released on to the collector, immediately followed by the formation of the polymer beat Taylor cone ejecting a jet. The droplets accumulated in one area forming a solution layer on the collector linear to the tip. No fibres collected on solution layer. Any fibres depositing on this region dissolved in to the solution layer increasing its volume with the addition of drops that reached this region. Up to 4 visible minijets were observed spinning fibres. However, the multiple jets were more unstable compared to the release of the single jet and not all the fibres reached the collector. The fibres would spread laterally from the tip and collect on surrounding surfaces

of the machine and casing. Droplet spraying was reduced by adjusting the height. The height of the tank was adjusted from 25cm to 25.5cm to reduce droplets released. Adjusting the height to 27.5cm had a greater effect as results showed less or no solution was collected on the target and fewer drops were released in comparison to the experiments using the previous tank height.

Observations at Parameters of 15cm collection distance and 20kV applied voltage using PVA 6%

Initially a single jet emerged which remained throughout the experiment. No drops were ejected but a small region of solution formed on the target linear to the tip. Successive fibres spun and collected on this region dissolved onto the solution layer. The Taylor cone had the polymer beat releasing a single jet for the majority of the experiment. The instability of the jet caused the fibres to be collected surrounding surfaces. The height was not adjusted and remained 25cm throughout the experiment. Altering the tank height did not eliminate the polymer beat and remained at which no droplets.

4.5.3. PVA 8%

Observations at Parameters of 10cm collection distance and 12kV applied voltage using PVA 8%

Initially a drop was released which was immediately followed by the formation of another spherical drop which simultaneously released either one main jet or up to 3 or 4 minijets. The formation of multiple jets occurred in the initial five minutes of ES and lasted for a few seconds. The minijets observed were highly unstable from jet initiation, with maybe one or two of the minijets fibres reaching the collector. The minijets rotated and alternated the

point of release randomly from the surface of the Taylor cone. The fibres of the minijets also collected on the surrounding surfaces. Fibre webs formed, bound from the bottom region of the collector extending on to the machine platform. The minijets electrospun for brief period, immediately followed by a single stable jet extending from the Taylor cone. Electrospinning of the single fibre occurs for a few minutes before another drop is released and the whole process is repeated.

The process described of the initial release of a droplet leading up to the spinning of a single jet gave a sequence of drop formation then its release, followed by jet formation then its release, then resuming back to drop formation, was repeated throughout the electrospinning process. This resulted in numerous drops accumulating on the collector which were subsequently covered by fibres. Due to coverage of the collector by fibres the drops fell from the tip on to the extension web of fibres formed between the bottom region of the collector and machine platform.

Observations at Parameters of 10cm collection distance and 20kV applied voltage using PVA 8%

Initially the Taylor cone was formed but alternated between retreating back into the needle from the tip, or spraying of the solution onto the target for a few seconds and then reforming the Taylor cone releasing a single jet. To eliminate the problem of maintaining the Taylor cone, the tank height was adjusted to achieve an adequate flow rate. The height of the solution tank initially was set at 24.5cm, at this height the solution was held within the needle and didn't drip out from the tip. It was increased to 28cm at which a drop of the solution formed on the tip. The drop aided the spinning process and produced two or three

minijets. The multiple jets reached the collector, depositing the fibres and there was sufficient deposition, an extension of fibres began to spin from the collector forming a mini-mesh of fibres, held linearly between the tip and collector by the electric field. The height was adjusted to 27cm at which a single jet ejected from the Taylor cone. However, when the fibres reached the collector, only solution was observed collecting on the region linear with the tip. Any subsequent deposition of fibres in this region dissolved into the solution drop and only led to the increases of the drop size on the target. Regions surrounding the drop of solution collected fibres and the area of deposition increased with subsequent electrospinning.

Observations at Parameters of 15cm collection distance and 12kV applied voltage using

PVA 8%

Initially, large drops were released from the needle tip on to the target for the first ten minutes of electrospinning at these parameters. As droplets stopped ejecting, a gradual build up of a single droplet on the tip was observed which grew large distorting the Taylor cone shape. As solution volume of the drop increased it was dragged by its weight to the base of the needle tip. After the drop shifted to the tip base, another Taylor cone immersed from the needle tip and electrospinning of the solution was initiated. The Taylor cone was surrounded by the solution drop which aided in maintaining the process and not allowing the needle tip to dry up due its higher viscosity. The source of the fibre spinning alternated between electrospinning directly from the needle tip and spinning from the adhering droplet on the outer surface of the needle. The droplet eventually was ejected from the tip but replaced by another droplet in the same manner described previously. The height was

adjusted between 25 cm to 26cm, which reduced the size of the droplet remaining on the needle tip but droplets continued to be ejected onto the target.

Observations at Parameters of 15cm collection distance and 20kV applied voltage using PVA 8%

Under the influence of the charge, the Taylor cone elongated towards the collector losing its shape. The elongated drop either ejected on to the collector, followed by the immediate formation of another Taylor cone that released a single jet, or the drop ejected dual jets aiming at the collector or the drop would retreat back within the needle to repeat the either one of the previous processes mentioned. However, the drop retreating into the needle from the tip was less common and occurred more in the initial part of the experiment. The elongation of the drop was temporary lasted from a few seconds to minutes but this proved to be an obstruction in the needle preventing jet initiation. The electrospinning mainly alternated between spinning dual or single jets and ejecting droplets onto the collector.

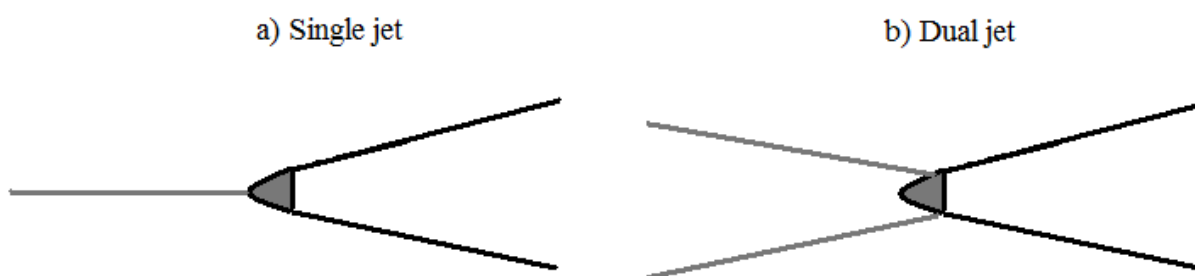


Figure 128. a) Single jet and b) Dual jets

Droplet Formation and Ejection onto the Collector

Images below show the sequence of the electrospinning jet forming a droplet, ejecting it and resuming back to electrospinning as described previously.



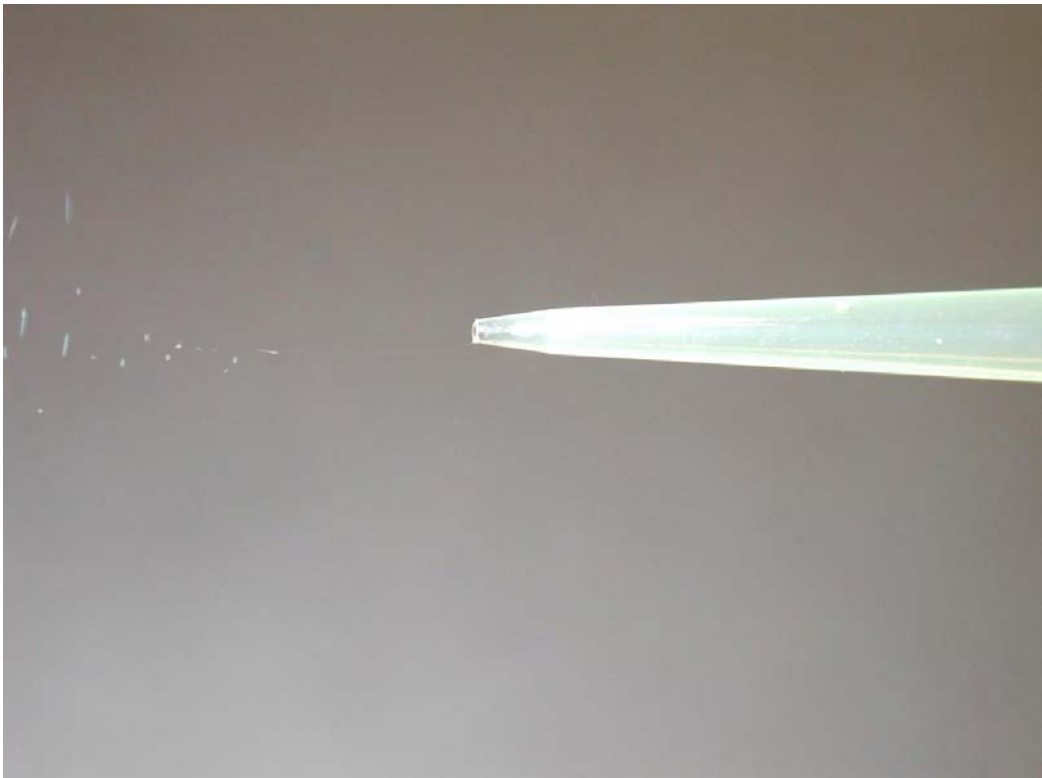
Figure 129a. *Electrospinning jet.*



b. *Electrospinning jet stops.*



c. Drop grows larger at the tip protrudes towards the collector.



d. Drop is ejected and electrospinning jet forms immediately and continues the process.

5. DISCUSSION

5.1. Effect of Solution Concentration

The solution concentration had a significant effect on the fibre diameter and morphology. At lower concentrations of PVA 4% and PVA 6% beaded fibres were produced and at PVA 8% smooth fibres were formed.

Beaded fibres formed as a result of the low viscosity and the dominating effect of the surface tension in the solution. Droplets also formed during the electrospinning process due to the effect of the surface tension and deposited on the collector. The stretching of the jet caused the spherical shaped beads to become more spindle-like shape. Average fibre diameter was significantly affected by increasing solution concentration. Results indicated that thinner fibres were attainable with lower concentration and the diameter increases with increasing concentration, whilst maintaining other variable process parameters.

The droplets and frequency of beading are reduced with increasing concentration from PVA 4% to 6%. Increasing the concentration up to PVA 8% eliminated the ejection of droplets and beading, to form smooth fibres. At higher concentrations the viscosity of the solution is higher which results in increased chain entanglements preventing the break-up of the jet into small droplets. The jet is able to elongate further during its flight under the influence of the columbic stress and become thinner. Higher solution concentration with the associated higher viscosity enabled the charged jet to withstand the stretching under columbic force to yield smoother fibres with larger diameters.

The smallest average fibre diameter was obtained with PVA 4% and the largest fibre diameter was obtained with PVA 8%. Diameters for PVA 4% ranged from 43-92nm, PVA 6% ranged from 72-128nm and PVA 8% ranged from 144-215nm. The average fibre diameter increases with increasing concentration (Figures 9, 11, 13 and 15). Figure 9 shows diameter size approximately doubles with concentration increase; PVA 4%, with 44nm, PVA 6% with 91nm and PVA 8% 195nm. Large spherical beads with thin cylindrical fibres linking the beads together are formed resulting in beaded fibres at PVA 4% shown in Figure 8a. With PVA 6% the bead sizes considerably smaller with greater density of fibres intercepting the beads (Figure 8b). Fibres formed with PVA 8% have no beads and the morphology varies between cylindrical and flat ribbon fibres (Figure 8c, 10c and 12c). Fibre morphology shows to change from cylindrical to a combination of cylindrical and flat ribbon fibres with increasing concentration (Figure 8, 10 and 12). This shows that solution concentration had an obvious effect on the average fibre diameter and morphology. Thinner and beaded fibres are obtained with lower concentration solutions and smooth larger diameter fibres are obtained at higher concentrations.

Studies have shown that at higher concentrations, the viscosity is higher which results in increased chain entanglements that prevent the breakup of the jet into small droplets. The jet is able to elongate further during its flight under the influence of the columbic stress and become thinner. Higher concentration with the associated higher viscosity enabled the charged jet to withstand the stretching under columbic force to yield smoother fibres with larger diameters. Qiang *et al* (2007) found thinner PVA fibres were attainable with lower concentration and the fibre diameter increased with increasing concentration, whilst maintaining other variable process parameters. At higher concentrations, the charged jet

had a greater resistance to the stretching of the jet due to its high viscosity resulting in larger diameter of as spun fibres from about 371nm at 6% concentration to approximately 676nm at 9% concentration. The charged jet dried more easily with increasing concentration. The amount of solvent present in the jet is reduced as the concentration increases allowing the jet to dry during elongation⁶⁰. Zhang *et al* (2005) found beaded fibres were formed at 6% PVA concentration with an average fibre diameter measured between the beads from 73nm to 91nm. The morphology changed with increasing concentration from beaded to uniform, smoother fibres with increased fibre diameter between 196nm to 296nm. Fibre forming ceased beyond 8.3% concentration and large droplets were formed instead which fell on the target irrespective of the voltage applied⁶¹. Koski *et al* (2004) found the PVA fibre diameters increased with increasing Mw and concentration⁶². Ding *et al* (2002) found the increasing PVA solution concentration eliminated bead formation and the fibre diameter increased with increasing solution concentration⁶³. Tao *et al* (2007) found the morphology of the fibres changed with increasing concentration, whilst maintaining a constant M_w of PVA¹⁶. At 18,000 g/mol M_w the transition from beads to spherical beaded fibres occurred at 16% PVA concentration. At 18% concentration fibres with spindle-like beads were electrospun and at 22% more stable and smoother fibres formed. Above 22% the fibrous structures began to change to flat ribbon fibres, which were evident at 27%. Study concluded at any M_w the concentration will influence the composition of the solution jet, therefore, affecting the morphology of the fibres produced¹⁶.

Koski *et al* (2004) investigated the effect of Mw on the fibres produced via electrospinning using PVA solutions of various Mw at different concentrations⁶². Overall findings indicated that each Mw required a minimum concentration at which a stabilised fibrous structure

could be achieved⁶². Tao *et al* (2007) investigated structural transitions of electrospun PVA fibre determined by the M_w and solution concentration. The study outlined that at any M_w the solution concentration will influence the composition of the jet and, in turn, the morphology of the fibres produced. The C_i and C_f of PVA with M_w of 18,000 g/mol is 14% and 22%, respectively¹⁶.

A factor which determines the stabilisation of the fibrous structure is the solution concentration⁶². The Berry number $[\eta]C$, whereby $[\eta]$, the intrinsic viscosity, C the solution concentration can define a value at which fibre diameter and morphology alters according to the concentration with relation to the M_w of the polymer^{16,34}. In dilute PVA solutions the degree of chain entanglement is less and is defined as $[\eta]C < 1$ ⁶². As the concentration increases from dilute to semi-dilute solution the polymer chains begin to entangle with each other in the solution and is defined as $[\eta]C > 4$ for PVA aqueous solutions⁶². At a given value of $[\eta]C$ changing either $[\eta]$ or C can affect the electrospun structure⁶². The Mark-Houwink equation defines the intrinsic viscosity for PVA in water⁶².

$$[\eta] = 6.51 \times 10^{-4} M_w^{0.628}$$

The polymer chain entanglement regimes for the PVA solutions used in this study were calculated. Using PVA of M_w 72,000, PVA 4% had the entanglement regime of $[\eta]C=3$, PVA 6% had $[\eta]C=4$ and PVA 8% had $[\eta]C=6$. The results of this study show at $[\eta]C > 3$ the polymer chain entanglement regime is high enough to allow fibrous structures to form. Between $3 < [\eta]C < 4$ only beaded fibres were formed. At $[\eta]C > 6$ the polymer chain entanglements increased and smooth fibres form with no beads.

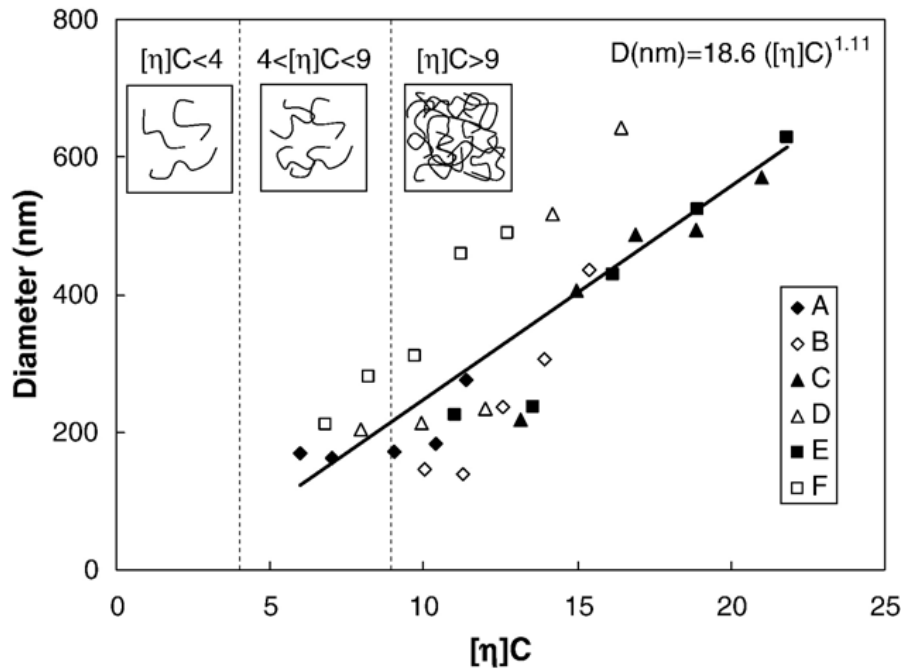


Figure 130. The average fibre diameter with the Berry number for PVA at M_w of A: 9500g/mol, B: 18,000g/mol, C: 40,500g/mol, D: 67,000g/mol, E: 93,500g/mol & F: 155,000g/mol. The $[\eta]C$ critical values for the transition from extremely dilute to dilute to highly entangled polymer chain regimes are shown¹⁶.

The fibre diameter distribution increased with increasing concentration, at collection distances and applied voltages of 10cm with 12kV (Figures 16-18), 15cm with 12kV (Figures 19-21) and 15cm with 20kV (Figures 22-24). At parameters of 10cm and 20kV the fibre diameter distribution increased from PVA 4% to PVA 6% and decreased from PVA 6% to PVA 8% (Figure 25-27). The smallest diameters were found with PVA 4% electrospun fibres (Figures 16, 19 and 25) and the largest with PVA 8% (Figures 18, 21 and 24). This suggests that increasing the solution concentration increased the fibre diameter distribution depending on the parameters used. Zhang *et al* (2005) found that fibre diameter distribution increased with increasing solution concentration from PVA 6% to PVA 7% and from PVA 7% to PVA 8%⁶¹. Qiang *et al* (2007) found the diameter distribution decreased

with increasing solution concentration of PVA 6% to PVA 7% to PVA 8% but increased from PVA 8% to PVA 9%⁶⁰.

The deposition rate increased with increasing concentration at the parameter of 12kV and 10cm collection distance (Figure 28). The rate increased from concentration of PVA 6% to PVA 8% at parameters of 20kV and 10cm (Figure 29), 12kV and 15cm (Figure 30), and 20kV and 15cm (Figure 31). At the same parameters the deposition rate decreased with increasing concentration from PVA 4% to PVA 6% (Figure 29, 30 and 31). At parameters of 12kV and 15cm there was slight decrease in deposition rate from PVA 4% to PVA 6% and a slight increase from PVA 6% to PVA 8% (Figure 30). The deposition rate was affected by the solution concentration by either increasing or decreasing deposition with increasing concentration.

However, the deposition area varied with the parameters and in some cases fibres may have accumulated in a specific region over a small area or dispersed over a larger area. Diagrams of the fibre deposition areas show how varying the concentration affected the sizes of these areas. Eda *et al* (2001) found that a smaller deposition area is obtained with electrospun fibres by increasing the concentration¹⁵. The onset of the jet instability occurs at a further distance from the capillary tip. The viscoelastic force is sufficient enough to withstand the electrical bending instability to allow the jet to leave the needle tip and travel for a longer distance in a straight path before bending instability initiates¹⁵. Ramakrishna (2005) stated that the projection of the jet in this manner reduces the jet path and the resultant bending instability of the jet deposits over a smaller region¹⁹. The fibres collected from these regions have large diameters as they have undergone less stretching from the

reduced jet path¹⁹. The samples taken to measure mass of the electrospun material in a specific area, does not take into account the area over which the deposition spreads. Therefore, more fibres may be deposited on the collector at a specific concentration but the measurements of deposition rate does not take this into account, therefore, a higher or lower deposition rate is recorded.

5.2. Effect of Applied Voltage

Increasing the voltage has shown to effect the electrospun product whilst maintaining other variables using solutions of PVA 4%, PVA 6% and PVA 8%. The average fibre diameter, morphology, fibre diameter distribution and deposition rate were influenced by the application of increasing voltage.

The affect on the average fibre diameter was shown whilst using PVA 4%. Increasing the applied voltage from 8kV to 12kV reduced the average fibre diameter (Figure 33, 35 and 37). The diameter did not change with further increasing the voltage to 20kV (Figure 33, 35 and 37). The morphology consisted of beaded fibres with various bead morphologies (Figure 32, 34 and 36). Elongated beads were observed with applying 8kV and 12kV at 7cm and 15cm collection distance (Figure 32 and 34). Fibre webbing was observed using 20kV at 10cm collection distance (Figure 34c). These results showed that increasing the applied voltage stretched the jet under the actions of the forces producing a narrower jet and ultimately thinner fibres with PVA 4%.

Findings show whilst using PVA 6%, the average fibre diameter increased from 18kV to 20kV at 10cm collection distance (Figure 39) and at a longer distance the diameter decreased it

(Figure 41). Increasing the voltage from 12kV to 18kV decreased the average fibre diameter slightly at 10cm collection distance (Figure 39) and a slightly increased at 15cm collection distance (Figure 41). The bead density decreased at 10cm collection distance (Figure 38) but increased at 15cm (Figure 40). The morphology varied with increasing voltage as spindle-like beads on fibres formed at 12kV and 20kV but whilst using 18kV fibre webs were formed at 10cm collection distance (Figure 38b). The beads on the fibres changed from spindle-like to spherical morphology as the voltage increased at 15cm collection distance (Figure 40).

Whilst using PVA 8%, average fibre diameter decreased with increasing voltage at 10cm collection distance (Figure 43) and diameter increased slightly at 15cm collection distance (Figure 45). The average fibre diameters were larger at 15cm (Figure 45) compared to 10cm collection distance (Figure 43). At 12kV smooth, cylindrical and uniform fibres were formed (Figure 42) and at 20kV fibres of undulating diameters with mixed morphologies of cylindrical and flat ribbon were formed (Figure 44). Increasing the voltage to 20kV at both of the short and long collection distances showed fibre webs formed, which also contributed to the flat appearances of the fibres, at 10cm collection distance (Figure 42) and flat ribbon fibres which spread over fibres deposited beneath formed at 15cm collection distance (Figure 44). The smooth fibres merged to form a single larger diameter fibre (Figure 42 and 44) regardless of the applied voltage. Generally, with using PVA 8%, increasing voltage at a shorter distance decreased the average fibre diameter but at a longer distance slightly increased the diameter.

These results show that increasing the applied voltage can form thinner PVA fibres. The increase in the electric field strength corresponding to the increase in voltage enhances the

electrostatic repulsive forces in the fluid jet. The jet stretched under the actions of the forces, producing a narrower jet and ultimately thinner fibres. However, increasing voltage can also increase fibre diameter as the jet accelerates more and more solution is removed from the capillary tip^{30,61,63}. Singh *et al* (2009) found similar affects of the increasing voltage on the fibre diameter. As the voltage increased the fibre diameter initially increased and then gradually decreased with further increasing voltage⁶⁴. Zhang *et al* (2005) found that increasing the applied voltage slightly increased the diameter of PVA fibres⁶¹. A voltage applied above 10kV produced a higher frequency of thin fibres possessing diameters less than 100nm⁶¹. Qiang *et al* (2007) found whilst maintaining all other variables the average fibre diameter increased with the increasing of the spinning voltage showing a monotonic increase from 410nm at 17.5kV to 524nm at 22.5kV⁶⁰. Therefore, lower spinning voltage was more efficient at producing thinner fibre⁶⁰.

The fibre diameter distribution was affected by the increasing voltage. Using PVA 4% the fibre diameter distribution decreased with increasing voltage (Figure 47-53). Using PVA 6% showed that the fibre distribution decreased from 12kV to 18kV (Figure 54 and 55), and increased from 18kV to 20kV (Figure 55 and 56) with increasing voltage at 10cm collection distance. The distribution decreased with increasing voltage using PVA 6% at 15cm collection distance (Figure 57 and 58). Using PVA 8% the fibre diameter distribution increased with increasing voltage (Figures 60-63). The results show that using a lower concentration solution, the distribution is generally lower at higher voltages. Using a higher concentration solution larger fibre diameter distribution is obtained. Zhang *et al* (2005) found that a voltage applied above 10kV produced a higher frequency of thin PVA fibres possessing diameters less than 100nm but there was also a broader distribution of fibre

diameters when 10kV to 13kV were applied. Whilst at low voltages of 5kV, the distribution of the fibre diameters in comparison was lower⁶¹. Qiang *et al* (2007) found that greater uniformity and a narrower distribution of fibres were obtained at lower voltages of 17.5kV, whereas, at higher voltage of 20kV to 22.5kV there is a broader distribution of fibres⁶⁰.

The bead morphology was specifically analysed to observe what changes occur with beads on fibres whilst increasing the voltage. Using PVA 4% the bead size (length and width) decreased with increasing voltage (Figures 110 to 112) with the exception of the increased bead width from 12kV to 20kV at 15cm collection distance (Figure 112). At 8kV mainly elongated beads were formed, at 12kV bead morphology consisted a mixture of spherical, spindle-bead, spindle-like, and elongated bead morphologies and at 20kV mainly spherical beads were observed as well as fibre webbing which formed at 10cm collection distance and a few elongated beads also formed at 15cm collection distance (Figure 32, 34 and 36). Larger beads on fibres were formed at lower voltages consisting of mainly elongated beads using PVA 4%.

Using PVA 6%, the bead size increased from 12kV to 18kV but decreased from 18kV to 20kV at 10cm collection distance (Figure 113). The morphology consisted of spindle-like beads on fibres at 12kV, larger beads with spindle-like and spindle-bead morphologies with fibres webs were formed at 18kV and mainly spindle-like beads with fibre webs formed at 20kV (Figure 38 and 113). The bead width decreased from 12kV to 18kV and increased from 18kV to 20kV and the bead length decreased with increasing voltage at 15cm collection distance (Figure 114). However, in comparison to the changes in bead width which was less than

50nm, the decrease in bead length was greater with changes of approximately 200-300nm with increasing voltage (Figure 114). The bead morphology changed from spindle-like at 12kV and 18kV, to spherical at 20kV and bead density also increased (Figure 40 and 114). At higher voltages either spherical or spindle-like beads were formed using PVA 6%. No elongated beads were formed using this solution.

The results have shown that depending on the voltage, the morphology and number of the beads on the beaded fibres formed varied using the lower concentration solutions. Dietzel *et al* (2001) found smooth fibres formed at low voltage application and highly beaded fibres at a higher voltage²¹. The high voltage increased jet velocity drawing more solution from the tip²⁹. Increasing the voltage increased the acceleration of the jet which caused it to stretch and thin the diameter but alternately increased chances of bead formation²⁸. Beaded fibres began to form and bead density increased²¹. Samatham and Kim (2006) found elongated beads on fibres formed as a result the beads stretched by the electrostatic forces³³.

The deposition rate was affected by the increasing voltage. Whilst using PVA 4% the deposition rate increased with increasing voltage (Figure 64). For PVA 6%, the deposition rate varied, as it increased from 12kV to 18kV, then decreased from 18kV to 20kV (Figure 65). For PVA 8%, deposition rate decreased with increasing voltage at 10cm collection distance and increased at 15cm collection distance (Figure 66). A higher deposition rate can be due to the increased solution removal from increasing voltage³⁸. Multiple jet formation observed with electrospinning PVA 4%, PVA 6% and PVA 8% at specific parameters resulted in larger collection regions on the collector. As a result, less fibres accumulate in a specific

region and may have possibly recorded a lower mass of electrospun material depending on which region of the collector the samples were taken from^{10,21}. The increased deposition of fibres may have resulted from the increased acceleration of the jet which draws more solution from the tip depositing more fibres on the collector⁶⁴.

5.3. Effect of Collection Distance

The results showed that altering the collection distance had an effect on the electrospun material whilst maintaining other variables, using PVA 4%, PVA 6% and PVA 8% solutions. Using PVA 4% the average fibre diameter increased with increasing collection distance at 8kV (Figure 68). Increasing the collection distance at 12kV did not affect the average fibre diameter as it decreased only slightly from 47nm to 43nm (Figure 70). The fibre diameter increased with increasing collection distance from 10cm to 15cm at 20kV (Figure 72). The distance of 7cm at 20kV was too short to deposit any fibres as the solvent did not evaporate sufficiently from the jet prior to reaching the collector, instead a layer of dissolved fibres formed on the collector (Figure 71). The fibre morphology consisted of only beaded fibres with PVA 4%. Fibre webs formed at shorter collection distances, which reduced to form distinctly separate beaded fibres with increasing collection distance (Figures 67, 69 and 71).

Whilst using PVA 6%, the average fibre diameter decreased from 7cm to 10cm collection distance and increased slightly from 10cm to 15cm collection distance at 12kV (Figure 74). The average fibre diameter increased with increasing collection distance at 18kV, (Figure 76) and the diameter decreased at 20kV (Figure 78). The bead density reduces with increasing collection distance at 12kV and 18kV, whereas the density increased at 20kV (Figure 73, 75 and 77). The morphology of the beads changed from spherical to spindle-like at 18kV and

spindle-like to spherical at 20kV (Figure 75 and 77). Increasing the collection distance at 12kV did not alter the bead morphology and a mixture of spherical and spindle-like beads were formed (Figure 73). Regions of fibre webs were formed which diminished with increasing collection distance (Figure 73, 75 and 77).

Findings showed whilst using PVA 8%, the average fibre diameter increased with increasing collection distance (Figure 80 and 82). Increasing the collection distance at 12kV did not alter the fibre morphology but adhering fibres were formed in some regions at 10cm collection distance which diminished with increasing collection distance (Figure 79). Fibre webs are formed at a shorter collection distance with some indications of flat ribbon fibre formation at 20kV (Figure 81). The fibre webbing reduced with increasing collection distance and a mixture of flat ribbon and cylindrical fibres were formed (Figure 79 and 81). Larger average fibre diameters were obtained at longer distances using PVA 8%. Smooth and beadless fibres were formed using PVA 8% (Figure 79 and 81).

Findings showed the fibre diameter decreased with increasing collection distance as the flight path of the jet increases from the capillary to the collector, increasing its total flight path allowing more time for solvent evaporation and elongation⁶⁴. Alternatively, the fibre diameter increased with increasing collection distance as the effect of the electrostatic field is weakened by increased distance between the needle tip and collector, therefore, reducing the stretching of the jet during its flight to the collector and forming larger fibres. Qiang *et al* (2007) found the diameters of electrospun PVA fibres decreased slightly with increasing collection distance⁶⁰. Reneker *et al* (2000) stated that smaller diameter fibres were obtained by increasing the distance due to the effect of the charged jet⁹. The charged

jet released from the Taylor cone travels in a linear trajectory for a short distance before the jet undergoes bending instability, which causes unstable looping and further thinning producing narrower fibres^{9,60}. Supaphol *et al* (2008) found the fibre diameter to increase from collection distance of 3cm to 5cm and from 17cm to 20cm. However, as the collection distance increased from 5cm to 17cm the fibre diameter decreased⁵⁷. Ding *et al* (2002) found the fibre diameter increased slightly with increasing collection distance⁶⁴. Zhang *et al* (2005) found varying the distance showed to have no significant effect on morphology of the resultant PVA fibres⁶¹.

The fibre morphology was affected by increasing the collection distance. At shorter distances the fibres appear wet on reaching the collector and adhere to other fibres and beaded fibres on the collector forming fibre webs. Fibre webs were formed using all the solutions (PVA 4%, PVA 6% and PVA 8%) which occurred at 10cm collection distance and shorter distances. A short collection distance can lead to insufficient evaporation of the solvent from the jet before reaching the collector. When the fibres reach the collector they dissolve and conglutinate on to each other^{29,64,65}. Increasing the collection distance can reduce conglutination and fibre webbing forming distinctly separated nanofibres, observed with PVA 4%, PVA 6% and PVA 8%.

The fibre diameter distribution increased with increasing the collection distance from 10cm to 15cm using PVA 4% at 8kV (Figures 84 and 85) and at 12kV (Figures 87 and 88), PVA 6% at 12kV (Figures 92 and 93) and at 18kV (Figures 94 and 95), and PVA 8% at 12kV (Figures 99 and 100) and at 20kV (Figures 101 and 102). The fibre diameter distribution decreased as collection distance increased from 7cm to 10cm distance using PVA 4% at 8kV (Figures 83

and 84), also using PVA 6% at 12kV (Figure 91 and 92) and from 10cm to 15cm collection distance using PVA 6% at 20kV (Figures 96 and 97). No change in the fibre diameter distribution 7cm to 10cm collection distance using PVA 4% at 12kV from (Figures 86 and 87) and from 10cm to 15cm collection distance at 20kV (Figures 89 and 90). The increasing collection distance affected the fibre diameter distribution by either increasing or decreasing the diameter distribution or having no effect at all.

Supaphol *et al* (2008) found the fibre diameter distribution decreased as the collection distance increased from 5cm to 15cm, however, from 15cm to 20cm the diameter distribution increased slightly⁵⁷. The increase collection distance reduces the electric field strength. This reduces the effect of the Columbic and electrostatic forces within the jet causing the bending instability to initiate closer to the needle tip. As a result, the jet path trajectory is increased and the jet thinning is reduced, therefore forming larger fibres. Alternatively, the increased flight time of the jet allowed more time for the jet to stretch forming thinner fibres. However, where increasing the collection distance has no effect on the fibre diameter indicated that fibres dried sufficiently within the given collection distance and could not be stretched further^{57,64}. Singh *et al* (2009) found the average fibre diameter increased with increasing distance but the deposition area of the fibres also increased with fewer fibres reaching the collector⁶⁴.

The bead morphology and size for PVA 4% and PVA 6% were analysed. Whilst using PVA 4%, the bead size increased with increasing collection distance at 8kV (Figure 115), also at 20kV (Figure 117) and from 7cm to 10cm distance at 12kV (Figure 116). From the collection distance of 10cm to 15cm the bead length increased but the bead width decreased at 12kV

(Figure 116). The morphology of the beads on the fibres remained as elongated beads with increasing collection distance at 8kV (Figure 115). Increasing collection distance changed the morphology from elongated beads to spindle-like beads at 12kV (Figure 116) and only spherical beads were formed at 20kV (Figure 117). Increasing the collection distance can increase bead size at high and low constant voltages. The increased collection distance increased the bead length whilst reducing the bead width. As the beads stretched they appeared spindle-like.

Using PVA 6%, the bead size decreased with increasing collection distance at 18kV (Figure 119) and 20kV (Figure 120). As the collection distance increased from 7cm to 10cm the bead length decreased by 543nm and bead width increased by 3nm, from 10cm to 15cm the bead length increased by 379nm and the bead width increased by 35nm, at 12kV (Figure 118). As the collection distance increased the beads maintained the combination of spherical and spindle-like morphology at 12kV. The bead morphology changed with increasing collection distance from spherical to spindle-like at 18kV and from spindle-like to spherical beads at 20kV (Figure 118 to 120). The fibre morphology changes with increasing collection distance with PVA 6%. As the collection distance increased, bead density reduced at 12kV (Figure 73) and 18kV (Figure 75), whereas it increases at 20kV (Figure 77). Increasing the collection distance can decrease the bead size, or increase bead width and decrease the bead length. As a result the beads appear spherical.

Increasing the collection distance increases the flight time²⁸. The increased flight time the increased the solvent evaporation rate, also allowed more time to stretch and elongate the jet. As the jet stretches, the spherical beads stretch to spindle-like beads^{20,28}. Alternatively,

the weakened electric field due to the increased distance can reduce the stretching which causes spindle-like beads to become spherical^{20,23}. This explains the changes in morphology of the beads as the collection distance increased with the beaded fibres formed using PVA 4% and PVA 6% solutions.

The effect of collection distance on the deposition rate for PVA 4%, PVA 6% and PVA 8% was analysed. Results showed whilst using PVA 4% as the collection distance increased the deposition rate increased from 7cm to 10cm collection distance at 8kV but decreased slightly from 10cm to 15cm collection distance (Figure 103). The deposition rate decreased with increasing collection distance at 12kV (Figure 103). The deposition rate decreased with increasing collection distance at 20kV (Figure 103). Whilst using PVA 6%, the deposition rate decreased with increasing collection distance at 12kV (Figure 104). The deposition rate decreases but slightly at 18kV (Figure 104). The deposition rate increased with increasing collection distance at 20kV (Figure 104). Whilst using PVA 8%, the deposition rate decreased with increasing collection distance at 12kV and 20kV (Figure 105). Generally, the deposition rate decreased as the collection distance increased. This suggests that the increased collection distance reduced the electric field strength, therefore, reducing the draw stress of the jet and depositing fewer fibres on the collector. However, the increased collection distance may have been too far for all the fibre electrospun to reach the collector. Zhao et al (2004) found too large distances resulted in no fibres reaching the collector⁴⁴. Therefore, fibres may form but necessarily deposit on the collector. During the electrospinning process fibres deposited on to surrounding surfaces as well as on the collector.

5.4. Electrospinning Process: Jet formation and Deposition

The fibres deposited on the collector and formed a visible circular or oval-shaped white layer which gradually became larger with subsequent deposition of fibres, spreading from the region of the collector in line with the needle (central region) outwards towards the edges of the collector. The central region coverage of the collector may have reduced the potential difference present which attracted the jet to collector. This could have resulted in the fibres depositing on other regions of the collector with less coverage on which the potential difference could attract the jet. This ultimately formed larger deposition areas of the fibres collected. On observing the electrospinning process, it was evident that once there was sufficient coverage of the central region of the collector, the fibre deposition area became larger (Appendix VIII).

Droplets of solution were released continuously with lower concentration solutions release, may be due to the coverage of the collector by fibres which reduced the potential difference between the needle and the collector (Appendix IX). The low viscosity of the low concentration solutions caused the surface tension to dominate which resulted in droplets ejecting instead of a jet forming from a Taylor cone at the needle tip²¹. The problem was solved by adjusting the solution tank height reduce or increase the solution flow to the tip. However, this didn't necessarily eliminate droplet formation but did sometimes reduce it. The droplet formation during electrospinning ceased jet and fibre formation. Large droplets were ejected on to the collector causing an inaccurate measure of the output of electrospun fibres from the machine within the given experimental time. The mass collected includes droplets deposited with the fibres. The height was adjusted regularly to maintain an adequate solution flow rate to the tip and reduce or eliminate droplet formation.

6. CONCLUSION

This study investigated the effects of solution concentration, applied voltage and collection distance on electrospun fibres of PVA solutions. Solutions of PVA 4%, PVA 6% and PVA 8% were electrospun using the ES1a electrospinning machine, New Zealand (2007).

The results of this study showed that the solution concentration affected the fibre morphology and the average fibre diameter. At lower concentrations beaded fibres were formed. At a higher concentration smooth fibres were obtained. The chain entanglement regime had increased with increasing concentration showing PVA 4% with $[\eta]C= 3$, PVA 6% with $[\eta]C= 4$ and PVA 8% with $[\eta]C= 6$. The greater increase between PVA 6% and PVA 8% led to the significant morphological change from beaded to smooth fibres. The fibre diameter had also increased with the concentration. This concludes that it is essential to control solution concentration to manipulate fibre morphology and diameter.

The solution concentration also effected the fibre diameter distribution. At given parameters consisting of combinations of either 12kV or 20kV with a collection distance of either 10cm or 15cm, an increase in fibre diameter distribution was observed with the results. Except with the results of parameters 10cm and 20kV where the fibre diameter distribution decreased from PVA 6% to PVA 8%. However, determined from the results the solution concentration showed to generally have the effect of increasing the fibre diameter distribution.

The effect increasing solution concentration had on deposition rate varied with the parameters used. An obvious increase was observed with parameters of 12kV and 10cm.

Only slight changes were observed using parameters of 12kV and 15cm. However, with parameters of 20kV and 10cm, also 20kV and 15cm the deposition rate decreased from PVA 4% to PVA 6% and increased from PVA 6% to PVA 8% with increasing concentration. Generally, there is a higher productivity using a higher concentration solution. It is evident from the results that solution concentration affects productivity of the nanofibres and depending on specific collection distance and voltage used the productivity may be greater, less or have little effect at all.

Manipulation process parameters were equally as influential on fibre formation. Increasing the applied voltage affected the fibre morphology and diameter. Depending on the solution concentration increasing the voltage formed either thinner or larger fibres and affected the bead morphology. Using PVA 4% increasing the voltage formed thinner beaded fibres with elongated beads as the voltage increased to 12kV. Whilst using PVA 4% the beads formed on fibres at lower voltages were elongated and larger in comparison to beads formed at higher voltages which were mainly spherical. Applying higher voltages of 18kV and 20kV on PVA 6% solution formed either spherical or spindle-like beads but no elongated beads on fibres were observed.

Whilst using PVA 6% the effect of increasing the voltage was also influenced by the collection distance. The results show that the fibre diameter decreased from 12kV to 18kV and increased from 18kV to 20kV at 10cm collection distance. The opposite effect of increasing the voltage occurs at 15cm collection distance with the fibre diameter increasing from 12kV to 18kV and decreasing from 18kV to 20kV. Morphology of the beaded on the beaded fibres varied at 12kV and 20kV, also fibre webs forming at 18kV with 10cm

collection distance. However, at 15cm collection distance the morphology distinctly altered from spindle-like to spherical morphology as the voltage increased. Similar influence of the increasing collection distance with the increasing voltage is observed whilst using PVA 8%. Using PVA 8% the results show that the fibre diameter increases with increasing voltage at 10cm collection distance. At a longer collection distance of 15cm the fibre diameter slightly increased as the voltage increased. The fibre morphology consisted of smooth and more uniform fibres at a lower voltage of 12kV. At a higher voltage of 20kV the fibres had undulating diameters and a mixture of cylindrical and flat ribbon morphologies with fibre webbing also observed.

Whilst using PVA 4% the fibre diameter increased with increasing collection distance from 10cm to 15cm at 8kV and 20kV, with only a slight decrease observed at 12kV. Fibre webs observed at shorter distances had diminished when the collection distance increased to 10cm and then 15cm. Variation in the fibre diameter was observed whilst using PVA 6%. At this concentration, the effect increasing the collection distance was also affected by the voltage applied. Increasing the collection distance at 12kV showed little variation in the fibre diameter. More variations were observed at higher voltages. However, the difference in results of the fibres formed was distinct at 18kV and 20kV. The study showed that a slight variation of the applied voltage greatly influenced the composition of the fibres. This was observed whilst increasing the collection distance at 18kV which showed the fibre diameter decreased and the morphology of beads on the fibres changed from spherical to spindle-like. Increasing the collection distance at 20kV decreased the diameter and the beads changed from spindle-like to spherical. Adhering fibres and fibre webs were observed at a

shorter collection distance whilst using PVA 8%. Increasing the collection distance resulted in larger fibres being formed.

Effects of the increasing voltage on the fibre diameter distribution were analysed. The increasing the voltage influenced the fibre diameter distribution by either narrowing or widening it. The diameter distribution had decreased with increasing voltage using PVA 4% and from 12kV to 18kV using PVA 6% at 10cm collection distance. However, the distribution increased using PVA 6% from 18kV to 20kV at 10cm collection distance, also whilst using PVA 6% at 15cm collection distance and for PVA 8% as the voltage increased. The study shows that at lower concentrations increasing the voltage narrows the fibre diameter distribution, whilst at a higher concentration increasing the voltage increases the distribution. However, whilst using PVA 6% the effect of increasing voltage shows both the increase in fibre diameter distribution from 12kV to 18kV and decrease from 18kV to 20kV at 10cm collection distance. This has shown the sensitivity of altering the applied voltage and its effect on the fibre formation such that a large increase in voltage, as well as a slight increase can evidently alter the variation in diameters of fibres.

The deposition rate was also affected by the increasing voltage. As the applied voltage increased the deposition rate increased for PVA 4 %, decreased for PVA 8% and for PVA 6% increased from 12kV to 18kV but decreased from 18kV to 20kV. This proved that increasing the voltage controlled the productivity of fibres either resulting in producing more or less nanofibres per unit time of production. The effect of the increasing collection distance on the deposition rate showed an increase observed only using PVA 4% at 8kV from 7cm to 10cm and with PVA 6% at 20kV. The rest of the results using PVA 4%, PVA 6% and PVA 8%

showed a decrease in deposition rate with increasing collection distance which concluded that increasing the collection distance can potentially decrease productivity of nanofibres.

Increasing the collection distance effected the fibre formation but this was also influenced by the solution concentration and the applied voltage. At a shorter collection distance fibre webs were more likely to form which distorted the fibre morphology. This effect was more evident whilst using PVA 4% and PVA 6% at 7cm collection distance and at 10cm collection distance for all the PVA solutions. Increasing the collection distance for all the solutions resulted in more distinct fibre formation, whilst also altering the fibre diameter and morphology. An adequate distance was required between the tip and collector to allow time for fibres to dry sufficiently before reaching the collector. Fibre diameter distribution varied with increasing collection distance at a given voltage whilst using PVA 4% and PVA 6% but with using PVA 8% the distribution had only increased with increasing collection distance.

Generally, the deposition rate decreased with increasing collection distance with the exception of PVA 6% at 20kV that showed an increased deposition rate.

Observations were made of the jet formation and electrospinning phases of PVA 4%, PVA 6% and PVA 8%. Solutions of PVA 4% electrospun with a constant polymer beat and at a regular pace with little obstruction to production processes. In comparison, the PVA 6% the solution electrospun whilst randomly releasing droplets of the solution on to the collector that halted electrospinning temporarily but otherwise maintaining a jet with a constant polymer beat. Solutions of PVA 8% electrospun without a polymer beat and randomly

formed dual or triple minijets on the needle tip. However, electrospinning with all the solutions was simple and effective.

This study demonstrated that nanofibres could be obtained using the ES1a machine but the quality and size of the fibres formed depended greatly on the correct combination of solution properties and process parameters. The solution concentration showed the most evident effect on the diameter and morphology of fibres formed. A certain degree of polymer chain entanglements were necessary to form smooth and beaded fibres which were only obtained using PVA 8%. The collection distance was a crucial parameter to manipulate as at shorter distances fibre webs were more likely to form that distorted and merged the fibres on reaching the collector. Sufficient collection distance was required in order to obtain single dry fibres. The applied voltage affected the morphology and number of beads formed on beaded fibres of PVA 4% and PVA 6%. Varying the process parameters showed the different effects this had on the resultant fibres formed. Either increasing the collection distance or the applied voltage or a combination of both showed this altered the dimensions of the fibres. This effect was clearly observed with each solution. However, altering the process parameters for PVA 4% and PVA 6% could not eliminate the bead formation due to insufficient chain entanglement but it could reduce the number and size of beads on the fibres formed. The solution concentration determined the type of fibre formed, hence smooth or beaded fibres, and the voltage and collection distance controlled the quality, for example, reducing or increasing the fibre diameter.

The solution concentration, voltage and collection distance affected the fibre diameter, morphology, fibre diameter distribution and deposition rate. Electrospinning PVA was

simple and fibres of nanometre range could easily be formed. This study shows that structures can be manipulated at a nanoscale level with electrospinning. Electrospinning PVA may prove to be beneficial biocompatible material in the field of nanomedicine for the fabrication of tissue engineering scaffolds used for the replacement of injured or diseased soft tissue.

7. FUTURE WORKS

This study has proven that fabricating nanofibres is relatively simple and effective. Investigation into controlling the parameters and calibrating of the ES1a machine has given knowledge of the productivity and structure of nanofibres formed whilst electrospinning PVA solutions.

Further work can investigate into obtaining specific structures that can mimic the architecture or topography of certain biological structures. The results of this study consisted of the collection of randomly orientated fibres. However, further studies can be conducted into collecting aligned nanofibres or experimentation of fabricating different nanofibre structures of PVA solutions using textured collectors.

My main purpose to use PVA for this study was its potential as a biomedical material for tissue engineering scaffolds. To investigate this potential further cell culture studies will be needed which analyse its biocompatibility with soft tissue cells invitro. Experimentation can be carried out to determine the response tissue cells have to such nanoscale structures produced by electrospinning.

Further work can be done into exploring the different nanostructures that can be produced using the ES1a machine, whilst also investigating the invitro cell reaction to the nanostructures produced.

8. APPENDICES

I. PVA 4% Calibration of Flow Rate on ES1a

Calibration using volume of 3mls of PVA 4% solution.

Parameters – 10cm collection distance, 12kV applied voltage, Tank height = 21.5cm

Time (hr)	Volume reading (ml)	Observations
0	3	
1	2.5	Polymer bead, droplets on collector
2	2.3	
3	2.2	
4	2.1	Needle tip dried out
5	2.1	Volume loss by drops and fibre-forming

Aluminium foil collector mass = 1.46g

Aluminium foil collector + PVA deposited mass = 1.50g

Ila) PVA 4% Calibration of Flow Rate on ES1a

Calibration using volume of 3mls of PVA 4% solution

Parameters – 10cm collection distance, 12kV applied voltage, Tank height = 21cm

Time (hr)	Volume reading (ml)	Observations
0	3	
0.5	2.9	Polymer beat, single jet
1	2.8	No polymer beat
1.5	2.7	
2	2.6	
2.5	2.5	Polymer beat, single jet
3	2.4	
3.5	2.3	
4	2.2	
4.5	2.1	
5	2	
5.5	1.9	
6	1.8	
6.5	1.7	
7	1.7	

Aluminium foil collector mass = 1.45g

Aluminium foil collector + PVA deposited mass = 1.48g

Ilb) PVA 4% Calibration of Flow Rate on ES1a

Calibration using volume of 3mls of PVA 4% solution

Parameters – 10cm collection distance, 12kV applied voltage, Tank height = 21cm

Volume reading (ml)	Time	Observations
3	0	
2.8	49 min	Polymer beat, single jet
2.6	2hrs	
2.4	3hrs	
2.2	3hrs 44min	
2.0	4hrs 47min	
1.8	6hrs	

Aluminium foil collector mass = 1.45g

Aluminium foil collector + PVA deposited mass = 1.48g

IIIa) PVA 6% Calibration of Flow Rate on ES1a

Calibration using volume of 3mls of PVA 6% solution

Parameters – 10cm collection distance, 12kV applied voltage, Tank height = 21cm

Time (hr)	Volume reading (ml)	Observations
0	3	
0.5	2.8	Volume loss via droplet ejection
1	2.6	and fibre forming
1.5	2.3	
2	2.2	Continuous droplet ejection, no jet

Aluminium foil collector mass = 1.36g

Aluminium foil collector + PVA deposited mass = 1.42g

IIIb) PVA 6% Calibration of Flow Rate on ES1a

Calibration using volume of 3mls of PVA 6% solution

Parameters – 10cm collection distance, 12kV applied voltage, Tank height = 22cm

Volume reading (ml)	Time	Observations
3	0	
2.9	12 min	No polymer beat, single jet
2.8	27 min	
2.7	40 min	
2.6	52 min	
2.5	1 hr 5 min	
2.4	1 hr 15 min	
2.3	1 hr 30 min	
2.2	1 hr 40 min	Continuous droplet ejection, no jet

Aluminium foil collector mass = 1.45g

Aluminium foil collector + PVA deposited mass = 1.48g

IVa) PVA 6% Calibration of Flow Rate on ES1a

Calibration using volume of 3mls of PVA 6% solution

Parameters – 15cm collection distance, 20kV applied voltage, Tank height = 22cm

Time (hr)	Volume reading (ml)	Observations
0	3	
0.5	2.6	Volume loss via droplet ejection and fibre forming
1	2.2	
1.5	1.8	

IVb) PVA 6% Calibration of Flow Rate on ES1a

Calibration using volume of 3mls of PVA 6% solution

Parameters – 15cm collection distance, 20kV applied voltage, Tank height = 22cm

Volume reading (ml)	Time	Observations
3	0	
2.8	13 min	No polymer beat, single jet
2.6	24 min	
2.4	39 min	
2.2	50 min	
2.0	1 hr 9 min	
1.8	1 hr 23 min	

Va) PVA 8% Calibration of Flow Rate on ES1a

Calibration using volume of 3mls of PVA 8% solution

Parameters – 10cm collection distance, 12kV applied voltage, Tank height = 22cm

Time (min)	Volume reading (ml)	Observations
0	3	
15	2.8	Single jet, no droplets
30	2.6	

Vb) PVA 8% Calibration of Flow Rate on ES1a

Calibration using volume of 3mls of PVA 8% solution

Parameters – 10cm collection distance, 12kV applied voltage, Tank height = 22cm

Volume reading (ml)	Time	Observations
3	0	
2.8	16 min	No polymer beat, single jet
2.6	29 min	Droplet ejection

VIa) PVA 8% Calibration of Flow Rate on ES1a

Calibration using volume of 3mls of PVA 8% solution

Parameters – 10cm collection distance, 12kV applied voltage, Tank height = 22.1cm

Time	Volume reading (ml)	Observations
0 min	3	
15 min	2.8	Single jet
30 min	2.7	
45 min	2.6	
1hr	2.5	
1hr 15min	2.4	
1hr 30 min	2.3	
1hr 30 min	2.2	
2 hrs	2.2	

VIb) PVA 8% Calibration of Flow Rate on ES1a

Calibration using volume of 3mls of PVA 8% solution

Parameters – 10cm collection distance, 12kV applied voltage, Tank height = 22.1cm

Volume reading (ml)	Time	Observations
3	0	
2.8	9 min	Single jet
2.6	33 min	
2.4	1 hr 5 min	
2.2	1 hr 50 min	

Appendix VII

Concentration

Polymer Chain Entanglement Regime

The Mark-Houwink equation defines the intrinsic viscosity, $[\eta]$, for PVA in water⁶².

$$[\eta] = 6.51 \times 10^{-4} M_w^{0.628}$$

Berry number: $[\eta]C$

$[\eta]$: Intrinsic viscosity

C: Concentration

PVA M_w : 72,000 g/mol

PVA Concentrations used:

- PVA 4%
- PVA 6%
- PVA 8%

Calculating Intrinsic Viscosity

$$[\eta] = 6.51 \times 10^{-4} M_w^{0.628}$$

$$[\eta] = 6.51 \times 10^{-4} (72,000)^{0.628}$$

$$[\eta] = 0.73$$

Calculating Berry number: $[\eta]C$

$$C = \text{PVA 4\%} \quad [\eta]C = 0.73 \times 4$$

$$[\eta] = 0.73 \quad [\eta]C = 2.92$$

Chain entanglement regime **PVA 4%: $[\eta]C = 3$**

$$C = \text{PVA 6\%} \quad [\eta]C = 0.73 \times 6$$

$$[\eta] = 0.73 \quad [\eta]C = 4.38$$

Chain entanglement regime **PVA 6%: $[\eta]C = 4$**

$$C = \text{PVA 8\%} \quad [\eta]C = 0.73 \times 8$$

$$[\eta] = 0.73 \quad [\eta]C = 5.84$$

Chain entanglement regime **PVA 8%: $[\eta]C = 6$**

Appendix VIII

Deposition Area of PVA Nanofibres

The solutions were electrospun and the product deposited on the Al foil collector. The following images are of the deposition areas of the electrospun material. Each variable investigated consisted of four experiments. The deposition areas consist of the rectangular Al foil collector with the shape of the deposited electrospun fibres.

The tables below show the measurements which consist of the length and width (length/width=L↕W↔) of the deposition, an image of the deposition area (DA) and the measured mass in grams of electrospun PVA obtained on the collector.

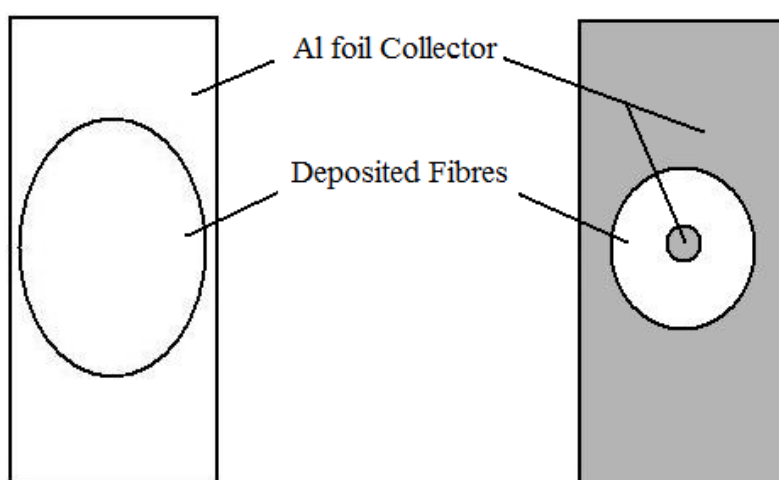


Figure 131. Image above shows the collector and region of collection. The image on the left gives an example of the deposition which comprises of an oval shaped collection with no visible region of the collector surface within the deposition. The image on the right is an example of a ringed collection which consists of the circular deposition of PVA with a region in the centre of the visible collector surface.

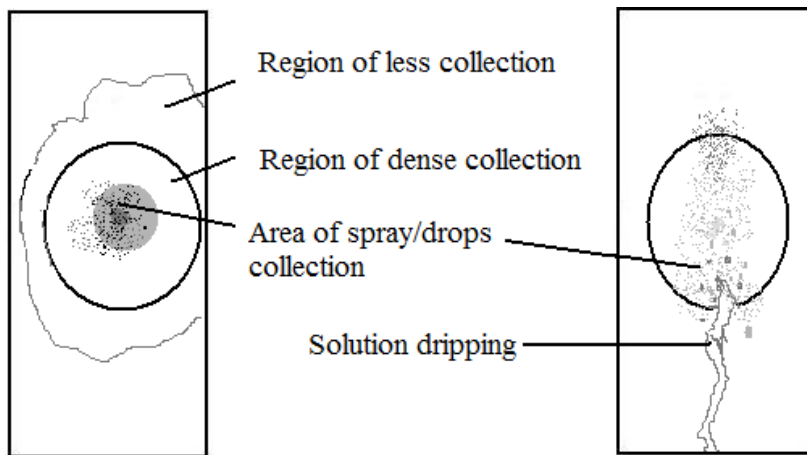


Figure 132. The image above shows the fibre collection, spraying, ejection of drops on the collector and regions of the solution collection due to insufficient drying the jet before reaching the collector.

Deposition Area of Fibres from Electrospun PVA 4% Solutions

Deposition area= DA, (length/width=L↕W↔)

EXP 1	EXP2	EXP3	EXP4
DA= 20cm /10 cm	DA=20/12cm	DA= 19cm/10.5cm	DA=19/11cm
PVA=0.01g	PVA=0.01g	PVA=0.02g	PVA=0.01g

Table 1. PVA 4%, 12kV, 15cm, H=25cm

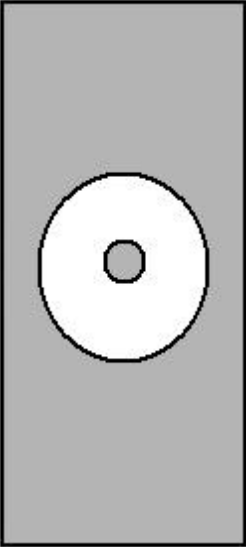
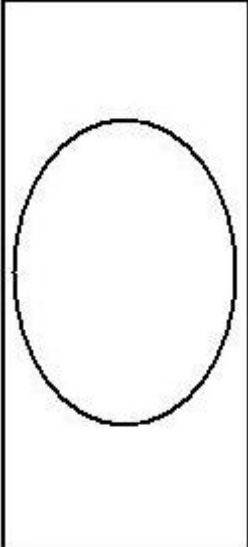
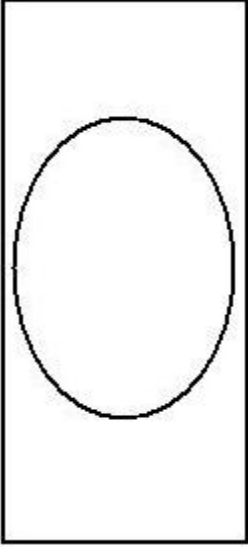
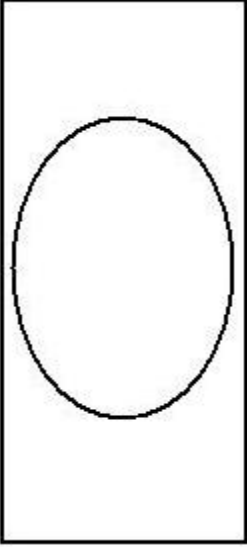
EXP 1	EXP2	EXP3	EXP4
DA= 11/9cm	DA=13/10cm	DA= 13/11cm	DA=13/9cm
			
PVA=0.03g	PVA=0.01g	PVA=0.02g	PVA=0.01g

Table 2. PVA 4%, 12kV, 10cm, H=25cm

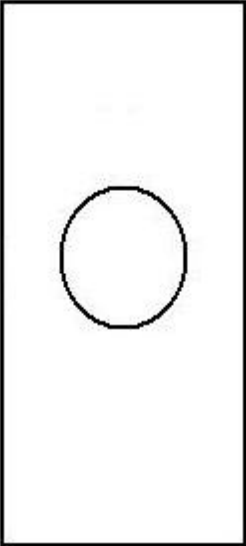
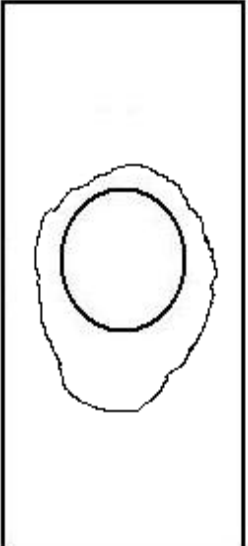
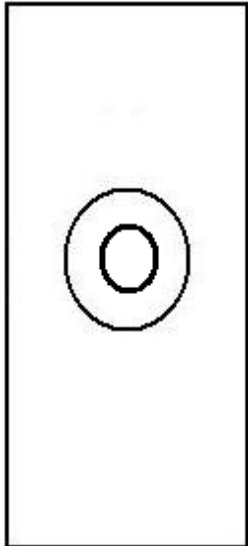
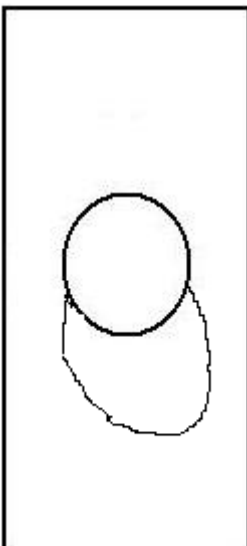
EXP 1	EXP2	EXP3	EXP4
DA= 8.5/7cm	DA=9/7.5cm	DA= 8/7cm	DA=9/7cm
			
PVA=0.07g	PVA=0.05g	PVA=0.05g	PVA=0.03g

Table 3. PVA 4%, 20kV, 10cm, H=25cm

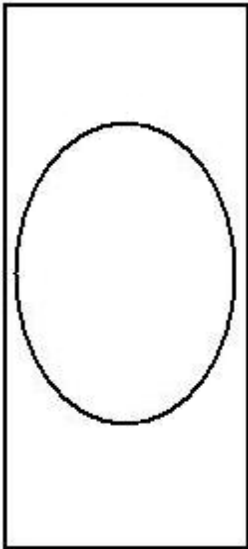
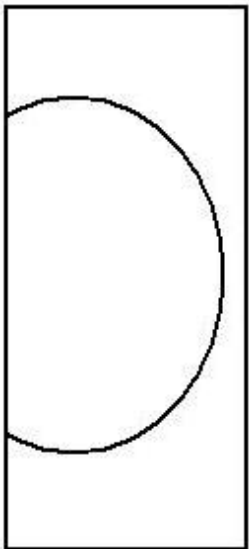
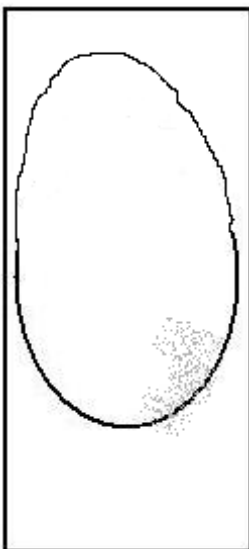
EXP 1 (H=24cm)	EXP2 (H=25cm)	EXP3 (H=25cm)	EXP4 (H=24cm)
DA= 18/9cm	DA=15/10cm	DA= 13/11cm	DA=20/10cm
			
PVA=0.03g	PVA=0.01g	PVA=0.04g	PVA=0.04g

Table 4. PVA 4%, 20kV, 15cm, H=24-25cm

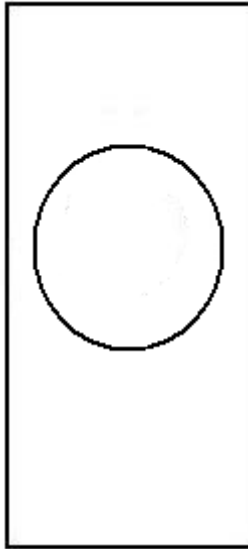
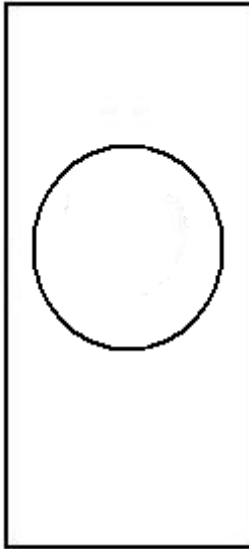
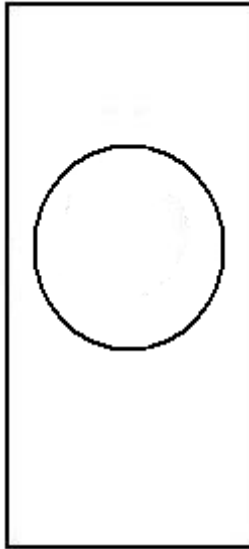
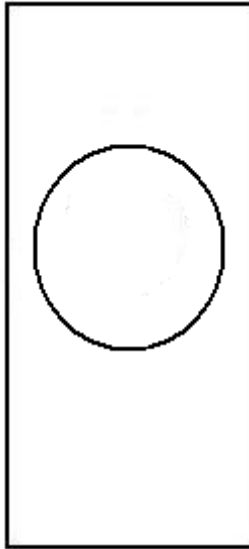
EXP 1 (H=25cm)	EXP2 (H=25cm)	EXP3 (H=25cm)	EXP4 (H=24cm)
DA= 11/10cm	DA=11/11cm	DA= 12.5/10.5cm	DA=10/10.5cm
			
PVA=0.01g	PVA=0.01g	PVA=0.01g	PVA=0.01g

Table 5. PVA 4%, 8kV, 10cm, H=24-25cm

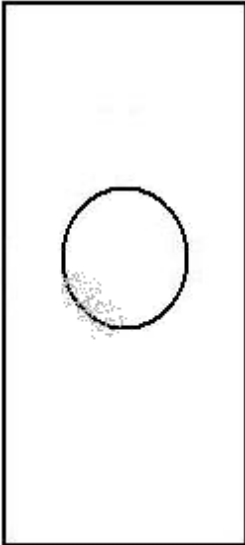
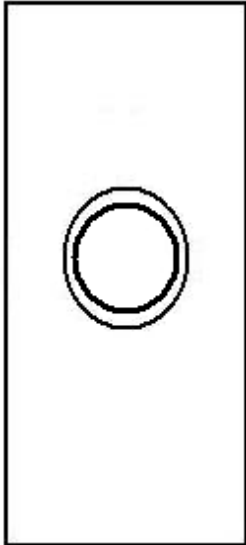
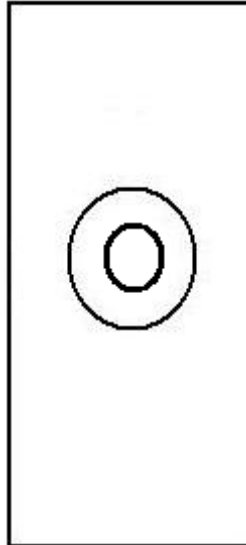
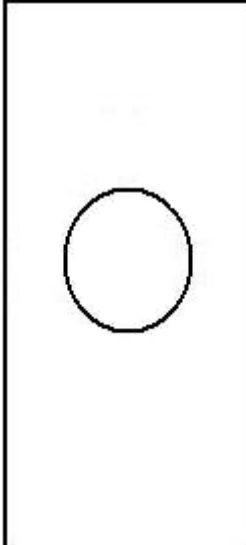
EXP 1	EXP2	EXP3	EXP4
DA= 8.5/7.5cm	DA=8/8.5cm	DA= 7.5/8.5cm	DA=8/8.5cm
			
PVA=0.01g	PVA=0.01g	PVA=0.02g	PVA=0.02g

Table 6. PVA 4%, 12kV, 7cm, H=25cm

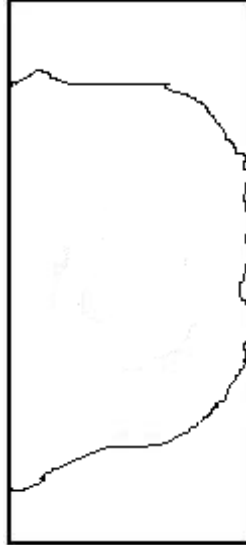
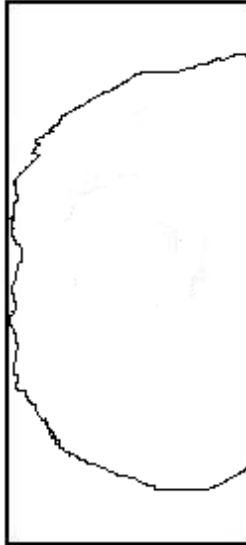
EXP 1 (H=25cm)	EXP2 (H=25cm)	EXP3 (H=24.5cm)	EXP4 (H=24.5cm)
DA= 20/10.5cm	DA=20/11.5cm	DA= 21/10cm	DA= 21/10cm
			
PVA=0.01g	PVA=0.01g	PVA=0.01g	PVA=0.01g

Table 7. PVA 4%, 8kV, 15cm, H=24.5-25cm

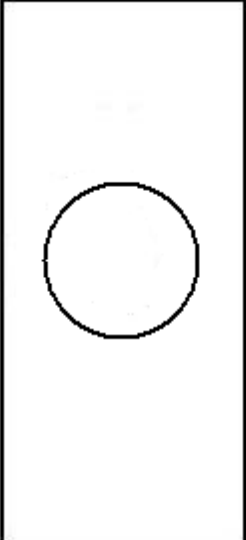
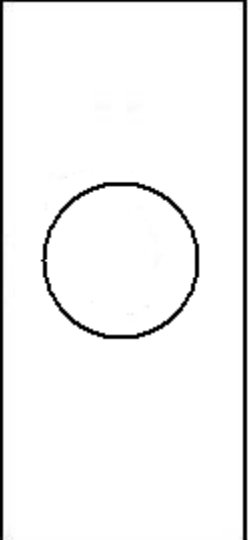
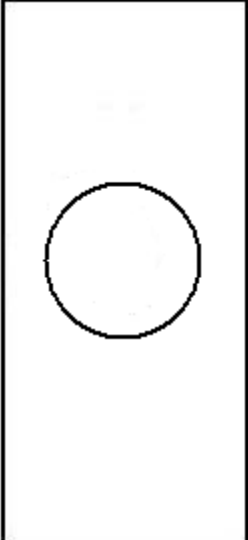
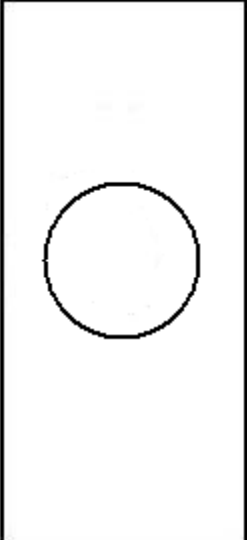
EXP 1 (H=25cm)	EXP2 (H=25cm)	EXP3 (H=24.5cm)	EXP4 (H=24.5cm)
DA= 9/9cm	DA=9.5/9.5cm	DA= 8.5/8.5cm	DA=9.5/9.5cm
			
PVA=0.01g	PVA=0.01g	PVA=0.01g	PVA=0.01g

Table 8. PVA 4%, 8kV, 7cm, H=25cm

Deposition Area of Fibres from Electrospun PVA 6% Solutions

Deposition area= DA, (length/width=L↕W↔)

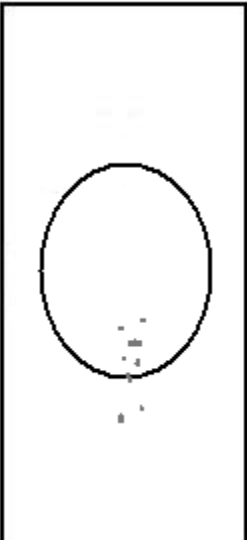
EXP 1 (H=25cm)	EXP2 (H=25cm)	EXP3 (H=25cm)	EXP4 (H=25.5cm)
DA= 13/8.5cm	DA=13/9cm	DA= 12/9.5cm	DA=12/9.5cm
			
PVA=0.14g	PVA=0.20g	PVA=0.17g	PVA=0.13g

Table 9. PVA 6%, 12kV, 10cm, H=25-25.5cm

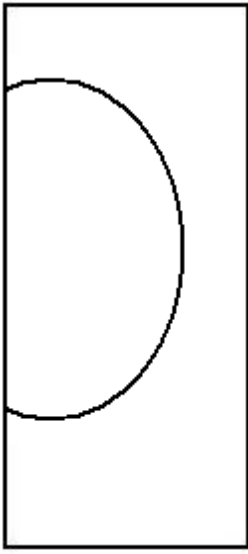
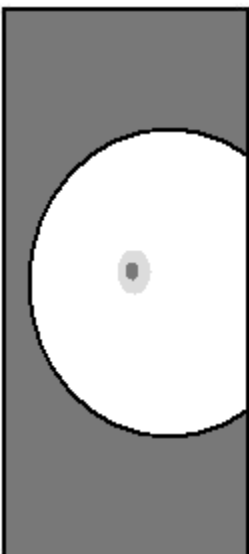
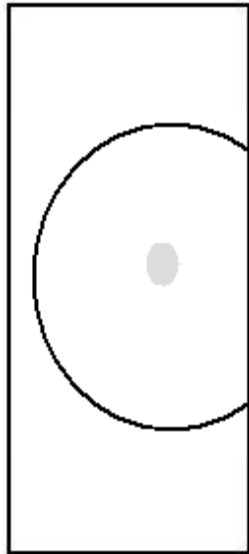
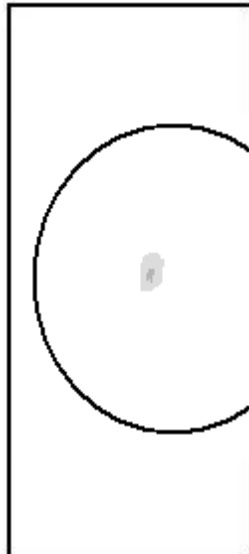
EXP 1	EXP2	EXP3	EXP4)
DA= 18/8.5cm	DA=15/10cm	DA= 14/9.5cm	DA=14/10.5cm
			
PVA=0.07g	PVA=0.08g	PVA=0.07g	PVA=0.08g

Table 10. PVA 6%, 20kV, 15cm, H=25cm

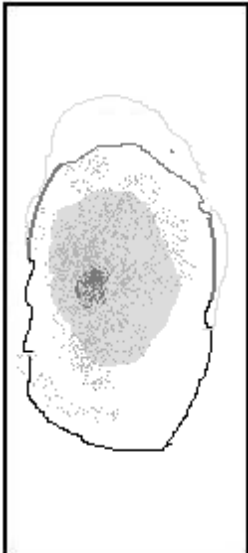
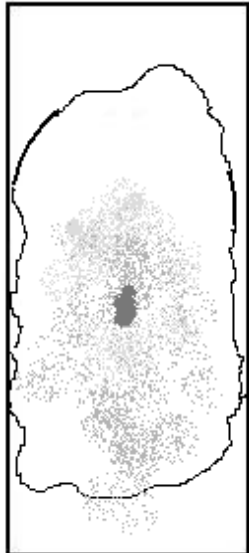
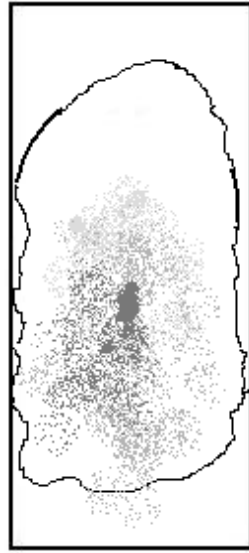
EXP 1 (H=24.5cm)	EXP2(H=24.5cm)(FIB)	EXP3 (H=24cm)	EXP4 (H=24.5cm)
DA= 16/9cm	DA=23/10cm	DA= 21/10cm	DA=20/9.5cm
			
PVA=0.02g	PVA=0.1g	PVA=0.17g	PVA=0.09g

Table 11. PVA 6%, 20kV, 10cm, H=24-24.5cm

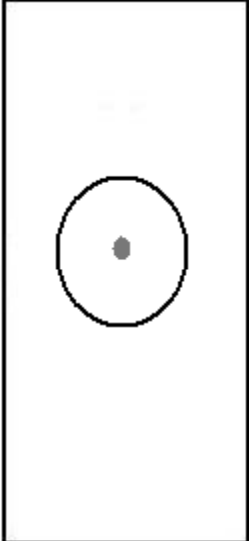
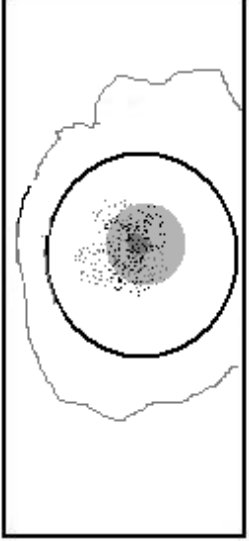
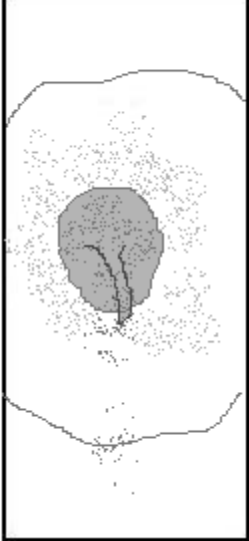
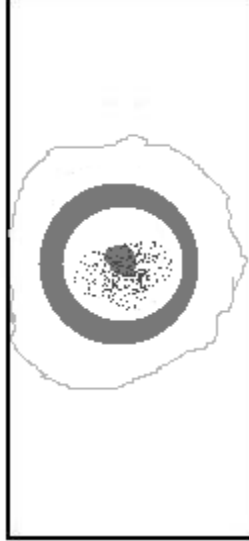
EXP 1	EXP2 (FIB)	EXP3 (FIB)	EXP4)(FIB)
DA= 8/7cm	DA=17/9.5cm	DA= 22/11.5cm	DA=13/11cm
			
PVA=0.1g	PVA=0.01g	PVA=0.17g	PVA=0.14g

Table 12. PVA 6%, 18kV, 10cm, H=25cm

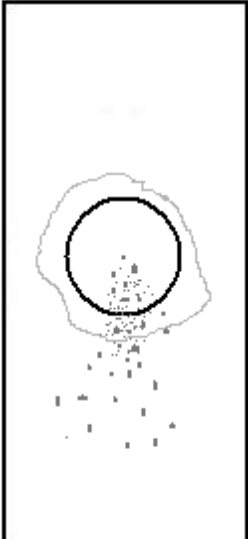
EXP 1 (H=25cm)	EXP2 (H=24.5cm)	EXP3 (H=24.5cm)	EXP4 (H=24.5cm)
DA= 12/9.5cm	DA=8.5/10cm	DA= 7/6.5cm	DA=12/7.5cm
			
PVA=0.05g	PVA=0.02g	PVA=0.02g	PVA=0.01g

Table 13. PVA 6%, 12kV, 7cm, H=24.5-25cm

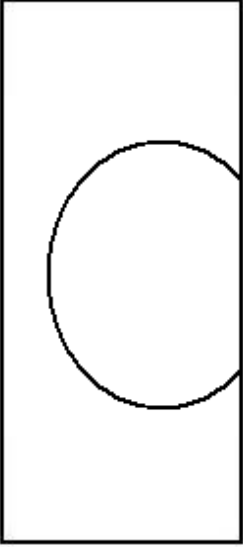
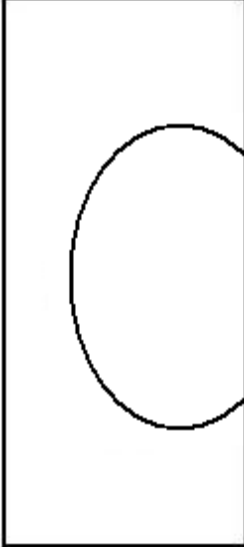
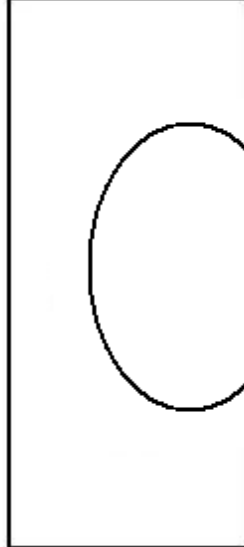
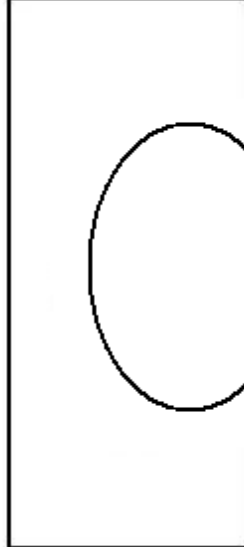
EXP 1	EXP2	EXP3	EXP4
DA= 16/9.5cm	DA=16/8.5cm	DA= 15/9cm	DA=16/9cm
			
PVA=0.03g	PVA=0.04g	PVA=0.04g	PVA=0.05g

Table 14. PVA 6%, 18kV, 15cm, H=25cm

EXP 1 (H=25cm)	EXP2 (H=25cm)	EXP3 (H=25.5cm)	EXP4 (H=25.5cm)
DA= 22/9.5cm	DA=23/10cm	DA= 23/9.5cm	DA= 23/9.5cm
			
PVA=0.17g	PVA=0.09g	PVA=0.09g	PVA=0.05g

Table 15. PVA 6%, 12kV, 15cm, H=25.5-25cm

Deposition Area of Fibres from Electrospun PVA 8% Solutions

Deposition area= DA, (length/width=L↕W↔)

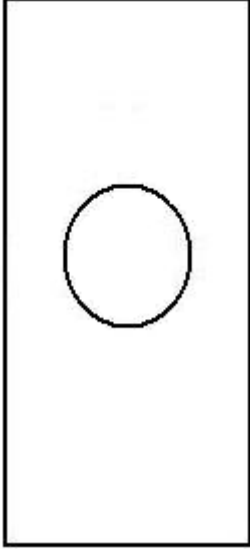
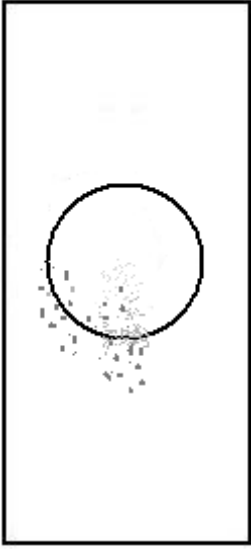
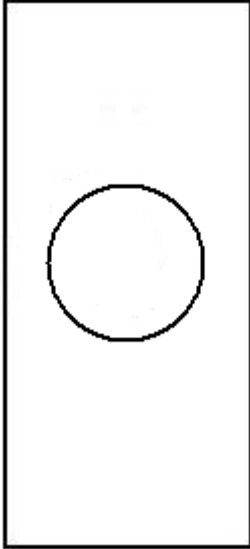
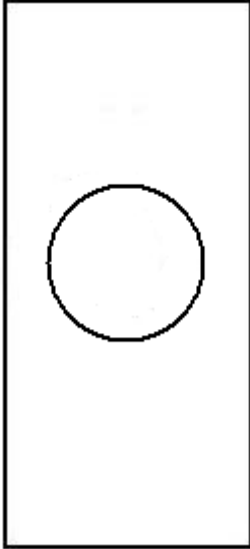
EXP 1 (H=26cm)	EXP2 (H=25cm)	EXP3 (H=25cm)	EXP4 (H=25cm)
DA= 7.5/7.5cm	DA=10.5/8.5cm	DA= 9.5/8.5cm	DA=9/9cm
			
PVA=0.05g	PVA=0.03g	PVA=0.02g	PVA=0.02g

Table 16. PVA 8%, 12kV, 10cm, H=25-26cm

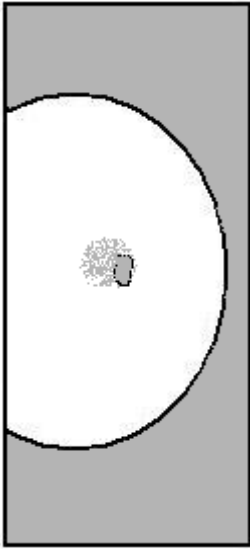
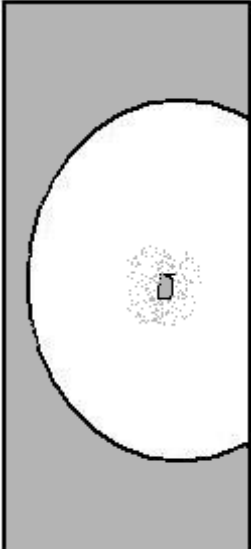
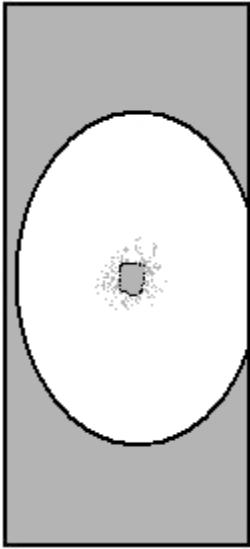
EXP 1 (H=26cm)	EXP2 (H=26cm)	EXP3 (H=25cm)	EXP4 (H=26cm)
DA=23/10.5cm	DA=23/11.5cm	DA= 20/10.5cm	DA=18/10cm
			
PVA=0.09g	PVA=0.06g	PVA=0.08g	PVA=0.14g

Table 17. PVA 8%, 20kV, 10cm, H=25-26cm

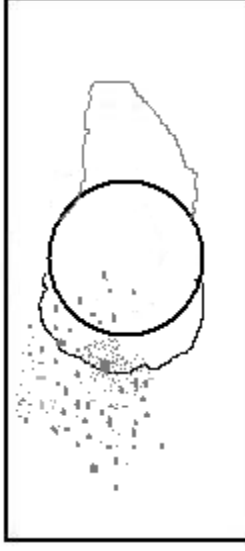
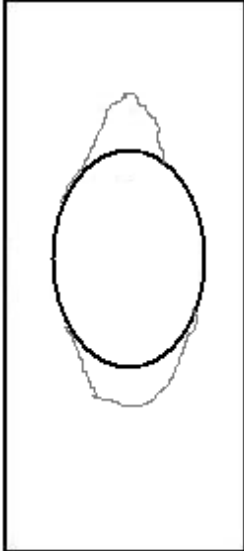
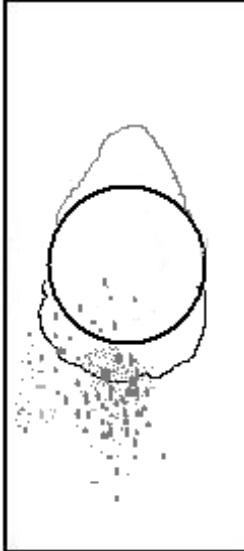
EXP 1 (H=25cm)	EXP2 (H=25cm)	EXP3 (H=26cm)	EXP4 (H=26cm)
DA=14/9cm	DA=12.5/10cm	DA= 15/8.5cm	DA=14/9.5cm
			
PVA=0.01g	PVA=0.03g	PVA=0.03g	PVA=0.02g

Table 18. PVA 8%, 12kV, 15cm, H=25-26cm

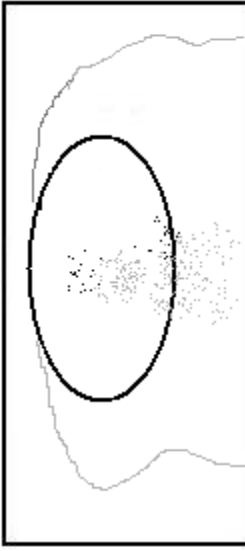
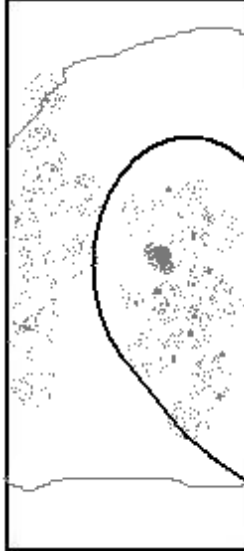
EXP 1	EXP2	EXP3	EXP4
DA=20/10cm	DA=24/11cm	DA= 22/10.5cm	DA=14/10.5cm
			
PVA=0.12g	PVA=0.03g	PVA=0.03g	PVA=0.09g

Table 19. PVA 8%, 20kV, 15cm, H=26cm

9. REFERENCES

1. Greiner Andreas & Wendorff J.H. Electrospinning: A Fascinating Method for the Preparation of Ultrathin Fibers. *Angew. Chem. Int. Ed.*, 2007, 46;5670-5703
2. Kumar S.G., Nukavarapu S.P., James R., Hogan M.V. and Laurencin C.T. Recent Patents on Electrospun Biomedical Nanostructures: An Overview. *Recent Patents on Biomedical Engineering*, 2008, 1;68-78.
3. Venugopal J., Low S., Choon A.T. & Ramakrishna S. Interaction of cells and nanofibre scaffolds in tissue engineering. *Journal of Biomedical Materials Research Part B: Applied Biomaterials*, 2007,84B;34-48.
4. Venugopal J., Y. Z. Zhang and S. Ramakrishna. Electrospun nanofibres: biomedical applications. *J Nanoengineering and Nanosystems*, 2005, 218; 35-45
5. Gomes D.S., da Silvia A.N.R., Morimoto N. I., Mendes L.T.F., Furlan R. & Ramos I. Characterization of an electrospinning process using different PAN/DMF concentrations. *Polímeros*, 2007, 17;206-211.
6. Teo W.E. & Ramakrishna S. A review on electrospinning design and nanofibre assemblies. *Nanotechnology*, 2006, 17;R89-R106
7. Reneker D. H. & Chun I. Nanometre diameter fibres of polymer, produced by electrospinning. *Nanotechnology*, 1996, 7;216-223.
8. Shenoy S., W. D. Bates, H. L. Frisch and G. E. Wnek. Role of chain entanglements on fibre formation during electrospinning of polymer solutions: good solvent, non-specific polymer-polymer interaction limit. *Polymer* 2005, 46;3372-3384.

9. Reneker D.H., Yarin A.L., Fong H. & Koombhongse S. Bending instability of electrically charged liquid jets of polymer solutions in electrospinning. *Journal of Applied Physics*, 2000, 87;4531-4547.
10. Demir M.M., Yilgor I., & Erman B. Electrospinning of polyurethane fibers. *Polymer*, 2002, 43;3303-3309.
11. Doshi J. & Reneker D.H. Electrospinning Process and Applications of Electrospun Fibers. *Journal of Electrostatics*, 1995, 35;151-160.
12. Rutledge G. C. & Fridrikh S. V. Formation of Fibre by Electrospinning. *Advanced Drug Delivery Views*, 2007, 59;1384-1391
13. Lee J. S., Choi K. H., Ghim H. D., Kim S.S., Chun D. H., Kim H. Y. & Lyoo W.S. Role of molecular weight of atactic poly(vinyl alcohol) (PVA) in the structure and properties of PVA nanofabric prepared by electrospinning. *Journal of Applied Material Science*, 2004, 93;1638-1646.
14. Haghi A.K. & Akbari M. Trends in electrospinning of natural nanofibres. *Physica Status Solidi*, 2007, 204;1830-1834
15. Eda G., Liu J, Shivkumar S. Flight of path of electrospun polystyrene solutions: Effects of molecular weight and concentrations. *Materials Letters*, 2001, 67;1451-1455.
16. Tao J., Shivkumar S. Molecular weight dependent structural regimes during the electrospinning of PVA. *Materials Letters*, 2007,61;2325:2328.
17. Weiwei Z., Zhu M., Yang W., Yu H. Chen Y. And Zhang Y. Experimental Study on the Relationship between Jet Instability and Formation of Beaded Fibres during Electrospinning. *Polymer Engineering and Science*, 2005, 45; 704-709

18. Teraoka I. *Polymer Solutions: an introduction to physical properties*. Wiley Publishers, New York & Canada, 2002.
19. Ramakrishna S., Fujihara K., Teo W-E., Lim T-C., & Ma Z. *An Introduction to Electrospinning and Nanofibers*. World Scientific Publishing, London, 2005.
20. Lee K.H., Kim H.Y., Band H.J., Jung Y.H., and Lee S.G. The change of bead morphology formed on electrospun polystyrene fibres. *Polymer*, 2003, 44;4029-4034.
21. Dietzel J. M., Kleinmeyer J., Harris D. & Beck Tan N. C. The effect of processing variables on the morphology of electrospun nanofibres and textiles. *Polymer*, 2001, 42;261-272.
22. Megelski S., Stephens J.S. Chase D.B. and Rabolt J.F. Micro- and Nanostructured Surface Morphology on Electrospun Polymer Fibres. *Macromolecules*, 2002;8456-66.
23. Zhong X., Kim K., Fang D., Ran S., Hsiao B. S. & Chu B. Structure and process relationship of electrospun bioabsorbable nanofibre membranes. *Polymer*, 2002, 43;4403-4412.
24. Liu Y., He J-H., Yu J-Y. & Zeng H-M. Controlling numbers and sizes of beads in electrospun nanofibres. *Polymer International*, 2008, 57;632-636
25. Kong C. S., Lee T.H., Lee S. H. & Kim H.S. Nano-web formation by the electrospinning at various electric fields. *Journal of Material Science*, 2007,42;8106-8112
26. Jarusuwannaporn T., Hongrojjanawiwat W., Jitjaicham S., Wannatong L., Nithitanakul M., Pattamaprom C., Khoombhongse P., Rangkupan R. & Supaphol P. Effect of solvents on electro-spinnability of polystyrene solutions and

- morphological appearance of resulting electrospun polystyrene fibers. *European Polymer Journal*, 2005, 41;409-421
27. Reneker D.H. & Yarin A.L. Electrospinning Jets and Polymer Nanofibres. *Polymer*, 2008, 48; 2387-2425.
28. Homayoni H., Ravandi S.H.A. & Valizadeh M. Electrospinning of chitosan nanofibers: Processing optimization. *Carbohydrate Polymers*, 2009, 77;656-661.)
29. Buchko C. J., Chen L.C., Shen Y. & Martin D. C. Processing and microstructural characterisation of porous biocompatible protein polymer thin films. *Polymer*, 1999, 40; 7397-7407.
30. Heikkila P. & Harlin A. Parameter study of electrospinning of polyamide-6. *European Polymer Journal*, 2008, 44;3067-3079
31. Patra S. N., Easteal A. J. & Bhattacharyya D. Parametric study of manufacturing poly(lactic) acid nanofibrous mat by electrospinning. *Journal of material Science*, 2009,44;647-654
32. Chen Z.G., Wei B., Mo X-M. & Cui F-Z. Diameter control of electrospun chitosan-collagen fibers. *Journal of Polymer Science Part B: Polymer Physics*, 2009, 47; 1946-1955
33. Samatham R. & Kim K.J. Electric Current as a Control Variable in the Electrospinning Process. *Polymer Engineering and Science*, 2006, 46;954-959.
34. Gupta P., Elkins C., Long T.E., and Wilkes G.L. Electrospinning of linear homopolymers of poly(methyl methacrylate): exploring relationships between fibre formation, viscosity, molecular weight and concentration in a good solvent. *Polymer*, 2005, 46;4799-4810

35. Tripatanasuwan S., Zhong Z. & Reneker D.H. Effect of evaporation and solidification of the charged jet in electrospinning of poly(ethylene oxide) aqueous solution. *Polymer*, 2007, 48;5742-46
36. Sukigara S., Gandhi M., Ayutsede J., Micklus M. & Ko F. Regeneration of *Bombyx mori* silk by electrospinning. Part 2. Process optimization and empirical modelling using response surface methodology. *Polymer*, 2004, 45;3701-3708.
37. Krishnappa R.V. N., Desai K. & Sung C. M. Morphological study of electrospun polycarbonates as a function of the solvent and processing voltage. *Journal of Material Science*, 2003, 38;2357-2365.
38. Subbiah T., Bhat G. S., Tock R.W., Parameswaran S. & Ramkumar S.S. Electrospinning of Nanofibres. *Journal of Applied Polymer Science*, 2005, 96;557-569.
39. Baumgarten P.K. Electrostatic spinning of acrylic microfibers. *Journal of Colloid and Interface Science*, 1971, 36;71-79
40. Yuan X., Zhang Y., Dong C. & Sheng J. Morphology of ultrafine polysulfone fibres prepared by electrospinning. *Polymer International*, 2004, 45;1704-1710
41. Li Y., Huang Z. & Lu Y. Electrospinning of nylon-6,6,1010 terpolymer. *European Polymer Journal*, 2006, 42;1696-1704
42. Ayutsede J., Gandhi M., Sukigara S., Micklus M., Chen H.E. & Ko F. Regeneration of *Bombyx mori* silk by electrospinning. Part 3: characterisation of electrospun nonwoven mat. *Polymer*, 2005, 46;1625-1634.
43. Yördem O.S., Papila M. & Menceloğlu Y.Z. Effects of electrospinning parameters on polyacrylonitrile nanofibre diameter: An investigation by response surface methodology. *Materials and Design*, 2008, 29;34-44.

44. Zhao S., Wu X., Wang L. & Huang Y. Electrospinning of ethyl-cyanoethyl cellulose/tetrahydrofuran solutions. *Journal of Applied Polymer Science*, 2004, 91;242-246
45. Frenot A. & Chronakis I.S. Polymer nanofibres assembled by electrospinning. *Current Opinion in Colloid and Interface Science*, 2003, 8;64-75
46. Chew S.Y., Wen Y., Dzenis Y. And Leong K.W. The Role of Electrospinning in the Emerging Field of Nanomedicine. *Curr. Pharm. Des.*, 2006;12(36);4751-4470
47. Li W-J., Laurencin C.T., Catterson E.J., Tuan R.S. & Ko F.K. Electrospun nanofibrous structure: A novel scaffold for tissue engineering. *Journal of Biomedical Materials Research*, 2002, 60;613-621
48. Sill T.J. & von Recum H.A. Electrospinning: Applications in drug delivery and tissue engineering. *Biomaterials*, 2008, 29;1989-2006.)
49. Bhattarai S.R., Bhattarai N., Yi H.K., Hwang P.H., Cha I.I. & Kim H.Y. Novel biodegradable electrospun membrane: scaffold for tissue engineering. *Biomaterials*, 2004, 25; 2595-2602
50. Zhang Y.Z., Feng Y., Huang Z-M., Ramakrishna S. & Lim C.T. Fabrication of porous electrospun nanofibres. *Nanotechnology*, 2006, 17;901-908
51. Li Dan & Xia Y., Electrospinning of Nanofibres: Reinventing the Wheel? *Advanced Materials*, 2004, 16;1151-1170
52. Guiping M.A., Dongzhi Y., Yingshan Z., Yu J. & Jun N. Preparation and characterization of chitosan/poly(vinyl alcohol)/poly(vinyl pyrrolidone) electrospun fibres. *Frontiers of Materials Science in China*, 2007, 1; 432-436.
53. Marten F.L. Vinyl Alcohol Polymers, *Kirk-Othmer Encyclopaedia of Chemical Technology*, 2002, Wiley, New York, NY 2002 Online.

54. Yang Q. Li Z, Hong Y., Zhoa Y., Qiu S, Wang C. & Wei Y. Influence of solvents on the formation of ultrathin uniform poly(vinyl pyrrolidone) nanofibers with electrospinning. *Journal of Polymer Science Part B: Polymer Physics*, 2004, 42; 3721-3726.
55. Briscoe B., Luckham P. & Zhu S. The effects of hydrogen bonding upon the viscosity of aqueous poly(vinyl alcohol) solutions. *Polymer*, 2000, 41;3851-3860
56. Katti D.S., Robinson K.W., Ko F.K. & Laurencin C.T. Bioresorbable Nanofibre-Based Systems for Wound Healing and Drug Delivery: Optimization of Fabrication Parameters. *Journal of Applied Materials Research Part B: Applied Biomaterials* 70B,2004;286-296
57. Supaphol P. & Chuangchote S. On the Electrospinning of Poly (vinyl alcohol) Nanofibre Mats: A revisit. *Journal of Applied Polymer Science*, 2008, 108; 969-978.
58. Stanger J., Tucker N., Wallace A., Larsen. N., Staiger M. & Reeves R. The Effect of Electrode Configuration and Substrate Material on Mass Deposition Rate of Electrospinning. *Journal of Applied Polymer Science*, 2009, 112; 1729-1737.
59. Fong H., Chun I. and Reneker D. H. Beaded nanofibres formed during electrospinning. *Polymer*, 1999, 40;4585-4592.
60. Qiang L., Jia Z., Yang Y., Wang L. & Guan Z. Preparation and Properties of PVA Nanofibres by Electrospinning. *International Conference on Solid Dielectrics*, Winchester, UK, July8-13, 2007
61. Zhang C., Yuan X., Wu L., Han Y., Sheng J. Study on morphology of electrospun poly(vinyl alcohol) mats. *European Polymer Journal* 2005, 41; 423

62. Koski A., Yim K. & Shivkumar S. Effect of Molecular Weight on Fibrous PVA Produced by Electrospinning. *Materials Letters*, 2004, 58;493-497.
63. Ding B., Kim H-Y., Lee S-C., Lee D-R. & Choi K-J. Preparation and Characterisation of Nanoscaled Poly(vinyl alcohol) Fibres via Electrospinning. *Fibres and Polymers*, 2002, 3;73-79.
64. Singh S., Lakshmi S. G. & Vijaykumar M. Effect of Process Parameters on the Microstructural Characteristics of Electrospun Poly(Vinyl Alcohol) Fibre Mats. *Nanobiotechnology*, 2009, pages 1-7.
65. Chang C., Limkrailassiri K., & Lin L. Continuous near- field electrospinning for large area deposition of orderly nanofibre patterns. *Applied Physic Letters*, 2008, 93.